

Dihydrogen Activation at Non-Metallic Centers

Inauguraldissertation

zur

Erlangung der Würde eines Doktors der Philosophie

vorgelegt der

Philosophisch-Naturwissenschaftlichen Fakultät

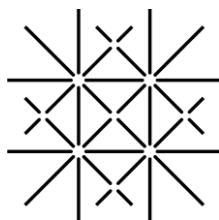
der Universität Basel

von

Johanna Auth

aus Marburg, Deutschland

Basel, 2015



UNI
BASEL

Genehmigt von der Philosophisch-Naturwissenschaftlichen Fakultät
auf Antrag von

Prof. Dr. Andreas Pfaltz

Prof. Dr. Helma Wennemers

Basel, den 17. Februar 2015

Prof. Dr. Jörg Schibler

Dekan

für Micha und meine Familie

This thesis was supervised by Prof. Dr. Andreas Pfaltz from April 2011 to March 2015 at the University of Basel, Department of Chemistry.

Parts of this work have been previously published:

“Synthesis of functionalized pyridinium salts bearing a free amino group”

J. Auth, P. Mauleón, A. Pfaltz, *ARKIVOC* **2014**, 154.

Acknowledgements

First and foremost, I would like to thank Prof. Dr. Andreas Pfaltz for the opportunity to work on his research group and for constant support and confidence.

Special thanks goes to Prof. Dr. Helma Wennemers, who agreed to co-examine this thesis and to Prof. Dr. Dennis Gillingham for charring the examination.

I am very grateful to Dr. Paolo Tosatti, Dr. Alex Marti and Dr. Pablo Mauleón for the time they invested for critically proofreading and improving this manuscript.

I am extremely thankful to Dr. Pablo Mauleón for his constant support and advice during the course of this research. His helpful suggestions and valuable scientific input were instrumental to this work. Moreover, I would like to thank the whole activation team Dr. Jaroslav Padevet, Dr. Sabrina Peixoto, Dr. Paolo Tosatti, and Dr. Alex Marti for the fruitful discussions and support in every chemical issue.

Furthermore, I thank all the members of the Pfaltz group, and especially those of lab 204, for the fruitful working atmosphere and for making my time enjoyable.

I am very grateful to Dr. Jaroslav Padevet for recording numerous NMR experiments and helpful discussions of technical matters. I would also like to thank Dr. Florian Bächle and Patrick Isenegger for measuring ESI mass spectra. I want to thank Dr. Heinz Nadig who measured the EI and FAB mass spectra and Werner Kirsch and Sylvie Mittelheisser who determined all the elemental analyses. Moreover, Markus Neuburger is gratefully acknowledged for collecting the X-ray data.

I want to thank all former and current member of the workshop team for their technical support.

I thank Marina Mambelli Johnson for all organization work beyond chemistry.

Financial support by the Swiss National Science Foundation and the University of Basel is gratefully acknowledged.

Ein besonderer Dank gilt auch allen Freunden von der Universität Bielefeld. Ohne euch wäre das Studium nur halb so schön gewesen!

Schliesslich möchte ich mich bei meiner ganzen Familie und allen Freunden bedanken, besonders bei meinen Eltern und bei meiner Schwester. Vielen Dank dass ihr mich stetig auf meinem Lebensweg begleitet habt und ich immer auf eure Unterstützung vertrauen konnte.

Zu guter Letzt möchte ich mich bei Micha für seine stetige Unterstützung, das Verständnis, die Geduld und Liebe, die er mir während meinen Studium entgegengebracht hat und mich auch in schwierigen Situation stets aufs Neue motiviert hat.

Table of Contents

1	INTRODUCTION	3
1.1	DIHYDROGEN ACTIVATION AT NON-METALLIC CENTERS	3
1.2	FRUSTRATED LEWIS PAIRS	5
1.2.1	MECHANISTIC INVESTIGATIONS	10
1.3	NAD ⁺ /NADH REDUCTIONS AND ANALOGUES	12
1.4	THESIS OUTLINE	14
2.	SUMMARY OF PREVIOUS RESULTS OBTAINED IN THE PFALTZ GROUP	19
2.1.	PYRIDINIUM ALKOXIDES	19
2.2.	PYRIDINIUM AMIDINES	22
3.	INTRAMOLECULAR PYRIDINIUM-BASED FLP SYSTEMS	27
3.1.	INTRODUCTION	27
3.1.1.	OBJECTIVE OF THIS WORK	28
3.1.2.	DFT CALCULATIONS ON FLP SYSTEMS FOR H ₂ ACTIVATION	28
3.2.	SYNTHESIS	30
3.2.1.	RETROSYNTHETIC ANALYSIS	30
3.2.2.	SYNTHESIS OF BENZYLIC AMINES	31
3.2.3.	PROTONATION	33
3.2.4.	METHYLATION	36
3.2.5.	DEPROTONATION	44
3.3.	HYDROGENATION OF AMINO-PYRIDINIUM SALTS	47
4.	BIMOLECULAR PYRIDINIUM-BASED FLP SYSTEMS	53
4.1.	INTRODUCTION	53
4.1.1.	FLP FORMATION WITH STERICALLY HINDERED PHENOLATES	53
4.1.2.	OBJECTIVE OF THIS WORK	54
4.1.3.	DFT CALCULATIONS ON FLP SYSTEMS FOR H ₂ ACTIVATION	54
4.2.	SYNTHESIS	55
4.2.1.	PREPARATION OF <i>N</i> -ACYL AMMONIUM SALTS	55
4.2.2.	PREPARATION OF AUTHENTIC SAMPLES	58
4.3.	DIHYDROGEN ACTIVATION RESULTS	59
4.4.	REACTION WITH DEUTERIUM GAS	66
4.5.	REDUCTIONS WITH 1,4-DHP	67
4.6.	SUMMARY	69

5.	REVISION OF THE PROPOSED MODEL FOR H₂ ACTIVATION: HANTZSCH ANALOGUES IN PYRIDYLIDENE CHEMISTRY	73
5.1.	INTRODUCTION	73
5.1.1.	OBJECTIVE OF THIS WORK	77
5.2.	<i>N</i>-ARYL HANTZSCH ESTERS	78
5.2.1.	PREPARATION	78
5.2.2.	DIHYDROGEN ACTIVATION EXPERIMENTS	80
5.2.3.	DEUTERATION EXPERIMENTS	82
5.2.4.	POSSIBLE APPLICATIONS OF HANTZSCH ESTER 175	83
5.3.	<i>N</i>-ARYL NICOTINAMIDE DERIVATIVES	85
5.3.1.	PREPARATION	85
5.3.2.	PREPARATION OF AUTHENTIC SAMPLES OF DIHYDROPYRIDINES	87
5.3.3.	DIHYDROGEN ACTIVATION STUDIES	87
5.3.4.	DEUTERATION STUDIES	89
5.3.5.	POSSIBLE APPLICATION OF NICOTINAMIDE 200	90
5.4.	SUMMARY	90
6.	ARYL SUBSTITUTED PYRIDYLIDENES IN DIHYDROGEN ACTIVATION	93
6.1.	INTRODUCTION	93
6.2.	OBJECTIVE OF THIS WORK	93
6.3.	DFT CALCULATIONS ON PYRIDYLIDENES FOR H₂ ACTIVATION	94
6.4.	SYNTHESIS	95
6.4.1.	PREPARATION OF TRIARYL-PYRIDINIUM SALTS	95
6.4.2.	PREPARATION OF AUTHENTIC SAMPLES	98
6.4.3.	PREPARATION OF <i>N</i> - <i>TERT</i> -ALKYLPYRIDINIUM SALTS	99
6.5.	DIHYDROGEN ACTIVATION RESULTS	100
6.5.1.	HYDROGENATION OF TRIARYL-PYRIDINIUM SALTS	100
6.5.2.	HYDROGENATION OF <i>N</i> - <i>TERT</i> -ALKYLPYRIDINIUM SALTS	106
6.5.3.	REACTION WITH DEUTERIUM GAS	107
6.6.	OPTIMIZATION	108
6.6.1.	VARIATION OF THE BASE	108
6.7.	APPLICATION	112
6.7.1.	REDUCTION WITH AUTHENTIC SAMPLES	112
6.7.2.	<i>IN-SITU</i> REDUCTION	118
6.8.	SUMMARY	120
7	EXPERIMENTAL PART	123
7.1	WORKING TECHNIQUES AND REAGENTS	123
7.2	ANALYTICAL METHODS	123
7.3	INTRAMOLECULAR PYRIDINIUM-BASED FLP SYSTEMS	126
7.3.1	SYNTHESIS OF BENZYLIC AMINES	126
7.3.2	SYNTHESIS OF AMINO-PYRIDINIUM SALTS	133
7.4	BIMOLECULAR PYRIDINIUM-BASED FLP SYSTEMS	143
7.4.1	SYNTHESIS OF PYRIDINIUM SALTS	143

7.4.2	PHENOLATES	149
7.5	REVISION OF THE PROPOSED MODEL FOR H ₂ ACTIVATION: HANTZSCH ANALOGUES IN PYRIDYLIDENE CHEMISTRY	152
7.5.1	SYNTHESIS OF <i>N</i> -ARYL HANTZSCH ESTERS	152
7.5.2	SYNTHESIS OF <i>N</i> -ARYL NICOTINAMIDE DERIVATIVES	157
7.6	ARYL SUBSTITUTED PYRIDYLIDENES IN DIHYDROGEN ACTIVATION	166
7.6.1	SYNTHESIS OF PYRIDINIUM SALTS	166
7.6.2	SYNTHESIS OF <i>N</i> - <i>tert</i> -ALKYLPYRIDINIUM SALTS	174
7.6.3	ACTIVATION AT ELEVATED PRESSURE	176
7.6.4	ANALYTICAL DATA FOR THE ACTIVATION PRODUCTS	176
7.6.5	SYNTHESIS OF SUBSTRATES	179
7.6.6	REDUCTION WITH AUTHENTIC SAMPLES	183
7.6.7	<i>IN-SITU</i> REDUCTION	184
7.6.8	ANALYTICAL DATA FOR THE REDUCED SUBSTRATES	184
8.	APPENDIX	189
8.1.	CRYSTALLOGRAPHIC DATA	189
8.2.	LIST OF ABBREVIATIONS	190
9.	REFERENCES	195
10	SUMMARY	201

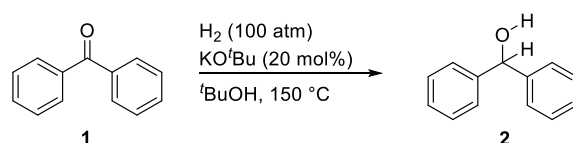
Chapter 1

1 Introduction

1.1 Dihydrogen Activation at Non-Metallic Centers

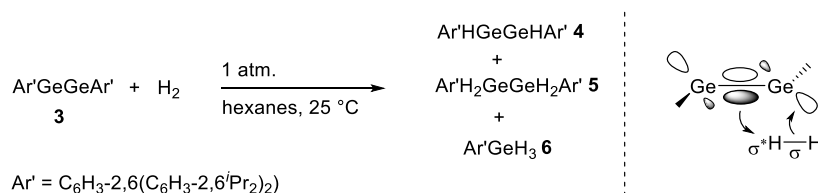
Catalytic hydrogenation is a powerful tool to reduce saturated organic compounds and this transformation is extensively used in industrial processes, for example for the processing of crude oils or for the production of ammonia-based fertilizer through the *HABER-BOSCH* process.^[1] Moreover, hydrogenations find wide industrial application in the production of pharmaceuticals, fine chemicals, flavors and vitamins.^[2-5] Furthermore, the utilization of hydrogen gas as replacement of fossil fuels has triggered the interest of the society as it is a cleaner and more sustainable energy source. Consequently, any improvement of the efficiency of the catalyst would be beneficial to lower the cost of these valuable processes. As the H₂ molecule possess as very strong two electron H–H bond (104.2 kcal/mol), it first needs to be cleaved, or “activated” and the splitting usually requires the action of a transition metal catalyst such as palladium, platinum or iridium. Both the mechanism and application of transition metal catalyzed hydrogenations have been the subject of numerous studies and the impact of this research was awarded with the Nobel Prize in 2001.^[6-7] However, these transition metal catalyzed used in industrial processes can be expensive and environmentally harmful.

The possibility of developing transition-metal-free methods for the hydrogenation of organic compounds has attracted considerable interest in recent years. *WALLING* and *BOLLYKY* showed fifty years ago that potassium *tert*-butoxide induces hydrogenation of benzophenone (**1**) to diphenylmethanol (**2**) at high temperature and high pressure (*Scheme 1.1*).^[8] However, due to the harsh reaction conditions, the substrate scope was restricted to robust non-enolizable ketones.



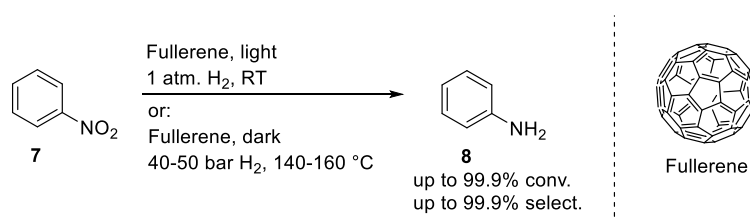
Scheme 1.1. Reduction of benzophenone.

Dihydrogen activation by a nonmetallic main-group compound has been observed by *POWER* and co-workers.^[9] They synthesized a stable digermine complex **3**, which reacts rapidly with H₂ at room temperature and ambient pressure. Mechanistic studies showed electrons are donated to an empty nonbonding orbital and back-donating from the π -bond orbital of the Ge-Ge double bond facilitate dihydrogen cleavage (*Scheme 1.2*).



Scheme 1.2. Dihydrogen activation by an unsaturated heavier main group compound.

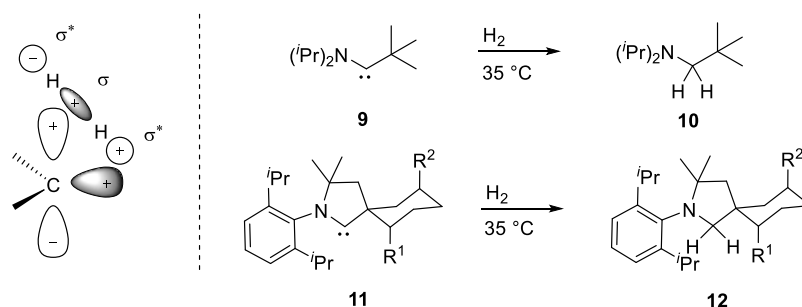
The group of *XU* reported that neutral fullerene, the fullerene anion, and their combination are adequate catalysts for the reduction of aromatic nitro compounds to the corresponding amino aromatics. Their system performed with high conversion and selectivity under UV irradiation under ambient conditions or in the dark under forcing conditions. However, the mechanism of the dihydrogen activation is not fully understood for this system (*Scheme 1.3*).



Scheme 1.3. Catalytic hydrogenation of nitrobenzene on C₆₀ catalyst.

In 2007, *BERTRAND* and co-workers showed that dihydrogen can be activated by stable singlet carbenes.^[10] The team realized that singlet carbenes and many transition-metal complexes share a common frontier orbital pattern, approximate energy and occupancy. Taking advantage of this fact, stabilized acyclic and cyclic (alkyl)(amino)carbenes like **9** and **11** were designed which can cleave dihydrogen, forming alkane products (*Scheme 1.4*). According to the rationale proposed by *BERTRAND et al.* the hydrogen cleavage occurs through donation of the dihydrogen σ -bonding orbital into the vacant orbital of the singlet carbene, leaving

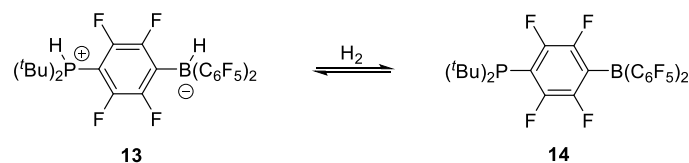
sufficient overlap for the carbene lone pair to populate the H₂ antibonding σ^* orbital. Consequently, the H–H bond is weakened and heterolytic cleavage occurs.



Scheme 1.4. Activation of H₂ by singlet carbene.

1.2 Frustrated Lewis Pairs

In an even more promising development, the group of *STEPHAN* synthesized a non-metallic compound that allows for the reversible heterolytic cleavage of dihydrogen.^[11-14] The success of *STEPHAN*'s model relies on the implementation of the concept of “antagonistic”^[15-16] or “frustrated”^[17-18] Lewis pairs (FLPs). In such systems, sterically hindered Lewis donors and acceptors are combined. Their steric demands preclude formation of simple Lewis acid-base adducts, allowing for the subsequent synergistic action of both Lewis acid and base on H₂ and other molecules.^[19] These new systems, based on phosphinoboranes, can add H₂ at 25 °C and expel it again by heating at 100 °C. Upon heterolytic hydrogen cleavage, a proton is bound to the phosphorous atom and a hydride to the boron atom of the resulting phosphonium borate (*Scheme 1.5*).



Scheme 1.5. First intramolecular FLP system developed by *STEPHAN et al.*^[11]

These transformations have triggered considerable interest in the field, and catalytic applications of this strategy are currently being pursued by several groups.^[20-21] For example, *STEPHAN* has demonstrated that the system described in *Scheme 1.5* can be deployed for the

catalytic hydrogenation of imines.^[22] To achieve catalysis, it is required that the B–N dative bond formed between the “activator” and the product upon reduction of the imine is broken, thus releasing the phosphinoborane species which can subsequently activate again H₂, re-entering the catalytic cycle. This can be readily achieved by simple heating the solutions between 80 and 120 °C. In this fashion, thermal dissociation of amine occurs and the catalytic reduction of imines takes place under 1–5 bar of H₂.

The group of *ERKER* has developed a new system based on ethylene-linked (Mes)₂P(C₂H₄)B(C₂F₅)₂ (Mes=2,4,6-trimethylphenyl, *Figure 1.1, 15*).^[23] This compound was shown to also activate H₂, forming the corresponding phosphonium borate. Although the reaction was not thermally reversible, the salt was able to reduce benzaldehyde. In more recent efforts, *ERKER* and co-workers have reported a related olefinic linked phosphine borane (*Figure 1.1, 16*)^[24] which also activates H₂ and has been employed to effect the catalytic reduction of imines and enamines at room temperature. The same research group has also developed an interesting reversible system based on the 1,8-diphosphino-naphthalene phosphine (*Figure 1.1, 17*).^[25] In combination with B(C₆F₅)₃, the bisphosphine **17** has been shown to efficiently activate dihydrogen and to undergo H₂ extrusion when heated at 60 °C, to regenerate the FLP. Catalytic reduction of silyl enol ethers has been achieved at 25 °C under H₂ pressure of 2 bar. Moreover, the activation of H₂ deploying a zirconocene derivative (Mes₂PC₅H₄)₂ZrCl₂ in combination with B(C₆F₅)₃ under very mild conditions is described (*Figure 1.1, 18*).^[26]

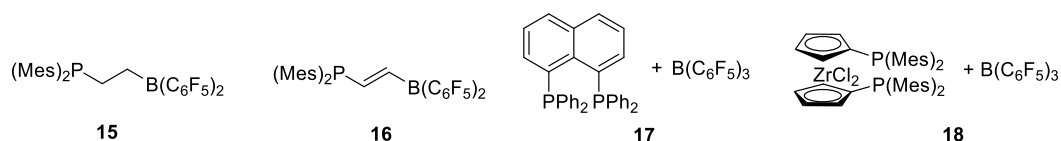


Figure 1.1. Phosphane/borane systems.

STEPHAN and co-workers reported that the reaction of the imine ^tBuN=CPh(H) and B(C₆F₅)₃ leads to an adduct, which can activate dihydrogen at 80 °C and 4–5 bar of hydrogen pressure. (*Figure 1.2, 19*).^[27] Subsequent heating of this adduct under hydrogen pressure leads to full reduction of the aromatic ring.^[28] The group of *REPO* and *RIEGER* have reported the catalytic hydrogenation of imines and enamines.^[29] Their approach relies on the use of a linked amino-borane (*Figure 1.2, 20*) species derived from a sterically encumbered amine which is used in

place of bulky phosphines. Furthermore, they also demonstrated that a similar intermolecular FLP can activate dihydrogen under mild conditions as well and was applied to the stoichiometric reduction of benzaldehyde (Figure 1.2, **21**).^[30] The group of Soós designed novel intermolecular FLP catalysts based on the finding that increasing the steric bulk of the *ortho*-substituted aryl group of the boron centers enables the use of non-bulky amines (Figure 1.2, **22**).^[31] More recently, WANG *et al.* reported that the secondary borane with extremely bulky and electron-withdrawing 2,4,6-tris(trifluoromethyl)phenyl groups in combination with simple sterically less demanding amines, can activate hydrogen under mild conditions (Figure 1.2, **23**).^[32] Similar to the described zirconocene-phosphine derivative **18** described above, ERKER *et al.* found out that the reaction of a zirconocene-amine derivative with $B(C_6F_5)_3$ in the presence of H_2 leads to the cleavage of the H–H bond (Figure 1.2, **24**). Moreover, this FLP system can also be used as catalyst for the reduction of imines and silyl enol ethers.^[26]

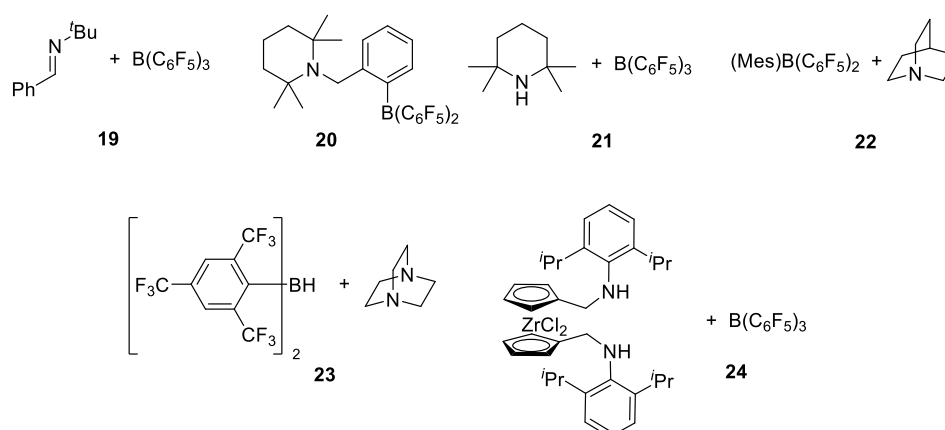
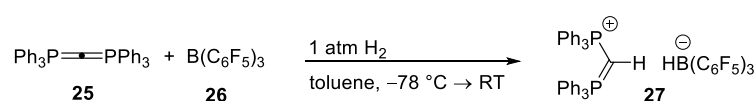


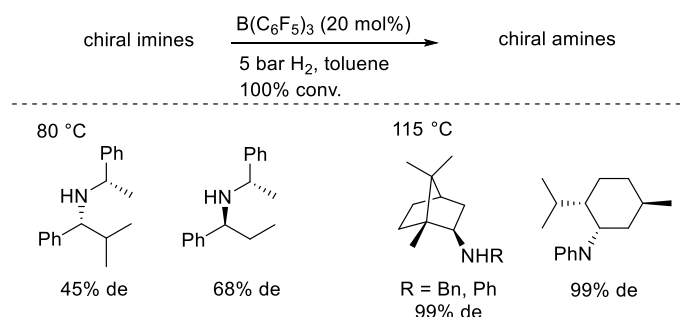
Figure 1.2. Amine/borane systems.

ALCARAZO *et al.* showed that the pair of hexaphenylcarbodiphosphorane and $B(C_6F_5)_3$ is also capable of activating dihydrogen. Moreover, this new carbon-based FLP is also able to open ethers and lactones through C–O bond cleavage and to activate the Si–H bond of silanes. The researchers suggest that the reactivity occurs through the unusual electronic distribution around the central carbon(0) atom (Scheme 1.6).^[33]



Scheme 1.6. Dihydrogen activation of hexaphenylcarbodiphosphorane and $B(C_6F_5)_3$.

The field of metal-free hydrogenation has been extended to the possibility of enantioselective reduction. For example, a highly diastereoselective catalytic hydrogenation of imines was successfully achieved by combination of chiral imines and $B(C_6F_5)_3$ as catalyst (*Scheme 1.7*).^[34]



Scheme 1.7. Diastereoselective hydrogenation of chiral imines catalyzed by $B(C_6F_5)_3$, selected examples.

Soon after the first report of chiral boranes as catalysts for asymmetric hydrogenation by *KLANKERMAYER*,^[35] the investigation of new chiral FLPs started. Chiral boranes such as **28** and **29** have been employed in hydrogen activation together with tBu_3P . Using these systems, significant enantioselectivity has been achieved for the catalytic hydrogenation of prochiral imines.^[36] However, very few chiral FLP catalyst are known and enantioselective reactions mediated by such compounds are very rare and so far, not very efficient.^[37-41]

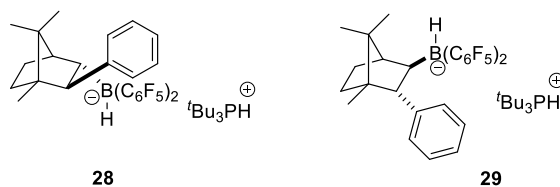
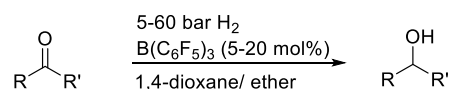


Figure 1.3. Chiral FLPs used for reduction of imines.

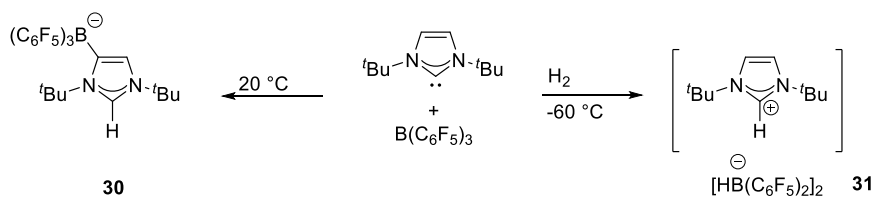
Very recently, the groups of *ASHLEY* and *STEPHAN* reported on the reduction of C=O bonds employing FLP catalysts.^[42-43] These reactions are the first examples of completely metal-free catalytic hydrogenation of carbonyl compounds, a transformation which was not possible with the initial phosphine-based FLP systems. The authors use solutions of $B(C_6F_5)_3$ in either 1,4-dioxane or diethylether to hydrogenate various alkyl and aryl ketones and aldehydes under mild reaction conditions. The reductions proceed *via* a FLP mechanism in which the solvent serves as a weak Brønsted base (*Scheme 1.8*). Interestingly, the ring-opening of 1,4-dioxane was not observed, in contrast to the previously reported opening of THF with FLP

based systems.^[44] That might be due to the fact that 1,4-dioxane is a weaker donor than THF but still sufficiently Lewis basic to activate H₂.



Scheme 1.8. B(C₆F₅)₃-Catalyzed hydrogenation of aldehydes and ketones.

The combination of a Lewis acid/base is not only limited to bulky phosphines and amines in combination with B(C₆F₅)₃. In 2008, the groups of *STEPHAN* and *TAMM* reported simultaneously the incorporation of sterically hindered *N*-heterocyclic carbenes (NHCs) to FLP chemistry.^[45-46] The reaction of 1,3-di-*tert*-butylimidazolin-2-ylidene with B(C₆F₅)₃ affords a strong adduct **30**, whereas the reaction at low temperature gives an FLP which cleaves H₂ heterolytically to form the imidazolium hydroborate **31** (*Scheme 1.9*).

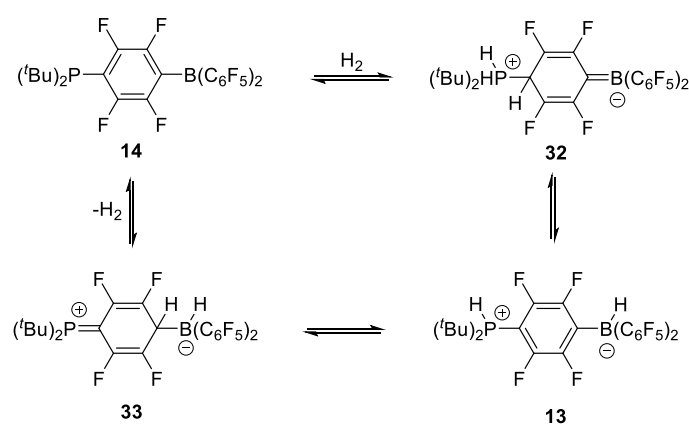


Scheme 1.9. Reactions of NHCs with B(C₆F₅)₃

Unfortunately, attempts to enhance the scope of Lewis acids to less electrophilic boranes such as Ph₃B together with hindered phosphines has shown low reactivity in the activation of dihydrogen,^[47-48] although recently interesting results have been reported for the activation of other small molecules like CO₂.^[48-49] Certainly, the possibility of employing milder Lewis acids for FLP chemistry would be a great improvement towards functional group tolerance as well as stability and handling of the borane species by avoiding the use of these highly reactive, air and moisture sensitive compounds. As reported by *PARADIES* and co-workers, the employment of the weaker Lewis acid (2,6-F₂-C₆H₃)₃B shows interesting tolerance to various functional groups in FLP catalyzed hydrogenations,^[50] but the research in this field is still in early stages.

1.2.1 Mechanistic Investigations

The details of the mechanism of action of reversible H₂ activation by a FLP system have been the subject of numerous studies. In their first report in 2006, *STEPHAN* and co-workers proposed a stepwise mechanism, in which the proton migrates across the molecule's arene linker to the hydride, and the two recombine to form dihydrogen. In the reverse reaction, the authors proposed that H₂ likely attaches to boron, and then a proton migrates to the phosphorous atom (*Scheme 1.10*).^[11-12]



Scheme 1.10. Initially proposed mechanism for H₂ splitting.

Mechanistic investigations by the *ERKER* and *GRIMME* research groups published in 2010 suggest that FLPs are heterolytic cleavage is induced by polarization caused by the electronic field created by their donor/acceptor atoms based on DFT studies (*Figure 1.4*).^{[51],[52]}

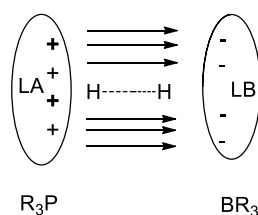


Figure 1.4. H₂ activation in the electric field created by an FLP.

According to their model, the step with the highest energy barrier is the entrance of the H₂ molecule into the FLP cavity. Afterwards the reaction proceed without a barrier, and the authors suggests that the splitting of dihydrogen does not require specific H₂/FLP orbital

interactions. Nevertheless, these mechanistic studies are limited in their explanation of FLP chemistry, as they only describe the initial part of the reaction (*Figure 1.5*).

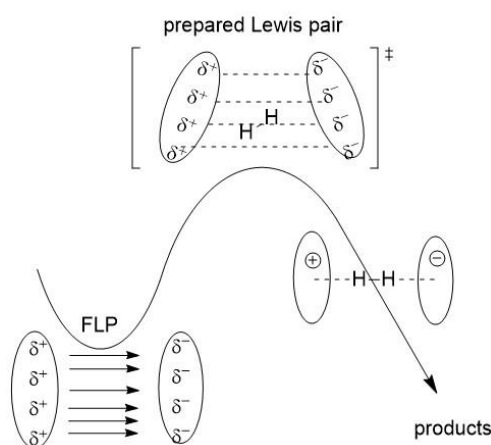


Figure 1.5. Energy profile of the H₂ splitting by an FLP.

Recently, PÁPAI and co-workers stated that the “*electron-donation-based picture of hydrogen splitting by FLPs need not be abandoned*”. They concluded from their computational studies that FLPs with similar reactivity show tremendously different electronic field characteristics. Moreover, the DFT studies indicate that the electronic field is not present in cavities, but as spherical regions around the donor/acceptor atoms, which are too weak to account for the electronic structure of the transition state. Consequently, the polarization of the H–H bond can be better interpreted as the results of orbital interactions. Their detailed mechanistic analysis revealed that the dihydrogen activation occurs through σ -donation of H₂ to the Lewis acceptor and simultaneous electron back donation to H₂ (*Figure 1.6*).^[53]

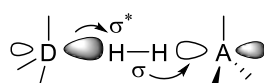


Figure 1.6. Electron transfer model.

1.3 NAD⁺/NADH reductions and analogues

Redox transformations in living organisms rarely occur in the absence of metal-free systems. Living organisms typically rely on organic coenzymes such as nicotinamide adenine dinucleotide (NADH, *Figure 1.7, 34*) in combination with metalloenzymes.

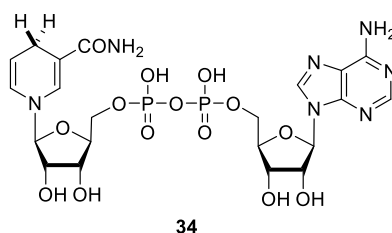
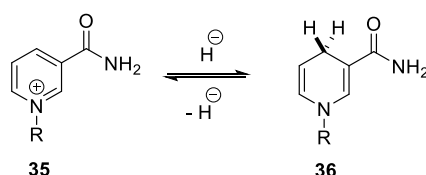


Figure 1.7. Nicotinamide adenine dinucleotide, NADH.

NADH is an ubiquitous biological reductant. In metabolism, NAD⁺ is involved in redox reactions, carrying electrons from one reaction to another. The coenzyme is, therefore, found in its oxidized form NAD⁺ and its reduced form NADH, which can then be deployed as reagents for redox reactions through hydride transfer. These reactions are the main function of NAD⁺ and are reversible (*Scheme 1.11*).^[54]



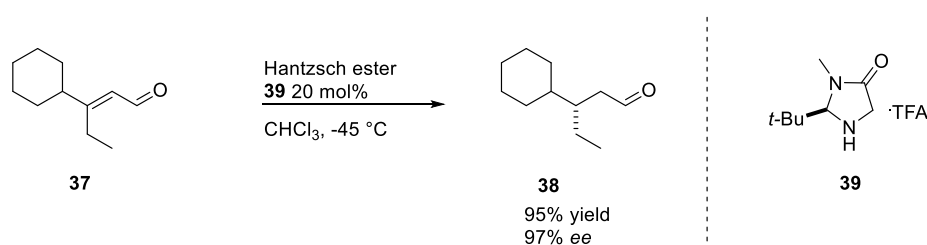
Scheme 1.11. Redox chemistry of NADH, R represents the dinucleotide moiety of NADH.

The study of NADH and analogues based on dihydropyridines systems started receiving more attention after the exact structure of NADH was published in the late 1950s.^[55] The selective nature of NADH reductions led to the interesting possibility of developing stereoselective reducing agents similar to NADH. *WESTHEIMER* was the first to demonstrate that a synthetic NADH mimic was able to reduce a dye into its corresponding base.^[56] Based on these results, the development of dihydropyridines became an intensively investigated field.^[55, 57-59] Subsequent studies found that dihydropyridines can be used as effective reagents to reduce

organic substrates for example imines,^[60] aldehydes,^[61] ketones^[62] and other functional groups.^[63]

With the development of new NADH mimics, the chemistry of dihydropyridines and particularly of Hantzsch esters was studied. Closely related to NADH, Hantzsch esters were first discovered by *HANTZSCH* in 1882.^[64] Hydride abstractions from Hantzsch esters and analogues have found numerous applications in organic synthesis, enabling for example catalytic transformations through pyridinium salt and 1,4 dihydropyridine systems.^[59] Moreover, Hantzsch esters exhibit important pharmacological properties such as antihypertensive, antibiotic, anti-inflammatory and antifungal activity.^[65-66]

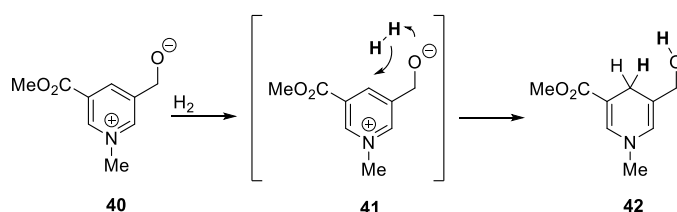
One of the several interesting properties of Hantzsch esters resides in their ability to participate as reducing agents in the organocatalytic hydrogenation of some organic compounds. In 2004, *MACMILLAN*^[67] and *LIST*^[68] independently reported the development of organocatalytic enantioselective transfer hydrogenation strategies using iminium catalysts and Hantzsch esters to reduce α,β -unsaturated carbonyl compounds. They described a chemical reduction wherein enzymes and cofactors are replaced by small molecule organocatalysts and dihydropyridines systems. These novel iminium catalytic reductions are highly efficient and enantioselective, and constitute powerful strategies for the enantioselective formation of C–H stereogenic centers. For example, high levels of enantiocontrol are observed for the enantioselective reduction of α,β -unsaturated aldehydes **37** using dihydropyridine analogues in the presence of iminium catalyst **39** (*Scheme 1.12*).^[69]



Scheme 1.12. Organocatalytic α,β -unsaturated aldehyde reduction using Hantzsch esters.

1.4 Thesis Outline

The activation of H₂ by Frustrated Lewis Pairs is nowadays an established method for the heterolytic cleavage of dihydrogen without the presence of transition-metal catalysts. As mentioned above, *WALLING* and *BOLLYKY* demonstrated the ability of ketones to act as hydride acceptors in H₂ activation processes.^[8] Compared to benzophenone, a pyridinium compound is expected to be a much stronger hydride acceptor. The use of a strong base like an alkoxide or a basic amine might enable the use of weak hydride acceptors such as pyridinium salts. Preliminary DFT calculations were performed on the system shown in *Scheme 1.13* which suggest that the dihydrogen cleavage might occur through a concerted reaction of H₂ and the zwitterionic pyridinium derivative **41**. The calculated activation barrier for this process is moderate with about 13 kcal/mol.

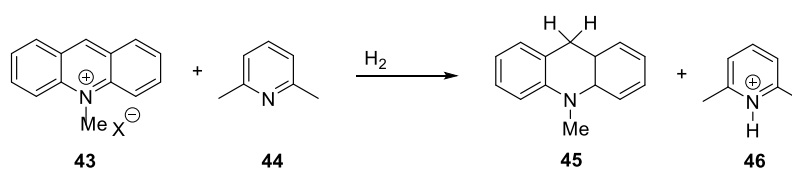


Scheme 1.13. DFT studies on alkoxy-pyridinium systems.

The aim of this thesis was to develop new systems for heterolytic dihydrogen activation and catalytic hydrogenation that combine relatively strong bases, and pyridinium salts as hydride acceptors. These electrophilic centers are much less Lewis acidic than the fluorinated arylboranes used in conventional FLP systems, and the implementation of systems of this type would considerably enhance the scope of nonmetal-based catalytic hydrogenation.

The initial part of this Thesis describes attempts at developing systems containing pyridinium salts as hydride acceptors in combination with different bases. The following two chapters describe efforts on a related system, also based on the use of pyridinium ions but conceptually different in its approach towards dihydrogen activation, since it relies on the generation of highly reactive pyridylidenes by treatment of pyridinium salts with sufficiently strong bases.

After completion of the experiments of this thesis, the group of *INGLESON* reported on the development of a system which is conceptually similar to the ones investigated in the first part of this thesis. Their approach relied on the combination of *N*-methylacridinium salts **43** and 2,6-lutidine (**44**), which was shown to activate dihydrogen (*Scheme 1.14*).^[70] This work will be discussed in detail in *Chapter 5*.



Scheme 1.14. Dihydrogen activation by an *N*-methylacridinium salt and 2,6-lutidine.

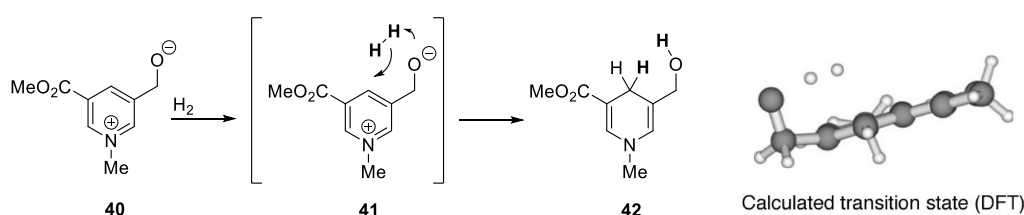
Chapter 2

2. Summary of Previous Results Obtained in the Pfaltz Group

The project of this doctoral thesis continues work initiated by Dr. *Pablo Mauleón*, who conducted post-doctoral studies in the research group of Prof. A. Pfaltz from January 2009 to August 2011. During that time, I joined the Pfaltz group working under the supervision of Dr. *Pablo Mauleón* as a master student. The results detailed below have been extracted from the report “*Alternatives to Standard Frustrated Lewis Pairs in the Reaction with Dihydrogen: Experimental and Computational Studies*” by Dr. *Pablo Mauleón*. They are included with the aim of better contextualizing the project and explain where it stemmed from.

2.1. Pyridinium Alkoxides

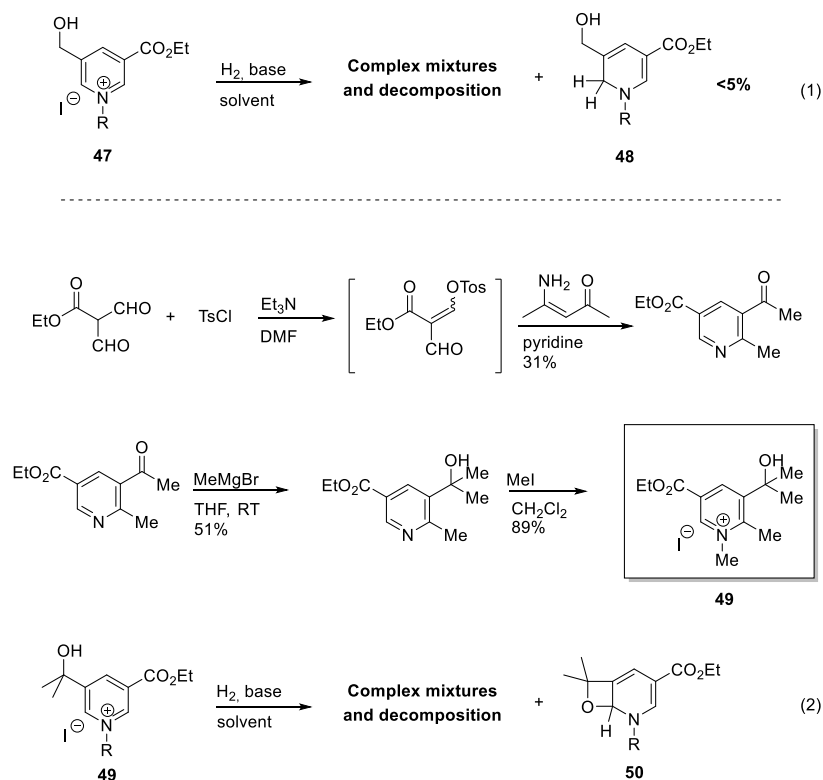
Preliminary DFT calculations were performed on the system shown in *Scheme 2.1*. A reaction path involving a concerted, strongly exothermic reaction of the zwitterionic pyridinium derivative with dihydrogen was found, leading to the corresponding 1,4-dihydropyridine with an activation barrier of ca. 13 kcal/mol. MP2 calculations, which yield more realistic transition state energies, gave a value of 21 kcal/mol. In the transition state shown below (*Scheme 2.1*), one hydrogen atom strongly interacts with the basic oxygen atom, while the electrophilic center at C4 interacts with the elongated σ -bond of the dihydrogen molecule. Obviously, the calculated energies are not reliable numbers, and further calculations including solvent effects would be necessary for obtaining more realistic transition state energies. Nevertheless, the results show that this reaction is, at least in principle, a feasible process.



Scheme 2.1. Preliminary DFT studies.

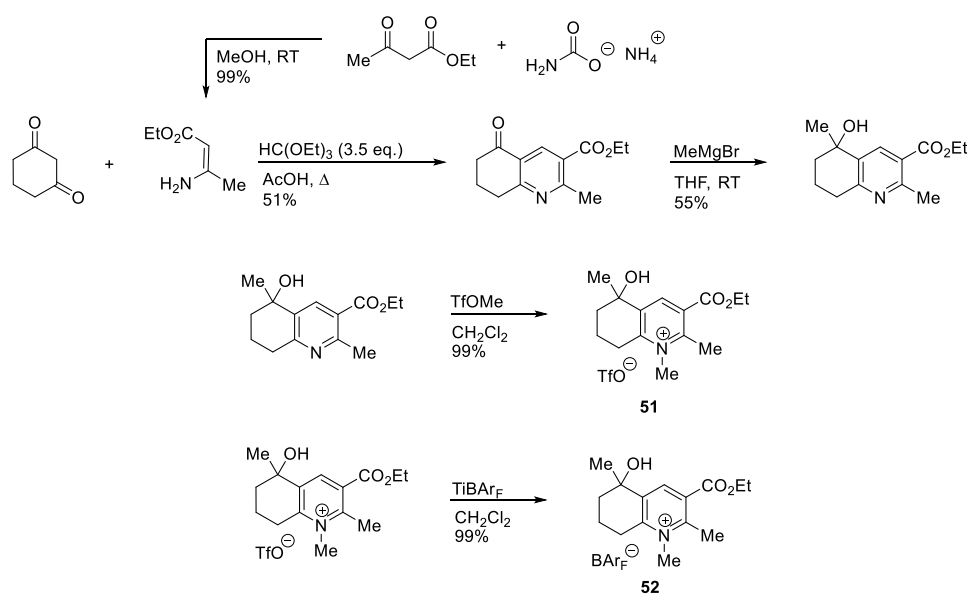
With these estimations in hand, initial efforts were directed towards the development of systems which incorporate a pyridinium ring and a free alcohol placed in a position that is in principle ideal to adopt the required conformation. In this context, several model substrates such as those indicated in *Scheme 2.2* were prepared and tested. Unfortunately, no success was achieved with the systems explored; the tests often led to either decomposition of the starting material, or to complex reaction mixtures from which no products originated from dihydrogen activation were detected. Problems associated with the nucleophilicity of these alkoxides occasionally led to the formation of intramolecular addition of the alkoxide to the electrophilic pyridinium systems. Nevertheless, meaningful conclusions from these experiments were drawn:

1. A disproportionation process can take place if primary alcohols are used (*Scheme 2.2*, eq. 1).
2. The studies indicate that pyridinium salts undergo intramolecular nucleophilic addition in the presence of alcohols and a base even if that entails formation of strained four-membered heterocycles (*Scheme 2.2*, eq. 2).



Scheme 2.2. Pyridinium salts: first generation.

Based on these results, the model system was revised and a second generation of potential pyridinium-based dihydrogen activators was prepared. The main difference between the two models was the introduction of a rigid carbon backbone, which in theory should preclude intramolecular nucleophilic addition of the deprotonated alcohols to the pyridinium ring. Additionally, this new design included tertiary alcohols in order to prevent disproportionation reactions as well as intermolecular nucleophilic additions. The synthetic sequence optimized for these compounds is detailed in *Scheme 2.3*. The structure of the target compounds was confirmed by X-ray analysis (*Figure 2.1*).



Scheme 2.3. Pyridinium salts: second generation.

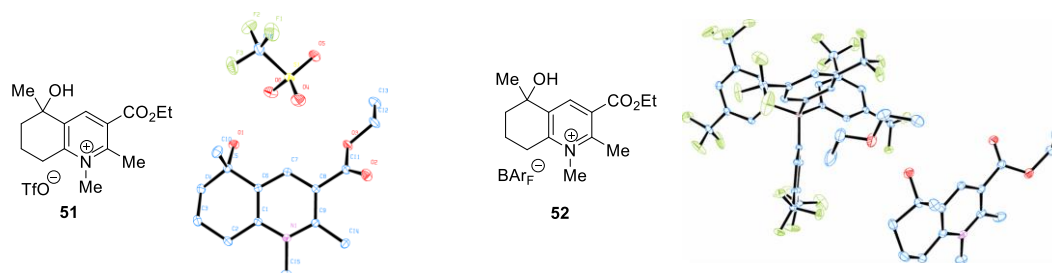
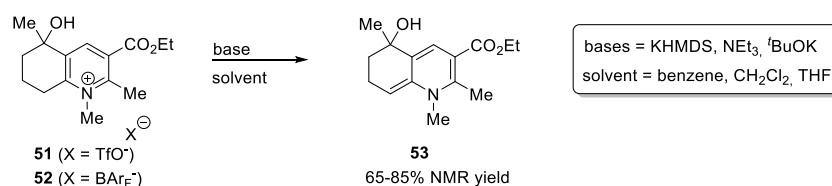


Figure 2.1. X-ray structures of and obtained for the second generation of pyridinium salts.

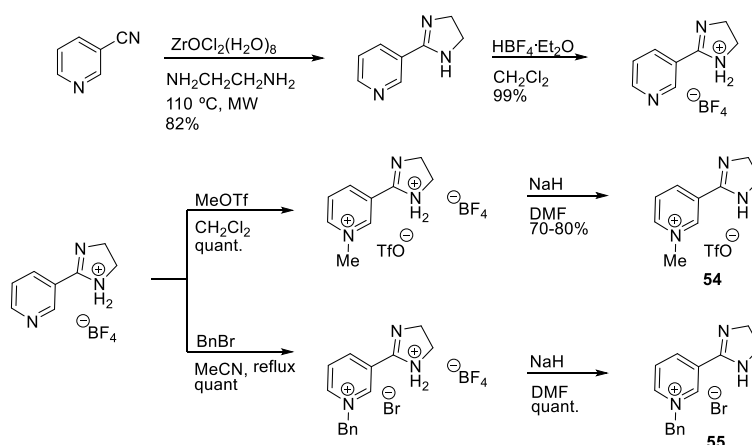
Once a synthetic route to prepare the desired salts was found, they were treated with different bases to test their reactivity in the absence of hydrogen (*Scheme 2.4*). In all cases the formation of varying amounts of by-product **53** was observed, which result from deprotonation of the relatively acidic proton in the alkyl groups next to the pyridinium ring.



Scheme 2.4. Reactivity observed for the second generation of pyridinium salts.

2.2. Pyridinium Amidines

The results obtained thus far suggested that the design of more robust systems, as well as tuning the basicity of the nitrogen, might be necessary. Along these lines, systems containing more basic amines such as amidines were explored, and replacement of the *N*-methyl group by a more robust benzyl group was tested. An easy way to prepare multigram quantities of desired amidines **54** and **55** is detailed in *Scheme 2.5*. DFT studies were conducted to find theoretical support for the working hypothesis. The effect of substitution on both, the aromatic ring and the amidine, was examined to see if it could have an influence on the activation barrier for the H₂ splitting. Very similar results (26.1–31.6 kcal/mol) were found for the different substitution patterns studied (*Figure 2.2*, right).



Scheme 2.5. General strategy for the preparation of pyridinium/amidines systems.

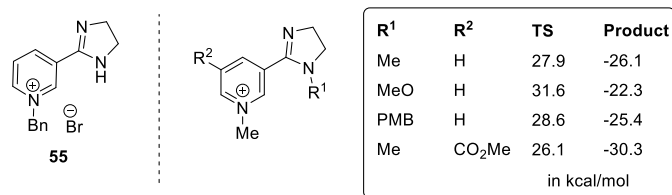
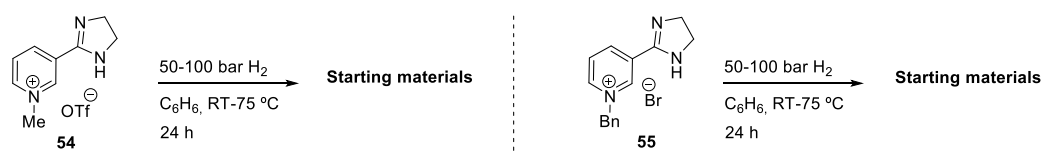


Figure 2.2. DFT studies on pyridinium/amidinium systems.

Following the sequence detailed above, two candidates were synthesized and tested in the reaction with H₂ in benzene at different reaction temperatures and hydrogen pressures. Although these compounds were found to be more robust than their predecessors and were perfectly stable under the reaction conditions, no products derived from H₂ activation was ever detected in the reaction mixtures (*Scheme 2.6*).



Scheme 2.6. Attempted dihydrogen activation with pyridinium/amidinium systems.

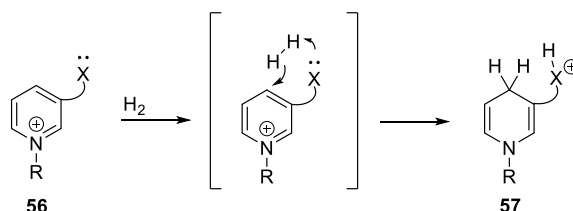
Chapter 3

3. Intramolecular Pyridinium-Based FLP Systems

3.1. Introduction

Although the catalytic efficiency and scope of FLP systems are still limited, the results obtained employing Frustrated Lewis Pairs indicate that it might be possible to develop practical systems for H₂ activation based on simple organic compounds. As explained in the introduction, FLPs rely on steric interactions in order to avoid formation of a stable Lewis acid-Lewis base complex. Thus, only systems based on very strong Lewis acids (such as B(C₆F₅)₃ and related compounds) and P and N bases with bulky substituents have been used so far.

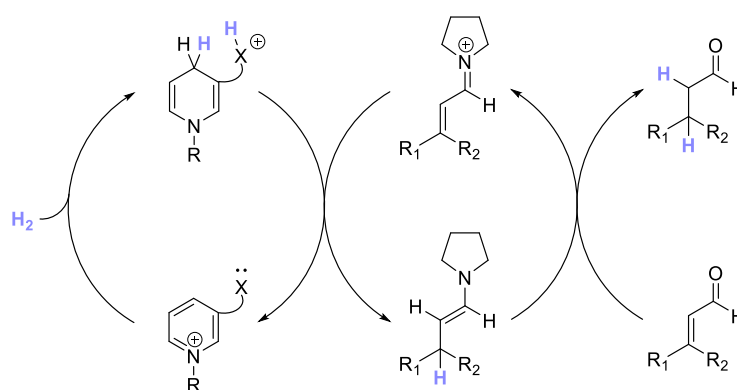
As mentioned above, *WALLING* and *BOLLYKY* demonstrated the ability of ketones to act as hydride acceptors in H₂ activation processes.^[8] Compared to benzophenone, a pyridinium compound is expected to be a much stronger hydride acceptor. The use of a strong base like a basic amine might enable the use of weak hydride acceptors such as pyridinium salts. Additionally, the intramolecular nature of H₂ activation which involves a concerted action of the pyridinium salt and the base should significantly lower the activation energy of the H–H bond cleavage and H₂ splitting should occur under mild reaction conditions. Thus, the first objective of this work was to develop an efficient system for heterolytic H₂ activation containing basic amines as an alternative to bulky phosphines as proton acceptor, and a pyridinium salt as a hydride acceptor. The reactivity and stability of pyridinium derivatives of this type can be tuned by modification of the basic site X and/or by introduction of additional substituents in the aromatic ring (*Scheme 3.1*).



Scheme 3.1. Proposed interaction between H₂ and pyridinium salts.

3.1.1. Objective of This Work

The aim of this project was the development of a synthesis towards pyridinium amides. Once the preparation could be achieved, the idea was to test these pyridinium salts for H₂ activation reactions. If proof of principle for the process could be found, the second goal would be the investigation of the synthetic applications of the system. In this context, the reduced compounds could be used as a hydride donor for the reduction of electrophilic C=C, C=O or C=N bonds. The combination of this H₂ activation process with the organocatalyzed reduction of α,β -unsaturated aldehydes developed by *LIST*^[68] and *MACMILLAN*^[67] would be an appropriate candidate for this purpose as depicted in *Scheme 3.2*.



Scheme 3.2. Proposed interaction between H₂ and pyridinium salts.

3.1.2. DFT Calculations on FLP Systems for H₂ Activation

DFT studies were conducted by *PADEVET* using a B3LYP DFT method and 6-311+G(d) basis set with one diffuse function on heavy atoms, because the molecule bears charges on the nitrogen atoms. All substrate geometries were optimized to their energetic minima and final energies were used without vibrational ZPE (zero point energy) corrections. The transition state was confirmed by frequency calculations and had only one negative “eigenvalue”.

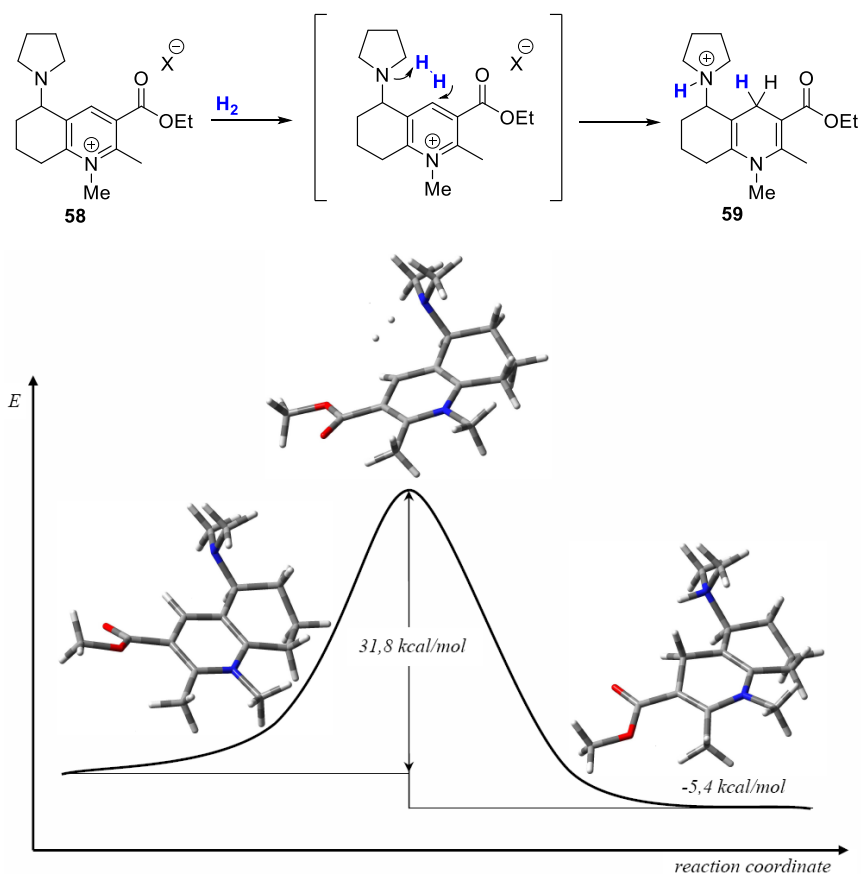


Figure 3.1. Calculated energy profile for the H-H cleavage step obtained by DFT calculations.

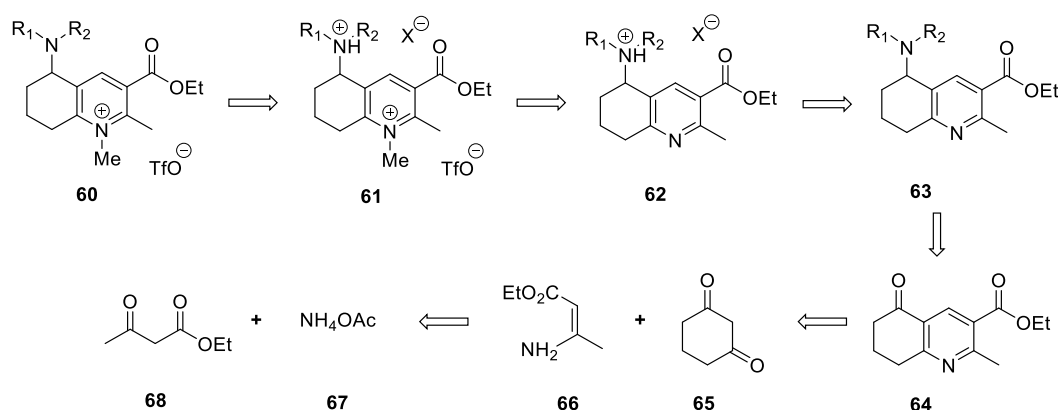
According to these studies, the process is indeed feasible and has a calculated activation energy for the hydrogen splitting by a model substrate slightly over 30 kcal/mol (Figure 3.1). Although high, the activation energy required for the process could be reached by using forcing conditions such as elevated temperature or high pressure. The calculations also show an energetic difference of around 5 kcal/mol between substrate and product, which suggests that the process might be reversible under the reaction conditions.

Future calculations will focus on the impact of factors like temperature and pressure on the activation energy, as well as on introducing PCM (Polarizable Continuum Model) to model potential solvent effects.

3.2. Synthesis

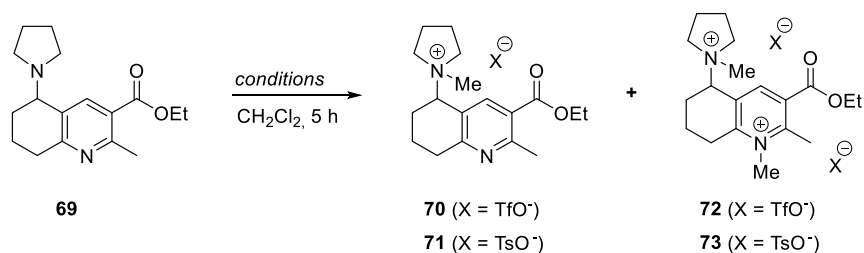
3.2.1. Retrosynthetic Analysis

A possible way to prepare the desired pyridinium salts **60** is shown in *Scheme 3.3*. β -Amino- α,β -unsaturated ester **66** can be prepared in one step by reaction of β -ketoester **68** with ammonium carbamate.^[71] Its condensation with 1,3-cyclohexadione (**65**) should result in the formation of ketone **64**.^[72] This ketone would be an interesting building block for the preparation of amine **63** by reductive amination with a variety of amines and a reducing agent such as sodium borohydride.^[73] Alternatively, the amine **63** could also be prepared *via* reduction of ketone **64** and subsequent *MITSUNOBU* reaction.^[74-75]



Scheme 3.3. Retrosynthesis of pyridinium salts **60**.

Preliminary results showed that direct methylation of amine **69** with two different methylating reagents resulted in the formation of two main compounds: **70**, in which the tertiary amine was methylated, and compound **72**, in which both nitrogen atoms were methylated (*Table 3.1*).

Table 3.1. Preliminary results.

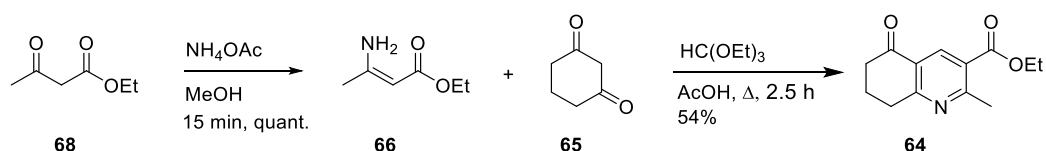
Entry	Reagent	Eq.	Product	Ratio ^[a]
1	MeOTf	1.1	70 + 72	1:1
2		0.9	70 + 72	2:1
3	MeOTs	0.9	71 + 73	1:1

[a] Estimated by ¹H NMR analysis of the crude reaction mixture.

In light of these results, it became evident that the amine functionality needed to be protected for the preparation of the desired pyridinium salts **60**. Capitalizing on the different basicities of both nitrogen atoms, selective protonation of the tertiary amine would provide an effective method for the desired protection. Upon protonation, subsequent treatment with a methylating agent such as methyl trifluoromethanesulfonate should result in the formation of biscation **61**.^[76] This step might be more problematic because hindered and electron poor amine **63** is less nucleophilic than a normal pyridine. Finally, simple deprotonation of pyridinium salts **61** should afford the desired compounds.

3.2.2. Synthesis of Benzylic Amines

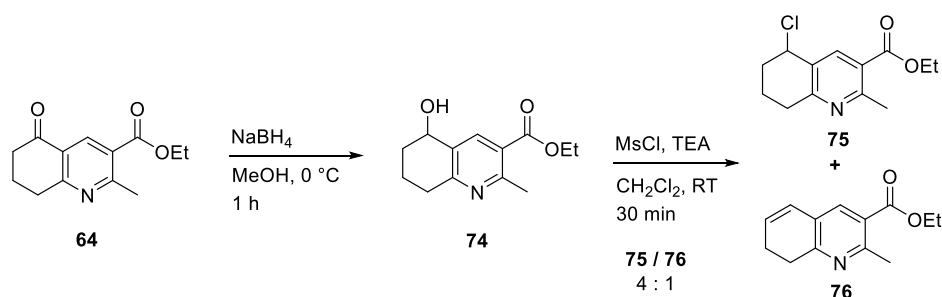
Ketone **64** was easily prepared in two steps from commercially available compounds (Scheme 3.4) following an established procedure:^[71-72] first, treatment of ethyl acetoacetate (**68**) with one equivalent of ammonium carbamate (**67**) in MeOH gave (Z)-ethyl 3-aminobut-2-enoate (**66**) in quantitative yield.^[71] Then, condensation of enoate **66** with 1,3-cyclohexadione and ethyl orthoformate in refluxing acetic acid led to formation of desired ketone **64** in moderate but acceptable yield (54%).^[72]



Scheme 3.4. Synthesis of ketone **64**.

From this point, a logical route to prepare amine **63** would involve reductive amination of ketone **64** with a secondary amine and an appropriate reducing agent.^{[73],[77]} However, this method gave the desired product in very low yield, along with substantial formation of side products. Attempts to prepare the amine **63** via a *MITSUNOBU* reaction from alcohol **74** were unsuccessful and only decomposition of the starting materials were observed.

At this point, a three step procedure involving reduction of the ketone to the alcohol and formation of the desired amine via mesylation and subsequent displacement with a secondary amine was studied. The substitution of methanesulfonate with various amines has been successfully implemented for the synthesis of the corresponding substituted amines.^[78] Reduction of ketone **64** with NaBH_4 in MeOH gave the alcohol **74** in quantitative yields (*Scheme 3.5*). Subsequent treatment with MsCl in the presence of triethylamine should have led to the corresponding methanesulfonate. However, the mesylated compound was not observed; instead, the reaction generated a 4:1 mixture of chloride **75** and alkene **76** (*Scheme 3.5*). Although the reasons for the formation of chloride **75** remain unclear, formation of compound **76** can be easily explained by a known competing dehydration reaction, which occurs before complete mesylation has been achieved.^[79] These compounds were easily separated by column chromatography.

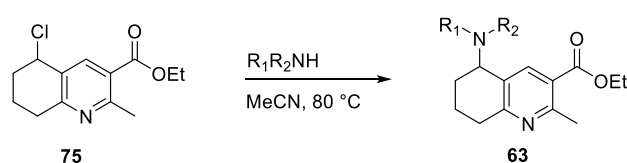


Scheme 3.5. Reduction to the alcohol **74**, followed by treatment with MsCl.

Nevertheless, chloride **75** reacted with a variety of secondary amines in refluxing acetonitrile and as a result the desired amines were generally obtained in good to excellent yields (*Table 3.2*). It was found that cyclic secondary amines (entries 2-5) reacted in good to

excellent yields. The reaction with D-prolinol (entry 5) generated two diastereomers which were easily separated by column chromatography. In contrast to the cyclic amines, diethylamine (entry 1) reacted poorly, probably due to the somewhat lower nucleophilicity of diethylamine, and even at longer reaction times the conversion could not be increased. Following this synthetic procedure, up to four grams of the desired amines were prepared from commercially available and inexpensive starting materials. Additionally, purification of the crude mixture resulted in formation of very stable and easy-to-handle solids.

Table 3.2. Reaction of chloride **75** with secondary amines.



Entry	Amine	Product	t [h]	Yield [%] ^[a]
1		77	48	5 ^[b]
2		69	24	98
3		78	20	80
4		79	20	78
5		80	18	67 ^[c]

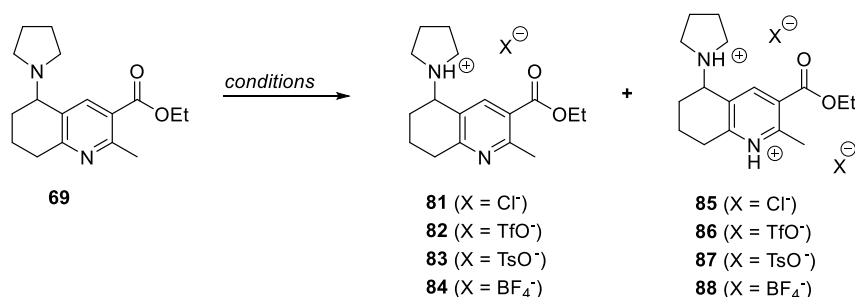
[a] Pure isolated product after chromatography, [b] Estimated by ¹H NMR analysis of the crude reaction mixture, [c] Combined yield of both diastereoisomers.

3.2.3. Protonation

As mentioned above, hampering the nucleophilicity of the tertiary amine is necessary for the selective methylation of the nitrogen in the pyridine ring. To achieve this goal, simple protonation of the nitrogen at the amine was investigated. If successful, this method should provide a very practical and easily removed “protecting group”.

Typically, strong acids are used to protonate tertiary amines.^[80] Considering the higher basicity of amines compared to pyridines, the reaction should be selective at the amine adding only one equivalent of acid. Protonation at the pyridine unit should also be observed with more equivalents of acid. The results of the studies with model amine **69** and several Brønsted acids are summarized in *Table 3.3*.

Table 3.3. Protonation of amine **69**.



Entry	Acid	Eq.	Solvent	t [min]	Product	Conv. [%] ^[a]
1	HCl	1.0	Et ₂ O	10	81	--
2	TfOH	0.9	CH ₂ Cl ₂	20	82	77
3		2.0	CH ₂ Cl ₂	20	86	82
4	TosOH	0.9	CH ₂ Cl ₂	20	83	84
5		2.0	CH ₂ Cl ₂	20	87	90
6	HBF ₄	0.9	Et ₂ O	10	84	95
7		2.0	Et ₂ O	10	88	95

[a] Estimated by ¹H NMR analysis of the crude reaction mixture.

A first approach using HCl (2 m in diethylether) failed (entry 1). Instead of the desired protonation, the starting amine **69** underwent rapid decomposition. Protonation with trifluoromethanesulfonic acid (pK_a -14, entries 2 and 3) yielded the desired compound **82**, but this strong acid also led to the formation of unidentified side products. As a consequence, *p*-toluenesulfonic acid was tested because of its lower acidity (pK_a -2.8). Entries 4 and 5 indicate that compounds **83** and **87** can be prepared with *p*-toluenesulfonic acid with good

yields. The structure of compound **83** was unequivocally determined by single crystal X-ray crystallography (Figure 3.2).

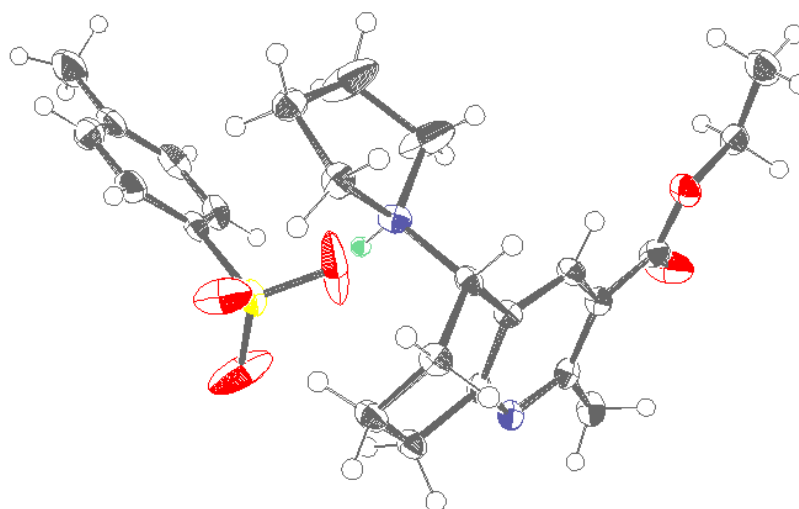
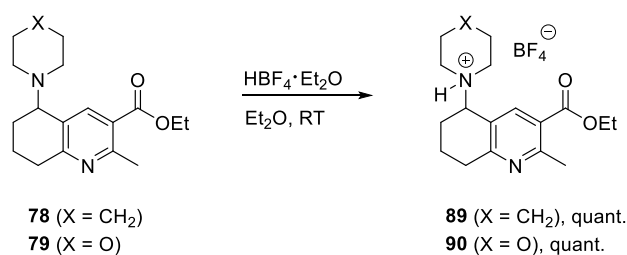


Figure 3.2. Ortep^[81] structure of **83**. Displacement ellipsoids for the non-hydrogen atoms are shown at 50% probability level.

Unfortunately, the resulting trifluoromethanesulfonate and *p*-toluenesulfonate salts proved to be highly sensitive to air and difficult to handle. Therefore, the behavior of an alternative proton source of comparable acidity was studied, specifically tetrafluoroboric acid diethyl etherate (pKa -0.4). Protonation took place very rapidly, the salt precipitated and could be easily filtered off, affording compound **84** in almost quantitative yield (entry 6). Additionally, the resulting salts were stable towards air and moisture, and the corresponding bisprotonated species **88** was not detected even when two equivalents of acid were added (entry 7).

Following the same strategy, the protonation of amines **78** and **79** with tetrafluoroboric acid diethyl etherate gave the protonated compounds **89** and **90** smoothly and quantitatively (Scheme 3.6).

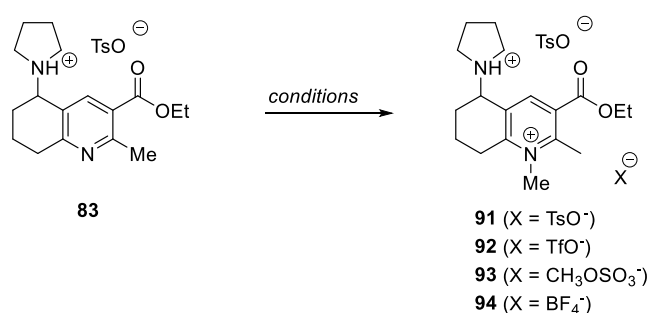


Scheme 3.6. Protonation of compounds **78** and **79** with HBF₄·Et₂O.

3.2.4. Methylation

After protonation of the tertiary amine, subsequent methylation should take place selectively at the pyridine nitrogen. Methylation of nucleophilic compounds is commonly performed using electrophilic methyl sources. For example, a powerful methylating reagent is methyl trifluoromethane sulfonate; other potentially interesting methylating agents are Meerwein's salt $[(\text{CH}_3)_3\text{O}(\text{BF}_4)]$, dimethyl sulfate or methyl tosylate. Therefore, the reaction of these selected methylating agents with model amine **83** was tested (Table 3.4).

Table 3.4. Methylation studies on model amine **83**.



Entry	Reagent	Eq.	Solvent	t [h]	T [°C]	Conv. [%] ^[a]
1		0.9	CH ₂ Cl ₂	0.5	RT	15
2	MeOTs	0.9	CH ₂ Cl ₂	3	RT	55
3		0.9	CH ₂ Cl ₂ ^[b]	3	RT	65
4	MeOTf	0.9	CH ₂ Cl ₂	0.5	RT	--
5		1.0	CH ₂ Cl ₂	24	RT	17
6	SO ₄ Me ₂	1.0	DCE ^[b]	24	80	--
7		1.0	CH ₂ Cl ₂	24	RT	5
8	Me ₃ OBF ₄	1.0	DCE ^[b]	24	80	18

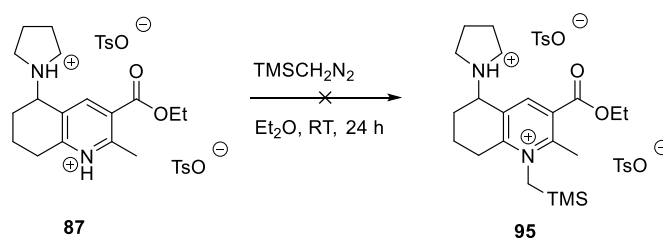
[a] Estimated by ¹H NMR analysis of the crude reaction mixture, [b] 4 Å mol. sieves was added to the reaction mixture.

The first reaction was set up with **83** and methyl tosylate in CH₂Cl₂ at room temperature (Table 3.4, entry 1). After 30 min, the solvent was evaporated and an off-white solid was obtained, which was analyzed by ¹H NMR indicating 15% conversion. Two clear diagnostic

peaks were used for the identification of the desired product in the crude reaction mixtures: first, the signal from the aromatic proton in the pyridine ring (which shifted downfield from 8.42 ppm to 8.86 ppm). Then, a singlet at 4.06 ppm was assigned as the newly incorporated methyl group. Slightly modified reaction conditions were applied (entries 2 and 3) which resulted in increased conversion (65%, entry 3), but unfortunately in this case the reaction did not take place cleanly. Surprisingly, the use of methyl triflate under these conditions did not result in the formation of the desired compound (entry 4). Instead of methylation of the pyridine, analysis of the ^1H NMR crude mixture showed formation of methyl tosylate, which suggests a methyl transfer from methyl triflate to tosylate.

To avoid side reactions like this, an alternative methylating agent was tested. The addition of one equivalent of dimethyl sulfate led to the desired bication in low yield (entry 5). Changing the solvent to DCE and longer reaction time resulted in no apparent improvement. Attempts with trimethyloxonium tetrafluoroborate showed also very low conversions (entries 7 and 8). Additionally, the use of activated molecular sieves as drying additives was shown to have little or no impact on the outcome of the reaction (*Table 3.4*, entries 3, 6 and 8).

The bisprotonated compound **87** could also be used to prepare the target compound **94** using diazomethane as methylating reagent. However, TMS protected diazomethane is much more convenient than diazomethane since it is more stable and can be purchased in organic solvents such as ether. Therefore, **87** was treated with one equivalent of TMS-diazomethane and was stirred at room temperature for one day (*Scheme 3.7*). The proton NMR of the crude material showed only decomposed products. Attempts to replace the counterion of **87** by treatment with salts like AgPF_6 , AgBF_4 and NaBF_4 were unsuccessful.

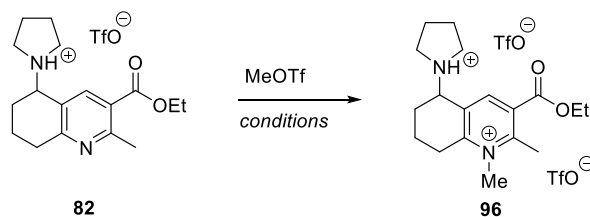


Scheme 3.7. Methylation of **87** with TMS-diazomethane.

As methyl trifluoromethane sulfonate showed interaction with tosylate, a potential solution would involve the use of triflate as counterion of both (*Table 3.5*). For that reason, compound **82** was treated with 0.9 equivalents of methyl trifluoromethane sulfonate in

dichloromethane. After 30 min of stirring, a mixture of products was observed by ^1H NMR. Purification *via* column chromatography (*basic*-alumina, $\text{CH}_2\text{Cl}_2/\text{MeOH}$ 10:1) led to the free amine **69**. Higher temperatures and longer reaction times did not alter the outcome of the reaction and only decomposition products were generated.

Table 3.5. Methylation experiments on compound **82**.

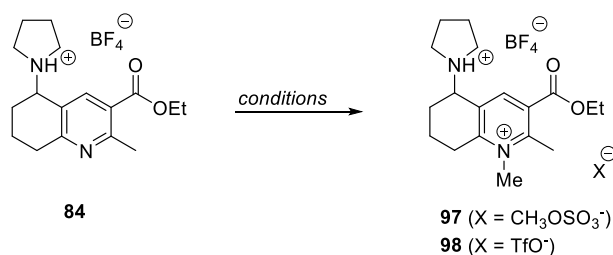


Entry	MeOTf [eq.]	Solvent	t [h]	T [°C]	Conv. [%] ^[a]
1	0.9	CH_2Cl_2	0.5	RT	--
2	0.9	DCE	4	80	--

[a] Estimated by ^1H NMR analysis of the crude reaction mixture.

Since the methylation studies performed on protonated amines **82** and **83** did not provide satisfactory results, the attention was turned to the stable BF_4 salt **84**. Two main test series were carried out using MeOTf and Me_3OBF_4 as methylating agents. However, the number of options for solvents was limited because of the low solubility of salt **84**.

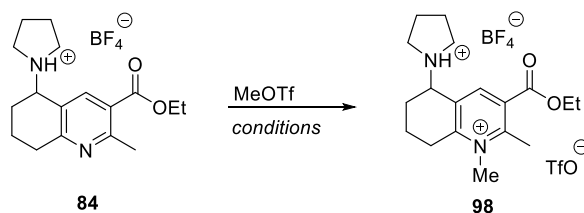
First, the use of highly polar solvents was investigated. A previous study using dimethylsulfate and MeOTf in DMSO showed no conversion at all (*Table 3.6*, entries 1 and 2). The best result was achieved after 1.5 h (29% conversion, entry 3), but the bication seemed not to be stable for a long time (10% conversion, entry 4). Addition of two equivalents of methyl trifluoromethane sulfonate, as well as increasing the reaction temperature did not improve the conversion, affording mixtures of unidentified products.

Table 3.6. Formation of biscations **96** and **97** in highly polar solvents.

Entry	Reagent	Eq.	Solvent	t [h]	T [°C]	Conv. [%] ^[a]
1	SO ₄ Me ₂	1	DMSO	18	RT	--
2		1	DMSO	1	RT	--
3		1	DMF	1.5	RT	29
4	MeOTf	1	DMF	48	RT	10
5		1	DMF	24	70	--
6		2	DMF	24	RT	--
7		2	DMF ^[b]	24	70	--

[a] Estimated by ¹H NMR analysis of the crude reaction mixture, [b] 4 Å mol. sieves was added to the reaction mixture.

In light of these negative results, the need to switch to less polar solvents such as Et₂O, THF or dioxane became evident. Of these three, dioxane seemed to be the most appropriate due to the higher solubility of protonated compound **84** in it. Although **84** was not fully soluble in dioxane, it gradually dissolved after addition of methyl trifluoromethane sulfonate since the biscation is soluble in dioxane. The results are detailed in *Table 3.7*.

Table 3.7. Alkylation of compound **84** with methyl trifluoromethane sulfonate in dioxane.

Entry	MeOTf [Eq.]	Solvent	Conc. [mol/L]	t [h]	T [°C]	Conv. [%] ^[a]
1	1	dioxane	0.2	18	RT	22
2	1	dioxane	0.2	18	50	12
3	1	dioxane/DMF 10:1	0.2	18	RT	19
4	1	dioxane	0.1	18	RT	33
5	1	dioxane	0.1	1.5	RT	38
6	1	dioxane	0.1	4	RT	47
7	1	dioxane	0.05	4	RT	56
8	1	dioxane	0.02	4	RT	70
9	1	dioxane	0.02	4	50	29
10	1	dioxane	0.05	4	0–15	100
11	2	dioxane	0.05	4	RT	25
12	4	dioxane	0.2	4	RT	29

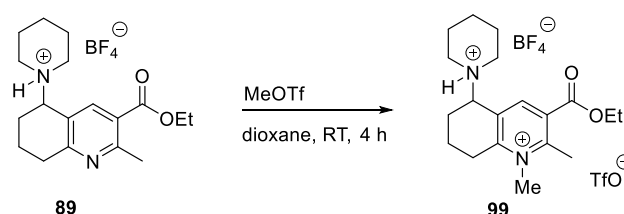
[a] Estimated by ¹H NMR analysis of the crude reaction mixture.

First, increasing of the temperature from RT to 50 °C had a negative impact on the reactivity (entries 1 and 2). Because of the low solubility of compound **84** in dioxane, the addition of 10% of DMF was tested to help solubility, but the reaction was slower in this case (entry 3). Interestingly, an attempt performed at shorter reaction time showed slightly better conversion (entry 5), which is consistent with the observation that biscations are unstable and probably decompose after extended reaction times. A ¹H NMR study was performed to more accurately determine the effect of time on the reactivity. To achieve this, a NMR scale reaction

was set up with a 0.1 M solution of compound **84** in dioxane-*d*₈. After addition of one equivalent of MeOTf, a ¹H NMR was recorded every 20 min for 12 hours. The results showed that after 4 hours the reaction did not proceed further. Consequently, the following reactions were conducted for 4 hours to establish appropriate reactivity comparison.

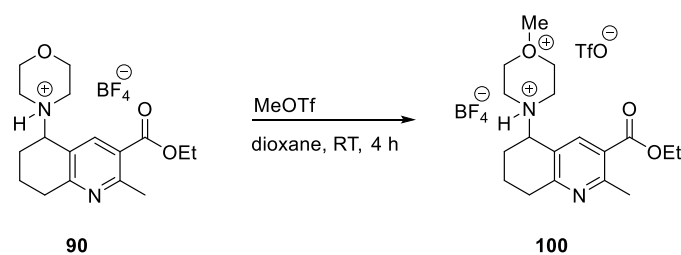
It turned out that not only the reaction time, but also the concentration of the solution had an impact on the outcome of the transformation. Lowering the concentration from 0.2 M to 0.1 M increased the yield from 22% to 47% (entry 6). When the concentration was lowered to 0.02 M and the yield further increased to 70% (entry 8). The influence of the temperature at low concentrations was also investigated. The results showed again that the reaction performed better at room temperature than at higher temperatures (entries 8 and 9). At 0 °C, the ¹H NMR spectra showed no starting materials, but the formation of an uncharacterized side product was observed (entry 10). The addition of more equivalents of MeOTf had no positive effect on the outcome of the reaction (entries 11 and 12).

In summary, the best combination was a 0.02 M solution of compound **84** in dioxane, stirred at room temperature for 4 h (entry 8). Under these conditions, conversions in the range of 70% could be consistently obtained and ¹H NMR showed the formation of the bication as the major product. Similarly, protonated piperidine **89** was methylated in 60% yield (*Scheme 3.8*).



Scheme 3.8. Formation of the bication from protonated piperidine **89**.

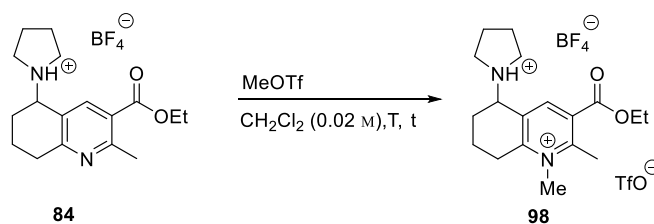
All crude ¹H NMR spectra showed one peak at 4.00 ppm, which was initially assigned as unreacted MeOTf. However, removal of this impurity by washing with pentane and solvent mixtures of pentane and ether was ineffective after five cycles of washing and drying under high vacuum overnight. This impurity could be attributed to interactions of MeOTf with the solvent, since it is known that esters of trifluoromethane sulfonic acid are initiators for the polymerization of tetrahydrofuran.^[82] In accordance with this hypothesis, NMR analysis of the methylation of protonated morpholine **90** (*Scheme 3.9*) showed that the reaction took place at the oxygen instead of the pyridine-nitrogen affording the undesired product **100**.



Scheme 3.9. Methylation of protonated morpholine **90**.

To avoid interactions with dioxane, the methylation was tested in dichloromethane at low concentration (*Table 3.8*). No reactivity was observed at low temperatures (entries 1 and 2). Although at room temperature satisfactory conversions were achieved, the formation of side products was observed in every case (entries 3-5). Since the removal of these side products was not possible the attention was turned back to dioxane.

Table 3.8. Reaction of compound **84** with methyl trifluoromethane sulfonate in dichloromethane.



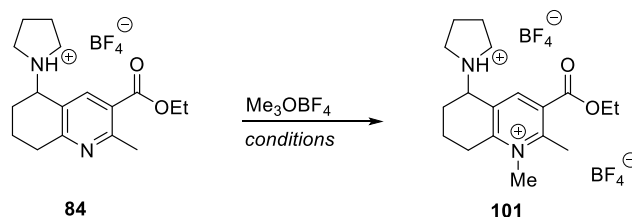
Entry	MeOTf [Eq.]	t [h]	T [°C]	Conv. [%] ^[a]
1	1	0.5	0	-
2	1	0.5	-20	-
3	1	8	RT	20
4	1	24	RT	59
5	2	24	RT	76

[a] Estimated by ¹H NMR analysis of the crude reaction mixture.

The suitability of Me₃OBF₄ as methylating reagent was also studied (*Table 3.9*). In DCE, no conversion was observed (entry 1). In DMF, the conversions were rather poor (entries 2 and 3). In dioxane, generally higher conversions could be obtained (entries 4 and 5). A subtle influence of the substrate concentration was noted in every case, the conversions being higher at lower

concentration (23% to 36%, entries 5 and 6). Adding 5 or 10 equivalents of the reagent showed generally higher conversion (entries 6 and 8), whereas higher temperatures had the opposite effect (entries 9 and 10). The best result was obtained at a concentration of 0.05 M and using 10 equivalents of Me_3OBF_4 (44%, entry 8), but also the formation of unidentified side products was observed under these conditions.

Table 3.9. Methylation experiments using trimethyloxonium tetrafluoroborate.



Entry	Me_3OBF_4 [Eq.]	Solvent	Conc. [mol/L]	t [h]	T [°C]	Conv. [%] ^[a]
1	1	DCE ^[b]	0.2	0.5	80	--
2	1	DMF	0.2	24	RT	10
3	1	DMF	0.2	24	70	--
4	1	dioxane	0.2	4	RT	18
5	5	dioxane	0.1	4	RT	23
6	5	dioxane	0.05	4	RT	36
7	10	dioxane	0.1	4	RT	38
8	10	dioxane	0.05	4	RT	44
9	10	dioxane	0.1	4	50	17
10	10	dioxane	0.05	4	50	21

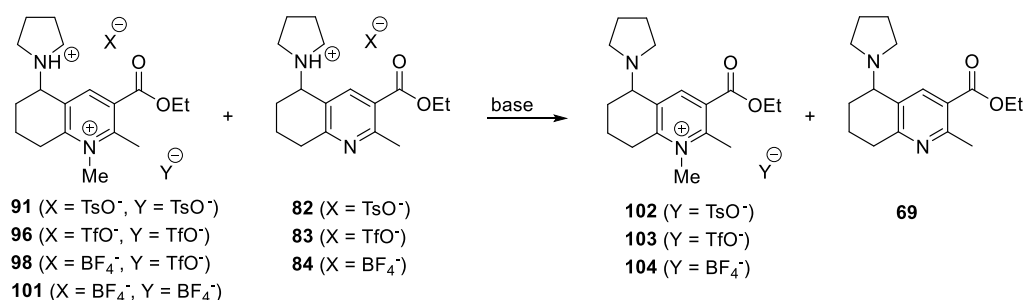
[a] Estimated by ^1H NMR analysis of the crude reaction mixture, [b] 4 Å mol. sieves was added to the reaction mixture.

In summary, the best results for the methylation of compound **84** were achieved at low concentration (0.05 M) and using 10 equivalent of Me_3OBF_4 . In general, methyl trifluoromethane sulfonate proved to be a superior reagent for the methylation of the free pyridines. It is important to mention that in all cases the biscationic compounds could not be

isolated because of their high hygroscopy and low stability. Formation and conversions were studied by ^1H NMR analysis of the crude reaction mixtures.

3.2.5. Deprotonation

In looking at deprotonation conditions, different non-nucleophilic bases with sufficient basicity such as triethylamine, Hünig's base or DBU were studied first. As mentioned above, the biscations could not be isolated: instead, the crude reaction mixtures were directly treated with base, thus generating the desired compounds along with minor amounts of the corresponding initial amines. Separation and purification were done after this step, because of the ease in handling both the product and the corresponding regenerated amine (*Scheme 3.10*).

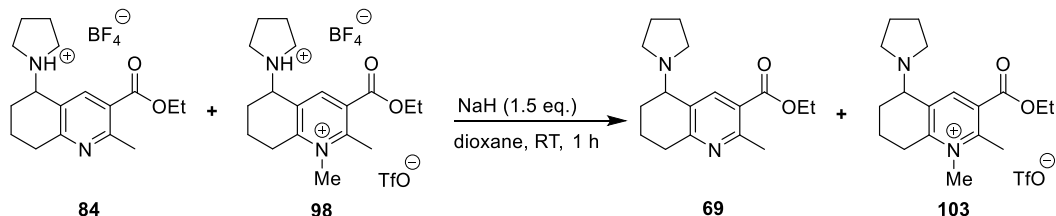


Scheme 3.10. Deprotonation strategy.

Treatment of the biscation with triethylamine or Hünig's base resulted in clean deprotonation. ^1H NMR showed two diagnostic peaks for **103**: the aromatic proton was shifted from 8.14 ppm to 8.65 ppm and the additional methyl group was detected at 4.06 ppm. The formation of the free amine could also be followed by TLC (SiO₂, cyclohexane/EtOAc 3:1). However, the separation of the protonated base from the product proved to be a non-trivial problem: column chromatography on basic alumina led only to the free amine **69**, suggesting that the desired product underwent demethylation on the column.

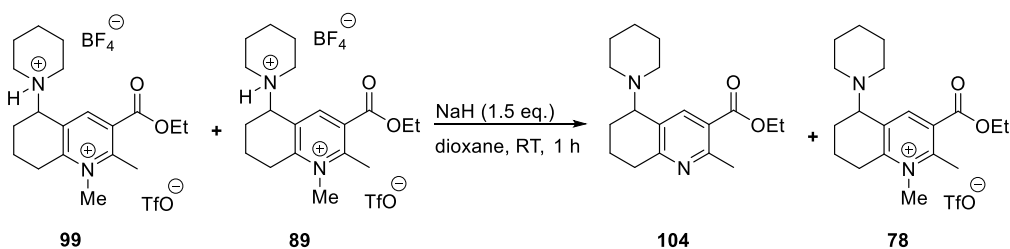
To avoid problems removing the protonated base, sodium hydride was chosen as a logical alternative because the protonated base in this case would be hydrogen gas. Addition of 1.5 equivalents of sodium hydride to the crude mixture in dioxane yielded the pyridinium salt **103** (*Scheme 3.11*). Due to the better solubility of the free amine **69**, it was now possible

to separate the two compounds simply by washing with pentane. The generated NaBF_4 could then be removed by dissolving pyridinium salt **103** in dichloromethane followed by filtration over an HPLC filter.



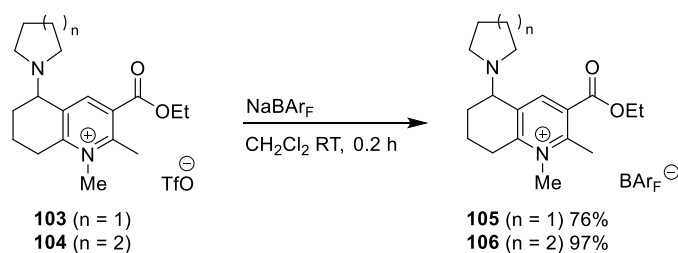
Scheme 3.11. Deprotonation of compounds **84** and **98**.

The described method was also applied to form the pyridinium salt of biscation **99** (*Scheme 3.12*).



Scheme 3.12. Deprotonation of compounds **99** and **89**.

It is known that trifluoromethane sulfonate is a moderately strong coordinating anion.^[83] To test the potential influence of the coordinating ability of the anion in the developed system, pyridinium salts with less coordinating counterion such as BAR_F were prepared.^[84] For their synthesis, the previously prepared salts were simply treated with NaBAR_F to obtain the BAR_F salt, and then filtered to remove NaOTf (*Scheme 3.13*).



Scheme 3.13. BAR_F salts **105** and **106**.

Several stationary phases (including deactivated silica and *basic*-alumina) were tried for the purification of triflate salt **103** and BAr_F salt **106** by column chromatography. Unfortunately, triflate salt **103** decomposed in all cases, whereas the BAr_F salt **106** seemed to be slightly more stable, although small impurities and by-products were always detected. Better results could be obtained when washing the salt carefully with pentane, but unfortunately completely pure compounds were never obtained. While none of the different salts could be analyzed by X-ray diffraction, pyridinium salt **106** was fully characterized by NMR spectroscopy. The ¹H NMR spectra showed two singlets from the methyl groups on the pyridine ring at 4.12 ppm and 3.01 ppm. Using HSQC, the corresponding carbon resonances were found at 40.6 ppm and 18.6 ppm. All quaternary carbons on the pyridine ring were determined by ¹³C APT. HMBC spectra showed that one methyl group (4.12 ppm) is correlated over three bonds to two quaternary carbons (158.3 ppm and 154.8 ppm) of the pyridine ring (*Figure 3.3*). The aromatic proton (8.99 ppm) was also in correlation to the same two quaternary carbons, whereas the second methyl group (3.01 ppm) showed different correlations. Consequently, it was confirmed by NMR that the methyl group with the signal at 4.01 ppm is attached to the nitrogen at the pyridinium ring. Additionally, the fragmentations observed by MS spectroscopy consistently showed loss of the amine moiety, and in all cases the mass of 232 *m/z* was detected.

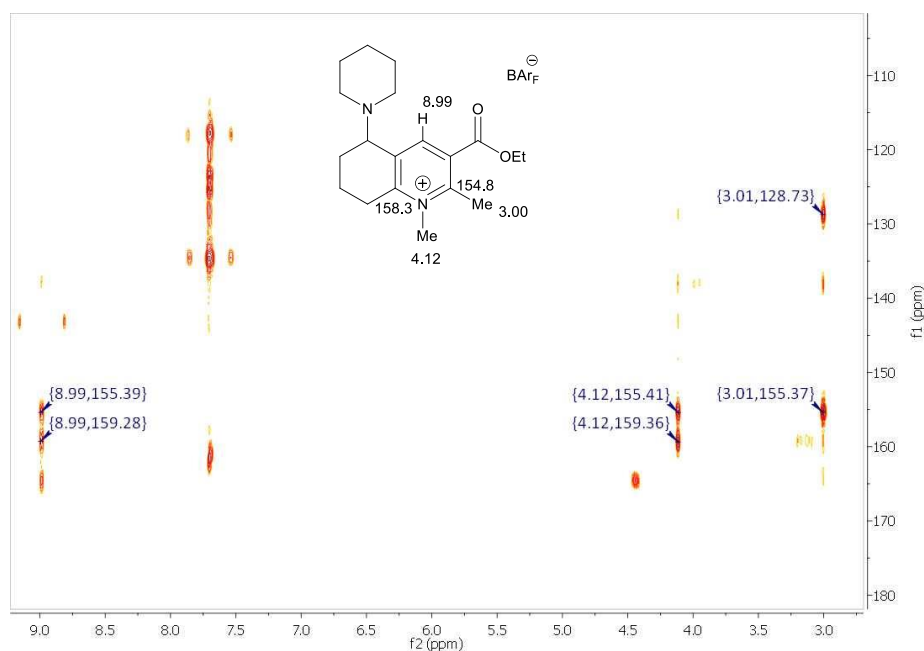
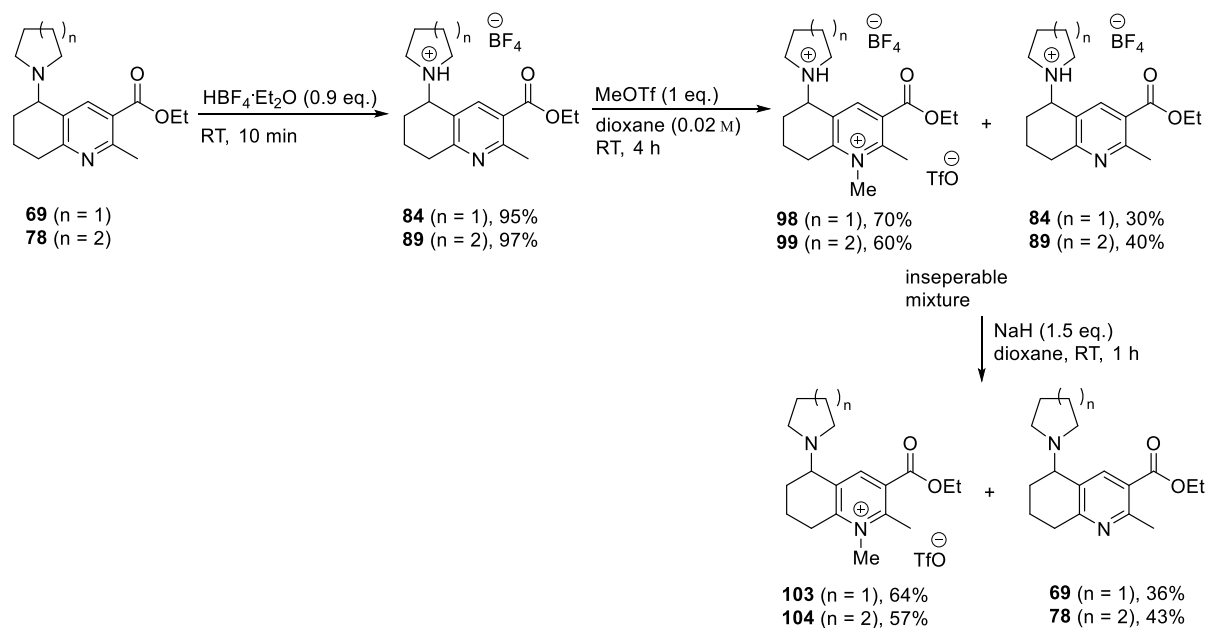


Figure 3.3. HMBC measurements of compound **106**.

In summary, the desired amino-pyridinium salt **103** and **104** could be synthesized with an overall yield of 43% (**103**) and 33% (**104**) starting from the benzylic amines **69** and **78**, which can be rediscovered after the sequence. The best reaction conditions for the key steps are shown in *Scheme 3.14*.



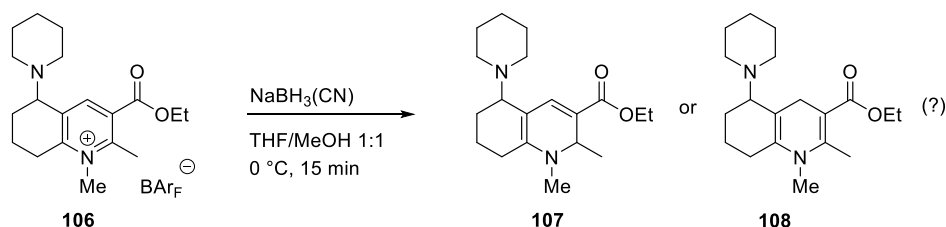
Scheme 3.14. Overview of synthetic pathway towards amino-pyridinium salts **103** and **104**.

3.3. Hydrogenation of Amino-Pyridinium Salts

As explained in the Introduction, the target molecules were developed based on the assumption that a pyridinium salt could act as a hydride acceptor and a basic amine as proton acceptor. Then, H₂ splitting should occur without the need of other additives. Having prepared four different pyridinium salts, different conditions were tested to evaluate their potential as H₂ activators.

Initially, the pyridinium salt **106** was reduced with NaBH₃(CN) as hydride source. The purpose of this experiment was two-fold: first, to prove the capability of the prepared pyridinium salts to act as hydride acceptor. Second, to obtain authentic samples of the desired dihydropyridines that constitute the products of dihydrogen activation. The reaction was carried out in a 1:1 mixture of THF/MeOH at 0 °C. The ¹H NMR spectra showed that all starting

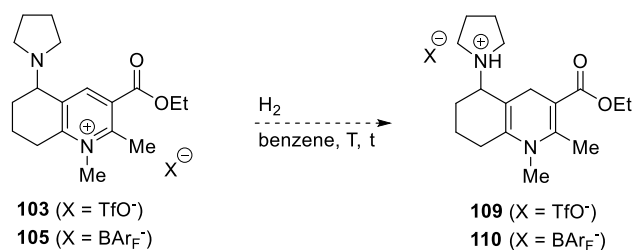
materials were consumed, since the resonance of the aromatic proton at 8.91 ppm disappeared and that a mixture of products was generated. Purification by column chromatography led to a mixture of three unidentified compounds. Mass spectrometry showed the expected fragmentation for the dihydropyridine **107** or **108** (Scheme 3.15).



Scheme 3.15. Reduction of **106**.

Pyridinium salt **103** was chosen as model substrate for the initial hydrogenations (Table 3.10). The first experiments were carried out at room temperature under different hydrogen pressures (entries 1-3). Under these conditions, no reaction was observed and ^1H NMR analysis showed only unreacted starting materials. Similar results were obtained under more forcing conditions (entries 4 and 5). The hydrogenation experiments were also performed on BAr_F salt **105**. Again, ^1H NMR analysis of the crude reaction mixtures indicated no reaction (entries 6 and 7).

Table 3.10. Hydrogenation of pyridinium salts **103** and **105**.



Entry	Substrate	H_2 [bar]	Conc. [mol/L]	T [°C]	t [h]	Conv. [%] ^[a]
1		1	0.2	RT	3	--
2		10	0.2	RT	3	--
3	103	100	0.2	RT	3	--
4		100	0.2	50	18	--
5		100	0.2	75	18	--

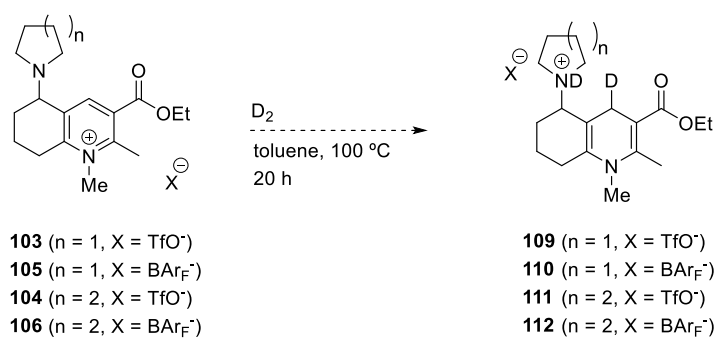
6	105	50	0.1	RT	13	--
7		100	0.1	RT	15	--

[a] Estimated by ^1H NMR analysis of the crude reaction mixture.

At this point, further experiments were carried out using deuterium gas instead of hydrogen. This change was based on the reasoning that ^2H NMR would represent a very selective tool to detect even traces of species resulting from deuterium activation. Indeed, ^2H NMR analysis would reveal only deuterium-containing species, eliminating the signals of all the hydrogen atoms that complicate the spectrum interpretation and the detection of desired products in the case of standard hydrogenation and ^1H NMR analysis. Moreover, observation of deuterated species could only be attributed to an interaction between pyridinium ions and D_2 , and would thus constitute a proof of principle for the proposed hypothesis.

The deuteration experiments were performed on all the pyridinium salts obtained thus far. For these experiments, the solvent was changed to toluene because of its higher boiling point. The results are summarized in *Table 3.11*.

Table 3.11. Deuteration experiments on pyridinium salts.



Entry	Substrate	D_2 [bar]	Conv. [%] ^[a]
1	103	100	--
2		50	--
3	105	100	--
4		50	--

5	104	100	--
6		50	--
7	106	100	--
8		50	--

[a] Estimated by ^1H NMR analysis of the crude reaction mixture.

Unfortunately, the results of these experiments were inconclusive. ^2H NMR showed several signals that could be attributed to deuterium incorporation, but a control experiment performed solely on non-deuterated benzene (no substrate) with D_2 revealed the same spectroscopic pattern. This does not necessarily mean that deuterium splitting did not happen: the signals corresponding to the desired compounds could easily be in the same region as the artifacts, thus making identification of the compounds difficult. Most of the starting materials reacted and a mixture of different compounds was observed. Attempts to purify the mixture by column chromatography provided no clean product.

At this point, two experiments were performed to check the stability of pyridinium ion **106**: first, it was dissolved in toluene and stirred at $100\text{ }^\circ\text{C}$ for 24 h. Under these conditions, the salt proved to be stable, which initially suggested that the mixture of products obtained after treatment with D_2 might result from a subsequent reaction with the amine-pyridinium salts. However, a second experiment performed on a solution of **106** in toluene at $100\text{ }^\circ\text{C}$ and under 100 bar of an inert gas (nitrogen) showed a similar NMR pattern to that observed for the high temperature/high pressure deuteration experiments. Although this result does not disprove the possibility on H_2 activation, it clearly indicates that the developed system needs to be more robust in order to withstand potentially forcing reaction conditions.

Chapter 4

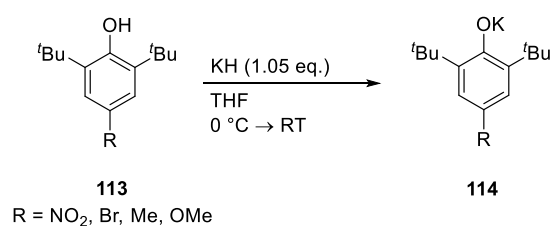
4. Bimolecular Pyridinium-Based FLP Systems

4.1. Introduction

4.1.1. FLP Formation with Sterically Hindered Phenolates

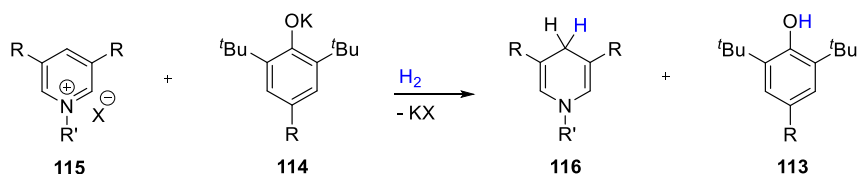
The previous study on intramolecular FLPs suggested that these systems are not suitable for the reaction with dihydrogen. They are not reactive enough and decompose under more forcing reaction conditions, and should therefore be more robust.

After the pioneering work of *STEPHAN*, a number of FLPs were found to activate small molecules such as H₂, CO₂ and N₂O.^[19] In such systems, sterically encumbered Lewis donors and acceptors are combined, leading to an unquenched reactivity. In order to achieve hydrogen splitting, the Lewis acidity and basicity must be correctly matched, but also steric constraints must be sufficient to preclude formation of Lewis adducts. While searching for alternative of Frustrated Lewis Pairs, it was assumed that sterically hindered phenolates could serve as basic partners in these processes. In particular, the employment of analogues of butylated hydroxytoluene (BHT) for the formation of a FLP was envisioned, having a pK_a of 12.2. BHT is used as an antioxidant food additive (E321), antioxidant in cosmetics, pharmaceuticals, polymers, electrical oils and edible oils.^[85] The sterically demanding ^tBu-groups should significantly lower the possibility of nucleophilic additions. Thanks to their widespread occurrence, BHT and many of its derivatives can be found easily even as commercially available compounds. Furthermore non commercial BHT derivatives can be prepared from inexpensive starting materials. For these characteristics and for the possibility to easily screen a large variety of bases whose properties can be finely tuned, BHT derivatives were considered as ideal bases to pair with pyridinium salts as Lewis acids. The synthesis of hindered phenolates was carried out according to *Scheme 4.1*.



Scheme 4.1. Synthesis of phenolates.

The combination of electrophilic pyridinium salts and basic phenolates should lead to the formation of a Frustrated Lewis Pair and should facilitate dihydrogen cleavage (*Scheme 4.2*).



Scheme 4.2. Proposed interaction between pyridinium salts and BHT derivatives.

4.1.2. Objective of This Work

The work described in this chapter was aimed at the development of new FLPs. First, the preparation of stable pyridinium salts needed to be studied. Variation of the ester functionalities at the 3 and 5 position of the heterocycle led to pyridinium salts with different sterical and electronical properties, which can influence the electrophilicity of the pyridinium salt. On the other hand, the incorporation of different substituents at the *para*-position of the phenol ring of the BHT derivative could have an influence on its reactivity. In addition, the reactivity of the system in the presence of hydrogen gas needed to be explored. If proof of principle for the process could be found, the next goal of the project would be the investigation of catalytic transformations based on the successful frustrated Lewis pair.

4.1.3. DFT Calculations on FLP Systems for H₂ Activation

DFT studies performed by *PADEVET* indicated that the reaction between *N*-acylpyridinium salts and hindered phenolates with dihydrogen has a relatively low activation energy (19.30 kcal/mol), which in principle should be accessible at higher temperatures (*Figure 4.1*).

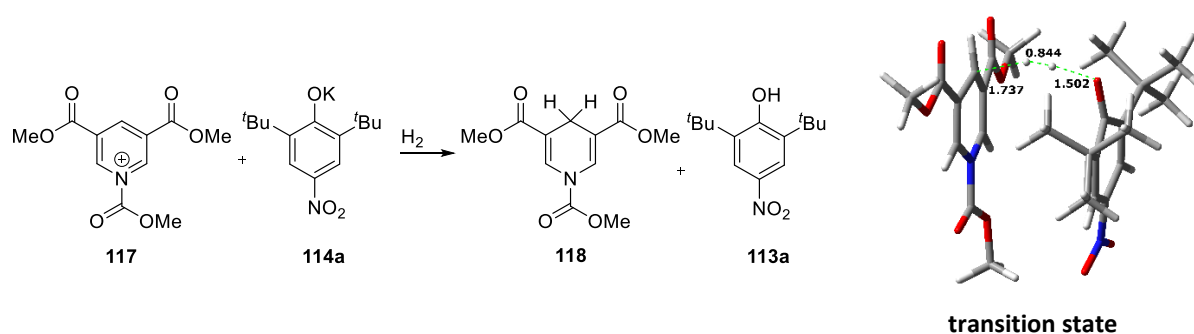


Figure 4.1. DFT studies on the reaction of *N*-acylpyridinium salts and hindered phenolates with H_2 .

These studies also indicated that variation of the substitution pattern of the pyridine ring could lead to a lowering of the activation barrier (18.20 kcal/mol) for H_2 splitting (Figure 4.2).

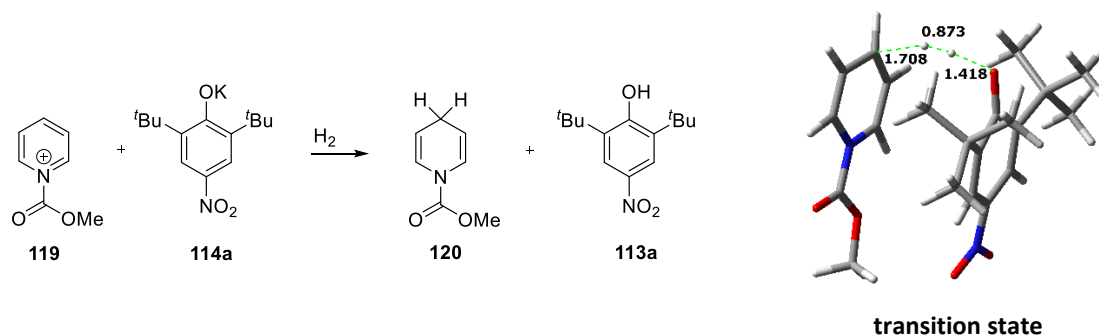
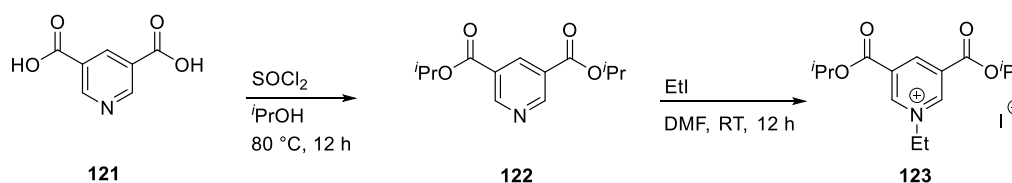


Figure 4.2. DFT studies on the reaction of *N*-acylpyridinium salts and hindered phenolates with H_2 .

4.2. Synthesis

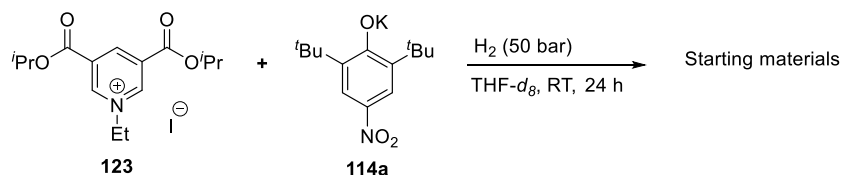
4.2.1. Preparation of *N*-Acyl Ammonium Salts

In a preliminary study, alkylated pyridinium salts were synthesized. A logical route to prepare pyridinium salts such as **123** would involve esterification of the 3,5-pyridinedicarboxylic acid (**121**) followed by reaction with an alkylating reagent such as ethyl iodide (Scheme 4.3).



Scheme 4.3. Synthesis of bisester **122**, followed by reaction with ethyl iodide.

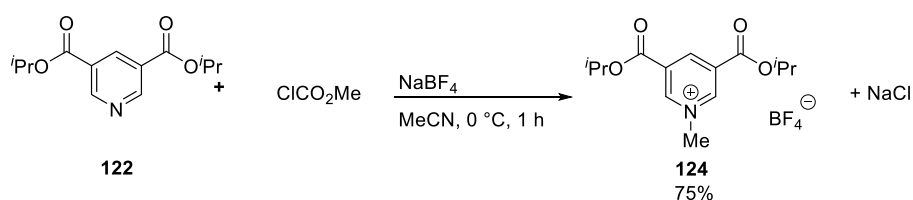
The product **123** proved to be not very stable and needed to be stored in the glove box. However, it was tested in combination with *p*NO₂-BHT **114a** in dihydrogen activation reactions (Scheme 4.4).



Scheme 4.4. Alkylated pyridinium salts in attempted H₂ activation reactions.

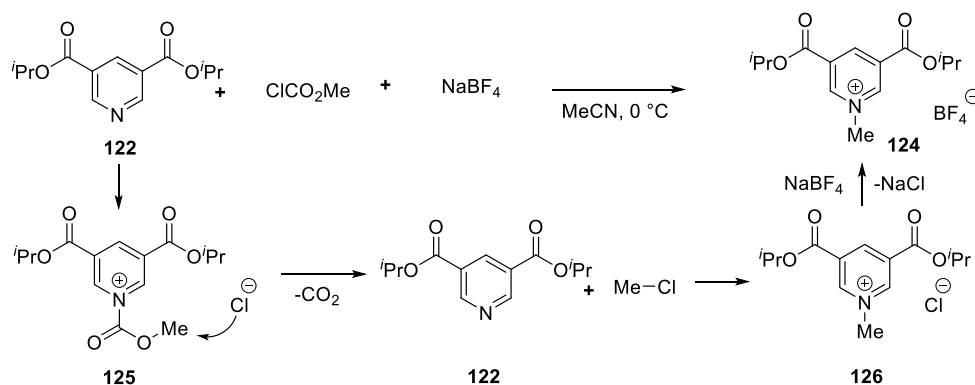
As shown in Scheme 4.4, only unreacted starting materials were recovered. This observation indicated that the system is not reactive enough. The reactivity could be increased by preparing pyridinium salts bearing acyl groups directly attached to the pyridine nitrogen atom.

The desired *N*-acyl pyridinium salts were prepared following a literature known protocol from KING.^[86] Reaction of the corresponding pyridine with methyl chloroformate in the presence of NaBF₄ should lead to the desired *N*-acyl pyridinium salt. Analysis of the product showed that pyridinium salt did not possess an acyl fragment bound to the nitrogen atom. Instead, the pyridinium salt bearing a methyl group was isolated (Scheme 4.5).



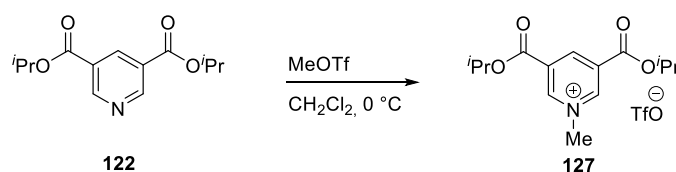
Scheme 4.5. Preparation of pyridinium salt **124**.

It has been reported that *N*-acyl ammonium salts undergo CO₂ extrusion processes in the presence of chloride anions, thus forming the corresponding *N*-methyl pyridinium salts, as described in Scheme 4.6.^[87]



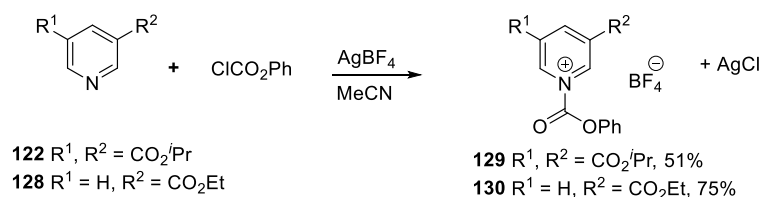
Scheme 4.6. Amine deacylation/alkylation with acyl chlorides.

To confirm this assumption, pyridine **122** was treated with methyl trifluoromethane sulfonate in dichloromethane at $0\text{ }^\circ\text{C}$. After 10 min, the reaction was completed and gave a colorless solid (*Scheme 4.7*). ^1H NMR analysis showed the same NMR pattern observed for the alkylated product.



Scheme 4.7. Methylation of **122** with methyl triflate.

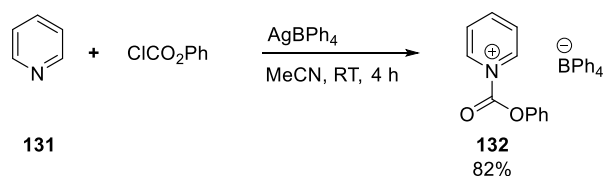
To avoid the undesired alkylation, a reagent without alkyl groups needed to be used. Therefore, different pyridines were tested in the acylation with phenyl chloroformate as acylating agent. The synthesis proved to be challenging because the products were not stable towards air and moisture and required Schlenk conditions during the synthesis and work-up and the formation of side products during the reaction was observed. In an effort to impair the reactivity of the undesired chloride anion, formation of AgCl as an inert side product of the reaction was deemed beneficial. Therefore, AgBF_4 was selected as the salt of choice to replace NaBF_4 . As a result, a significant improvement was observed when AgBF_4 was used instead of NaBF_4 . The ^1H NMR spectrum indicated that the reaction proceeded more cleanly and afforded only the desired product. For pyridinium ion **129**, the reaction performed best for 1 h at $0\text{ }^\circ\text{C}$, whereas for product **130** 4 h at room temperature was needed. With the optimized procedure in hand, two different pyridinium salts could be synthesized in moderate to good yields (*Scheme 4.8*).



Scheme 4.8. Synthesis of *N*-acyl ammonium salts.

Both compounds were sensitive towards air and moisture; monoester **130** was stable in the glove box for one week, whereas bisester **129** started to decompose immediately and was not used for further studies.

The synthesis of the unsubstituted pyridinium salt **132** was achieved by following a literature protocol, in which AgBPh₄ is used instead of AgBF₄, giving the desired bench stable product in good yields (*Scheme 4.9*).^[88]

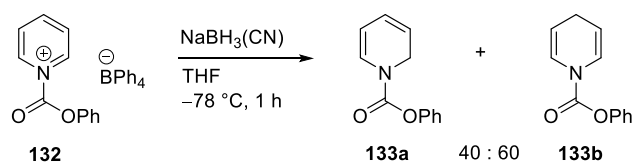


Scheme 4.9. Synthesis of pyridinium salt **132**.

4.2.2. Preparation of Authentic Samples

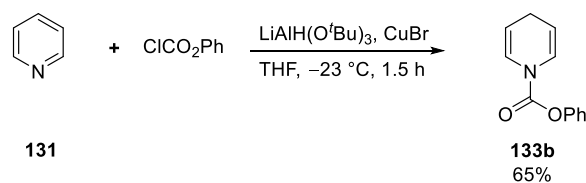
The preparation of authentic samples of the desired dihydropyridines was necessary to compare them with the products of dihydrogen activation experiments and, moreover, to prove the capability of the prepared pyridinium salts to act as hydride acceptor.

Initially, pyridinium salt **132** was reduced using NaBH₃(CN) as hydride source. ¹H NMR analysis of the reaction mixture revealed the presence of a mixture consisting of 1,2- and 1,4-DHP in a 40 to 60 ratio (*Scheme 4.10*). Separation by column chromatography was not successful due to the very similar polarity of both compounds.



Scheme 4.10. Reduction of pyridinium salt **132** with $\text{NaBH}_3(\text{CN})$.

Alternatively, the 1,4-DHP **133b** could be prepared selectively *via* copper hydride reduction developed by COMINS.^[89] By using a mixture of lithium tri-*tert*-butoxyaluminium hydride and cuprous bromide in THF, a hydrido copper reagent was generated *in situ*. Under these conditions, the desired 1,4-DHP **133b** was obtained with perfect regioselectivity although the yield was only moderate.

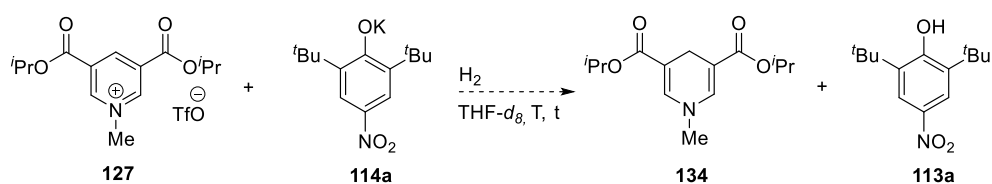


Scheme 4.11. Preparation of 1,4-DHP **133b**.

The established procedure was then tested for the reduction of the monoester **130**. ^1H NMR analysis indicated the formation of a mixture of products, among which one compound could be identified as 1,4-DHP by 2D NMR analysis. Numerous attempts to isolate the corresponding monoester failed due to decomposition of the product.

4.3. Dihydrogen Activation Results

In order to evaluate the potential of the developed FLPs, initial dihydrogen activation reactions with compounds **129** and **144a** were carried out. The reactions were performed in deuterated solvent (0.1 M) which allowed to directly analyze the crude reaction mixtures. The results of these reactions are summarized in *Table 4.1*.

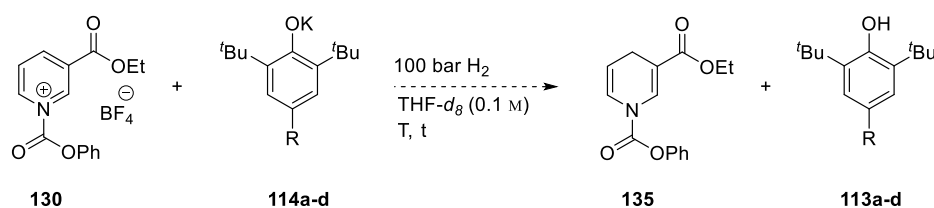
Table 4.1. Hydrogenation experiments.

Entry	H ₂ [bar]	T [°C]	t [h]	Conv. [%] ^[a]
1	50	RT	48	mixture
2	50	RT	96	mixture
3	50	50	48	decomposition
4	100	RT	48	mixture
5	100	RT	96	mixture

[a] Estimated by ¹H NMR analysis of the crude reaction mixture.

Unfortunately, all experiments gave similar product mixtures and decomposition was observed at higher temperature (entry 3). The crude mixtures still contained unreacted pyridinium salt, but interestingly ¹H NMR revealed around 50% protonation of *p*NO₂-BHTK. Increasing the hydrogen pressure and the reaction time did not improve the outcome of the reaction (entries 2 and 6). Purification of the product mixture by column chromatography was not successful. Several solid phases were tested and neutral alumina was found to be the best method of choice. Attempts to isolate the products failed as they seemed to be unstable and decomposed.

As explained above, alkylated pyridinium salts might not be reactive enough. Therefore the more reactive *N*-acyl ammonium salts were used for further testing as summarized in *Table 4.2*.

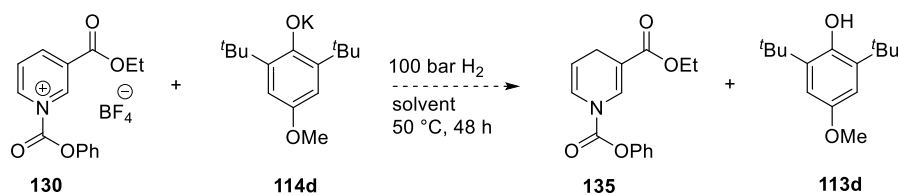
Table 4.2. Hydrogenation experiments with BHT derivatives.

Entry	R	T [°C]	t [h]	Conv. [%] ^[a]
1		50	48	--
2		50	96	mixture
3	NO ₂	100	48	mixture
4	114a	120	48	mixture
5		170	48	mixture
6		50	48	--
7	Br	100	48	--
8	114b	120	48	--
9		170	48	mixture
10		50	48	mixture
11	Me	100	48	mixture
12	114c	120	48	mixture
13		170	48	mixture
14		50	48	mixture
15	OMe	100	48	mixture
16	114d	120	48	mixture
17		170	48	mixture

[a] Estimated by ¹H NMR analysis of the crude reaction mixture.

In most cases, complex product mixtures were observed, which could not be purified and seemed to decompose at higher temperatures. Only reaction with *p*Br-BHTK gave no reaction at temperatures up to 120 °C and the starting materials were fully recovered (entries 6-8). At higher temperatures, a mixture was obtained (entry 9). Reaction with *p*OMe-BHTK led to the cleanest spectra (entries 14-17), therefore it was chosen for the next experiments.

It was reasoned that reactions at higher concentration might facilitate dihydrogen activation by bringing the interacting molecules closer together. Therefore, the concentration of pyridinium salt **130** was increased to 1 M instead of 0.1 M. Also, different solvents were tested as reported in *Table 4.3*.

Table 4.3. Solvent screening at different concentrations.

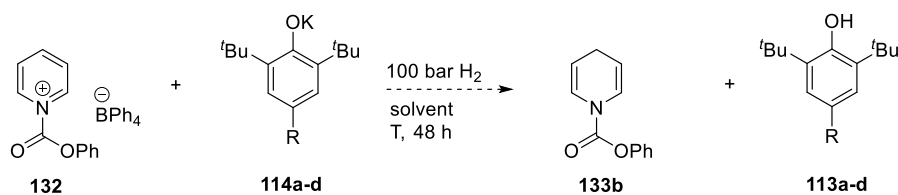
Entry	Solvent	Conc. [mol/l]	Conv. [%] ^[a]
1	THF- <i>d</i> ₈	0.1	mixture
2		1	mixture
3	CD ₂ Cl ₂	0.1	mixture
4		1	mixture
5	benzene- <i>d</i> ₆	0.1	mixture
6		1	mixture

[a] Estimated by ¹H NMR analysis of the crude reaction mixture.

When the reaction was carried out in different solvents mainly complex product mixtures were observed and the desired dihydropyridine was not formed. Increasing the concentration did not overcome this issue.

The results obtained thus so far were inconclusive. In all cases, partial protonation of the phenolate was observed. Furthermore, partial consumption of the pyridinium salt was observed in several instances. Comparison of the NMR data with the authentic samples of dihydropyridines could not definitely clarify if the desired DHP has been formed, since the crude NMR spectra indicated a complex product mixture and purification of this mixture was not possible. NMR analysis suggested that these products might be formed by decomposition of the starting materials.

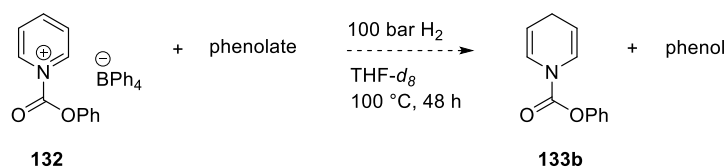
In light of these unsatisfactory results, further studies were conducted with the more stable pyridinium salt **132**. The solubility of **132** was found to be poor in most organic solvents, it only fully dissolved in DMSO (*Table 4.4*).

Table 4.4. Hydrogenation experiments with pyridinium salt **132**.

Entry	R	Solvent	T [°C]	Conv. [%] ^[a]
1		THF- <i>d</i> ₈	100	--
2	NO ₂	DMSO- <i>d</i> ₆	100	--
3	114a	DMSO- <i>d</i> ₆	150	--
4		THF- <i>d</i> ₈	100	--
5	Br	DMSO- <i>d</i> ₆	100	--
6	114b	DMSO- <i>d</i> ₆	150	--
7		THF- <i>d</i> ₈	100	--
8	Me	DMSO- <i>d</i> ₆	100	--
9	114c	DMSO- <i>d</i> ₆	150	--
10		THF- <i>d</i> ₈	100	--
11	OMe	DMSO- <i>d</i> ₆	100	--
12	114d	DMSO- <i>d</i> ₆	150	--

[a] Estimated by ¹H NMR analysis of the crude reaction mixture.

In all cases no reaction was observed and the starting materials were fully recovered, even when more harsh reaction conditions such as 150 °C and 100 bar H₂ were applied. A possible explanation for the lack of reactivity might be that the pyridinium salts are not electrophilic enough or that the phenolates are not basic enough. Consequently, other sterically hindered phenolates with similar pK_A values were tested (*Table 4.5*).

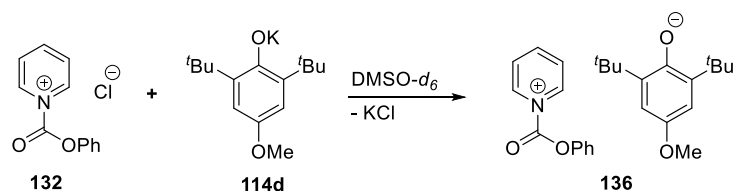
Table 4.5. Screening of phenolates.

Entry	Phenolate	Conv. [%] ^[a]
1		--
2		--
3		--
4		--

[a] Estimated by ¹H NMR analysis of the crude reaction mixture.

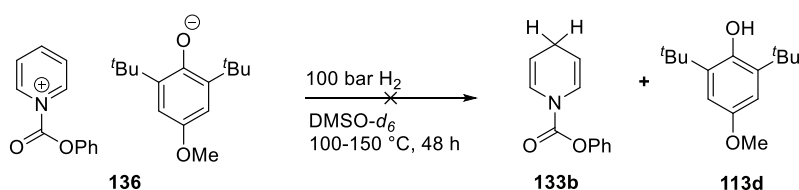
Again, no reaction was observed. As described above, the concentration of the reaction might be crucial for the reactivity. If the BHT derivative could serve as counterion of the pyridinium ion, the two interacting compounds would be very close together (*Scheme 4.12*). The formation, starting from the chloride salt, should be easily achieved by dissolving both compounds, stirring and filtrating the generated KCl. Distillation of the solvent should yield the corresponding pyridinium salt/BHT pair **136**.

A variety of different solvents were tested for this transformation, but only DMSO proved to be a suitable solvent. In the other cases, either the pyridinium salt was unstable or the phenolate was protonated. Due to the high boiling point of DMSO, the solvent could not be removed. Therefore the solution, which was sensitive towards air and moisture, was directly used for the dihydrogen activation reactions.



Scheme 4.12. Formation of pyridinium salt/BHT ion pair **136**.

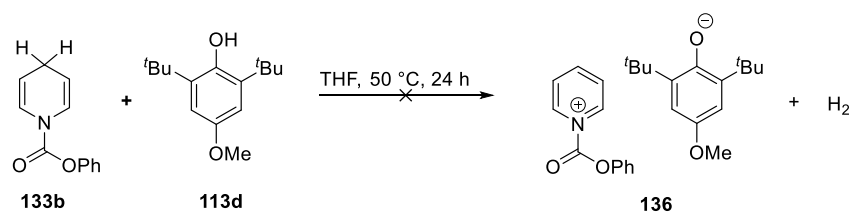
The formed potassium chloride is soluble in DMSO, but its presence during the activation reaction should not have a significant influence. The ion pair was then tested for H₂ activation reactions as depicted in *Scheme 4.13*.



Scheme 4.13. Hydrogenation experiments with pyridinium salt/BHT ion **136**.

At 100 °C, mostly starting materials were observed. When the reaction temperature was increased to 150 °C, decomposition of the ion pair was detected.

Consequently, a compatibility test of hindered phenolates with 1,4-DHP **133b** was carried out. Interestingly, no spontaneous evolution of H₂ was observed upon mixing the dihydropyridine derivative with phenol **114d**, even after heating to 50 °C for 24 h. This indicates that the equilibrium of this reaction lies on the DHP/BHT side.



Scheme 4.14. Compatibility of the DHP **133b** and a BHT derivative **113d**.

4.4. Reaction with Deuterium Gas

One of the main problems associated with pyridinium salts pertains to their intrinsic relatively low stability and high sensitivity to water. For that reason, NMR analysis of the crude reaction mixture is the preferred analytical method. In particular, ^2H -NMR should be an ideal method for detecting even trace amounts of deuterium incorporation, since incorporation of deuterium into the pyridinium salts can only be explained by activation of D_2 . Additionally, the calculated values of the kinetic isotope effect are not dramatically high, which suggests that the reactions with deuterium or hydrogen gas should proceed at similar rates. With that in mind, reactions of several pyridinium salts and BHT with deuterium gas were investigated.

Gratifyingly, when pyridinium salt **130** and $p\text{NO}_2$ -BHTK **114d** were subjected to the reaction conditions established in *Table 4.2* and with 85 bar of D_2 , a signal corresponding to deuterium incorporation was observed in the crude reactions mixture (*Figure 4.3*).

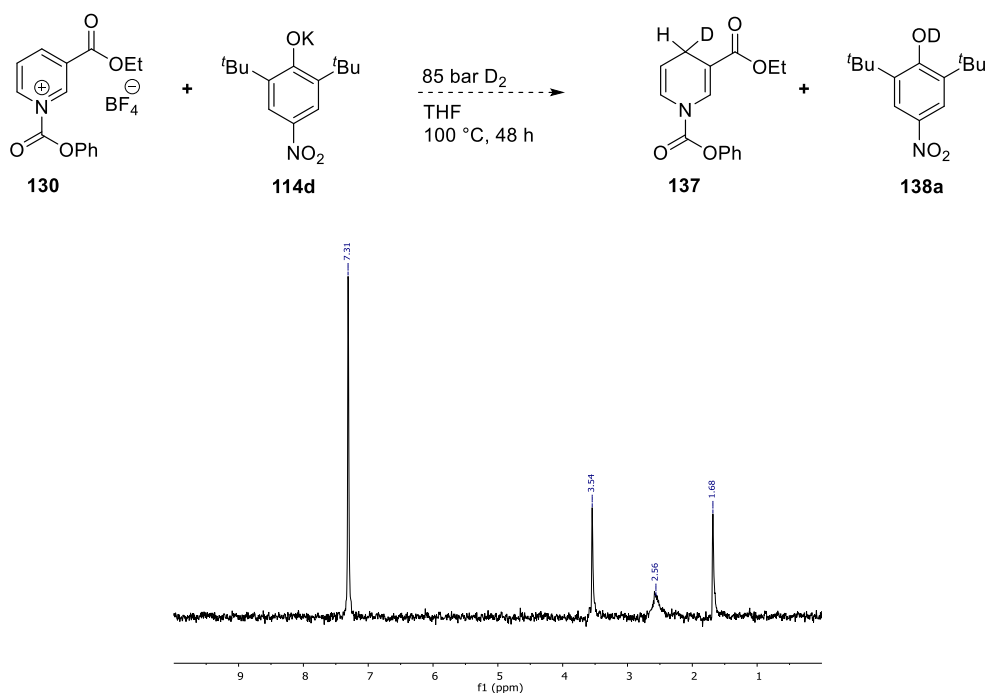


Figure 4.3. Reaction with deuterium gas. C_6D_6 (7.31 ppm) as internal standard in THF.

The broad signal observed at 2.56 ppm might result from the formation of D_2O or HDO during the activation process. To prove this hypothesis, a blind experiment was conducted. There, only THF and 85 bar of deuterium gas were heated to 50°C and stirred for 48 h. Most

surprisingly, the same signal at 2.50 ppm was observed in the spectra (Figure 4.4). Unfortunately, the deuterium signals did not correspond to the desired dihydropyridine **137**.

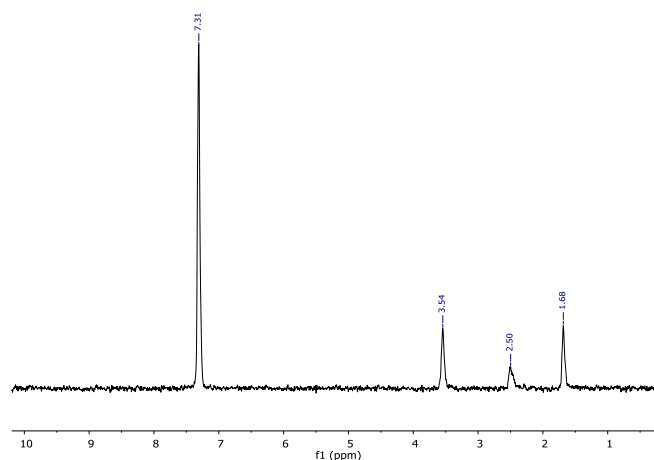
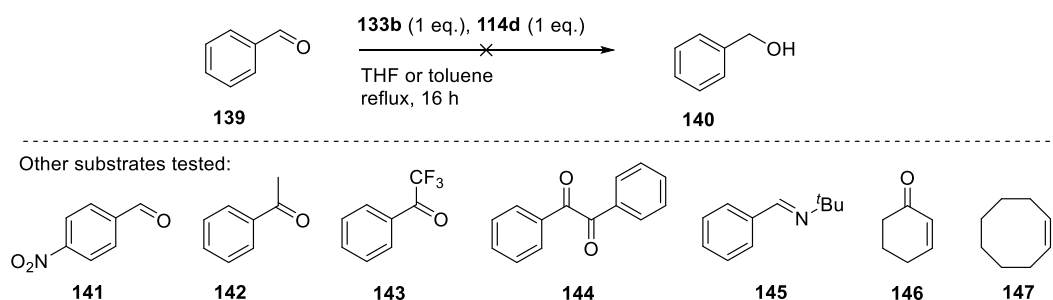


Figure 4.4. Blind test with pure solvent and deuterium gas. C₆D₆ (7.31 ppm) as internal standard in THF.

4.5. Reductions with 1,4-DHP

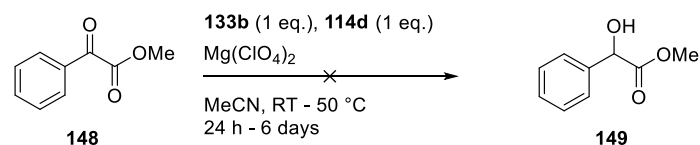
The first part of the project, dihydrogen activation by a newly developed FLP system, gave only negative results. The ability of the corresponding dihydropyridine to reduce substrates was then examined. A variety of substrates was tested for this transformation, but all attempts failed and only starting materials were observed (Scheme 4.15).



Scheme 4.15. Attempted reductions of various substrates using pyridinium **133b** and phenolate **114d**.

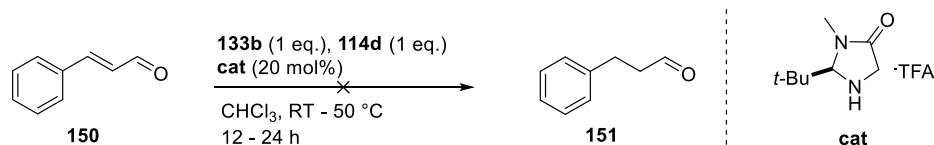
It has been reported in the literature that NADH models are able to reduce pyruvates into the corresponding β -hydroxyesters. These models were involved in the reduction of methyl benzoylformate in the presence of magnesium perchlorate, as described by LEVACHER.^[90]

Although numerous reaction conditions were tested, the reduced compound was not furnished.



Scheme 4.16. Attempted reduction of methyl benzoylformate (**148**).

A reason for the observed lack of reactivity might be that the substrates need to be more activated. As described in the previous chapter, organocatalytic transfer hydrogenations developed by *MACMILLAN* and *LIST* might be an adequate strategy for this purpose.^[67] Cinnamaldehyde was therefore treated with dihydropyridine **133b** and BHT derivative **114d** in the presence of the MacMillan catalyst, but unfortunately, no reaction occurred (*Scheme 4.17*).



Scheme 4.17. Attempted reduction of cinnamaldehyde (**150**).

Nevertheless, the reaction was carried out in the presence of **133b** and catalyst only, to evaluate if the BHT derivative had any influence. Again, no product formation was observed. As a control experiment, the reaction was set up with the Hantzsch ester and the reduced aldehyde was obtained in 74% yield using the described procedure.^[67] Surprisingly, when the reaction was repeated in the presence of the BHT derivative, the reduction of the aldehyde did not occur. These set of experiments indicate that not only the DHP is an unsuitable hydride donor, but also that the BHT inhibits the hydride transfer.

4.6. Summary

In summary, a series of *N*-acyl ammonium salts and phenolates derived from commercially available BHT derivatives were synthesized. While ester moieties on the pyridinium ring led to hygroscopic and rather unstable pyridinium salts, the unsubstituted derivative was isolated as a stable salt.

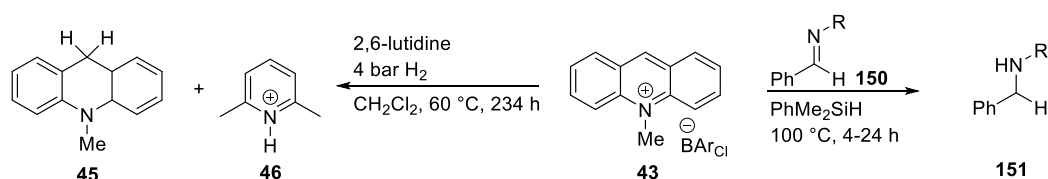
Applying these new FLP systems to dihydrogen activation, mostly no reaction was observed and starting materials were recovered. In some experiments, traces of new signals could be detected in the crude reaction mixture by NMR analysis, but the desired products could not be isolated. Furthermore, experiments with deuterium gas showed no incorporation of deuterium. Reduction experiments with the corresponding DHP and various electrophiles showed that the developed system is not able to transfer a hydride.

Chapter 5

5. Revision of the Proposed Model for H₂ Activation: Hantzsch Analogues in Pyridylidene Chemistry

5.1. Introduction

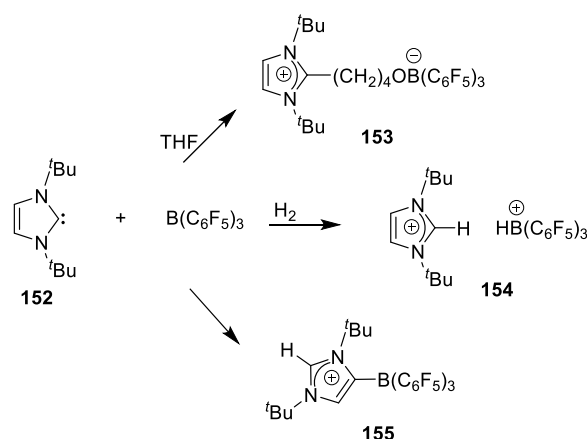
As explained in the thesis outline, the group of *INGLESON* very recently showed the activation of dihydrogen by using *N*-methylacridinium salts as Lewis acids and 2,6-lutidine as base.^[70] However, the reaction time to achieve adequate conversions for this process was almost two weeks, which is not very practical. Furthermore, *in situ* stoichiometric reduction was shown to take place with modest efficiency (around 25%). On the other hand, the ability of methylacridinium salts to activate Si–H bonds was exemplified by the reduction of imines using PhMe₂SiH as hydride source (*Scheme 5.1*).



Scheme 5.1. Dihydrogen activation by *N*-methylacridinium salt **43**, reduction of aldimines.

In light of the unsatisfactory results obtained so far in the *PFALTZ* group, and in hopes of finding more efficient systems using pyridinium salts as key partners in the activation of dihydrogen, investigation of an alternative approach towards H₂ activation was pursued.

The group of *TAMM* has demonstrated that *N*-heterocyclic carbenes in combination with a Lewis acidic borane can form a frustrated carbene-borane system, which is able to activate H–H, C–H and C–O bonds (*Scheme 5.2*).^[46] The scope of carbene-based Lewis Pairs for hydrogen activation was further broadened by *ARDUENGO et al.*^[91]



Scheme 5.2. Reactions of the frustrated carbene-borane Lewis Pair.

BERTRAND and co-workers were the first who discovered the ability of a single carbon center to split dihydrogen by nucleophilic activation.^[10] They found that singlet carbenes and many transition-metal complexes share a common pattern of frontier orbitals which are called *isolobal* (Figure 5.1).

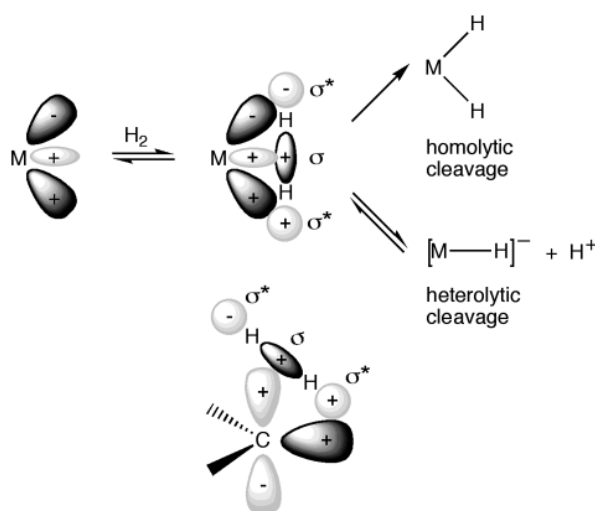
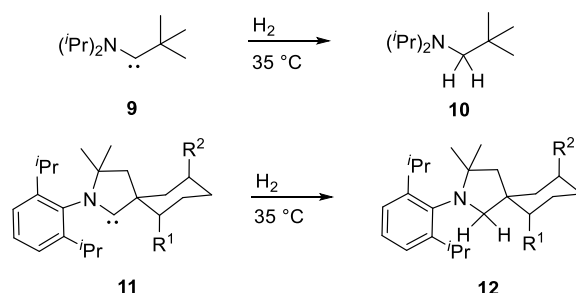


Figure 5.1: (Alkyl)(amino)carbenes activate H_2 under mild conditions.

The research team rationalized these findings invoking donation of the dihydrogen σ -bonding orbital into the vacant orbital of the singlet carbene, thus leaving sufficient overlap for the carbene lone pair to populate the H_2 antibonding σ^* orbital. Consequently, the H–H bond is weakened and heterolytic cleavage occurs. In their system, singlet acyclic and cyclic (alkyl)(amino)carbenes **9** and **11** are utilized to activate dihydrogen and even ammonia under

mild conditions (*Scheme 5.3*). *N*-heterocyclic carbenes do not react with hydrogen gas under these conditions.



Scheme 5.3. Singlet carbenes resemble transition metal centers.

The major drawback of *BERTRAND*'s system is the lack of reactivity of the resulting products. Once dihydrogen activation on the (alkyl)(amino)carbenes has taken place, the generated amine cannot undergo further reactions. Moreover, the process does not seem to be reversible since H₂ release was not observed.

To overcome the disadvantages of the system developed by *BERTRAND* (lack of potential applications), the lack of reactivity in the previously developed systems and the poor efficiency observed by *INGLESON*, the potential use of pyridinium salts in dihydrogen activation *via* carbene chemistry was envisioned. Specifically, it was reasoned that if a pyridinium salt **156** was deprotonated with a suitable base to form a pyridylidene **157**,^[92] this species might serve as reactive intermediate to activate dihydrogen (**158**), much like the aminocarbenes designed by *BERTRAND* (*Figure 5.2*),^[93] thus forming a dihydropyridine **159**. Furthermore, the resulting dihydropyridines might serve as efficient hydride donors in hydrogenations.

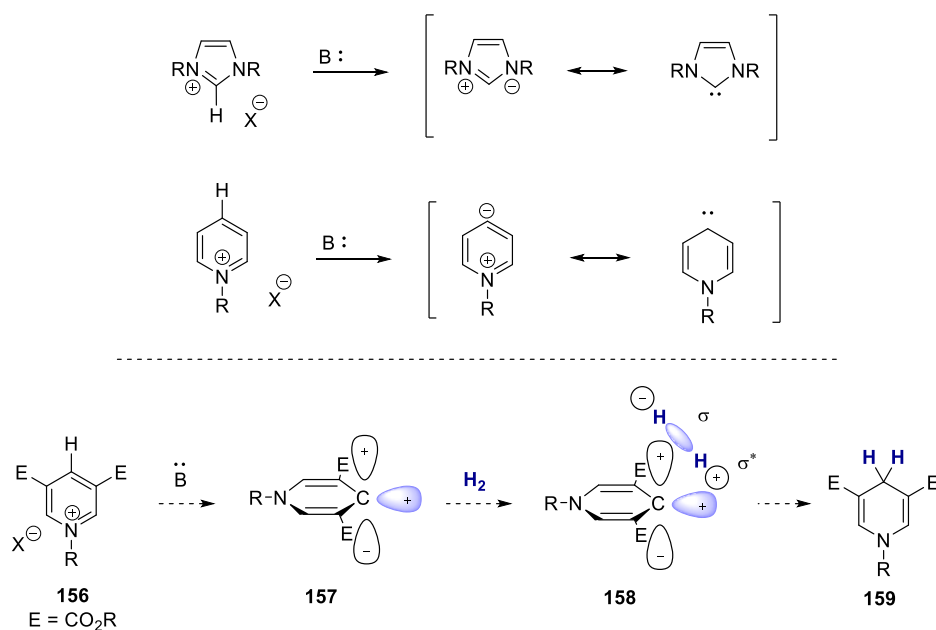
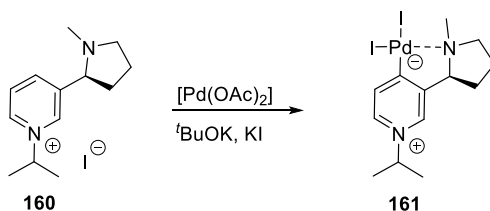


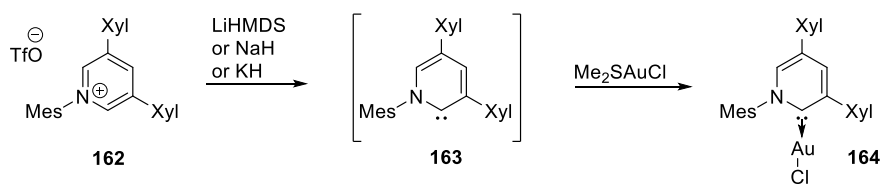
Figure 5.2: Formation of pyridylidenes by deprotonation of pyridinium salts, and general model of pyridylidenes in dihydrogen activation.

ALBRECHT et al. showed that catalytically active palladium pyridylidene complexes **161** can be formed from pyridinium ionic liquids such as *N*-heterocyclic carbene precursors **160** (*Scheme 5.4*).^[94]



Scheme 5.4. Formation of a palladium-pyridylidene *N*-heterocyclic carbene complex **161** in the presence of base.

ITAMI and coworkers described the formation of sterically hindered 1,3,5-triaryl pyridinium salt **162**, which can be deprotonated in the presence of a strong base to give the 2-pyridylidene **163** (*Scheme 5.5*).^[95]



Scheme 5.5. Base-promoted generation of 1,3,5-triaryl 2-pyridylidene **163** and trapping with Me₂SAuCl.

5.1.1. Objective of This Work

A prominent 1,4-dihydropyridine is the Hantzsch ester, which showed high reactivity in reductions where usually metal hydrides are employed.^[96-97] Compared to triaryl substituted pyridines, nicotinamides and Hantzsch esters possess electron withdrawing groups attached on the pyridine ring which increases the acidity of the aromatic proton and consequently facilitating the deprotonation. Therefore, the aim of this section was to synthesize stable *N*-aryl Hantzsch esters and *N*-aryl nicotinamides as depicted in *Figure 5.3*.

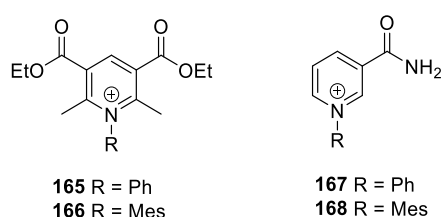


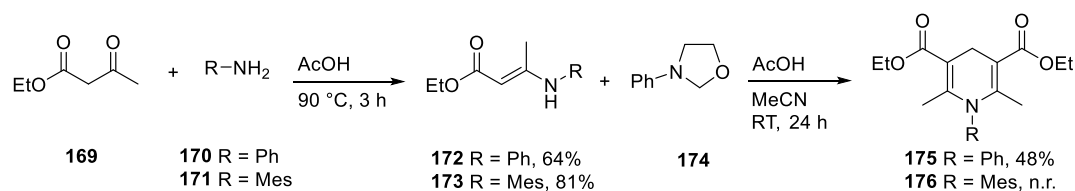
Figure 5.3. Target molecules.

Once the synthesis could be achieved, the idea was to test them in H₂ activation reactions in the presence of a strong base. If proof of principle for the dihydrogen activation could be found, the resulting substrates might be used as hydride donors in reduction of electrophilic C=C, C=O or C=N bonds. For example, *MACMILLAN* and co-workers used *N*-benzylnicotinamides for the enantioselective organocatalytic transfer hydrogenation of α,β -unsaturated aldehydes.^[69]

5.2. N-Aryl Hantzsch Esters

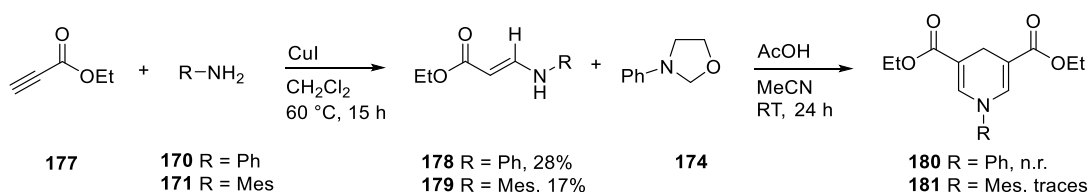
5.2.1. Preparation

The synthesis of the *N*-phenyl-Hantzsch ester was conducted using a procedure reported in the literature from commercially available starting materials.^[98-100] Condensation of the generated ethyl- β -anilincrotonate and 3-phenyl-1,3-oxazolidine (**174**) gave the desired 1,4-DHP **175** in moderate yield after column chromatography. However, reaction with the ethyl- β -mesitylcrotonate **173** led only to recovery of the starting materials (*Scheme 5.6*).



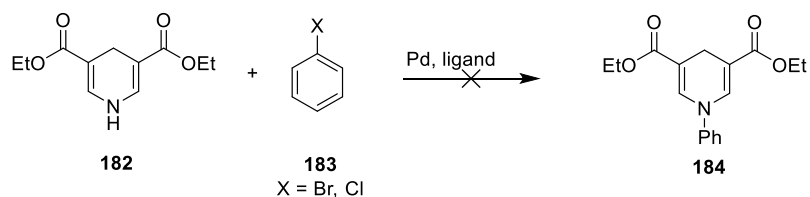
Scheme 5.6. Synthesis of *N*-aryl-Hantzsch esters **175** and **176**.

For the formation of the corresponding non-methylated Hantzsch esters, the desired enamines **178** and **179** were synthesized by reaction of ethyl propiolate and the corresponding amine in the presence of copper iodide.^[101] Both compounds were obtained in low yield. The following condensation led to a mixture of products, which proved to be difficult to purify due to similar polarity. Unfortunately, the desired product could not be isolated in reasonable yields (*Scheme 5.7*).



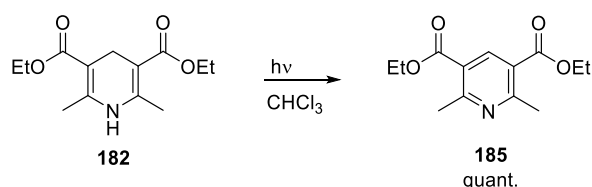
Scheme 5.7. Attempted synthesis of Hantzsch ester analogs.

A *BUCHWALD-HARTWIG AMINATION* was envisioned as a potential solution to this problem. It has been reported that piperidine reacts with arylchlorides in the presence of a palladium catalyst.^[102] However, although different ligands and conditions were tested for this transformation, the desired product could not be obtained (*Scheme 5.8*).



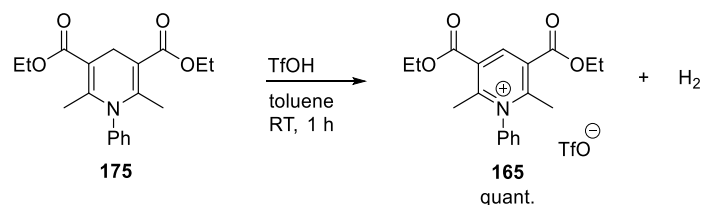
Scheme 5.8. Attempted Buchwald-Hartwig amination of 1,4-DHP **182**.

Usually, the transformation of dihydropyridines to the corresponding pyridinium salts includes the use of oxidizing agents such as nitric acids,^[64, 103] chromic acid,^[104] oxygen,^[105] iodine^[106] or sulfur.^[107-108] Newer approaches rely also on photoinduced aromatization. A procedure developed by *LIU* describes the oxidation of Hantzsch 1,4-DHPs through SET with CCl₄.^[109] Due to the high toxicity of CCl₄, the reaction was carried out in CHCl₃ instead. Gratifyingly, the reaction gave the desired pyridine **185** in quantitative yield (*Scheme 5.9*).



Scheme 5.9. Aromatization of 1,4-DHP **182**.

Interestingly, when 1,4-DHP **175** was treated with trifluoromethanesulfonic acid in dry toluene, the formation of a precipitate was observed. After separation and removal of the solvent, analysis by NMR indicated that the aromatized *N*-phenyl Hantzsch ester had been formed by extrusion of dihydrogen. This assumption was confirmed by HRMS of the pyridinium salt **165** (*Scheme 5.10*).

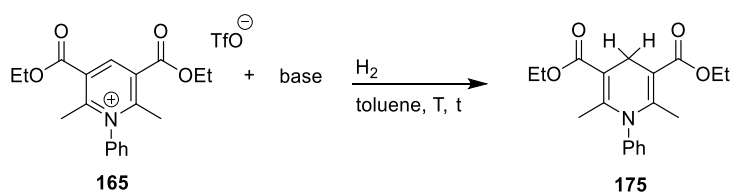


Scheme 5.10. Reaction of 1,4-DHP **175** with trifluoromethanesulfonic acid.

5.2.2. Dihydrogen Activation Experiments

The *N*-phenyl pyridinium salt **165** was then tested for the reaction with H₂ in the presence of base. In a first experiment, the pyridinium salt **165** was dissolved in toluene and LiHMDS was added, and then the autoclave was pressurized with 50 bar H₂. After four hours at 50 °C, analysis of the crude reaction mixture by ¹H NMR showed the formation of a complex product mixture, none of them being the desired 1,4-DHP **175** (Table 5.1, entry 1). In the presence of DBU and phosphacene P₁-^tBu, only decomposition of the starting material was observed (entries 2 and 3). Surprisingly, the use of a milder base showed the dihydropyridine **175** in low yields (entries 5 and 6). Higher conversions were obtained when more forcing conditions such as high pressure and high temperatures were applied (entries 8 and 9). The best result was achieved by increasing the reaction time to 24 h (entry 9).

Table 5.1. Dihydrogen activation experiments with different bases.

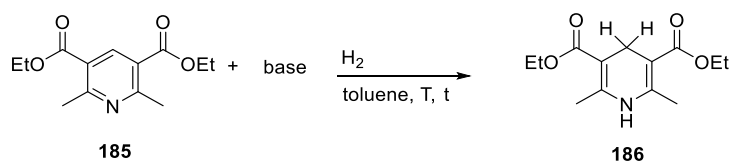


Entry	Base	H ₂ [bar]	T [°C]	t [h]	Conv. [%] ^[a]
1	LiHMDS	50	50	5	mixture
2	DBU	10	RT	4	decomposition
3	P ₁ - ^t Bu	10	RT	4	decomposition
4		10	RT	4	--
5		50	50	5	traces
6		50	100	5	15
7	DIPEA	100	50	5	--
8		100	100	5	12
9		100	100	16	32
10		100	100	24	23
11		35	100	16	28

[a] Estimated by ¹H NMR analysis of the crude reaction mixture.

The non-protected Hantzsch ester **185** showed poor reactivity upon treatment with base. With DIPEA, DBU or phosphacene P₁-^tBu, only starting materials were recovered (Table 5.2, entries 1-3). In the presence of LiHMDS, decomposition of the Hantzsch ester **185** was observed at 50 °C and 50 bar H₂ (entry 4). Lowering the hydrogen pressure and the reaction temperature led to a product mixture containing unreacted starting material as well as formation of new products (entry 5 and 6).

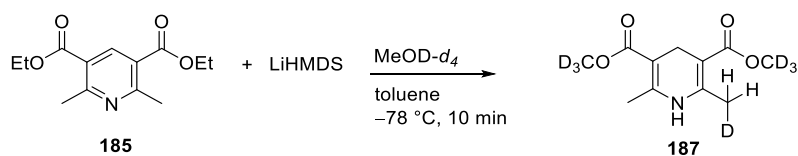
Table 5.2. Dihydrogen activation experiments with different bases.



Entry	Base	H ₂ [bar]	T [°C]	t [h]	Conv. [%] ^[a]
1	DIPEA	50	50	5	--
2	DBU	50	50	5	--
3	P ₁ - ^t Bu	50	50	5	--
4		50	50	5	decomposition
5	LiHMDS	1	0	5	mixture
6		1	-20	3.5	mixture

[a] Estimated by ¹H NMR analysis of the crude reaction mixture.

To gain more insight into the products formed during the H₂ activation reaction, a test experiment was conducted in which the Hantzsch ester **185** was quenched with MeOD-*d*₄ after treatment with LiHMDS. Analysis by NMR should then show if deuterium incorporation happened, and more importantly, in which position. Therefore, Hantzsch ester **185** was dissolved in toluene and the solution was cooled to -78 °C and LiHMDS was added. After 5 minutes, the reaction mixture was treated with MeOD-*d*₄. Analysis by ¹H and ²H NMR proved that compound **18** was formed as depicted in Scheme 5.11.



Scheme 5.11. Reaction of **185** with LiHMDS and MeOD-*d*₄.

Under basic conditions, transesterification of the ester groups took place as well as deprotonation and deuterium incorporation of the methyl groups. The signal of the ethyl ester groups could not be detected any more (*Figure 5.4, left*), however, ^2H NMR showed a singlet 3.90 ppm, which could be assigned to the newly formed methyl ester. Moreover, a multiplet at 2.44 ppm was observed, belonging to the methyl groups, which suggests that deprotonation of the methyl groups by LiHMDS happened.

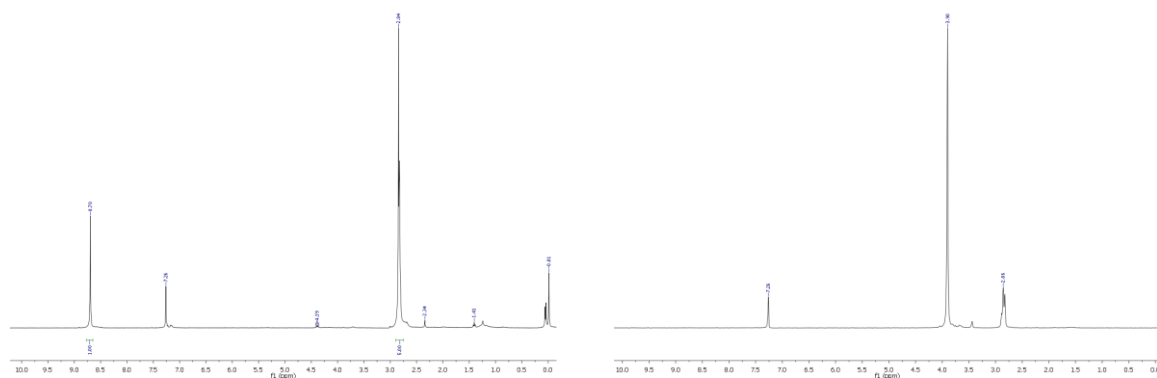
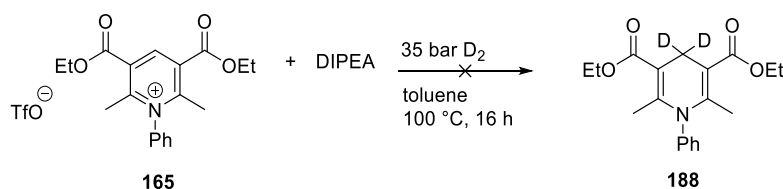


Figure 5.4. NMR spectra obtained of the reaction mixture: ^1H NMR (*left*) and ^2H NMR (*right*).

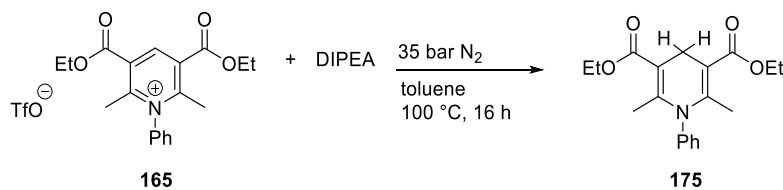
5.2.3. Deuteration Experiments

To clarify whether the dihydropyridine was formed by with *N*-phenyl Hantzsch ester **165** in the presence of DIPEA, experiments employing deuterium gas were conducted. Therefore, the pyridinium salt was treated with DIPEA and the autoclave was pressurized with 35 bar D_2 . Unfortunately, ^2H NMR analysis did not show a signal corresponding to a CD_2 fragment.



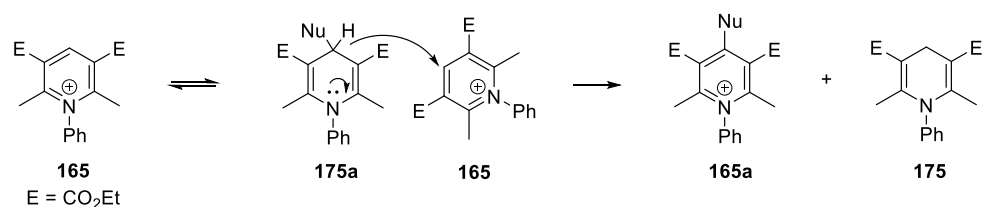
Scheme 5.12. Attempted deuterium activation.

A control experiment was conducted in which nitrogen gas was used. Although under these condition the formation of the corresponding 1,4-DHP **175** should not be possible, the ^1H NMR of the reaction mixture clearly showed a signal at 3.38 ppm of the CH_2 group (*Scheme 5.13*).



Scheme 5.13. Control experiment with N₂.

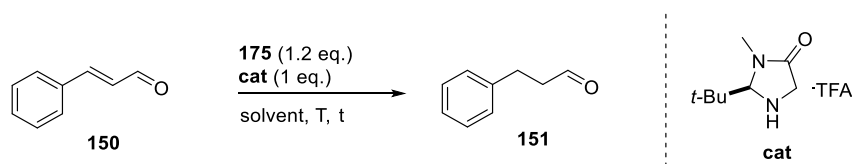
An alternative pathway leading to dihydropyridine **175** is shown in *Scheme 5.14*. Addition of a nucleophile (DIPEA, residual water, or **165** deprotonated at one of the methyl groups) could produce a dihydropyridine intermediate, which then transfers a hydride to the starting pyridinium salts **165**.^[110-112]



Scheme 5.14. Alternative pathway leading to dihydropyridine **175**.

5.2.4. Possible Applications of Hantzsch Ester **175**

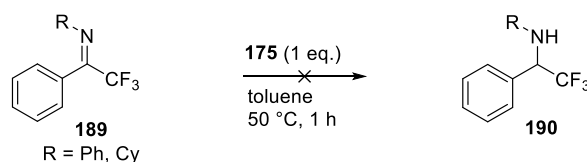
As described in the literature, regular Hantzsch esters in combination with organic catalysts are used as powerful tools to reduce α,β -unsaturated aldehydes substrates.^[67, 69] The ability of the prepared *N*-phenyl Hantzsch ester **175** to do this transformation was tested. Under the described reaction conditions, 21% conversion was observed (*Table 5.3*, entry 1). Extending the reaction time as well as lowering the reaction temperature gave only unreacted starting material (entries 2 and 3). Using the dihydrogen activation conditions (50 °C, 5 h) led to decomposition of the starting materials. As chloroform is not a suitable solvent for potential H₂ activation reactions the reductions were also carried out in THF and toluene. Unfortunately, all experiments showed no conversion the reduced compound (entries 5-8).

Table 5.3. Reduction of cinnamaldehyde (**150**) in the presence of Hantzsch ester **175** and MacMillan's catalyst.

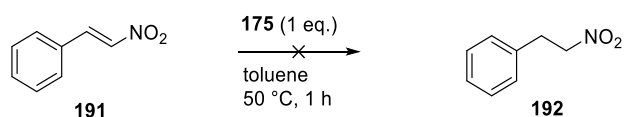
Entry	solvent	T [°C]	t [h]	Conv. [%] ^[a]
1		0	5	21
2	CHCl ₃	0	24	--
3		-30	24	--
4		50	5	decomposition
5	THF	0	1	--
6		0	1	--
7	toluene	0	24	--
8		50	5	--

[a] Estimated by ¹H NMR analysis of the crude reaction mixture.

Furthermore, *N*-aryl and -alkyl imines were tested, but the desired reduced imines could not be observed. In both cases, only unreacted starting material was recovered.

**Scheme 5.15.** Attempted reduction of activated imines.

Another appropriate substrate class for reduction are nitrostyrenes. Again, only unreacted starting material was recovered.

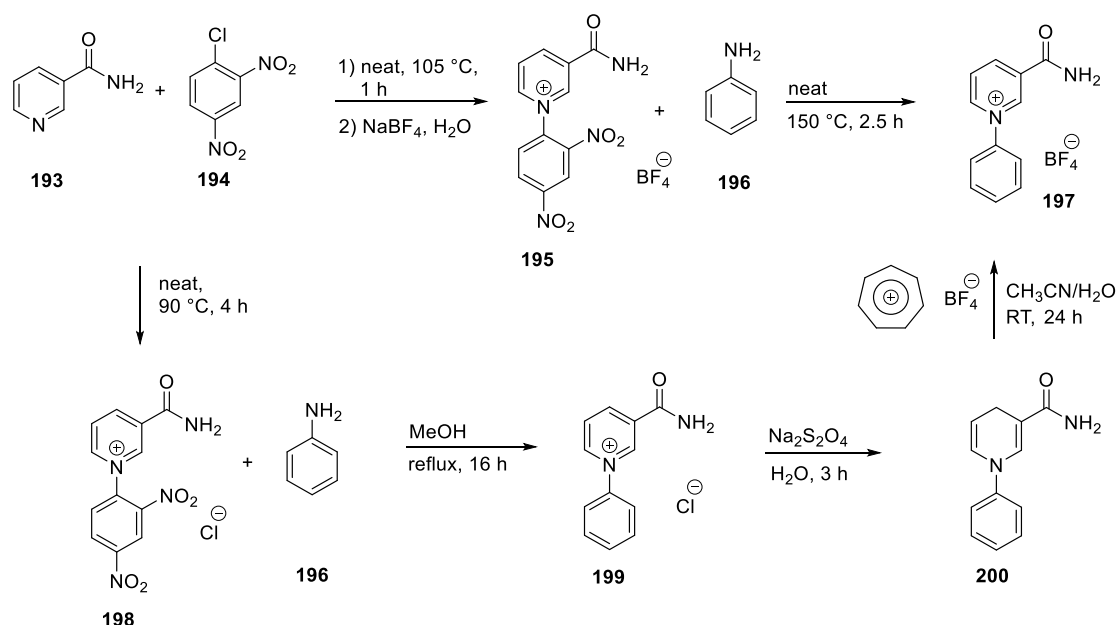
**Scheme 5.16.** Attempted reduction of nitrostyrene.

It was concluded that the *N*-phenyl Hantzsch ester **175** was a much weaker hydride donor compared to the non-protected Hantzsch ester.

5.3. *N*-Aryl Nicotinamide Derivatives

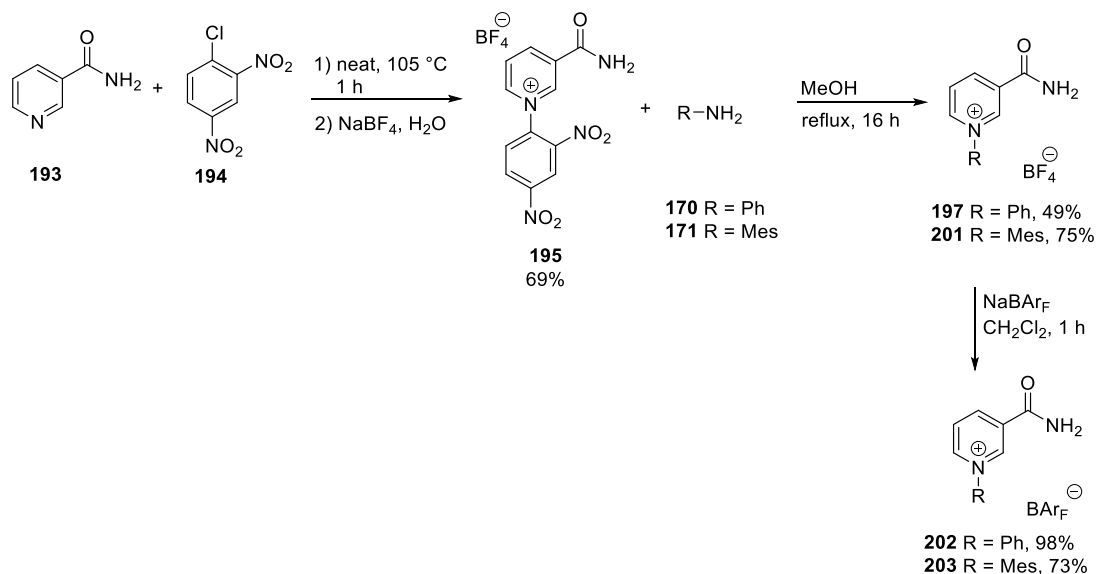
5.3.1. Preparation

Two different synthetic strategies were reported in the literature that resulted in formation of the desired *N*-aryl nicotinamide **197**, both from commercially available starting materials. One strategy involves formation of the Zincke salt **195**, as described by *HERDEWIJN*^[113] followed by Zincke reaction with aniline as described by *ITAMI*.^[95] Alternatively, the same product could be obtained from Zincke salt **199** followed by reduction and subsequent oxidation, as described by *BODOR*.^[114-115]



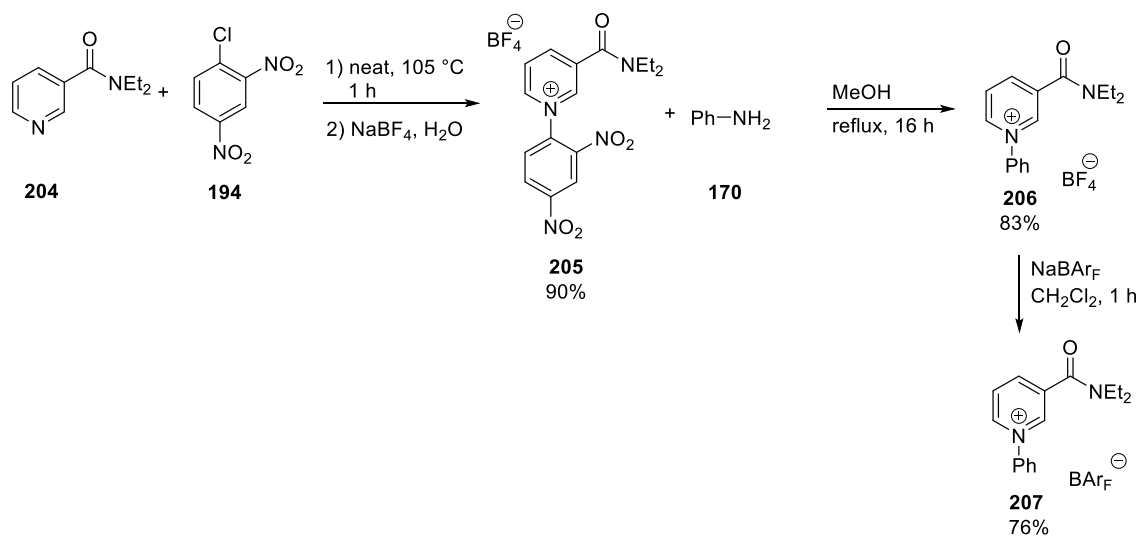
Scheme 5.17. Synthetic strategies towards **197**.

It turned out that a combination of both methods gave the best results. The Zincke salt **195** was prepared by heating the pyridine and the Zincke reagent neat at 105 °C for 1 h. Then, the crude reaction mixture was dissolved in water and NaBF₄ was added. The generated Zincke salt with BF₄ as counterion precipitates from water, and hence could be easily isolated by filtration. Subsequent reaction with aniline in methanol yielded the desired product **197** in moderate yield. Since the solubility of the *N*-aryl nicotinamide salt **197** was low, the counterion was changed to BAr_F, which significantly increased the solubility (*Scheme 5.18*).



Scheme 5.18. Synthesis of the *N*-aryl nicotinamides.

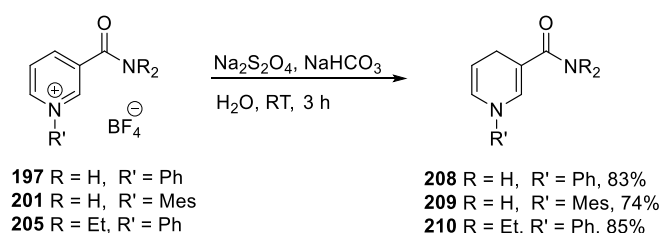
Alternatively, also the *N*-phenyl diethylnicotinamide **206** was synthesized. The ethyl groups should improve the solubility of the pyridinium salt and might inhibit possible interaction of the base with the amide previously described. Again, also the BAR_F salt **207** was synthesized (*Scheme 5.19*).



Scheme 5.19. Synthesis of the *N*-phenyldiethylnicotinamides **206** and **207**.

5.3.2. Preparation of Authentic Samples of Dihydropyridines

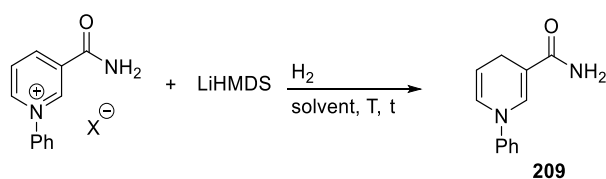
Before applying the pyridinium salts to H₂ activation reactions, it was necessary to prepare authentic samples of the corresponding dihydropyridines. Usually, the pyridinium salts are reduced with sodium borohydride in THF, but this method led only to a complex product mixture. Instead, reduction with sodium dithionite in water led to the desired dihydropyridines (Scheme 5.20).^[114]



Scheme 5.20. Reduction of *N*-aryl nicotinamide salts with Na₂S₂O₄.

5.3.3. Dihydrogen Activation Studies

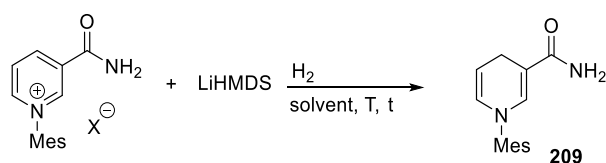
The prepared *N*-aryl nicotinamide salts **197** and **202** were then tested for H₂ activation reactions. When the BF₄ salt **197** was tested with toluene as solvent, no conversion was observed in any case, which might be due to the low solubility of the starting materials in toluene (Table 5.4, entries 1, 2 and 5). To overcome this issue, the solvent was changed to THF. With 50 bar H₂ pressure at 50 °C, traces of the desired DHP were observed (entries 3 and 6). Lowering the reaction temperature and increasing the pressure did not improve the reaction (entries 4 and 8). In contrast to that, when the reaction temperature was increased to 100 °C, the conversion improved up to 24% (entry 7).

Table 5.4. *N*-phenylnictoinamide salts **197** and **202** in attempted H₂ activation reactions.

Entry	X	solvent	H ₂ [bar]	T [°C]	Conv. [%] ^[a]
1		Toluene	50	50	--
2	197	Toluene	100	RT	--
3	BF ₄	THF	50	50	traces
4		THF	100	RT	--
5		Toluene	50	50	--
6	202	THF	50	50	traces
7	BAr _F	THF	50	100	24
8		THF	100	RT	--

[a] Estimated by ¹H NMR analysis of the crude reaction mixture.

N-Mesitylnictoinamide salts showed higher conversions than the previous tested *N*-phenylnictoinamide salts. In THF, conversion up to 60% were observed in case of the BF₄ salt **201** (Table 5.5, entry 2). Interestingly, the corresponding BAr_F salt **203** proved to be less reactive and the dihydropyridine was formed only in 21% conversion (entry 5).

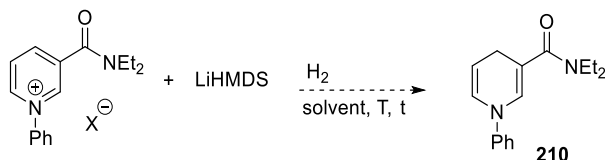
Table 5.5. *N*-Mesitylnictoinamide salts **201** and **203** in attempted H₂ activation reactions.

Entry	X	solvent	H ₂ [bar]	T [°C]	Conv. [%] ^[a]
1	201	THF	50	50	traces
2	BF ₄	THF	50	100	60
3		toluene	50	50	--
4	203	THF	50	50	--
5	BAr _F	THF	50	100	21
6		THF	100	RT	--

[a] Estimated by ¹H NMR analysis of the crude reaction mixture.

Finally, the pyridinium salts **206** and **207** derived from *N,N*-diethylnicotinamide were tested for the activation of H₂. Unfortunately, only decomposition of the starting material was observed in every case. (Table 5.6, entries 1-4).

Table 5.6. *N*-phenyldiethylnicotinamide salts **206** and **207** in H₂ activation reactions.

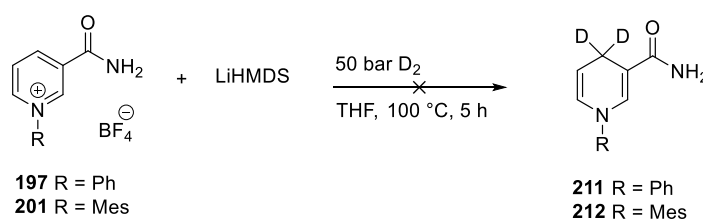


Entry	X	solvent	H ₂ [bar]	T [°C]	Conv. [%] ^[a]
1	206	THF	50	50	decomposition
2		THF	50	100	decomposition
3	BF ₄	toluene	50	50	decomposition
4	207	THF	50	50	decomposition
		BAr _F			

[a] Estimated by ¹H NMR analysis of the crude reaction mixture.

5.3.4. Deuteration Studies

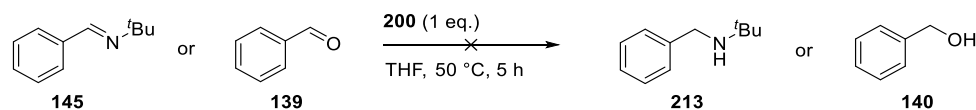
The best conditions (50 bar, 100 °C, 5 h) were then applied for the reaction of BF₄ salts **197** and **201** with deuterium gas. Unfortunately, the expected signals at 3.04 ppm and 3.06 ppm were not detected by ²H NMR, but ¹H NMR of the reaction mixture showed the presence of the CH₂ group. This finding means that the formation of the corresponding dihydropyridine did not take place *via* hydrogen activation. Similar to the tested *N*-phenyl Hantzsch ester, there might be an intermolecular hydride shift from an intermediate formed by addition of a nucleophile to the pyridinium salts, which could lead to reduction of the pyridinium salts.



Scheme 5.21. Attempted deuterium incorporation.

5.3.5. Possible Application of Nicotinamide 200

Again, the ability of the prepared *N*-phenyldihydropyridine **200** to reduce substrates was tested. No reduction occurred in the presence of a hindered imine or benzaldehyde.



Scheme 5.22. Attempted reduction of benzaldehyde and *N*-benzylidene-tert-butylamine.

5.4. Summary

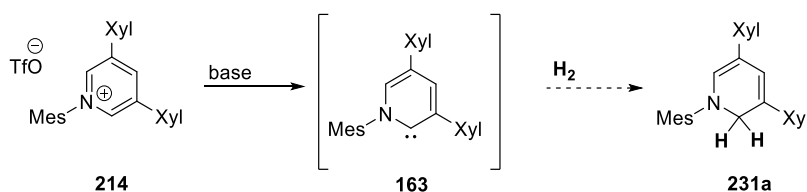
In summary, the synthesis of *N*-phenyl Hantzsch ester **165** and *N*-aryl nicotinamides **197**, **201** and **206** has been described. Both classes of pyridinium salts were tested for H₂ activation reactions. Although the formation of the corresponding dihydropyridines was observed, deuteration experiments proved that the reaction did not proceed *via* dihydrogen splitting. Furthermore, the ability of the obtained dihydropyridines to reduce substrates was evaluated. *N*-phenyl dihydropyridine **175** turned out to be a weaker hydride donor than standard Hantzsch esters. *N*-phenyldihydropyridine **200** originating from *N*-aryl nicotinamide **197** did not show any reactivity towards reduction of substrates.

Chapter 6

6. Aryl Substituted Pyridylidenes in Dihydrogen Activation

6.1. Introduction

As described in the previous chapter, the idea of pyridylidene as unconventional carbene in H_2 activation reactions was envisioned. Unfortunately, activation experiments with *N*-phenyl Hantzsch ester and *N*-aryl nicotinamide derivatives prepared during the course of the investigation were not successful. Alternatively, the sterically hindered 1,3,5-triaryl-2-pyridinium ions described by *ITAMI* and coworkers could be deployed target compounds. The pyridinium salt **162** can be deprotonated in the presence of a strong base to give 2-pyridylidene **163**.^[95] These highly reactive carbenes could then undergo formal addition of H_2 (Scheme 6.1).



Scheme 6.1. Synthesis of pyridylidenes and their proposed reactivity with dihydrogen.

6.2. Objective of This Work

Based on the idea outlined above, the synthesis of the described pyridinium salts was planned. Afterwards, the base-induced carbene formation followed by H_2 activation needed to be studied. If a proof of principle could be realized, the investigation of a catalytic application as described in the previous chapters would be the subject of further investigations. Furthermore, variation of the electronic features of the aromatic moieties might allow for catalyst optimization, hence opening new possibilities for reactivity.

6.3. DFT Calculations on Pyridylidenes for H₂ Activation

Preliminary DFT calculations were performed by *Padevet* on the system shown below, using LiHMDS as base for the formation of the pyridylidene. The calculated energy profile for the reaction of the mesitylpyridinium system described by *ITAMI* with H₂ is typical of an exothermic process. The calculations also indicate that the energy of the transition state is relatively low (20.1 kcal/mol). Therefore, it should be possible to overcome such an activation energy barrier carrying out the reaction at higher temperatures.

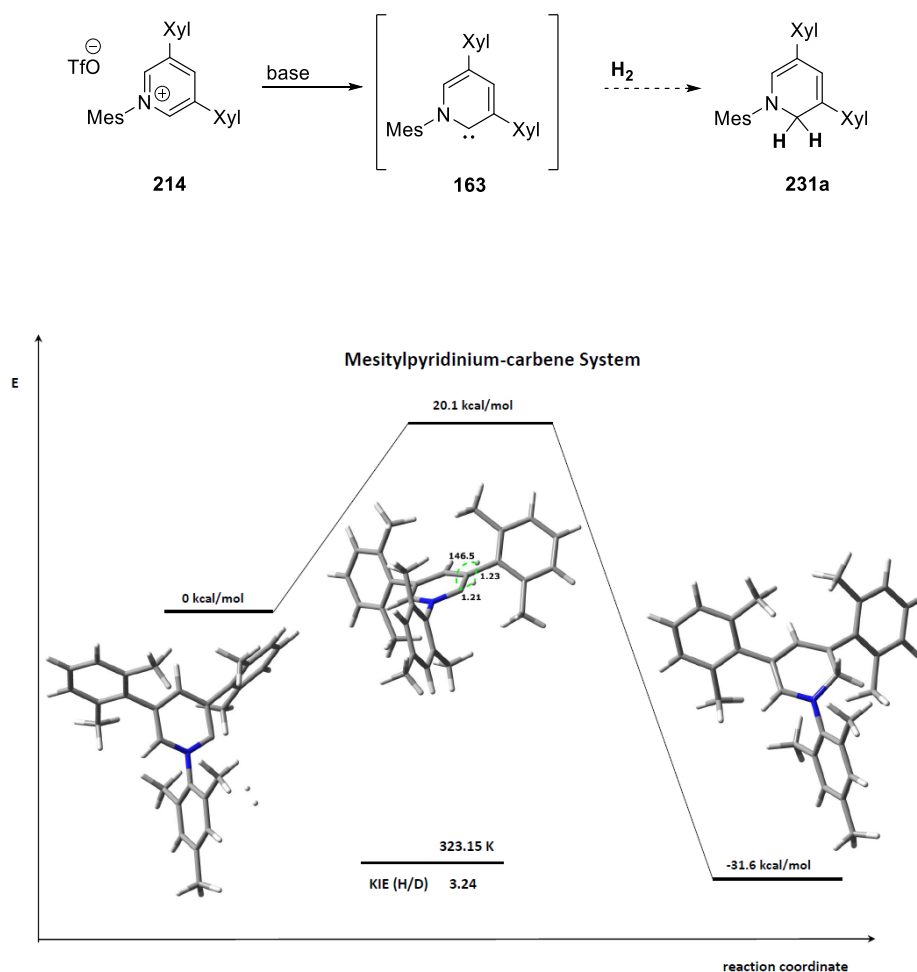


Figure 6.1. Energetic profile of the activation of H₂ by mesitylpyridinium systems.

If the H₂ activation experiments were successful, hydride transfer from the resulting dihydropyridines to electrophiles such as imines or ketones, would be investigated. To obtain insight into the energetic situation of the reduction step, calculations were conducted. The results obtained in these studies showed that the energy of the transition state is higher

compared to the activation step (27.3 kcal/mol), but still reachable under reasonable reaction conditions.

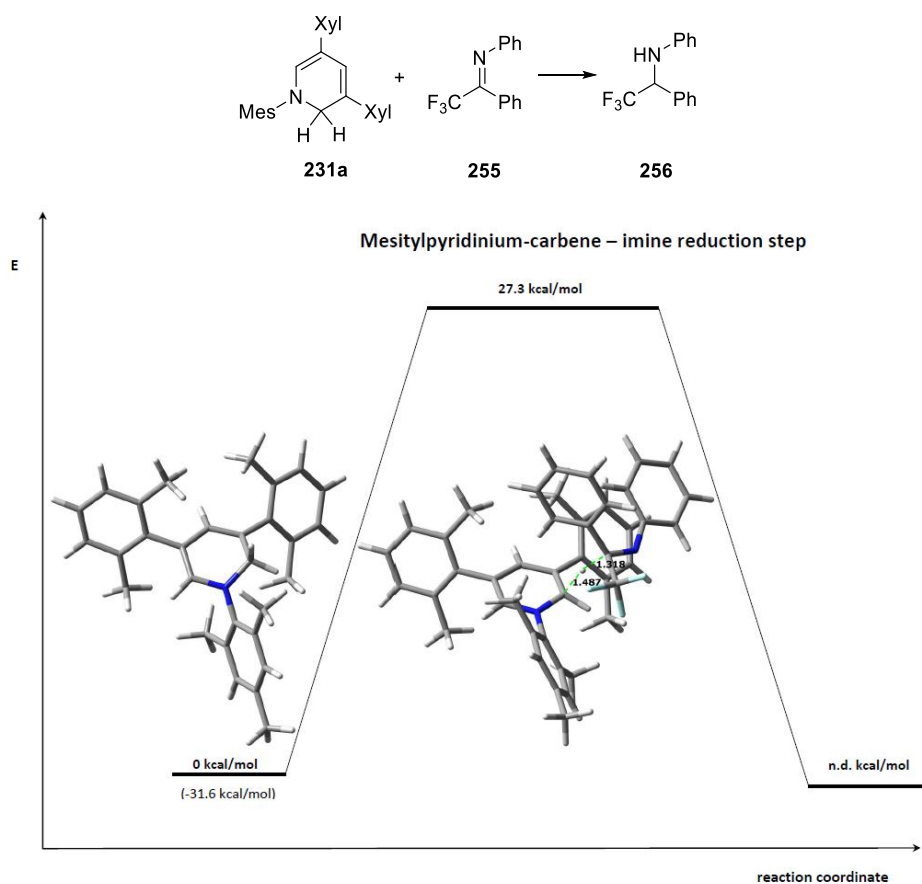


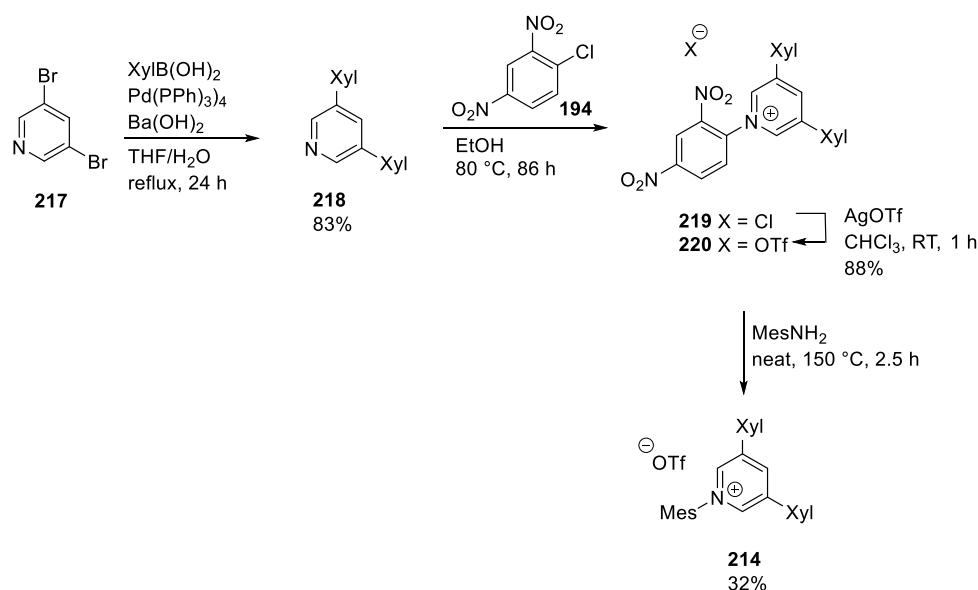
Figure 6.2. Energetic profile of the imine reduction step by mesitylpyridinium systems.

6.4. Synthesis

6.4.1. Preparation of Triaryl-Pyridinium Salts

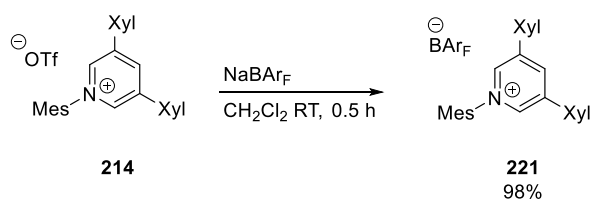
The pyridinium salt bearing three bulky aryl groups in the 1-, 3-, and 5-position was synthesized as described in the literature.^[95] Suzuki coupling of 3,5-dibromopyridine (**217**) and 2,6-dimethylphenylboronic acid (Xyl-B(OH)₂) in the presence of a palladium catalyst gave the corresponding pyridine **218** in 83% yield. Formation of the Zincke salt followed by counterion exchange afforded the Zincke salt **220** salt in high yields. Finally, the mesityl group was

introduced by Zincke reaction^[116] of **220** and 2,4,6-trimethylaniline to afford the desired product **214**.



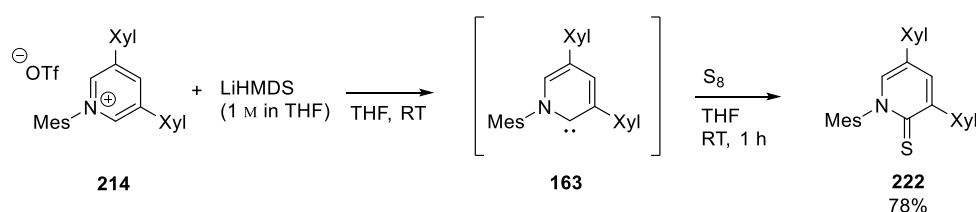
Scheme 6.2. Synthesis of pyridinium salt **214**.

The crucial reaction step is the last one, and in order to obtain the clean product **214**, careful purification proved to be essential to remove the presence of silver salts. Therefore, the crude reaction mixture was dissolved in toluene to precipitate the silver salts. After filtration, the excess of 2,4,6-trimethylamine had to be removed by vacuum distillation to facilitate crystallization of the product. After distillation, the product was recrystallized from toluene and chloroform to obtain the pyridinium salt **214** in 32% yield as an almost colorless solid. The whole sequence could be scaled up to 2 grams under the developed optimized reaction conditions. The corresponding BAR_F salt **221** could be prepared by dissolving **214** in dichloromethane and treatment with NaBAR_F followed by filtration of the precipitated sodium triflate (*Scheme 6.3*).



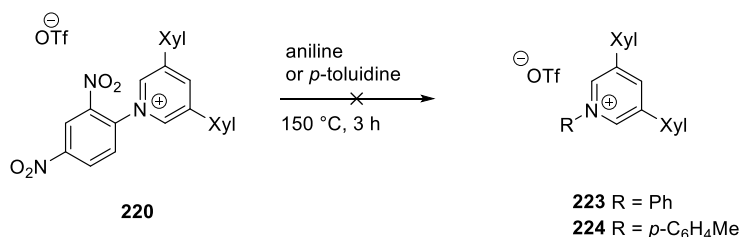
Scheme 6.3. Formation of pyridinium ion **221**.

Deprotonation of the pyridinium salt **214** by a strong base such as lithium hexamethyldisilazide (LiHMDS) leading to the formation of a pyridylidene species was described by *ITAMI*.^[95] The generation of the carbene was confirmed by trapping it with S₈ to form the corresponding 2-pyridinethione **222**, which could be characterized by NMR (*Scheme 6.4*). The 4-pyridylidene was not observed under these reaction conditions, which is in agreement with DFT calculations by the *ITAMI* group, who reported that the 2-pyridylidene is 13.3 kcal/mol more stable than the 4-pyridylidene. Unfortunately, the intermediate 2-pyridylidene could not be isolated or detected by NMR due to its high reactivity.



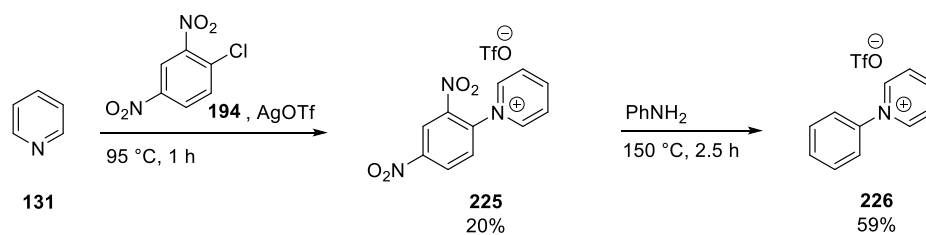
Scheme 6.4. Generation and trapping of 2-pyridylidene **163**.

With the Zincke salt **220** in hand, pyridinium salts with different substituents at the nitrogen atom could be synthesized. Introduction of the sterically less demanding phenyl or *para*-tolyl group was attempted but unfortunately the desired products were not obtained. The Zincke reaction gave only in very low yields and purification of the crude reaction mixture did not lead to the desired products (*Scheme 6.5*).



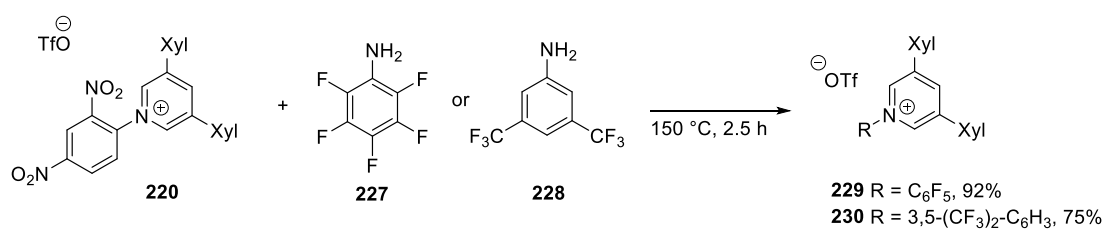
Scheme 6.5. Attempted synthesis of alternative pyridinium salts.

In a more successful approach, the synthesis of an *N*-phenylpyridinium salt was achieved. In this case pyridine was reacted with 1-chloro-2,4-dinitrobenzene to generate the Zincke salt **225**. Subsequent reaction with aniline gave the desired pyridinium salt in moderate yield (*Scheme 6.6*).



Scheme 6.6. Preparation of pyridinium salt **226**.

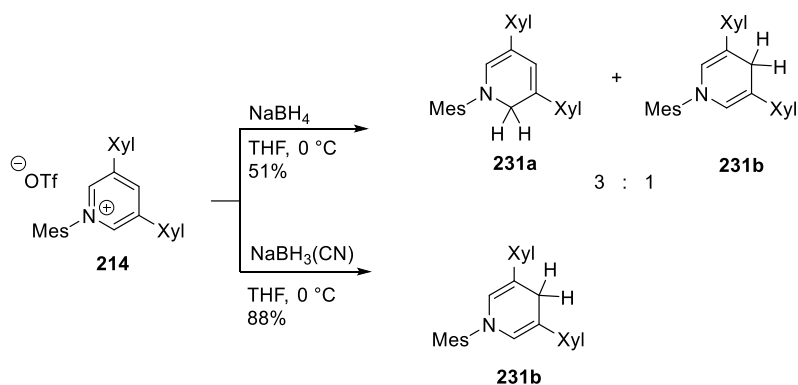
In principle, the reactivity of the pyridinium salt towards dihydrogen activation should be increased by introducing electron withdrawing groups attached to the nitrogen atom. Therefore, pyridinium salts with fluorinated phenyl groups were synthesized. Starting from the Zincke salt **220**, the fluorinated products **229** and **230** were obtained in good yields (*Scheme 6.7*).



Scheme 6.7. Synthesis of pyridinium triflates **229** and **230**.

6.4.2. Preparation of Authentic Samples

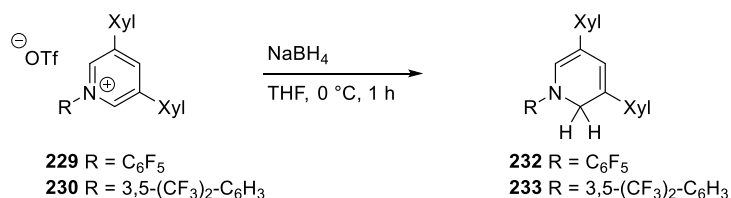
For the analysis of the H₂ activation experiments, it became necessary to prepare authentic samples of the corresponding dihydropyridines. Therefore, the pyridinium salt **214** was reduced with sodium borohydride as reducing agent. Interestingly, the reaction led to the 1,2-dihydropyridine **231a** (1,2-DHP) as major product containing small amounts of 1,4-dihydropyridine **231b** (1,4-DHP), whereas the reduction with sodium cyanoborohydride gave exclusively the 1,4-DHP **231b** (*Scheme 6.8*). Both products were identified by ²D NMR analysis. Both of these compounds are stable as solids, but tend to rearomatize in solution.



Scheme 6.8. Preparation of authentic samples of dihydropyridine **231a** and **231b**.

As next step, the implementation of a purification strategy was aimed, which could then be used for the purification of the dihydrogen activation reaction. Unfortunately, attempts to purify the 1,4-DHP **231b** by column chromatography were unsuccessful, even when neutral or basic alumina was used as solid phase. In contrast, filtration over neutral-alumina and ethyl acetate as eluent gave the 1,2-DHP **231a** as beige solid.

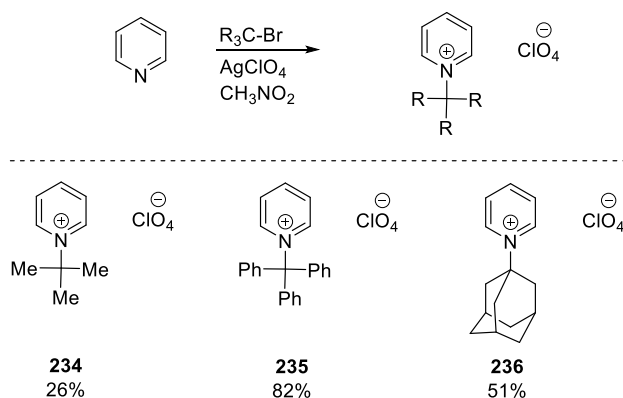
Reduction of fluorinated pyridinium salts **229** and **230** with sodium borohydride showed in both cases only traces of the corresponding reduced compounds (*Scheme 6.9*). Purification by column chromatography was not possible, as the products decomposed very rapidly.



Scheme 6.9. Preparation of authentic samples of dihydropyridines **232** and **233**.

6.4.3. Preparation of *N-tert*-Alkylpyridinium Salts

In an alternative approach, the synthesis of *N-tert*-alkylpyridinium salts was attempted. *N-tert*-alkylpyridinium salts could be prepared using the corresponding alkyl bromide and silver perchlorate in nitromethane (*Scheme 6.10*).^[117-118]



Scheme 6.10. Preparation of *N-tert*-alkylpyridinium salts.

As shown in *Scheme 6.10*, three different *N-tert*-alkylpyridinium salts could be synthesized. The *tert*-butylpyridinium salt **234** was obtained in poor yield, whereas **235** and **236** could be isolated in moderate to good yields. The synthesis of the 1-phenyl-2-dimethyl pyridinium salt was not successful. All salts were then tested in dihydrogen activation reactions.

6.5. Dihydrogen Activation Results

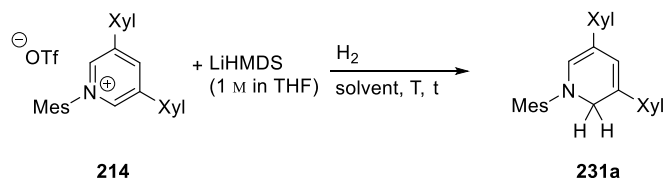
6.5.1. Hydrogenation of Triaryl-Pyridinium Salts

The prepared pyridinium salts were evaluated in base-induced dihydrogen activation reactions (*Table 6.1*). Firstly, very mild conditions such as those described by *BERTRAND* were tested.^[10] They used one equivalent of the carbene precursor and 2.25 equivalents of the base in a 1:1 mixture of THF and toluene. The reaction mixture was stirred for 20 minutes to ensure complete deprotonation. Afterwards, the reaction mixture was treated with 1 bar of hydrogen pressure. Analysis of the crude reaction mixture showed no product formation under these reaction conditions (*Table 6.1*, entries 1 and 2).

With the goal of applying more forcing reaction conditions, the reactions were set up in an autoclave under ambient pressure. The different set up would allow the use of higher hydrogen pressures instead of just 1 bar of gas, as reported by *BERTRAND* and co-workers. Again, after setting up the reaction, the resulting mixture was stirred for 20 minutes before

pressurizing with H₂. After the reaction was finished, the crude mixture was concentrated and dried under high vacuum and analyzed by NMR.

Table 6.1. Activation of H₂ under different reaction conditions.



Entry	H ₂ [bar]	T [°C]	t [h]	solvent	Conv. into 231a [%] ^[a]
1	1	40	2	THF/toluene	--
2	1	50	5	THF/toluene	--
3	50	50	24	THF/toluene	traces
4	100	50	24	THF/toluene	traces
5	100	RT	24	THF/toluene	--
6	10	50	24	THF/toluene	--
7	50	50	24	THF	traces
8	50	50	24	toluene	21
9	50	80	24	toluene	--
10	50	50	60	toluene	--
11	50	50	5	toluene	traces
12	100	50	24	toluene	30
13	100	80	24	toluene	16
14	100	50	15	toluene	33
15	100	50	30	toluene	13
16	100	50	5	toluene	51 ^[b]
17	100	50	2	toluene	10 ^[b]

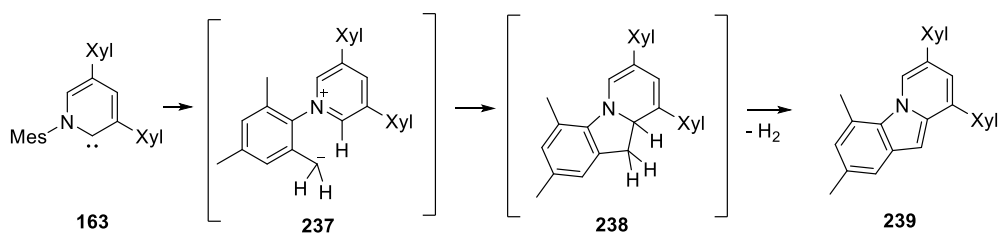
[a] Estimated by ¹H NMR analysis of the crude reaction mixture. [b] The autoclave was pressurized directly with H₂.

Using 50 and 100 bar of H₂ at 50 °C for 24 h, traces of the desired 1,2-DHP **231a** were observed by NMR (*Table 6.1*, entries 3 and 4). Lowering of the reaction temperature or the pressure did not lead to product formation (*Table 6.1*, entries 5 and 6).

When THF was used as solvent, only traces of the 1,2-DHP **231a** were observed. Changing the solvent to toluene improved the result significantly and 21% of the desired product was

observed (*Table 6.1*, entry 8). Although the pyridinium salt **214** is not fully soluble in toluene, the generated carbene went into solution once deprotonation happened. Higher temperatures and longer reaction times did not improve the outcome of the reaction and decomposition products were observed (*Table 6.1*, entries 9, 10 and 13). The pressure was increased to 100 bar H₂ which improved the conversion of **214** into **231a** was to 30% (*Table 6.1*, entry 12). Longer reaction times than 24 h were not beneficial to further increase the conversion, which is in the best case was around 30% (*Table 6.1*, entries 12, 14 and 15).

In every case the pyridinium salt **214** was completely consumed and a mixture of products was observed. Among the products formed the desired 1,2-DHP **231a** could be assigned by NMR. Column chromatography was used in order to purify the desired dihydropyridine, but as explained before, this material was found to be unstable under chromatographic conditions. Nevertheless, during these attempts to isolate the 1,2-DHP **231a** from the crude mixture, a major side product **239** was isolated as a yellow solid. NMR analysis revealed that such compound was formed as a result of a rearrangement reaction which has already been described by *ITAMI* (*Scheme 6.11*).^[95] The authors provided a plausible mechanism, in which a proton is transferred from the benzylic position of the mesityl group the carbene, generating a zwitterionic compound **237**. Nucleophilic attack of the reactive methylene leads to intermediate **238**, which rearomatizes under loss of H₂ to **239**.

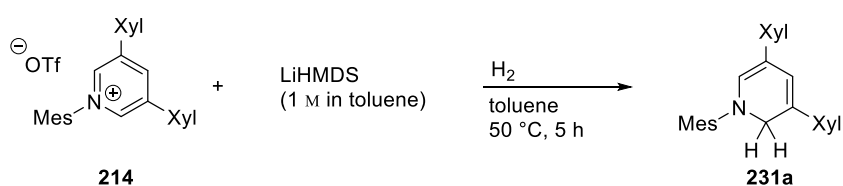


Scheme 6.11. Proposed mechanism for the conversion of pyridylidene **163** into byproduct **239**.

Therefore, it seems reasonable to assume that during the hydrogen activation a competitive reaction is taking place. Moreover, as the carbene is highly reactive, the intramolecular deprotonation might be faster than the hydrogen splitting. To inhibit this process, the autoclave was directly pressurized with H₂, thus avoiding the premix time of 20 minutes. By using the optimized reaction conditions (100 bar H₂, 50 °C), the conversion to **231a** could be improved up to 51% (*Table 6.1*, entry 15) and no byproduct **239** was formed.

As THF proved not be the best solvent, LiHMDS was changed from a 1.0 M solution in THF to a 1.0 M solution in toluene. Using this base under the optimized reaction conditions led to full conversion to the desired 1,2-DHP **231a**. A screening at different pressures revealed that full conversion of pyridinium ion **214** into 1,2-DHP **231a** also occurred at 50 bar H₂, but was incomplete at 10 bar H₂ (*Table 6.2*, entries 2 and 3). Consequently, further dihydrogen activation reactions were conducted using 50 bar H₂ at 50 °C in toluene as standard reaction conditions.

Table 6.2. Dihydrogen activation under optimized reaction conditions.

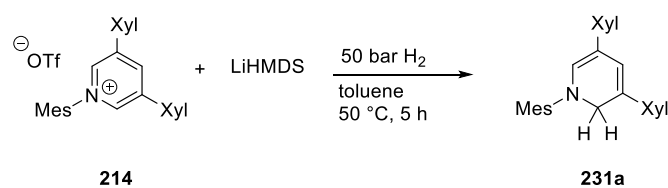


Entry	H ₂ [bar]	Conv. into 231a [%] ^[a]
1	100	100
2	50	100
3	10	71

[a] Estimated by ¹H NMR analysis of the crude reaction mixture.

The presence of the desired dihydropyridine **231a** was clearly observed by ¹H and ¹³C NMR. Comparison of the NMR data of the generated dihydropyridine and the authentic sample showed a perfect match. ¹³C NMR clearly confirmed the presence of the newly formed CH₂ group in the product **231a** at 52.0 ppm.

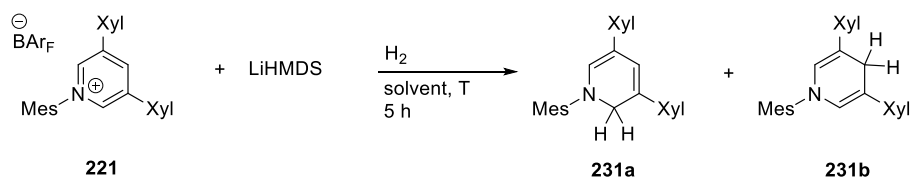
Furthermore, the amount of base was evaluated. As summarized in *Table 6.3*, the use of 0.5 eq. and 1 eq. of LiHMDS did not lead to product formation (entries 1 and 2). Increasing the amount of base to 1.5 eq. gave 21% conversion to the desired 1,2-DHP **231a** (entry 3). In order to reach full conversion, 2.25 eq. of LiHMDS were necessary (entry 4).

Table 6.3. Screening of the amount of base.

Entry	Pyridinium salt [eq.]	LiHMDS [eq.]	Conv. into 231a [%] ^[a]
1	1	0.5	--[b]
2	1	1	--[b]
3	1	1.5	21
4	1	2.25	100

[a] Estimated by ¹H NMR analysis of the crude reaction mixture, [b] Formation of side products detected.

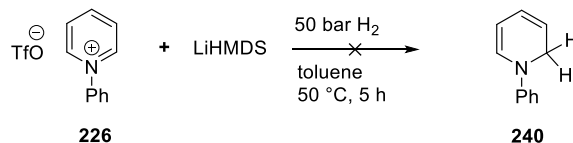
The influence of the counterion was also tested. The corresponding BAR_F salt **221** was used for H₂ activation reactions to study the influence of a sterically demanding non-coordinating counterion. Interestingly, whilst using standard reaction conditions, NMR analysis of the crude reaction mixture showed a 1:1 mixture of both, 1,2- and 1,4-DHP (*Table 6.4*, entry 1). The conversion towards both products could be increased by increasing the hydrogen pressure to 100 bar H₂ and the reaction temperature, although full conversion was not observed (entry 2). Changing the solvent to THF lead to 27% conversion to the 1,2-DHP **231a**. In this case, only the 1,2-DHP **231a** was formed.

Table 6.4. H₂ activation of the BAR_F salt **221**.

Entry	H ₂ [bar]	solvent	T [°C]	Conv. 231a [%] ^[a]	Conv. 231b [%] ^[a]
1	50	toluene	50	10	10
2	100	toluene	100	21	24
3	50	THF	50	27	--

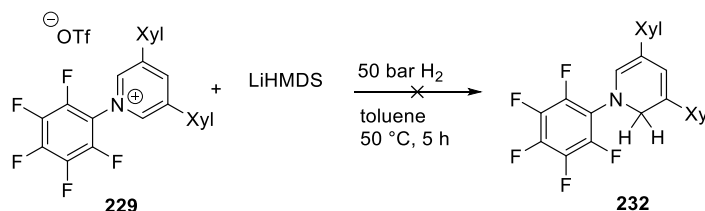
[a] Estimated by ¹H NMR analysis of the crude reaction mixture.

Furthermore, the *N*-phenylpyridinium salt **226** was tested for H₂ activation reactions. Under the established protocol, only decomposition of the starting materials were observed (*Scheme 6.12*).



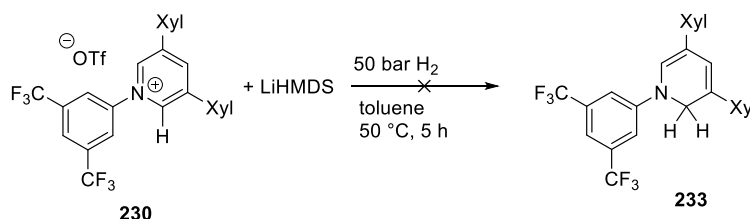
Scheme 6.12. Attempted H₂ activation using *N*-phenylpyridinium triflate **226**.

Fluorinated substituents at the nitrogen atom should increase the acidity of the pyridine H atoms. This would enable the use of a milder base for the pyridylidene formation. First, the pentafluoropyridinium triflate **229** was tested. In the presence of LiHMDS and standard reaction conditions, only decomposition was observed (*Scheme 6.13*).



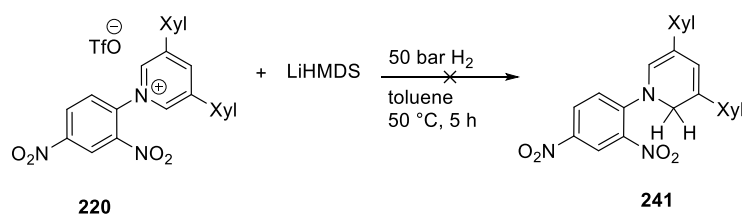
Scheme 6.13. Attempted H₂ activation with pentafluoropyridinium triflate **229**.

An alternative to the pentafluorophenyl derivative is the 3,5-bis(trifluoromethyl)-phenyl group since it has an similar electronic effect on the pyridinium ring. Again, it was tested for the H₂ activation, but reaction with LiHMDS led to decomposition (*Scheme 6.14*).



Scheme 6.14. Attempted H₂ activation with 3,5-bis(trifluoromethyl)-phenylpyridinium triflate **230**.

As the Zincke salt **220** itself is a pyridinium salt containing an electron withdrawing substituent, it might also be used for the H₂ activation process. Therefore the Zincke salt **220** was also tested for H₂ activation, but this approach led to decomposition only (*Scheme 6.15*).

Scheme 6.15. Attempted H₂ activation.

6.5.2. Hydrogenation of *N*-*tert*-Alkylpyridinium Salts

The prepared *N*-*tert*-alkylpyridinium salts were also tested for hydrogen activation under the optimized reaction conditions as summarized in *Table 6.5*. The reaction resulted in either formation of a complex product mixture or decomposition of the starting materials. The formation of the desired products was not observed. Due to these poor results, the *N*-*tert*-alkylpyridinium salts were not further studied.

Table 6.5. Dihydrogen activation using *N*-*tert*-alkylpyridinium salts.

Entry	pyridinium ion	Conv. [%] ^[a]
1	 234	Complex mixture
2	 235	Complex mixture
3	 236	decomposition

[a] Estimated by ¹H NMR analysis of the crude reaction mixture.

6.5.3. Reaction with Deuterium Gas

As explained in the previous chapters, to obtain further evidence for a dihydrogen cleavage process, a series of tests were run using D_2 gas instead of H_2 . 2H NMR should be an ideal method for detecting even trace amounts of the desired products.

First, the reaction was conducted under the standard reaction conditions established in the experiments with H_2 gas (50 bar D_2 , 50 °C, 5 h). If deuterium incorporation happened, a signal at around 4.31 ppm would be expected, since it should have the same shift as the CH_2 group observed after the hydrogen activation reaction described earlier. Gratifyingly, the 2H NMR of the reaction showed a signal at 4.30 ppm (*Figure 6.3*), which could be assigned to the CD_2 group. This result represented a clear proof of principle for the H_2 splitting process.

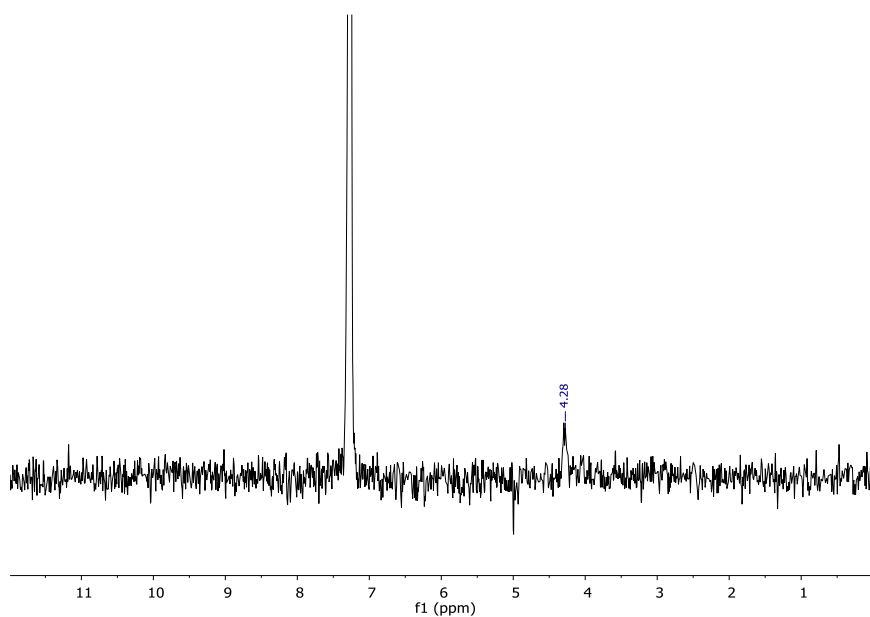


Figure 6.3. 2H NMR of deuterium splitting experiment, $CDCl_3$ (7.26 ppm) as internal standard in $CHCl_3$.

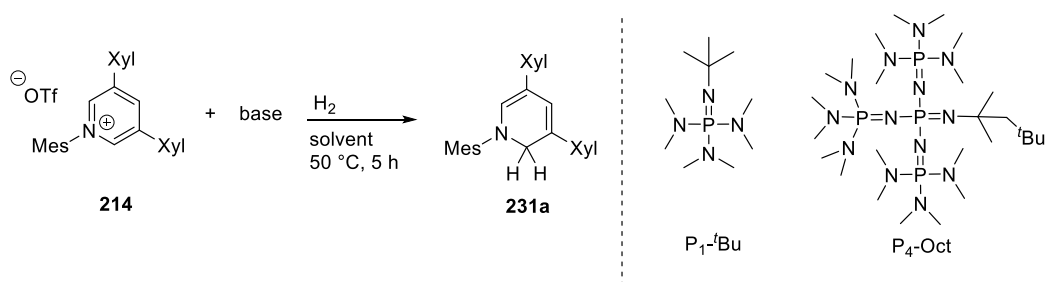
The 1H NMR of the reaction mixture also showed the presence of unreacted starting materials, which indicates that the reaction with deuterium gas needs longer to proceed. Consequently, the reaction time was prolonged to 24 h. The 2H NMR spectrum showed that the signal of the CD_2 group had increased. Furthermore, 1H NMR indicated full consumption of the starting materials. Calculations performed by *PADEVET* in the Pfaltz research group indicate that the kinetic isotope effect (KIE) has a value of 3.24. This means that the reaction with D_2 would be about three times slower than with H_2 .

Interestingly, the ^1H NMR analysis of the experiments with deuterium gas also showed the presence of 31% of the CH_2 group of the 1,2-DHP **231a** at 4.31 ppm. As 99.98% pure D_2 was used, the observed H_2 incorporation is assumed to result from hydride transfer between the dihydropyridine and the pyridinium salt. An experiment with a 4:1 mixture of D_2/H_2 was performed to see if the amount of non-deuterated 1,2-DHP **231a** can be increased. ^1H NMR analysis of the resulting reaction mixture revealed an increase from 31% to 63%. This finding clearly demonstrates the high reactivity of the carbene towards H_2 splitting.

6.6. Optimization

6.6.1. Variation of the Base

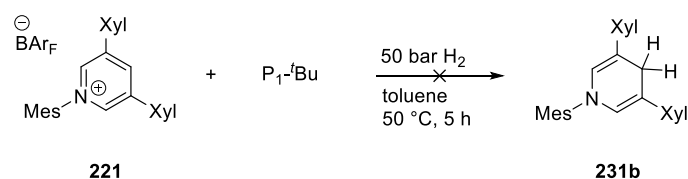
Having established a method to activate dihydrogen with 2-pyridylidenes, the next goal was to render the reaction catalytic. LiHMDS is a very strong base with a pK_a of 26, and for this reason the release of the proton from its conjugated acid is not favored: an alternative base of lower pK_a had to be found to facilitate catalysis. A potential solution could be represented by phosphazenes,^[119] which have a tunable basicity and are non-nucleophilic nitrogen bases. A prominent example of this class is the Schwesinger base^[119] with a pK_a of the conjugated acid of 42.7. Starting from the standard system, first test reactions with the pyridinium salt **214** and two different phosphazene bases $\text{P}_1\text{-}^t\text{Bu}$ and $\text{P}_4\text{-Oct}$ were conducted (*Table 6.6*). With toluene as solvent, no reaction was observed and only starting materials were recovered (entries 1 and 2). When THF was used instead, a mixture of products was observed containing traces of the desired 1,2-DHP (entries 3 and 4). Unfortunately, the mixture could not be further analyzed since the products were not stable and could not be isolated by column chromatography.

Table 6.6. Reactions with phosphazene bases.

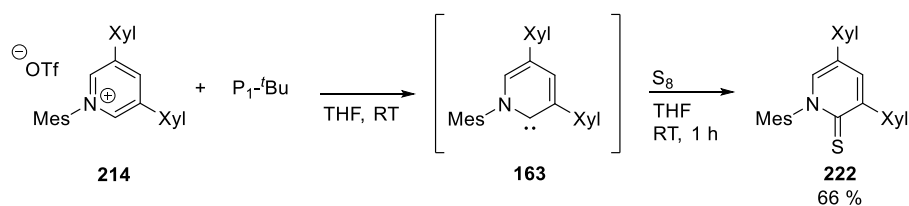
Entry	base	H ₂ [bar]	solvent	Conv. into 231a [%] ^[a]
1	P ₁ - ^t Bu	100	toluene	--
2	P ₁ - ^t Bu	50	toluene	--
3	P ₁ - ^t Bu	100	THF	mixture
4	P ₄ -Oct	50	THF	mixture

[a] Estimated by ¹H NMR analysis of the crude reaction mixture.

It appeared that in toluene, where only traces of the pyridinium salt **214** were dissolved, the base is not able to deprotonate the pyridinium salt **214**. In THF, the starting materials were completely soluble, but analysis of the crude reaction solution revealed a complex mixture of products. To overcome this issue, the corresponding BAr_F salt **221** was used instead (*Scheme 6.16*). Unfortunately, the desired 1,4-DHP **231b** could not be detected and formation of product mixtures was observed.

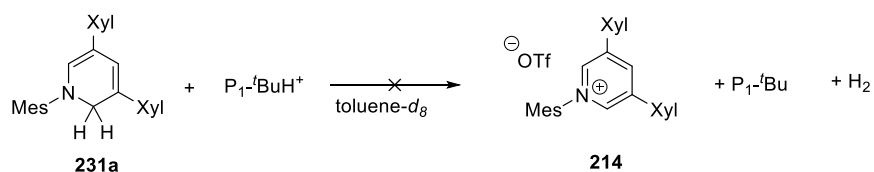
**Scheme 6.16.** Reaction with phosphazene base.

To test if the base was strong enough to deprotonate the pyridinium salt **214**, a test experiment was conducted in which the generated carbene **163** was quenched with sulfur as depicted in *Scheme 6.17*.



Scheme 6.17. Trapping of the pyridylidenes **163** with sulfur.

The corresponding sulfur compound **222** was formed with 66% yield. This clearly showed that the base was strong enough to deprotonate the pyridinium salt and H₂ activation should therefore be possible. A reason why the H₂ activation was not observed might be that H₂ activation is reversible with phosphazene bases. Thus an NMR experiment was conducted in which the 1,2-DHP **231a** and protonated P₁-^tBu, obtained from reaction with trifluoromethanesulfonic acid in toluene-*d*₈, were mixed to see if H₂ evolution would occur. Unfortunately, the experiment was not successful and no gas evolution could be detected (*Scheme 6.18*).



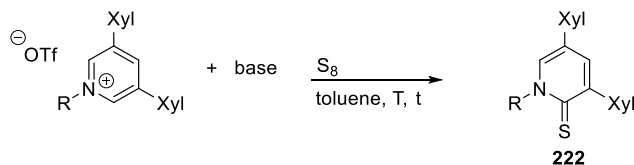
Scheme 6.18. H₂ release experiment.

The reaction with LiHMDS and the fluorinated pyridinium salts **229** and **230** only led to decomposition. Since the proton of the pyridinium ring in these systems should be more acidic, it might be possible to use a milder base such as diisopropylethylamine (DIPEA). Additionally, other strong bases were investigated: DBU, DIPEA, Verkade's base,^[119] and P₁-^tBu. First, the ability of the base to deprotonate the pyridinium salt was tested by quenching of the generated carbene with sulfur (*Table 6.7*).

In the case of pentafluorophenylpyridinium triflate **229**, decomposition was observed when DBU was used (entry 1). With DIPEA, no reaction was observed at room temperature (entry 2), but the formation of the desired product along with small impurities was detected when ambient reaction conditions were applied (entry 3). Lowering the reaction temperature to inhibit potential side reaction did not improve the outcome of the reaction (entry 4). Employing Verkade's base and P₁-^tBu resulted in the formation of complex product mixtures

(entries 5 and 6). Reaction of 3,5-bis(trifluoromethyl)-phenylpyridinium triflate **230** with the 4 different bases and S_8 gave complex mixture of products in every case (entries 7-10).

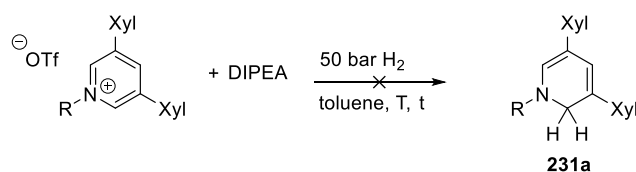
Table 6.7. S_8 trapping experiments with different bases.



Entry	R	base	T [°C]	t [h]	Conv. [%] ^[a]
1		DBU	RT	2	decomposition
2		DIPEA	RT	2	--
3		DIPEA	50	15	mixture
4		DIPEA	0	5	mixture
5		229	Verkade's base	RT	2
6		P_1 - ^t Bu	RT	2	mixture
7		DBU	RT	1	mixture
8		DIPEA	RT	1	mixture
9		Verkade's base	RT	1	mixture
10		230	P_1 - ^t Bu	RT	1

[a] Estimated by ¹H NMR analysis of the crude reaction mixture.

Although reaction with DIPEA led to the formation of mixtures, the ¹H NMR spectra of these reactions showed less byproducts compared to reaction with the other bases. Consequently, DIPEA was used for the reaction with dihydrogen (*Table 6.8*). The pentafluorophenylpyridinium salt showed a mixture of different products after 5 h at 50 °C, but the desired products were not observed. To prevent the formation of side products, the reaction temperature was lowered. The reactions were set up at -78 °C and the reaction with H₂ gas was conducted at 0 °C. Unfortunately, the same product mixture was observed (entry 2). Reaction with **230** and H₂ in the presence of DIPEA led to decomposition (entries 3 and 4).

Table 6.8. Attempted H₂ activation with DIPEA.

Entry	R	T [°C]	t [h]	Conv. [%] ^[a]
1		50	5	mixture
2	229	0	15	mixture
3		50	5	decomposition
4	230	0	15	decomposition

[a] Estimated by ¹H NMR analysis of the crude reaction mixture.

6.7. Application

6.7.1. Reduction with Authentic Samples

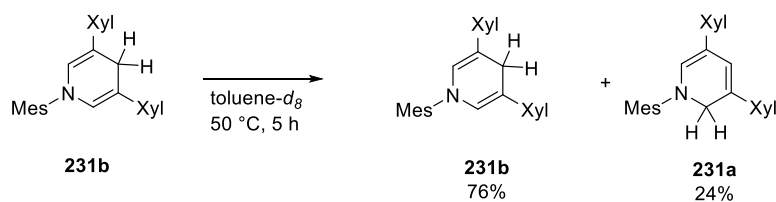
Dihydropyridines are known for their ability to reduce electrophilic C=C, C=O or C=N bonds. To show the utility of the developed dihydropyridines as reductants, test reactions were conducted starting from authentic samples. If reduction were observed in the isolated system, the substrate could then be used as trapping agent during the H₂ activation reaction. Both authentic samples, the 1,2-DHP **231a** and the 1,4-DHP **231b** were used for these reactions.

Table 6.9. Initial reductions of standard substrates.

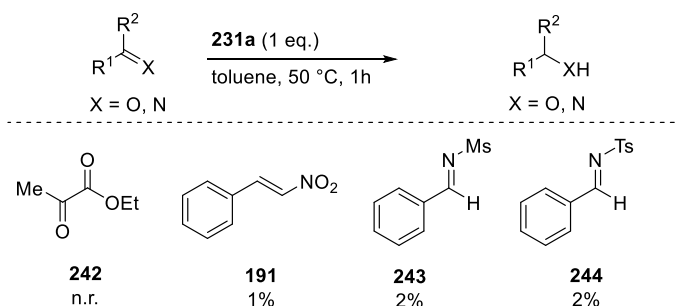
Entry	substrate	DHP	Conv. [%] ^[a]
1	139	1,2-DHP 231a	--
2	139	1,4-DHP 231b	--
3	145	1,2-DHP 231a	25
4	145	1,4-DHP 231b	--
5	142	1,2-DHP 231a	2
6	142	1,4-DHP 231b	1

[a] Estimated by ¹H NMR analysis of the crude reaction mixture.

The test reactions were set up in screw capped vials. After heating the reaction mixture to 50 °C for one hour, the solution was concentrated and analyzed by NMR. First, benzaldehyde was used as substrate. Both dihydropyridines showed no reactivity towards the aldehyde and only starting materials were recovered (*Table 6.9*, entries 1 and 2). Then, a sterically demanding imine was used, which is a standard substrate for the reduction with FLPs. In the case of 1,2-DHP **231a**, the ¹H NMR spectra showed around 25% conversion to the corresponding amine, whereas the 1,4-DHP **231b** showed no reactivity (entries 3 and 4). When acetophenone was used as substrate, only traces of the corresponding alcohol could be detected by ¹H NMR (entries 5 and 6). Interestingly, the 1,4-DHP **231b** showed less reactivity, but in every case mixtures of the 1,2-DHP **231a** and 1,4-DHP **231b** were observed. This indicates that by heating a solution of the 1,4-DHP **231b**, it interconverts into the thermodynamically more stable 1,2-DHP **231a**. Under H₂ activation conditions, 24% of the 1,2-DHP was observed as reported in *Scheme 6.19*.

**Scheme 6.19.** Interconversion of 1,4-DHP **231b** into 1,2-DHP **231a** under hydrogen activation conditions.

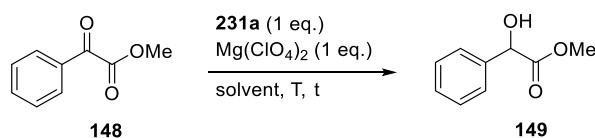
Based on these findings, further substrates were tested for the reduction only deploying the 1,2-DHP **231a**. There was no reduction towards activated C=O groups observed. Also nitroolefins and sulfonylimines showed only traces of reduction (*Scheme 6.20*).



Scheme 6.20. Reduction of various substrates.

In Nature, the most common example for reduction mediated by a dihydropyridine is the reduction process of NADH. The chemistry of NADH and NADH models has been extensively studied. Usually, they undergo reactions with pyruvate derivatives in the presence of magnesium perchlorate.^[90] Therefore, methyl benzoylformate was used as model substrate for the reduction with 1,2-DHP **231a**. In acetonitrile at room temperature, no reduction to the corresponding methyl mandelate was observed (*Table 6.10*, entry 1). The same result was observed when the reaction temperature was increased to 80 °C (entry 2). Unfortunately changing the solvent to toluene to reach higher reaction temperatures showed again no reduction (entry 3).

Table 6.10. Attempted reduction of methyl benzoylformate.

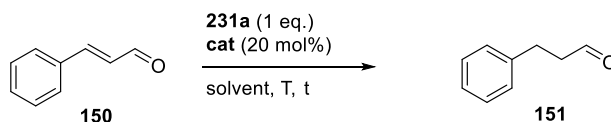


Entry	solvent	T [°C]	t [h]	Conv. [%] ^[a]
1	MeCN	RT	24	--
2	MeCN	80	24	--
3	toluene	110	24	--

[a] Estimated by ¹H NMR analysis of the crude reaction mixture.

Moreover, the organocatalytic reduction of α,β -unsaturated aldehydes was tested starting from the 1,2-DHP **231a**. Cinnamaldehyde (**150**) was used in the presence of the MACMILLAN catalyst,^[67] but the reaction showed only in one case the formation of a product mixture which, however, did not contain 3-phenylpropionaldehyde **151** (Table 6.11, entry 1). In the other cases, no reaction was observed (entries 2 and 3).

Table 6.11. Attempted organocatalytic reductions.

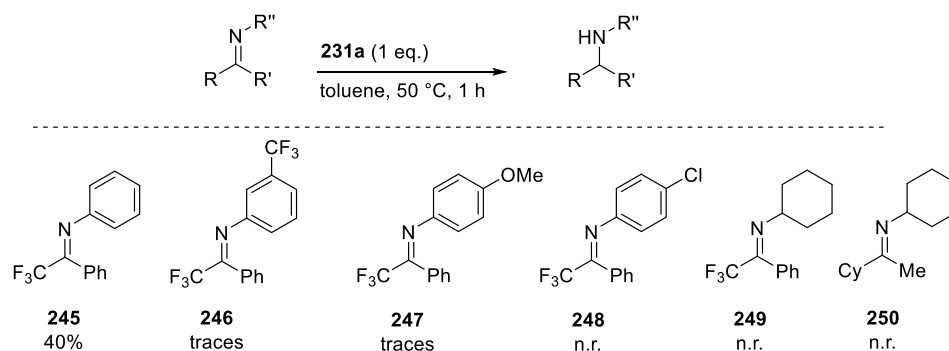


Entry	catalyst	solvent	T [°C]	t [h]	Conv. [%] ^[a]
1		THF	50	1	mixture
2		CHCl ₃	0	24	--
3		toluene	0	24	--
4		toluene	50	5	--
5		toluene	50	24	--
6		CHCl ₃	0	1	--
7		EtOH	78	24	--

[a] Estimated by ¹H NMR analysis of the crude reaction mixture.

The same reaction was conducted with pyrrolidine as catalyst, since it is similar to the JØRGENSEN catalyst,^[120] but less sterically demanding. Starting with the standard reaction conditions, no reaction was observed, even after longer reaction time (entries 4 and 5). In chloroform, and low temperature, again no conversion was detected (entry 6). As described in the literature, also ethanol was used as solvent. Again, cinnamaldehyde could not be reduced with the 1,2-DHP **231a** (entry 7).

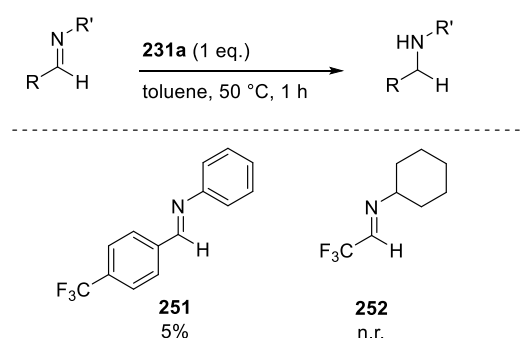
As the initial reduction of imines gave the most promising results so far, the ability of the 1,2-DHP **231a** to reduce these substrates was further investigated. In order to use more reactive and electrophilic substrates, a series of activated imines were synthesized and tested. First, ketimines **245-250** containing a CF₃ group were examined (Scheme 6.21).^[121]



Scheme 6.21. Reduction of ketimines.

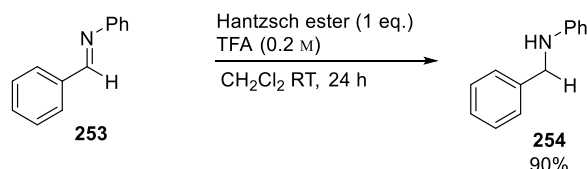
Gratifyingly, imine **245** could be reduced to the corresponding amine in 40% conversion as detected by ^1H NMR and GC/MS. For imines **246** and **247**, only traces (< 2%) of the amine were observed. The other imines could not be reduced by the 1,2-DHP. The same reactions were repeated in the presence of LiOTf and HMDS, since both compounds were formed during the hydrogen activation process. The reactions gave the same results as before, which means that these salts should have no influence on the reduction.

In the next step, two different aldimines were tested. Although aldimines are supposed to be more reactive, imine **251** could only be reduced with 5% conversion and imine **252** was not reduced at all (*Scheme 6.22*).



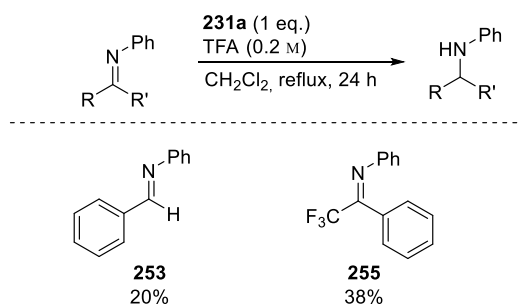
Scheme 6.22. Reduction of aldimines.

It has been reported that imines are not reduced by the Hantzsch ester in neutral media, but have to be activated prior to reduction by conversion into the iminium compounds by alkylation or by coordination to metal ions. The SINGH group reported that (*E*)-*N*-1-diphenylmethanimine (**253**) can be reduced to the corresponding amine in the presence of trifluoroacetic acid (TFA) in good yields (*Scheme 6.23*).^[122]



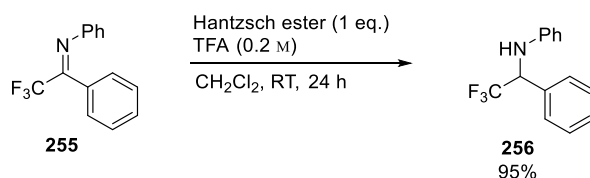
Scheme 6.23. Literature example of the reduction of an imine in the presence of trifluoroacetic acid.

Under the same reaction conditions, only conversion around 3% were observed when the Hantzsch ester was replaced with 1,2-DHP **231a**. In order to increase the conversion of the reduction of the developed system, the reaction mixture was heated to reflux for 24 h. For the same imine as used in the literature example, 20% conversion to the corresponding amine could be detected (*Scheme 6.24*). In the case of imine **255**, results similar to previous findings were observed.



Scheme 6.24. Reduction of imines with 1,2-DHP in the presence of TfOH.

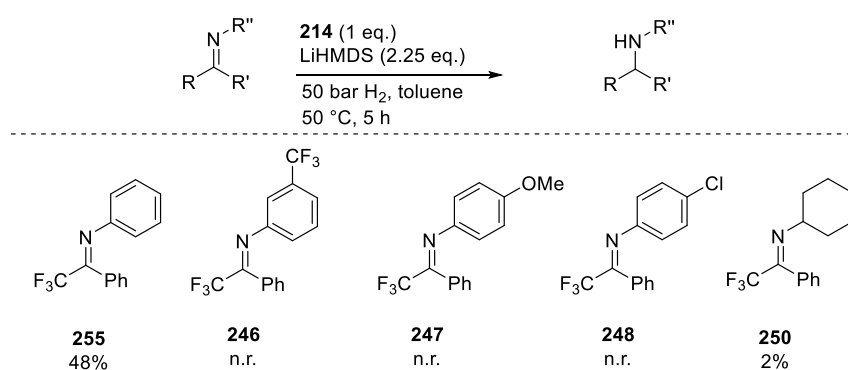
For comparison of the hydride donors, the reduction of imine **255** was carried out with the Hantzsch ester as hydride donor (*Scheme 6.25*). In this case, almost full conversion to the amine was observed. This indicates that the developed 1,2-dihydropyridine **231a** is a weaker hydride donor than the Hantzsch ester.



Scheme 6.25. Control experiment with Hantzsch ester.

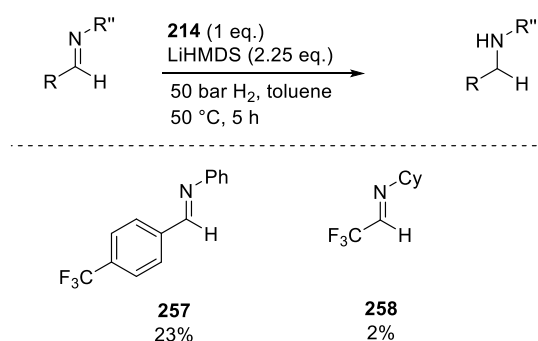
6.7.2. *In-Situ* Reduction

The reduction of imines, which so far had given the best results with the 1,2-DHP, served as starting point for this study. The conversion to the corresponding amine was analyzed by quantitative ^{19}F NMR. Due to the fact that all substrates contained a CF_3 group, the analysis by ^{19}F NMR proved to be an easy and effective method for this purpose. In a series of ketimines that were screened in this reaction, imine **255** stood out as the most promising substrate, providing a conversion of 48% (Scheme 6.23).



Scheme 6.26. *In-situ* screening with different ketimines.

Only moderate conversions were achieved by using aldimines. Compound **257** was reduced with 23% conversion, whereas reaction with **258** led only to traces of the desired amine.

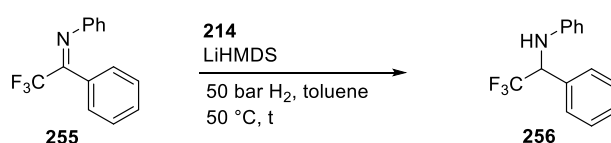


Scheme 6.27. *In-situ* screening with two aldimines.

In the next study, several conditions for the reduction of imine **255** were investigated. It turned out that the ratio between the reagents was crucial. Under standard reaction conditions, 48% conversion to the corresponding amine **256** was observed (Table 6.12, entry 1). Doubling the amount of imine increased the conversion to 92% (entry 2). In order to

get to full conversion, the reaction time was prolonged to 13 h. By doing this, higher conversions could be obtained, but also the formation of side products was observed (entries 3-5). Satisfyingly, lowering the amount of pyridinium salt to 20 mol% led to full reduction of the imine. However, it should be noted that the amount of base had to be in a 1:1 ratio with the imine, otherwise the conversion dropped significantly (entries 6 and 7). Lowering the amount of pyridinium salt to 10 or 5 mol% led to incomplete reduction as well as formation of side products (entries 8 and 9).

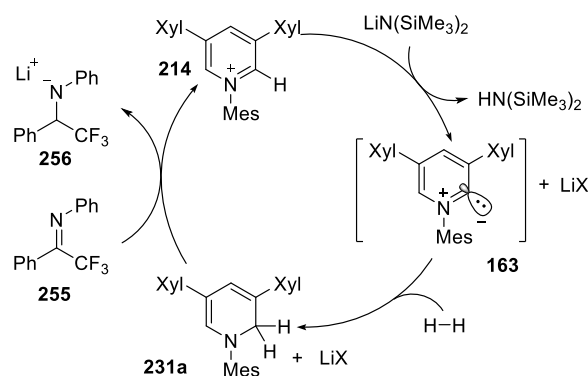
Table 6.12. Optimization of reaction conditions.



Entry	Pyridinium salt [eq.]	Imine [eq.]	LiHMDS [eq.]	t [h]	Conc. [g/mol]	Conv. 256 [%] ^[a]
1	1	1	2.25	5	0.1	48
2	1	2	2.25	5	0.1	92
3	1	1	2.25	13	0.1	95 ^[b]
4	1	2	2.25	13	0.1	95 ^[b]
5	1	1	1	13	0.02	10 ^[b]
6	0.2	1	1	5	0.1	100
7	0.2	1	0.5	5	0.1	10
8	0.1	1	1	5	0.1	65 ^[b]
9	0.05	1	1	5	0.1	85 ^[b]
10	--	1	2.25	5	0.1	--

[a] Estimated by ¹⁹F NMR analysis of the crude reaction mixture, [b] Formation of side products detected.

With the optimized reaction conditions in hand (50 bar H₂, 50 °C, 5 h, 20 mol% **214**), the reaction was performed on a preparative scale (0.27 mmol imine **255**). After column chromatography, amine **256** was obtained in 82% yield. In a control experiment without pyridinium salt **214** no amine **256** was formed (entry 10), ruling out base-induced heterolytic H₂ splitting. Based on these results and DFT calculations, a catalytic cycle for the observed imine reduction is proposed in *Scheme 6.28*.



Scheme 6.28. Proposed catalytic cycle

Pyridylidene **163** generated from pyridinium salt **214** can add H_2 to the carbenoid center of **163**. The resulting dihydropyridine **214** can act as reducing agent towards an imine.

6.8. Summary

In summary, the synthesis of several pyridinium salts was achieved. In the presence of LiHMDS, the corresponding pyridylidene was generated from the mesitylpyridinium salt and could be quenched by reaction with S_8 . Furthermore, an efficient process for the activation of dihydrogen via a pyridylidene intermediate was developed. Dihydrogen activation was confirmed by comparison of the obtained 1,2-dihydropyridine with authentic samples as well as splitting of D_2 and subsequent 2H NMR analysis. When the reaction was conducted in the presence of imine **255**, hydride transfer to the C=N bond was observed. In the presence of stoichiometric amounts of base, *in-situ* reduction of imine **255** gave full conversion with 20 mol% pyridinium salt **214** as catalyst.

Chapter 7

7 Experimental Part

7.1 Working Techniques and Reagents

The synthetic procedures were performed in oven-dried glassware under argon using Schlenk techniques or under purified nitrogen in a glovebox (Mbraun Labmaster 130). Commercially available reagents were purchased from *Acros*, *Aldrich*, *Alfa-Aesar*, *Fluka*, *Strem* or *TCl*. All chemicals were used as received from the chemical supplier without further purification unless otherwise noted. Dichloromethane, *n*-pentane and Et₂O were collected from a purification column system (PureSolve, Innovative Technology Inc.) or purchased from *Aldrich*, *Acros* or *Fluka* in septum-sealed bottles over molecular sieves. Column chromatographic purifications were performed on *Merck* silica gel 60 (particle size 40-63 nm) or *Aldrich* aluminum oxide (*neutral* or *basic*, particle size 0.05-0.15 mm, Brockmann Activity I). The eluents were of technical grade and distilled prior to use. The hydrogenation experiments were performed under purified nitrogen in a glovebox.

7.2 Analytical Methods

NMR-Spectroscopy: NMR spectra were measured on a Bruker DPX-NMR (400 MHz) or a Bruker Avance 500 (500 MHz) spectrometer equipped with BBO broadband probe heads. Chemical shifts (δ) are reported in parts per million (ppm) relative to residual solvent peaks and coupling constants (J) are reported in Hertz (Hz). Deuterated NMR solvents were obtained from Cambridge Isotope Laboratories, Inc. (Andover, MA, USA). The measurements were performed at 25 °C, if nothing else is reported. The chemical shift δ values were corrected to 7.26 ppm (¹H NMR) and 77.16 ppm (¹³C NMR) for CDCl₃, 3.31 ppm (¹H NMR) and 49.0 ppm (¹³C NMR) for MeOD-*d*₄, 2.50 ppm (¹H NMR) and 39.52 ppm (¹³C NMR) for DMSO-*d*₆. ¹⁹F NMR spectra relative to CFCl₃ (δ = 0 ppm). ²H NMR spectra relative to internal standard (deuterated solvent, 1 μ L) in non-deuterated solvent. ¹³C and ¹⁹F spectra were recorded ¹H-decoupled. For quantitative analysis of ¹⁹F spectra, an inverse gated method was used (10° pulse, relaxation time d_1 = 60 sec). The assignment of ¹H and ¹³C signals was realized with the help of DEPT and, if needed, two-dimensional correlation experiments (COSY, HMQC, HMBC and NOESY).

Multiplicities are assigned as follows: s (singlet), d (doublet), t (triplet), q (quartet), quin (quintet), sext (sextet), sept (septet), m (multiplet) and brs (broad singlet).

Mass spectrometry (MS): Mass spectra were measured by Dr. H. Nadig (Department of Chemistry, University of Basel) on VG70 250 spectrometer (electron-impact ionization, (EI)) or on a MAR 312 spectrometer (fast-atom bombardment (FAB)) mass spectrometers. FAB was performed with 3-nitrobenzyl alcohol (NBA) as matrix. The signals were given as mass-to-charge-ratio (m/z) with relative intensity in brackets.

Gas Chromatography-Mass Spectrometry (GC-MS): The GC-MS spectra were recorded on a HP5890 gas chromatograph with a HP5970A detector equipped with a Macherey and Nagel Optima5 (5% polyphenylmethylsiloxane column, 25 m x 0.2 mm x 35 μm), a HP5890 gas chromatograph with a HP5971 detector equipped with a Aglient HP1 (1% dimethylsiloxane column, 15 m x 0.2 mm x 33 μm). For both instruments the flow was set to 1 mL/min with 20:1 ratio. A Shimadzu GCMS-QP2010 SE equipped with a *Restek* RTx[®]-5MS (30 m x 0.2 mm x 0.2 μm) was used too. For this instrument the carrier pressure (He) was set to 100 kPa with 40:1 split ratio.

High resolution Mass Spectroscopy (HRMS): High resolution mass spectra were measured by Dr. H. Nadig (Department of Chemistry, University of Basel) on a Bruker maXIS 4G.

Infrared Spectroscopy (IR): The spectra were recorded on a *Shimadzu* FTIR-8400S Fourier Transform spectrometer with ATR/Golden Gate technology. The absorption bands are given in wavenumbers $\tilde{\nu}$ (cm^{-1}). The peak intensity is assigned with s (strong), m (medium), w (weak) and br (broad).

Elemental analysis (EA): Elemental analyses were measured by Mr. W. Kirsch and Sylvie Mittelheiser (Department of Chemistry, University of Basel) on a Leco CHN 900 analyzer or a Vario Micro Cube by Elementar (C, H, N detection). The data are indicated in mass percent.

Thin Layer Chromatography (TLC): TLC plates were obtained from *Macherey-Nagel* (Polygram SIL G/UV₂₅₄ and Polygram Alox N/UV₂₅₄, 0.2 mm silica with fluorescence indicator,

40 × 80 mm). For visualization UV light (254 nm, 366 nm) or basic permanganate solution [KMnO_4 (3 g), K_2CO_3 (20 g), 5% aqueous NaOH (5 mL), H_2O (300 mL)] were used.

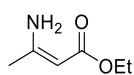
Melting points (m.p.): Melting points were determined on a Büchi 535 melting point apparatus and were not corrected.

Optical Rotations ($[\alpha]_D^{20}$): Optical rotations were measured on a Perkin Elmer Polarimeter 341, in a cuvette (1 dm cylindric cell) at 20 °C. The concentration (c) is given in g/100 mL.

7.3 Intramolecular Pyridinium-Based FLP Systems

7.3.1 Synthesis of Benzylic Amines

(Z)-Ethyl 3-aminobut-2-enoate (**68**)



To a solution of ethyl acetoacetat (19.4 mL, 154 mmol, 1.00 eq.) in methanol (160 mL) ammonium carbamate (11.7 g, 154 mmol, 1.00 eq.) was added in one portion. The resulting suspension was stirred at room temperature for 1.5 h. During that time all solid material was dissolved to obtain a clear yellow solution. The reaction mixture was concentrated to dryness yielding title compound **68** (19.8 g, quant.) as a yellow liquid. The analytical data match the literature values.^[123]

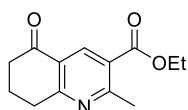
$C_6H_{11}NO_2$ (129.16 g mol⁻¹)

¹H-NMR (400 MHz, CDCl₃): δ = 7.62 (br, 2H, NH₂), 4.30 (s, 1H, CH), 3.90 (q, J = 7.1 Hz, 2H, CH₂CH₃), 1.71 (s, 3H, CH₃), 1.06 (t, J = 7.1 Hz, 3H, CH₂CH₃) ppm.

¹³C{¹H}-NMR (101 MHz, CDCl₃): δ = 170.5 (s, C=O), 160.6 (s, C-NH₂), 83.7 (s, CH), 58.6 (s, CH₂CH₃), 22.2 (s, CH₃), 14.8 (s, CH₂ CH₃) ppm.

TLC (SiO₂, cyclohexane/EtOAc 1:1): R_f = 0.36.

Ethyl 2-methyl-5-oxo-5,6,7,8-tetrahydroquinoline-3-carboxylate (**64**)



A solution of 1,3-cyclohexadione (17.3 g, 153 mmol, 1.00 eq.), triethyl orthoformate (90 mL, 540 mmol, 3.50 eq.) and (Z)-ethyl-3-aminobut-2-enoate (**68**) (19.8 g, 153 mmol, 1.00 eq.) in acetic acid (13 mL) was refluxed for 2.5 h under an argon atmosphere. Volatile compounds were removed *in vacuo*. The resulting residue was dissolved in EtOAc (200 mL) and washed with saturated Na₂CO₃ solution (150 mL) and brine (50 mL). The organic layers were concentrated to obtain crude material as red solid. Purification by column chromatography (SiO₂, 7 × 25 cm, cyclohexane/EtOAc 3:1) gave the desired product **64** (19.5 g, 54%) as an orange solid.

$C_{13}H_{15}NO_3$ (233.26 g mol⁻¹)

¹H-NMR (400 MHz, CDCl₃): δ = 8.70 (s, 1H, Ar-H), 4.36 (q, J = 7.1 Hz, 2H, CH₂CH₃), 3.11 (t, J = 6.2 Hz, 2H, CH₂CH₃), 2.84 (s, 3H, CH₃), 2.70-2.63 (m, 2H, CH₂), 2.21-2.14 (m, 2H, CH₂), 1.38 (t, J = 7.1 Hz, 3H, CH₂CH₃) ppm.

¹³C{¹H}-NMR (101 MHz, CDCl₃): δ = 197.5 (s, C=O), 166.2 (s, C=O), 166.0 (s, Ar-C), 164.6 (s, Ar-C), 137.8 (s, Ar-CH), 126.2 (s, Ar-C), 125.0 (s, Ar-C), 61.8 (s, CH₂CH₃), 38.9 (s, CH₂), 33.0 (s, CH₂), 25.6 (s, CH₂), 22.0 (s, CH₃), 14.7 (s, CH₂CH₃) ppm.

MS (EI, 70 eV) m/z (%): 233 (100) [M]⁺, 205 (99), 188 (72), 177 (63), 132 (14).

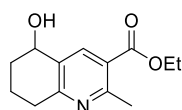
IR: $\tilde{\nu}$ = 2955w, 1721s, 1684s, 1586m, 1553m, 1434m, 1368m, 1244s, 1212s, 1179s, 1021m, 909w, 780m, 670w cm⁻¹.

EA: calc.: C 66.94, H 6.48, N 6.00; found: C 66.49, H 6.78, N 6.10.

TLC (SiO₂, cyclohexane/EtOAc 3:1): R_f = 0.25.

m.p.: 86-88 °C.

Ethyl 2-methyl-5-hydroxy-5,6,7,8-tetrahydroquinoline-3-carboxylate (**74**)



Ketone **64** (8.10 g, 34.7 mmol, 1.00 eq.) was dissolved in methanol (140 mL) and sodium borohydride (1.37 g, 34.7 mmol, 1.00 eq.) was added at 0 °C. The mixture was stirred for 1 h at RT. The obtained yellow solution was quenched with cold water (100 mL) and extracted with dichloromethane (3 × 50 mL). The combined organic layers were dried over MgSO₄ and filtered. Evaporation of the solvent gave the alcohol **74** (8.20 g, quant.) as a yellow solid.

$C_{13}H_{17}NO_3$ (235.38 g mol⁻¹)

¹H-NMR (400 MHz, CDCl₃): δ = 8.25 (s, 1H, Ar-H), 4.81 (s, 1H, CHCH₃), 4.35 (q, J = 7.1 Hz, 2H, CH₂CH₃), 3.00-2.79 (m, 2H, CH₂), 2.77 (s, 3H, CH₃), 2.31 (s, 1H, OH), 2.11-1.99 (m, 2H, CH₂), 1.90-1.79 (m, 2H, CH₂), 1.38 (t, J = 7.1 Hz, 3H, CH₂CH₃) ppm.

¹³C{¹H}-NMR (101 MHz, CDCl₃): δ = 167.0 (s, C=O), 160.2 (s, Ar-C), 158.5 (s, Ar-C), 139.3 (s, Ar-CH), 132.5 (s, Ar-C), 123.8 (s, Ar-C), 67.4 (s, CH), 61.5 (s, CH₂CH₃), 32.6 (s, CH₂), 32.4 (s, CH₂), 24.7 (s, CH₂), 19.0 (s, CH₃), 14.6 (s, CH₂CH₃) ppm.

MS (EI, 70 eV) m/z (%): 235 (43) $[M]^+$, 220 (26), 206 (100) $[M-CH_2CH_3]^+$, 190 (37), 179 (59), 162 (34), 151 (13), 144 (12), 77 (12), 65 (11).

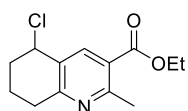
IR: $\tilde{\nu}$ = 3217w, 2932w, 1721s, 1564m, 1447m, 1322m, 1257s, 1156s, 1072s, 1021m, 956w cm^{-1} .

EA: calc.: C 66.36, H 7.28, N 5.95; found: C 65.58, H 7.48, N 5.96.

TLC (SiO₂, cyclohexane/EtOAc 2:1): R_f = 0.24.

m.p.: 70-72 °C.

Ethyl 5-chloro-2-methyl-5,6,7,8-tetrahydroquinoline-3-carboxylate (**75**)



To a solution of compound **74** (8.20 g, 34.9 mmol, 1.00 eq.) in dichloromethane (180 mL) and triethylamine (7.4 mL, 52.3 mmol, 1.50 eq.) was added methane sulfonylchloride (3.3 mL, 41.8 mmol, 1.20 eq.) at 0 °C.

The mixture was stirred at RT for 30 min. The obtained solution was extracted with H₂O (3 × 50 mL). The aqueous layers were back extracted each time with dichloromethane (2 × 20 mL). The combined organic layers were dried over MgSO₄, filtered and evaporated. Purification by column chromatography (SiO₂, 7 × 25 cm, cyclohexane/EtOAc 7:1,) afforded the desired product **75** (6.15 g, 81%) as an orange oil.

C₁₃H₁₆ClNO₂ (253.72 g mol⁻¹)

¹H-NMR (400 MHz, CDCl₃): δ = 8.18 (s, 1H, Ar-H), 5.26 (m, 1H, CH), 4.37 (q, J = 7.2 Hz, 2H, CH₂CH₃), 3.09-2.98 (m, 1H, CH₂), 2.92-2.80 (m, 1H, CH₂), 2.78 (s, 3H, CH₃), 2.32-2.13 (m, 3H, CH₂), 1.99-1.90 (m, 1H, CH₂), 1.39 (t, J = 7.1 Hz, 3H, CH₂CH₃) ppm.

¹³C{¹H}-NMR (101 MHz, CDCl₃): δ = 166.6 (s, C=O), 159.8 (s, Ar-C), 159.6 (s, Ar-C), 140.7 (s, Ar-CH), 129.9 (s, Ar-C), 124.0 (s, Ar-C), 61.6 (s, CH), 57.1 (s, CH₂CH₃), 32.8 (s, CH₂), 32.5 (s, CH₂), 25.1 (s, CH₂), 18.6 (s, CH₃), 14.7 (s, CH₂CH₃) ppm.

MS (EI, 70 eV) m/z (%): 253 (11) $[M]^+$, 218(100) $[M-CH_2CH_3]^+$, 190 (24), 144 (12).

IR: $\tilde{\nu}$ = 2950w, 2358w, 1722s, 1560w, 1445w, 1437w, 1269m, 1241w, 1179w, 1064w cm^{-1} .

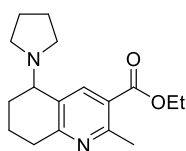
EA: calc.: C 61.54, H 6.36, N 5.52; found: C 61.37, H 6.47, N 5.50.

TLC (SiO₂, cyclohexane/EtOAc 2:1): R_f = 0.55.

Formation of Amines

General Procedure A: To a solution of **75** (1.00 eq.) in acetonitrile (0.2 M) was added the secondary amine (2.00 eq.) at 0 °C. The solution was heated to reflux (80 °C) for 24 hours. The reaction mixture was allowed to cool down to RT and the mixture was extracted with H₂O (30 mL). The aqueous layer was extracted with dichloromethane (3 × 20 mL). The combined organic layers were dried over MgSO₄, filtered and the solvent was removed under reduced pressure to give the desired product.

Ethyl 2-methyl-5-(pyrrolidin-1-yl)-5,6,7,8-tetrahydroquinoline-3-carboxylate (**69**)



The title compound **69** was obtained following the general procedure A using **75** (2.0 g, 6.38 mmol, 1.00 eq.), acetonitrile (30 mL) and pyrrolidine (1.05 mL, 12.8 mmol, 2.00 eq.), after purification by column chromatography (SiO₂, 3 × 15 cm, cyclohexane/EtOAc 3:1 → 1:2) as a yellow solid (1.80 g, 98%).

C₁₇H₂₄N₂O₂ (302.41 g mol⁻¹)

¹H-NMR (400 MHz, CDCl₃): δ = 8.13 (s, 1H, Ar-H), 4.41-4.29 (m, 2H, CH₂CH₃), 3.63-3.58 (m, 1H, CH), 3.05-2.95 (m, 1H, CH₂), 2.92-2.80 (m, 1H, CH₂), 2.76 (s, 3H, CH₃), 2.66-2.58 (m, 2H, CH₂), 2.49-2.41 (m, 2H, CH₂), 2.33-2.13 (m, 1H, CH₂), 1.98-1.87 (m, 1H, CH₂), 1.83-1.69 (m, 6H, 3 × CH₂), 1.38 (q, *J* = 7.1 Hz, 3H, CH₂CH₃) ppm.

¹³C{¹H}-NMR (101 MHz, CDCl₃): δ = 167.4 (s, C=O), 161.1 (s, Ar-C), 157.7 (s, Ar-C), 139.7 (s, Ar-CH), 131.8 (s, Ar-C), 122.9 (s, Ar-C), 61.3 (s, CH₂CH₃), 59.8 (s, CH), 50.2 (s, CH₂), 32.8 (s, CH₂), 24.8 (s, CH₂), 24.2 (s, CH₂), 24.0 (s, CH₂), 19.3 (s, CH₃), 14.7 (s, CH₂CH₃) ppm.

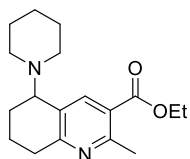
MS (EI, 70 eV) *m/z* (%): 288 (31) [M]⁺, 259 (35), 245 (13), 231 (29), 217 (100) [M-C₄H₉N]⁺, 190 (26), 172 (20), 144 (28), 70 (18).

IR: $\tilde{\nu}$ = 2978w, 2936w, 2880w, 1719m, 1455w, 1316s, 1262m, 1196m, 1140s, 1106s, 1057s, 1005s, 971m, 855w, 778s, 724m cm⁻¹.

EA: calc.: C 70.80, H 8.39 N 9.71; found: C 70.79, H 8.27, N 9.64.

TLC (SiO₂, cyclohexane/EtOAc 3:1): R_f = 0.15.

m.p.: 46-48 °C.

Ethyl 2-methyl-5-(piperidin-1-yl)-5,6,7,8-tetrahydroquinoline-3-carboxylate (78)

The title compound **78** was obtained following the general procedure A using **75** (2.00 g, 6.38 mmol, 1.00 eq.), acetonitrile (30 mL) and piperidine (1.3 mL, 12.8 mmol, 2.00 eq.), after purification by column chromatography (SiO₂, 3 × 15 cm, cyclohexane/EtOAc 40:1 → 2:1) as a colorless solid (1.53 g, 80%).

C₁₈H₂₆N₂O₂ (302.41 g mol⁻¹)

¹H-NMR (400 MHz, CDCl₃): δ = 8.47 (s, 1H, Ar-H), 4.37 (q, *J* = 7.1 Hz, 2H, CH₂CH₃), 3.77-3.71 (m, 1H, CHN), 2.91-2.82 (m, 2H, CH₂), 2.76 (s, 3H, CH₃), 2.54-2.46 (m, 2H, CH₂), 2.45-2.37 (m, 2H, CH₂), 2.13-2.03 (m, 2H, CH₂), 2.03-1.94 (m, 1H, CH₂), 1.79-1.64 (m, 1H, CH₂), 1.65-1.49 (m, 5H, CH₂), 1.49-1.42 (m, 1H, CH₂), 1.39 (q, *J* = 7.1 Hz, 3H, CH₂CH₃) ppm.

¹³C{¹H}-NMR (101 MHz, CDCl₃): δ = 167.7 (s, C=O), 161.2 (s, Ar-C), 157.2 (s, Ar-C), 138.7 (s, Ar-CH), 132.2 (s, Ar-C), 123.8 (s, Ar-C), 63.3 (s, CH), 61.3 (s, CH₂CH₃), 50.1 (s, CH₂), 33.2 (s, CH₂), 27.1 (s, CH₂), 25.2 (s, CH₂), 24.7 (s, CH₃), 21.6 (s, CH₂), 21.0 (s, CH₂), 14.7 (s, CH₂CH₃) ppm.

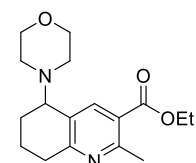
MS (EI, 70 eV) *m/z* (%): 302 (44) [M]⁺, 273 (35), 259 (38), 245 (11), 217 (100) [M-C₅H₁₀N]⁺, 201 (12), 190 (18), 172 (13), 144 (16), 86 (12).

IR: $\tilde{\nu}$ = 2940m, 2920m, 2362w, 1863w, 1715s, 1590w, 1550m, 1371w, 1251s, 1147s, 1107m, 1081m, 1054m, 961m cm⁻¹.

EA: calc.: C 71.49, H 8.67, N 9.26; found: C 71.39, H 8.59, N 9.18.

TLC (SiO₂, cyclohexane/EtOAc 2:1): R_f = 0.20.

m.p.: 55-57 °C.

Ethyl 2-methyl-5-morpholino-5,6,7,8-tetrahydroquinoline-3-carboxylate (79)

The title compound **79** was obtained following the general procedure A using **75** (2.00 g, 6.38 mmol, 1.00 eq.) in acetonitrile (30 mL) and morpholine (1.1 mL, 12.8 mmol, 2.00 eq.), after purification by column chromatography (SiO₂, 2 × 15 cm, cyclohexane/EtOAc, 20:1 → 7:1) as a colorless solid (1.50 g, 4.93 mmol, 78%).

$C_{17}H_{24}N_2O_3$ (304.38 g mol⁻¹)

¹H-NMR (400 MHz, CDCl₃): δ = 8.44 (s, 1H, Ar-H), 4.37 (q, J = 7.1 Hz, 2H, CH₂CH₃), 3.80-3.66 (m, 5H, CH, CH₂), 2.93-2.84 (m, 2H, CH₂), 2.75 (s, 3H, CH₃), 2.62-2.46 (m, 4H, CH₂), 2.16-2.06 (m, 1H, CH₂), 2.04-1.95 (m, 1H, CH₂), 1.41 (t, J = 7.1 Hz, 3H, CH₂CH₃) ppm.

¹³C{¹H}-NMR (101 MHz, CDCl₃): δ = 167.5 (s, C=O), 161.5 (s, Ar-C), 157.6 (s, Ar-C), 138.9 (s, Ar-CH), 131.0 (s, Ar-C), 123.8 (s, Ar-C), 68.0 (s, CH₂CH₃), 62.6 (s, CH), 61.4 (s, CH₂), 49.3 (s, CH₂), 33.1 (s, CH₂), 24.8 (s, CH₂), 21.3 (s, CH₂), 21.2 (s, CH₃), 14.7 (s, CH₃) ppm.

MS (EI, 70 eV) m/z (%): 304 (24) [M]⁺, 275 (10), 259 (11), 217(100) [M-C₄H₈NO]⁺, 190 (20), 172 (16), 144 (17), 86 (20).

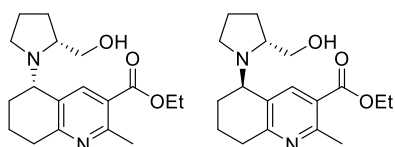
IR: $\tilde{\nu}$ = 2955w, 2840w, 2361w, 1715s, 1550m, 1439m, 1357w, 1325w, 1254s, 1153m, 1129m, 1114s, 1086w, 1057m, 1017m cm⁻¹.

EA: calc.: C 67.08, H 7.95, N 9.20; found: C 67.24, H 7.89, N 9.22.

TLC (SiO₂, cyclohexane/EtOAc 3:1): R_f = 0.19.

m.p.: 83-85 °C.

Ethyl 5-((R)-2-(hydroxymethyl)pyrrolidin-1-yl)-2-methyl-5,6,7,8-tetrahydroquinoline-3-carboxylate (80)



The title compound **80** was obtained following the general procedure A using **75** (1.00 g, 3.19 mmol, 1.00 eq.) in acetonitrile (15 mL) and *L*-prolinol (0.37 mL, 3.83 mmol, 1.20 eq.), after purification by column chromatography (SiO₂, 2 × 25 cm, cyclohexane/EtOAc 3:1 → 1:1) two separable diastereomers as a colorless oil (673 mg, 63% combined yield).

The absolute stereochemistry was not assigned due to the problems determine it using common NMR methods like 1D NOE difference and 2D NOESY.

The absolute stereochemistry was not assigned due to the problems determine it using common NMR methods like 1D NOE difference and 2D NOESY.

Compound 80a

$C_{18}H_{26}N_2O_3$ (318.41 g mol⁻¹)

¹H-NMR (400 MHz, CDCl₃): δ = 8.30 (s, 1H, Ar-H), 4.42-4.30 (m, 2H, CH₂CH₃), 4.09-4.03 (m, 1H, CH), 3.64 (dd, J = 10.8Hz, J = 4.0 Hz, 1H, CH₂-OH), 3.46 (dd, J = 10.8Hz, J = 2.7 Hz, 1H, CH₂-OH),

3.19 (m, 1H, CH), 2.94-2.88 (m, 2H, CH₂), 2.77 (s, 3H, CH₃), 2.67-2.58 (m, 1H, CH₂), 2.52-2.43 (m, 1H, CH₂), 2.16-2.08 (m, 1H, CH₂), 2.06-1.97 (m, 1H, CH₂), 1.97-1.81 (m, 1H, CH₂), 1.80-1.64 (m, 4H, CH₂), 1.39 (t, *J* = 7.1 Hz, 3H, CH₂CH₃) ppm.

¹³C{¹H}-NMR (101 MHz, CDCl₃): δ = 167.4 (s, C=O), 161.0 (s, Ar-C), 157.4 (s, Ar-C), 138.4 (s, Ar-CH), 132.0 (s, Ar-C), 124.0 (s, Ar-C), 62.6 (s, CH₂CH₃), 61.1 (s, CH₂), 60.0 (s, CH), 56.1 (s, CH), 46.6 (s, CH₂), 32.8 (s, CH₂), 28.9 (s, CH₂), 24.4 (s, CH₂), 24.3 (s, CH₃), 20.9 (s, CH₂), 20.8 (s, CH₂), 14.3 (s, CH₂CH₃) ppm.

MS (FAB NBA) *m/z* (%): 319 (96) [M]⁺, 287 (54), 218 (100) [M-C₅H₁₀NO]⁺, 190 (15).

IR: $\tilde{\nu}$ = 3350br, 2928w, 2860w, 1718s, 1593w, 1555w, 1443m, 1365w, 1259s, 1154w, 1059m, 784w cm⁻¹.

EA: calc.: C 67.90, H 8.23, N 8.80; found: C 67.71, H 8.12, N 8.75.

TLC (SiO₂, cyclohexane/EtOAc 1:1): R_f = 0.42.

[α]_D²⁰ = -112.5 (c = 1.08, CH₂Cl₂).

Compound 80b

C₁₈H₂₆N₂O₃ (318.41 g mol⁻¹)

¹H-NMR (400 MHz, CDCl₃): δ = 8.24 (s, 1H, Ar-H), 4.37 (q, *J* = 7.1 Hz, 2H, CH₂CH₃), 4.10-4.06 (m, 1H, CH), 3.33-3.25 (m, 3H, CH₂-OH, CH), 2.98-2.93 (m, 1H, CH₂), 2.92-2.85 (m, 2H, CH₂), 2.77 (s, 3H, CH₃), 2.74-2.64 (m, 2H, CH₂), 2.14-2.05 (m, 1H, CH₂), 2.04-1.89 (m, 2H, CH₂), 1.87-1.69 (m, 5H, 3 × CH₂), 1.40 (t, *J* = 7.1 Hz, 3H, CH₂CH₃) ppm.

¹³C{¹H}-NMR (101 MHz, CDCl₃): δ = 166.7 (s, C=O), 161.1 (s, Ar-C), 157.4 (s, Ar-C), 138.9 (s, Ar-CH), 131.1 (s, Ar-C), 122.7 (s, Ar-C), 61.7 (s, CH), 61.1 (s, CH₂CH₃), 60.0 (s, CH₂), 32.8 (s, CH₂), 29.2 (s, CH₂), 27.0 (s, CH₂), 24.4 (s, CH₂), 24.4 (s, CH₃), 20.9 (s, CH₂), 14.3 (s, CH₂CH₃) ppm.

MS (FAB NBA) *m/z* (%): 319 (100) [M]⁺, 287 (53), 218 (86) [M-C₅H₁₀NO]⁺, 190 (14).

IR: $\tilde{\nu}$ = 3355b, 2936w, 2866w, 1717s, 1594w, 1559w, 1442m, 1363w, 1259s, 1155w, 1059m, 783w, 665m cm⁻¹.

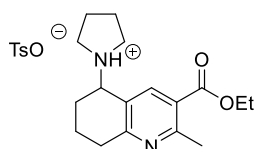
EA: calc.: C 67.90, H 8.23, N 8.80; found: C 67.65, H 8.15, N 8.76.

TLC (SiO₂, cyclohexane/EtOAc 1:1): R_f = 0.38.

[α]_D²⁰ = +26.8 (c = 1.06, CH₂Cl₂).

7.3.2 Synthesis of Amino-Pyridinium Salts

1-(3-(Ethoxycarbonyl)-2-methyl-5,6,7,8-tetrahydroquinolin-5-yl)pyrrolidin-1-ium 4-methylbenzenesulfonate (**83**)



To a solution of **69** (250 mg, 0.87 mmol, 1.00 eq.) in dichloromethane (4 mL) was added *p*-toluenesulfonic acid (150 mg, 0.80 mmol, 0.95 eq.). The mixture was stirred for 30 min at RT. Removal of the solvent *in vacuo* gave the title compound **83** (370 mg, 93%) as a colorless oil.

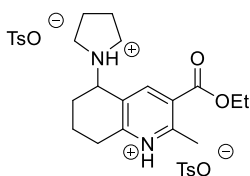
$C_{24}H_{32}N_2O_5S$ (460.59 g mol⁻¹)

¹H-NMR (400 MHz, CDCl₃): δ = 11.2 (br s, 1H, NH), 8.40 (s, 1H, Ar-H), 7.71 (d, *J* = 8.1 Hz, 2H, TsO⁻), 7.15 (d, *J* = 7.9 Hz, 2H, TsO⁻), 4.72-4.50 (m, 1H, CH), 4.36-4.21 (m, 2H, CH₂CH₃), 4.04-3.75 (m, 1H, CH₂), 3.73-3.43 (m, 1H, CH₂), 3.17-2.96 (m, 1H, CH₂), 2.96-2.83 (m, 1H, CH₂), 2.79 (s, 3H, CH₃), 2.34 (s, 3H, TsO⁻), 2.33-2.23 (m, 2H, CH₂), 2.19-1.93 (m, 5H, CH₂), 1.93-1.81 (m, 1H, CH₂), 1.79-1.58 (m, 1H, CH₂), 1.32 (t, *J* = 7.1 Hz, 3H, CH₂CH₃) ppm.

¹³C{¹H}-NMR (101 MHz, CDCl₃): δ = 166.4 (s, C=O), 161.7 (s, Ar-C), 142.8 (s, Ar-C), 140.4 (s, Ar-CH), 140.3 (s, Ar-C), 129.1 (s, Ar-C, TsO⁻), 126.1 (s, Ar-C, TsO⁻), 123.7 (s, Ar-C), 61.8 (s, CH₂CH₃), 61.6 (s, CH), 52.1 (s, CH₂), 32.0 (s, CH₂), 25.1 (s, CH₂), 24.9 (s, CH₂), 23.6 (s, CH₂), 21.7 (s, CH₃, TsO⁻), 18.1 (s, CH₃), 14.6 (s, CH₂CH₃) ppm.

MS (FAB NBA) *m/z* (%): 289 (100) [M-TsO⁻]⁺, 218.1 (44).

3-(Ethoxycarbonyl)-2-methyl-5-(pyrrolidin-1-ium-1-yl)-5,6,7,8-tetrahydroquinolin-1-ium 4-methylbenzenesulfonate (**87**)



To a solution of **69** (50 mg, 0.17 mmol, 1.00 eq.) in dichloromethane (0.8 mL) was added *p*-toluenesulfonic acid (66 mg, 0.34 mmol, 2.00 eq.). The mixture was stirred for 30 min at RT. Removal of the solvent *in vacuo* yielded the title compound **87** (75 mg, 94%) as a waxy solid.

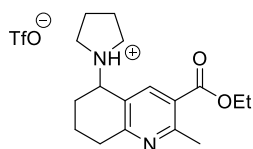
$C_{31}H_{40}N_2O_8S_2$ (632.79 g mol⁻¹)

¹H-NMR (400 MHz, CDCl₃): δ = 10.33 (br s, 1H, NH), 8.88 (s, 1H, Ar-H), 7.59 (d, J = 8.1 Hz, 4H, 2 x TsO⁻), 7.10 (d, J = 7.9 Hz, 4H, 2 x TsO⁻), 4.99 (s, 1H, CH), 4.32 (q, J = 7.12 Hz, 2H, CH₂CH₃), 3.59-3.37 (m, 3H, CH₂), 3.36-3.07 (m, 3H, CH₂), 2.88 (s, 3H, CH₃), 2.27 (s, 6H, 2 x TsO⁻), 2.26-2.14 (m, 2H, CH₂), 2.04-1.75 (m, 6H, CH₂), 1.32 (t, J = 7.1 Hz, 3H, CH₂CH₃) ppm.

¹³C{¹H}-NMR (101 MHz, CDCl₃): δ = 163.1 (s, C=O), 159.4 (s, Ar-C), 157.7 (s, Ar-C), 147.8 (s, Ar-C, 2 x TsO⁻), 142.8 (s, Ar-C, 2 x TsO⁻), 140.6 (s, Ar-CH), 129.3 (s, Ar-C, 2 x TsO⁻), 128.5 (s, Ar-C), 126.3 (s, Ar-C), 125.6 (s, Ar-C, 2 x TsO⁻), 63.2 (s, CH), 59.6 (s, CH₂CH₃), 53.9 (s, CH₂), 53.6 (s, CH₂), 27.8 (s, CH₂), 24.2 (s, CH₂), 23.2 (s, CH₂), 23.1 (s, CH₂), 21.7 (s, CH₃, 2 x TsO⁻), 20.4 (s, CH₃), 15.6 (s, CH₂), 14.5 (s, CH₂CH₃) ppm.

MS (FAB NBA) m/z (%): 461 (11) [M-TsO⁻]⁺, 290 (19) [M-2 x TsO⁻]⁺, 289 (100) [M-H⁺, -2 x TsO⁻]⁺, 218 (45) ppm.

1-(3-(Ethoxycarbonyl)-2-methyl-5,6,7,8-tetrahydroquinolin-5-yl)pyrrolidin-1-ium trifluoromethanesulfonate (82)



To a solution of **69** (10.7 mg, 0.037 mmol, 1.00 eq.) in dichloromethane (0.5 mL) was added trifluoromethanesulfonic acid (1 mM solution in dichloromethane, 33 μ L, 0.33 mmol, 0.95 eq.). The mixture was stirred for 20 min at RT. Removal of the solvent *in vacuo* gave the title compound **82** (15 mg, 96%) as a pale yellow oil.

$C_{18}H_{25}F_3N_2O_5S$ (438.46 g mol⁻¹)

¹H-NMR (400 MHz, CDCl₃): δ = 9.09 (br s, 1H, NH), 8.36 (s, 1H, Ar-H), 4.67-4.58 (m, 1H, CH), 4.46-4.30 (m, 2H, CH₂CH₃), 3.73-3.44 (m, 1H, CH₂), 3.27-3.14 (m, 2H, CH₂), 3.02-2.89 (m, 2H, CH₂), 2.83 (s, 3H, CH₃), 2.31-2.06 (m, 8H, CH₂), 2.06-1.93 (m, 1H, CH₂), 1.40 (t, J = 7.1 Hz, 3H, CH₂CH₃) ppm.

¹³C{¹H}-NMR (101 MHz, CDCl₃): δ = 166.5 (s, C=O), 162.0 (s, Ar-C), 159.8 (s, Ar-C), 141.1 (s, Ar-CH), 124.7 (s, Ar-C), 123.7 (s, Ar-C), 121.7 (q, J_{CF} = 320 Hz, CF₃), 62.1 (s, CH₂CH₃), 61.1 (s, CH), 53.5 (s, CH₂), 51.4 (s, CH₂), 32.0 (s, CH₂), 25.0 (s, CH₂), 24.4 (s, CH₂), 25.0 (s, CH₂), 23.5 (s, CH₂), 23.4 (s, CH₃), 17.7 (s, CH₂), 15.0 (s, CH₂CH₃) ppm.

$^{19}\text{F}\{^1\text{H}\}$ -NMR (376 MHz, CDCl_3): $\delta = -78.6$ (s, TfO^-) ppm.

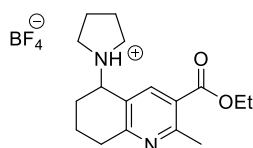
MS (FAB NBA) m/z (%): 289 (100) $[\text{M-TfO}]^+$, 218 (52).

Protonation with HBF_4

General Procedure B: To a solution of amine (1.00 eq.) in Et_2O (0.2 M) was added $\text{HBF}_4 \cdot \text{Et}_2\text{O}$ (0.95 eq.) dropwise. The mixture was stirred for 10 min at RT. The solvent was removed *in vacuo* and the residue was washed with dry *n*-pentane (2×2 mL) to obtain the desired compound.

All salts were not stable on column (silica and alumina), therefore precipitation was used for purification. The ^1H , ^{13}C and ^{19}F spectra matched with the expected data, but the measured value of the elemental analysis showed small differences.

1-(3-(Ethoxycarbonyl)-2-methyl-5,6,7,8-tetrahydroquinolin-5-yl)pyrrolidin-1-ium tetrafluoroborate (**84**)



The title compound **84** was obtained following the general procedure B using **69** (150 mg, 0.52 mmol, 1.00 eq.), Et_2O (2.5 mL) and $\text{HBF}_4 \cdot \text{Et}_2\text{O}$ (66.8 μL , 0.50 mmol, 0.95 eq.) as a colorless solid (190 mg, 97%).

$\text{C}_{17}\text{H}_{25}\text{BF}_4\text{N}_2\text{O}_2$ (376.20 g mol^{-1})

^1H -NMR (400 MHz, $\text{DMSO-}d_6$): $\delta = 9.39$ (brs, 1H, NH), 8.42 (s, 1H, Ar-H), 4.74-4.67 (m, 1H, CH), 4.41-4.26 (m, 2H, CH_2CH_3), 3.58-3.48 (m, 1H, CH_2), 3.45-3.33 (m, 1H, CH_2), 3.28-3.19 (m, 1H, CH_2), 3.15-2.98 (m, 2H, CH_2), 2.94-2.83 (m, 1H, CH_2), 2.73 (s, 3H, CH_3), 2.28-2.17 (m, 1H, CH_2), 2.27-1.90 (m, 4H, CH_2), 1.96-1.69 (m, 3H, CH_2), 1.33 (t, $J = 7.1$ Hz, 3H, CH_2CH_3).

$^{13}\text{C}\{^1\text{H}\}$ -NMR (101 MHz, $\text{DMSO-}d_6$): $\delta = 166.0$ (s, C=O), 161.4 (s, Ar-C), 159.2 (s, Ar-C), 142.4 (s, Ar-CH), 125.4 (s, Ar-C), 124.3 (s, Ar-C), 62.3 (s, CH_2CH_3), 53.4 (s, CH), 51.5 (s, CH_2), 31.2 (s, CH_2), 24.2 (s, CH_2), 23.5 (s, CH_2), 23.4 (s, CH_2), 17.5 (s, CH_3), 15.0 (s, CH_2CH_3) ppm.

$^{19}\text{F}\{^1\text{H}\}$ -NMR (376 MHz, $\text{DMSO-}d_6$): $\delta = -148.0$ (s, BF_4^-) ppm.

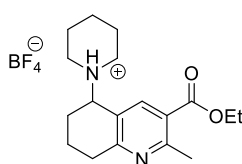
MS (FAB NBA) m/z (%): 377 (16) $[\text{M}]^+$, 289 (100) $[\text{M-BF}_4]^+$, 218 (51).

IR: $\tilde{\nu}$ = 3177w, 2966w, 2362w, 1718m, 1704w, 1423w, 1262s, 1150s, 1096w, 1060w, 910w cm^{-1} .

EA: calc.: C 54.28, H 6.70, N 7.45; found: C 56.38, H 6.85, N 7.86.

m.p.: 184-187 °C.

1-(3-(Ethoxycarbonyl)-2-methyl-5,6,7,8-tetrahydroquinolin-5-yl)piperidin-1-ium tetrafluoroborate (89)



The title compound **89** was obtained following the general procedure B using **78** (880 mg, 2.91 mmol, 1.00 eq.), Et₂O (14 mL) and HBF₄·Et₂O (0.37 mL, 0.50 mmol, 0.95 eq.) as a colorless solid (1.10 g, 97%).

C₁₈H₂₇BF₄N₂O₂ (390.22 g mol⁻¹)

¹H-NMR (400 MHz, DMSO-*d*₆): δ = 8.88 (br s, 1H, NH), 8.44 (s, 1H, Ar-H), 4.83-4.76 (m, 1H, CH), 4.41-4.27 (m, 2H, CH₂CH₃), 3.40-3.32 (m, 1H, CH₂), 3.19-3.00 (m, 2H, CH₂), 3.00-2.88 (m, 2H, CH₂), 2.96-2.75 (m, 1H, CH₂), 2.69 (s, 3H CH₃), 2.23-1.96 (m, 4H, CH₂), 1.89-1.49 (m, 6H, CH₂), 1.33 (t, *J* = 7.1 Hz, 3H, CH₂CH₃) ppm.

¹³C{¹H}-NMR (101 MHz, DMSO-*d*₆): δ = 167.7 (s, C=O), 164.6 (s, Ar-C), 157.2 (s, Ar-C), 138.7 (s, Ar-CH), 124.8 (s, Ar-C), 124.3 (s, Ar-C), 61.7 (s, CH₂CH₃), 61.2 (s, CH), 50.4 (s, CH₂), 47.6 (s, CH₂), 22.9 (s, CH₂), 22.7 (s, CH₂), 21.1 (s, CH₂), 18.2 (s, CH₂), 15.2 (s, CH₃), 14.5 (s, CH₂CH₃) ppm.

¹⁹F{¹H}-NMR (376 MHz, DMSO-*d*₆): δ = -148.0 (s, BF₄⁻) ppm.

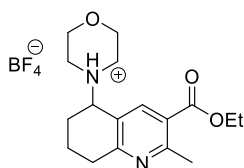
MS (FAB NBA) *m/z* (%): 303 (100) [M-BF₄]⁺, 218 (55) [M-BF₄, -C₅H₁₀N]⁺.

IR: $\tilde{\nu}$ = 3154w, 2948w, 1721m, 1558w, 1447w, 1263m, 1213w, 1144w, 1059s, 999s, 784w 684w cm^{-1} .

EA: calc.: C 55.40, H 6.97, N 7.18; found: C 56.56, H 6.93, N 7.21.

m.p.: 196-197 °C.

1-(3-(Ethoxycarbonyl)-2-methyl-5,6,7,8-tetrahydroquinolin-5-yl)morpholin-1-ium tetrafluoroborate (90)



The title compound **90** was obtained following the general procedure B using **79** (80.0 mg, 0.26 mmol, 1.00 eq.), Et₂O (1.5 mL) and HBF₄·Et₂O (34 μL, 0.25 mmol, 0.95 eq.) as a colorless solid (97.0 mg, 97%).

C₁₇H₂₅BF₄N₂O₃ (392.20 g mol⁻¹)

¹H-NMR (400 MHz, DMSO-*d*₆): δ = 9.37 (brs, 1H, NH), 8.36 (s, 1H, Ar-H), 4.75 (s, 1H, CH), 4.41-4.25 (m, 2H, CH₂CH₃), 4.02-3.89 (m, 2H, CH₂), 3.72-3.57 (m, 2H, CH₂), 3.40-3.19 (m, 2H, CH₂), 3.19-3.06 (m, 1H, CH₂), 3.06-2.95 (m, 1H, CH₂), 2.92-2.77 (m, 1H, CH₂), 2.71 (s, 3H CH₃), 2.38-2.22 (m, 1H, CH₂), 2.07-1.93 (m, 1H, CH₂), 1.88-1.73 (m, 1H, CH₂), 1.33 (t, *J* = 7.1 Hz, 3H, CH₂CH₃) ppm.

¹³C{¹H}-NMR (101 MHz, DMSO-*d*₆): δ = 165.0 (s, C=O), 160.4 (s, Ar-C), 159.7 (s, Ar-C), 145.5 (s, Ar-CH), 131.0 (s, Ar-C), 125.60 (s, Ar-C), 62.7 (s, CH₂CH₃), 62.2 (s, CH), 52.4 (s, CH₂), 50.6 (s, CH₂), 29.7 (s, CH₂), 22.5 (s, CH₂), 21.7 (s, CH₂), 17.8 (s, CH₃), 14.7 (s, CH₃) ppm.

¹⁹F{¹H}-NMR (376 MHz, DMSO-*d*₆): δ = -148.0 (s, BF₄⁻) ppm.

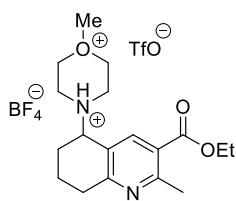
MS (FAB NBA) *m/z* (%): 305 (100) [M-BF₄]⁺, 218(54) [M-C₄H₈NO]⁺, 190 (11), 149 (15).

IR: $\tilde{\nu}$ = 3110w, 1726s, 1641m, 1407w, 1291m, 1101s, 1080s, 969s, 920m, 764m, 677w cm⁻¹.

EA: C 52.20, H 6.18, N 7.16; found: C 52.45, H 6.11, N 7.28.

m.p.: 252 °C.

4-(3-(Ethoxycarbonyl)-2-methyl-5,6,7,8-tetrahydroquinolin-5-yl)-1-methylmorpholine-1,4-dium tetrafluoroborate trifluoromethanesulfonate (100)



To a solution of **90** (90.0 mg, 0.23 mmol, 1.00 eq.) in dioxane (12 mL) and treated with methyl trifluorosulfonate (38.8 mg, 27 μL, 0.23 mmol, 1.00 eq.). The mixture was stirred for 4 h at RT. The solvent was removed *in vacuo* and the resulting yellow residue was washed with dry *n*-pentane

(2 × 2 mL) to obtain the biscation species **100** (118 mg, 93%).

$C_{19}H_{28}BF_7N_2O_6S$ (556.16 g mol⁻¹)

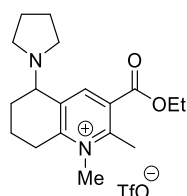
¹H-NMR (400 MHz, DMSO-*d*₆): δ = 9.37 (brs, 1H, NH), 8.36 (s, 1H, Ar-H), 4.75 (s, 1H, CH), 4.45-4.40 (m, 2H, CH₂), 4.40-4.28 (m, 2H, CH₂CH₃), 3.74-3.71 (m, 2H, CH₂), 3.67-3.63 (m, 2H, CH₂), 3.50-3.45 (m, 2H, CH₂), 3.39-3.34 (m, 2H, CH₂), 3.25 (s, 3H, CH₃), 3.23-3.19 (m, 2H, CH₂), 2.26 (s, 3H, CH₃), 1.33 (t, *J* = 7.1 Hz, 3H, CH₂CH₃) ppm.

¹³C{¹H}-NMR (101 MHz, DMSO-*d*₆): δ = 166.0 (s, C=O), 160.4 (s, Ar-C), 158.3 (s, Ar-C), 145.5 (s, Ar-CH), 131.0 (s, Ar-C), 125.9 (s, Ar-C), 121.4 (q, *J*_{CF} = 320 Hz, CF₃), 86.7 (s, CH₃), 62.7 (s, CH₂CH₃), 62.6 (s, CH), 48.9 (s, CH₂), 33.2 (s, CH₂), 22.6 (s, CH₂), 21.7 (s, CH₂), 17.8 (s, CH₃), 14.7 (s, CH₂CH₃) ppm.

¹⁹F{¹H}-NMR (376 MHz, DMSO-*d*₆): δ = -77.5 (s, TfO⁻), -148.0 (s, BF₄⁻) ppm.

MS (FAB NBA) *m/z* (%): 455 (21) [M-BF₄, -CH₃]⁺, 391 (14) [M-TfO⁻, -CH₃]⁺, 305 (100), [M-BF₄, -TfO⁻, -CH₃]⁺, 275 (12), 218 (40) [M-BF₄, -TfO⁻, -C₅H₁₂NO]⁺, 187 (52), 149 (17), 103 (13).

3-(Ethoxycarbonyl)-1,2-dimethyl-5-(pyrrolidin-1-yl)-5,6,7,8-tetrahydroquinolin-1-ium trifluoromethanesulfonate (103)



Fine powdered **84** (250 mg, 0.66 mmol, 1.0 eq.) was dissolved in dioxane (18 mL) and treated with methyl trifluorosulfonate (112 mg, 73 μ L, 0.66 mmol, 1.00 eq.). The mixture was stirred for 4 h at RT. The solvent was removed *in vacuo* and the resulting brown residue was washed with dry *n*-pentane (2 \times 2 mL) to obtain the bication species. The crude mixture was dissolved in dioxane (5 mL) and sodium hydride (25 mg, 0.99 mmol, 1.50 eq.) was added. The mixture was stirred for 30 min at RT. The obtained yellow solution was concentrated *in vacuo* and washed with dry *n*-pentane (2 \times 30 mL). The resulting solid material was dissolved in dichloromethane (2 mL) and filtered through a disposable HPLC filter (CHROMAFILL[®]0-20/15 MS, pore size 20 μ m). Evaporation of the solvent yielded the title compound **103** as a red oil (190 mg, 64%).

$C_{19}H_{27}F_3N_2O_5S$ (452.49 g mol⁻¹)

¹H-NMR (400 MHz, CDCl₃): δ = 8.67 (s, 1H, Ar-H), 4.47-4.37 (m, 2H, CH₂CH₃), 4.06 (s, 3H, N-CH₃), 3.91 (s, 1H, CH), 3.25-3.06 (m, 2H, CH₂), 2.91 (s, 3H, CH₃), 2.65-2.56 (m, 2H, CH₂), 2.47-2.40 (m,

2H, CH₂), 2.24-2.12 (m, 1H, CH₂), 1.91-1.76 (m, 3H, CH₂), 1.75-1.64 (m, 4H, CH₂), 1.35 (t, *J* = 7.1 Hz, 3H, CH₂CH₃) ppm.

¹³C{¹H}-NMR (101 MHz, CDCl₃): δ = 164.1 (s, C=O), 158.3 (s, Ar-C), 154.8 (s, Ar-C), 142.6 (s, Ar-CH), 137.5 (s, Ar-C), 123.0 (s, Ar-C), 121.7 (q, *J*_{CF} = 320 Hz, CF₃), 62.6 (s, CH₂CH₃), 57.8 (s, CH), 49.0 (s, CH₂), 40.6 (s, N-CH₃), 28.6 (s, CH₂), 23.2 (s, CH₂), 20.6 (s, CH₂), 18.1 (s, CH₃), 17.6 (s, CH₂), 13.7 (s, CH₂CH₃) ppm.

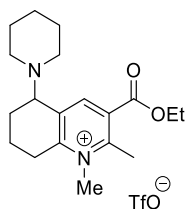
¹⁹F{¹H}-NMR (376 MHz, CDCl₃): δ = -77.4 (s, TfO⁻) ppm.

MS (FAB NBA) *m/z* (%): 303 (95) [M-TfO⁻]⁺, 232 (100) [M-TfO⁻, -C₄H₉N]⁺, 218 (11), 204 (18).

IR: $\tilde{\nu}$ = 2980w, 2955w, 1719m, 1455w, 1320s, 1262m, 1196m, 1140s, 1100m, 1057s, 1015s, 971m, 842w, 738m, 728m cm⁻¹.

EA: calc.: C 50.43, H 6.01, N 6.19; found: C 50.01 H 6.05, N 6.68.

3-(Ethoxycarbonyl)-1,2-dimethyl-5-(piperidin-1-yl)-5,6,7,8-tetrahydroquinolin-1-ium trifluoromethanesulfonate (104)



Fine powdered **89** (200 mg, 0.51 mmol, 1.00 eq.) was dissolved in dioxane (18 mL) and treated with methyl trifluorosulfonate (86.3 mg, 60 μL, 0.51 mmol, 1.00 eq.). The mixture was stirred for 4 h at RT. The solvent was removed *in vacuo* and the resulting brown residue was washed with dry *n*-pentane (2 × 2 mL) to obtain the bication species. The crude mixture was dissolved in dioxane (5 mL) and sodium hydride (20 mg, 0.77 mmol, 1.50 eq.) was added. The mixture was stirred for 30 min at RT. The obtained yellow solution was concentrated *in vacuo* and washed with dry *n*-pentane (2 × 30 mL). The resulting solid material was dissolved in dichloromethane (2 mL) and filtered through a disposable HPLC filter (CHROMAFILL®0-20/15 MS, pore size 20 μm). Evaporation of the solvent yielded the title compound **104** as a yellow oil (135 mg, 57%).

C₂₀H₂₉F₃N₂O₅S (466.51 g mol⁻¹)

¹H-NMR (400 MHz, CDCl₃): δ = 8.93 (s, 1H, Ar-*H*), 4.42 (q, *J* = 7.1 Hz, 2H, CH₂CH₃), 4.05 (s, 3H, N-CH₃), 4.00-3.91 (m, 1H, CH), 3.18-3.04 (m, 1H, CH₂), 2.94 (s, 3H, CH₃), 2.54-2.35 (m, 5H, CH₂),

2.26-2.10 (m, 1H, CH₂), 2.06-1.93 (m, 1H, CH₂), 1.89-1.65 (m, 2H, CH₂), 1.63-1.41 (m, 6H, CH₂), 1.36 (t, *J* = 7.1 Hz, 3H, CH₂CH₃) ppm.

¹³C{¹H}-NMR (101 MHz, CDCl₃): δ = 164.1 (s, C=O), 158.3 (s, Ar-C), 154.7 (s, Ar-C), 142.6 (s, Ar-CH), 137.4 (s, Ar-C), 128.2 (s, Ar-C), 121.9 (q, *J*_{CF} = 320 Hz, CF₃), 62.5 (s, CH₂CH₃), 61.4 (s, CH), 50.0 (s, CH₂), 40.5 (s, N-CH₃), 28.8 (s, CH₂), 26.2 (s, CH₂), 24.0 (s, CH₂), 19.5 (s, CH₂), 18.7 (s, CH₃), 18.1 (s, CH₂), 13.8 (s, CH₂CH₃) ppm.

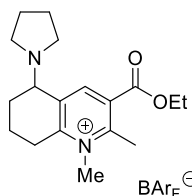
¹⁹F{¹H}-NMR (376 MHz, CDCl₃): δ = -77.5 (s, TfO⁻) ppm.

MS (FAB NBA) *m/z* (%): 317 (100) [M-TfO⁻]⁺, 232 (97)[M-TfO⁻, -C₅H₁₀N]⁺, 204 (13).

IR: $\tilde{\nu}$ = 2952m, 2920m, , 2362w, 1863w 1715s, 1590w, 1550m, 1371w, 1251s, 1147s, 1123m, 1071m, 886m cm⁻¹.

EA: calc.: C 51.49, H 6.27, N 6.00; found: C 51.08, H 6.33, N 6.23

3-(Ethoxycarbonyl)-1,2-dimethyl-5-(pyrrolidin-1-yl)-5,6,7,8-tetrahydroquinolin-1-ium tetrakis(3,5-bis(trifluoromethyl)phenyl)borate (105)



Compound **103** (250 mg, 0.55 mmol, 1.00 eq.) was dissolved in dichloromethane (3 mL) and NaBAr_F (490 mg, 0.55 mmol, 1.00 eq.) was added. The mixture was stirred for 20 min at RT and filtered through a disposable HPLC filter (CHROMAFILL®0-20/15 MS, pore size 20 μm). The solvent was removed *in vacuo* and the resulting residue was washed with dry *n*-pentane (2 × 2 mL) to give the BAr_F salt **105** (490 mg, 76%) as a green-brown solid.

C₅₀H₃₉BF₂₄N₂O₂ (1166.63 g mol⁻¹)

¹H-NMR (400 MHz, DMSO-*d*₆): δ = 8.68 (s, 1H, Ar-*H*), 7.74 (s, 4H, BAr_F-*H*), 7.63 (s, 8H, BAr_F-*H*), 4.42 (q, *J* = 7.0 Hz, 2H, CH₂CH₃), 4.06 (s, 3H, N-CH₃), 3.97-3.88 (m, 1H, CH), 3.22-3.11 (m, 2H, CH₂), 2.92 (s, 3H, CH₃), 2.68-2.55 (m, 2H, CH₂), 2.48-2.38 (m, 2H, CH₂), 2.26-2.02 (m, 1H, CH₂), 1.91-1.76 (m, 3H, CH₂), 1.74-1.64 (m, 4H, CH₂), 1.35 (t, *J* = 7.1 Hz, 3H, CH₂CH₃) ppm.

¹³C{¹H}-NMR (101 MHz, DMSO-*d*₆): δ = 164.1 (s, C=O), 161.0 (q, *J*_{BC} = 50 Hz, BAr_F), 158.3 (s, Ar-C), 154.8 (s, Ar-C), 142.6 (s, Ar-C), 137.5 (s, Ar-C), 134.0 (s, BAr_F), 128.7 (s, Ar-C), 128.4 (qq, *J*_{FC} = 30 Hz, *J*_{FC} = 3 Hz, BAr_F), 122.9 (q, *J*_{FC} = 273 Hz, BAr_F), 117.5 (sept, *J*_{FC} = 4 Hz, BAr_F), 62.6 (s,

CH₂CH₃), 57.8 (s, CH), 49.0 (s, CH₂), 40.6 (s, N-CH₃), 28.6 (s, CH₂), 23.2 (s, CH₂), 20.6 (s, CH₂), 18.1 (s, CH₃), 17.6 (s, CH₂), 13.7 (s, CH₂CH₃) ppm.

¹⁹F{¹H}-NMR (376 MHz, DMSO-*d*₆): δ = -61.4 (s, BAr_F⁻) ppm.

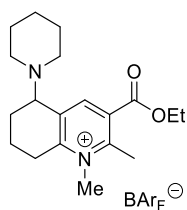
MS (FAB NBA) *m/z* (%): 303 (85) [M-BAr_F]⁺, 232 (100) [M-BAr_F, -C₄H₉N]⁺, 218 (6), 204 (18).

IR: $\tilde{\nu}$ = 2978w, 2938w, 2881w, 1710m, 1455w, 1316s, 1262m, 1196m, 1140s, 1106s, 1057s, 1005s, 971m, 855w, 778s cm⁻¹.

EA: calc.: C 51.48, H 3.37, 2.40; found: C 50.34, H 3.28 N 2.44.

m.p.: 55-57 °C.

3-(Ethoxycarbonyl)-1,2-dimethyl-5-(piperidin-1-yl)-5,6,7,8-tetrahydroquinolin-1-ium tetrakis(3,5-bis(trifluoromethyl)phenyl)borate (**106**)



Compound **104** (200 mg, 0.43 mmol, 1.00 eq.) was dissolved in dichloromethane (3 mL) and NaBAr_F (380 mg, 0.43 mmol, 1.00 eq.) was added. The mixture was stirred for 20 min at RT and filtered through a disposable HPLC filter (CHROMAFILL®0-20/15 MS, pore size 20 μm). The solvent was removed *in vacuo* and the resulting residue was washed with dry *n*-pentane (2 × 2 mL) to give the BAr_F salt **106** (490 mg, 97%) as a yellow solid.

C₅₁H₄₁F₂₄N₂O₂ (1180.66 g mol⁻¹)

¹H-NMR (500 MHz, DMSO-*d*₆): δ = 8.91 (s, 1H, Ar-*H*), 7.63 (s, 12H, BAr_F-*H*), 4.37 (q, *J* = 7.1 Hz, 2H, CH₂CH₃), 4.04 (s, 3H, N-CH₃), 3.93-3.87 (m, 1H, CH), 3.19-3.01 (m, 2H, CH₂), 2.93 (s, 3H, CH₃), 2.46-2.33 (m, 4H, CH₂), 2.18-2.10 (m, 1H, CH₂), 2.00-1.91 (m, 1H, CH₂), 1.77-1.64 (m, 1H, CH₂), 1.59-1.37 (m, 4H, CH₂), 1.37-1.30 (m, 3H, CH₂), 1.30 (t, *J* = 7.1 Hz, 3H, CH₂CH₃) ppm.

¹³C{¹H}-NMR (101 MHz, DMSO-*d*₆): δ = 164.1 (s, C=O), 161.0 (q, *J*_{BC} = 50 Hz, BAr_F), 158.3 (s, Ar-C), 154.8 (s, Ar-C), 142.6 (s, Ar-C), 137.5 (s, Ar-C), 134.0 (s, BAr_F), 128.8 (s, Ar-C), 128.2 (qq, *J*_{FC} = 30 Hz, *J*_{FC} = 3 Hz, BAr_F), 124.0 (q, *J*_{FC} = 273 Hz, BAr_FCF₃), 117.5 (sept, *J*_{FC} = 4 Hz, BAr_F), 62.4 (s, CH₂CH₃), 61.5 (s, CH), 48.9 (s, CH₂), 40.6 (s, N-CH₃), 28.8 (s, CH₂), 26.0 (s, CH₂), 23.8 (s, CH₂), 19.5 (s, CH₂), 18.6 (s, CH₃), 18.0 (s, CH₂), 13.6 (s, CH₂CH₃) ppm.

¹⁹F{¹H}-NMR (376 MHz, DMSO-*d*₆): δ = -61.4 (s, BAr_F⁻) ppm.

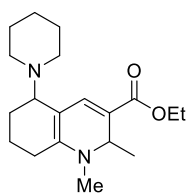
MS (FAB NBA) *m/z* (%): 317 (92) [M-BAr_F]⁺, 232 (100) [M-BAr_F, -C₅H₁₀N]⁺, 204 (18).

IR: $\tilde{\nu}$ = 2942w, 2921w, 2362w, 1877w 1699s, 1561w, 1519m, 1401w, 1243s, 1151s, 1123m, 1071m, 886m, 772w cm^{-1} .

EA: calc.: C 51.88, H 3.50, N 2.37; found: C 50.64, H 3.33 N 2.42.

m.p.: 55-57 °C.

Ethyl 1,2-dimethyl-5-(piperidin-1-yl)-1,2,5,6,7,8-hexahydroquinoline-3-carboxylate (107)



To a solution of **106** (35.0 mg, 0.03 mmol, 1.00 eq.) in THF/MeOH (1:1, 0.5 mL) was added sodium cyanoborohydride (1.90 mg, 0.03 mmol, 1.00 eq.) at 0 °C. The mixture was stirred for 15 min. Evaporation of the solvent and purification by flash chromatography (*n*-alumina, cyclohexane) yielded the

isomeric mixtures of the title compound **107** (4.50 mg, 48 %) as a yellow oil.

$\text{C}_{19}\text{H}_{30}\text{N}_2\text{O}_2$ (318.45 g mol^{-1})

Only diagnostic peaks are listed.

$^1\text{H-NMR}$ (400 MHz, $\text{DMSO-}d_6$): δ = 5.96 (s, 1H, =CH), 5.61 (s, 1H, =CH), 5.50 (s, 1H, =CH), 4.16 (q, J = 7.1 Hz, 2H, CH_2CH_3), 4.08-4.00 (m, 2H, CH_2CH_3), 3.96 (q, J = 7.1 Hz, 2H, CH_2CH_3); 2.97 (s, 3H, CH_3), 2.91 (s, 3H, CH_3), 2.87 (s, 3H, CH_3) ppm.

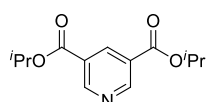
MS (FAB NBA) m/z (%): 236 (100) $[\text{M}-\text{C}_5\text{H}_{10}\text{N}]^+$, 191 (21), 178 (11), 167 (12), 149 (37), 133 (11), 123 (16), 95 (30), 83 (28), 57 (51).

TLC (*n*-alumina, cyclohexane/EtOAc 10:1): R_f = 0.20.

7.4 Bimolecular Pyridinium-Based FLP Systems

7.4.1 Synthesis of Pyridinium Salts

Diisopropyl pyridine-3,5-dicarboxylate (**122**)



Thionyl chloride (0.44 mL, 712 mg, 5.98 mmol, 2.00 eq.) was added dropwise over the course of 5 min to a stirred suspension of pyridine dicarboxylic acid (500 mg, 2.99 mmol, 1.00 eq.) in *i*PrOH (6 mL) at 0 °C. The white suspension was then refluxed overnight. After cooling to room temperature, EtOAc (10 mL) was added. To the suspension was added NaHCO₃ (5 mL) to neutralize any remaining SOCl₂ or HCl. The mixture was extracted with EtOAc (3 x 10 mL), dried over MgSO₄, and concentrated to afford a pale yellow oil. Purification by column chromatography (SiO₂, 6 x 25 cm, EtOAc/cyclohexane 1:10) gave the desired compound **122** as a pale yellow solid (320 mg, 43%). The analytical data match the literature values.^[124]

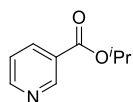
C₁₃H₁₇NO₄ (251.28 g mol⁻¹)

¹H-NMR (400 MHz, CDCl₃): δ = 9.31 (d, *J* = 2.1 Hz, 2H, Ar-*H*), 8.80 (t, *J* = 2.1 Hz, 1H, Ar-*H*), 5.29 (hept, *J* = 6.32 Hz, 2H, CH(CH₃)₂), 1.38 (d, *J* = 6.3 Hz, 12H, CH₃).

¹³C{¹H}-NMR (101 MHz, CDCl₃): 164.0 (s, C=O), 154.0 (s, Ar-CH), 137.8 (s, Ar-CH), 126.5 (s, Ar-C), 69.6 (s, CH(CH₃)₂), 21.9 (s, CH₃) ppm.

TLC (SiO₂, cyclohexane/EtOAc 10:1): R_f = 0.39.

Isopropyl nicotinate (**128**)



Thionyl chloride (1.18 mL, 1.94 g, 16.2 mmol, 1.00 eq.) was added dropwise over the course of 5 min to a stirred suspension of nicotinic acid (2.00 g, 16.2 mmol, 1.00 eq.) in *i*PrOH (35 mL) at 0 °C. The white suspension was then refluxed overnight. After cooling to room temperature, EtOAc (40 mL) was added. To the suspension was added NaHCO₃ (20 mL) to neutralize any remaining SOCl₂ or HCl. The mixture was extracted with EtOAc (3 x 40 mL), dried over MgSO₄, and concentrated to afford a pale yellow oil. Purification

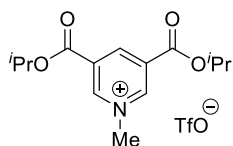
by column chromatography (SiO₂, 6 x 25 cm, EtOAc/cyclohexane 1:10) gave the desired compound **128** as a pale yellow solid (2.60 g, 97%). The analytical data match the literature values.^[124]

C₉H₁₁NO₂ (165.08 g mol⁻¹)

¹H-NMR (400 MHz, CDCl₃): δ = 9.19 (d, *J* = 1.9 Hz, 1H, Ar-*H*), 8.73 (dd, *J* = 4.9, 1.7 Hz, 1H, Ar-*H*), 8.26 (dt, *J* = 7.9, 1.9 Hz, 1H, Ar-*H*), 7.35 (dd, *J* = 7.9, 4.9 Hz, 1H, Ar-*H*), 5.25 (hept, *J* = 6.3 Hz, 1H, CH(CH₃)₂), 1.36 (d, *J* = 6.3 Hz, 6H, CH₃) ppm.

TLC (SiO₂, cyclohexane/EtOAc 10:1): R_f = 0.32.

3,5-bis(*iso*-Propoxycarbonyl)-1-methylpyridin-1-ium trifluoromethanesulfonate (**127**)



Methyl triflate (0.12 mL, 148 mg, 0.88 mmol, 1.00 eq.) was added to a solution of **122** (220 mg, 0.88 mmol, 1.00 eq.) in dichloromethane (4 mL) at 0 °C. The reaction mixture was stirred for 2 h at 0 °C. Evaporation of the solvent using high vacuum yielded the desired product **127** as a colorless solid (344 mg, 95%).

C₁₅H₂₀F₃NO₇S (415.38 g mol⁻¹)

¹H-NMR (400 MHz, CDCl₃): δ = 9.43 (d, *J* = 1.1 Hz, 2H, Ar-*H*), 9.28 (t, *J* = 1.5 Hz, 1H, Ar-*H*), 5.32 (hept, *J* = 6.3 Hz, 2H, CH(CH₃)₂), 4.68 (s, 3H, CH₃), 1.42 (d, *J* = 6.3 Hz, 12H, CH(CH₃)₂) ppm.

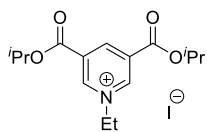
¹³C{¹H}-NMR (400 MHz, CDCl₃): 160.0 (s, C=O), 149.3 (s, Ar-CH), 144.7 (s, Ar-CH), 131.5 (s, Ar-C), 120.4 (q, *J*_{CF} = 320 Hz, CF₃), 72.3 (s, CH(CH₃)₂), 50.0 (s, CH₃), 21.6 (s, CH(CH₃)₂) ppm.

IR: $\tilde{\nu}$ = 3080w, 2991w, 2942w, 2882w, 2360w, 1732s, 1650w, 1464w, 1373m, 1324m, 1262s, 1195s, 1140s, 1107s, 1030s, 960m, 934w, 900w, 834w, 745m, 635s cm⁻¹.

MS (MALDI-TOF): *m/z* (%) = 266 ([M-(TfO)]⁺, 100)

HRMS (ESI-MS): calc. (*m/z*) for C₁₄H₂₀NO₄⁺: 266.1387 [M-(TfO)]⁺, found: 266.1389.

m.p.: 118-120 °C.

1-Ethyl-3,5-bis(*iso*-propoxycarbonyl)pyridin-1-ium iodide (123)

To a solution of diester **122** (100 mg, 0.39 mmol, 1.00 eq.) in DMF (1.0 mL) was added dropwise iodoethane (0.03 mL, 62.1 mg, 0.39 mmol, 1.00 eq.).

The mixture was stirred for 4 h at RT. The solvent was removed under high vacuum. The title product **123** was obtained as a brown solid (132 mg, 82%).

$C_{15}H_{22}INO_4$ (407.06 g mol⁻¹)

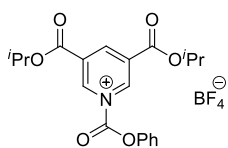
¹H-NMR (400 MHz, CDCl₃): δ = 9.78 (d, J = 1.7 Hz, 2H, Ar-*H*), 9.29 (t, J = 1.6 Hz, 1H, Ar-*H*), 5.30 (hept, J = 6.2 Hz, 2H, CH(CH₃)₂), 5.22 (q, J = 7.4 Hz, 2H, NCH₂CH₃), 1.82 (t, J = 7.4 Hz, 3H, NCH₂CH₃), 1.45 (d, J = 6.3 Hz, 12H, CH₃) ppm.

¹³C{¹H}-NMR (126 MHz, CDCl₃): 159.9 (s, C=O), 148.0 (s, Ar-CH), 145.2 (s, Ar-CH), 121.7 (s, Ar-C), 72.6 (s, CH(CH₃)₂), 59.3 (s, CH₂), 21.9 (s, CH(CH₃)₂) 16.7 (s, CH₃) ppm.

IR: $\tilde{\nu}$ = 1980w, 1724s, 1453w, 1372m, 1250s, 1186m, 1097s, 954w, 895w, 826m, 745m, 671w cm⁻¹.

MS (MALDI-TOF): m/z (%) = 280 ([M-(I)]⁺, 100)

HRMS (ESI-MS): calc. (m/z) for C₁₅H₂₂NO₄⁺: 280.1543 [M-(I)]⁺, found: 280.1545.

3,5-bis(*iso*-Propoxycarbonyl)-1-(phenoxycarbonyl)pyridin-1-ium tetrafluoroborate (129)

Phenyl chlorofomate (0.13 mL, 156 mg, 1.00 mmol, 1.00 eq.) and NaBF₄ (109 mg, 1.00 mmol, 1.00 eq.) were dissolved in acetonitrile (6 mL) and cooled to 0 °C. At this temperature, a solution of **122** (250 mg, 1.00 mmol, 1.00 eq.) in acetonitrile (1 mL) was added dropwise over 10 min and stirred for 1 h. The reaction mixture was filtered over a disposable HPLC filter (CHROMAFILL®0-20/15 MS, pore size 20 μ m) and the solvent was evaporated to dryness to give the title compound **129** as a colorless solid (230 mg, 51%).

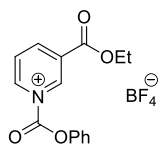
$C_{20}H_{22}BF_4NO_6$ (459.15 g mol⁻¹)

¹H-NMR (400 MHz, CDCl₃): δ = 9.41 (s, 2H, Ar-H), 9.31 (t, J = 1.7 Hz, 1H, Ar-H), 7.47-7.37 (m, 2H, Ar-H), 7.35-7.27 (m, 1H, Ar-H), 7.22-7.20 (m, 2H, Ar-H), 5.31 (hept, J = 6.3 Hz, 2H, CH(CH₃)₂), 1.44 (d, J = 6.3 Hz, 12H, CH₃) ppm.

¹³C{¹H}-NMR (126 MHz, CDCl₃): δ = 161.01 (s, CO₂Pr), 155.9 (s, CO₂Ph), 147.3 (s, Ar-CH), 144.1 (s, Ar-CH), 130.2 (s, Ar-C), 129.9 (s, Ar-CH), 127.2 (s, Ar-CH), 120.9 (s, Ar-C), 120.4 (s, Ar-CH), 71.7 (s, CH(CH₃)₂), 21.8 (s, CH(CH₃)₂) ppm.

¹⁹F{¹H} NMR (376 MHz, CDCl₃): δ = -152.2 (s, BF₄⁻) ppm.

3-(Ethoxycarbonyl)-1-(phenoxy carbonyl)pyridin-1-ium tetrafluoroborate (130)



The title compound **130** was obtained following the procedure of **129** using phenyl chloroformate (0.1 mL, 124 mg, 0.79 mmol, 1.20 eq.), AgBF₄ (155 mg, 0.79 mmol, 1.20 eq.), acetonitrile (3 mL) and ethyl nicotinate (0.09 mL, 100 mg, 0.66 mmol, 1.00 eq.) as a colorless solid (178 mg, 75%). The analytical data match the literature values.^[86]

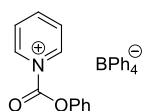
$C_{15}H_{14}BF_4NO_4$ (459.15 g mol⁻¹)

¹H-NMR (400 MHz, CDCl₃): δ = 9.28 (s, 1H, Ar-H), 9.00 (d, J = 5.1 Hz, 1H, Ar-H), 8.80 (d, J = 8.1 Hz, 1H, Ar-H), 7.96 (dd, J = 7.8 Hz, J = 5.9 Hz, 1H Ar-H), 7.41-7.37 (m, 3H, Ar-H), 7.27-7.22 (m, 2H, Ar-H), 4.44 (q, J = 7.1 Hz, 2H, CH₂CH₃), 1.39 (t, J = 7.1 Hz, 3H, CH₂CH₃) ppm.

¹³C{¹H}-NMR (101 MHz, CDCl₃): δ = 161.9 (s, CO₂Et), 151.0 (s, CO₂Ph), 146.4 (s, Ar-CH), 145.0 (s, Ar-CH), 143.8 (s, Ar-CH), 129.9 (s, Ar-C), 129.6 (s, Ar-CH), 127.1 (s, Ar-CH), 126.3 (s, Ar-CH), 120.4 (s, Ar-CH), 120.1 (s, Ar-C), 63.1 (s, CH₂CH₃), 14.1 (s, CH₂CH₃) ppm.

¹⁹F{¹H} NMR (376 MHz, CDCl₃): δ = -152.2 (s, BF₄⁻) ppm.

1-(Phenoxy carbonyl)pyridin-1-ium tetraphenylborate (132)



Pyridine (80.9 μ L, 79.1 mg, 1.00 mmol, 1.00 eq.) was added dropwise to a solution of phenyl chloroformate (0.13 mL, 163 mg, 1.04 mmol, 1.04 eq.) and sodium

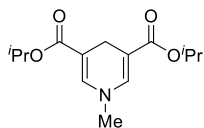
tetraphenylborate (342 mg, 1.00 mmol, 1.00 eq.) in anhydrous acetonitrile (7.5 mL) at 0 °C. The reaction mixture was stirred for 30 min. The solution was filtered over Celite® and the solvent was evaporated to give the product **132** as a yellow solid (423 mg, 82%). The analytical data match the literature values.^[88]

C₃₆H₃₀BNO₂ (519.45 g mol⁻¹)

¹H-NMR (400 MHz, CDCl₃): δ = 8.56 (d, *J* = 7.0 Hz, 2H, Ar-*H*), 8.59 (t, *J* = 7.7 Hz, 1H, Ar-*H*), 7.49 (t, *J* = 7.8 Hz, 2H, Ar-*H*), 7.35-7.29 (m, 3H, Ar-*H*), 7.20-7.18 (m, 2H, Ar-*H*) 7.18-7.15 (m, 8H, BPh₄⁻), 7.13 (d, *J* = 4.3 Hz, 8H, BPh₄⁻), 7.09-7.06 (m, 4H, BPh₄⁻) ppm.

¹³C{¹H}-NMR (101 MHz, CDCl₃): 150.2 (s, C=O), 149.1 (s, Ar-C), 132.8 (s, Ar-CH), 128.0 (s, Ar-CH), 127.7 (s, Ar-CH), 126.4 (s, Ar-CH), 125.2 (s, Ar-CH), 124.4 (s, Ar-C), 123.4 (s, Ar-CH), 119.0 (s, Ar-CH), 118.5 (s, Ar-CH), ppm.

Di-*iso*-propyl 1-methyl-1,4-dihydropyridine-3,5-dicarboxylate (**134**)



A cooled solution of **127** (500 mg, 1.20 mmol, 1.00 eq.) in THF (1 mL) was added dropwise to a solution of sodium cyanoborohydride (79.6 mg, 1.20 mmol, 1.00 eq.) in THF (6 mL) at -78 °C. The mixture was stirred for

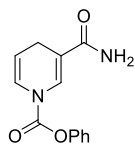
10 min. The reaction mixture was filtered through a disposable HPLC filter (CHROMAFILL®-20/15 MS, pore size 20 μm). Purification by filtration (*b*-alumina, 6 x 4 cm, EtOAc) and evaporation of the solvent yielded the desired product **134** as a yellow solid (130 mg, 41%)

C₁₄H₂₁NO₄ (267.15 g mol⁻¹)

¹H-NMR (400 MHz, CDCl₃): δ = 6.83 (s, 2H, NCH), 5.02 (hept, *J* = 6.3 Hz, 2H, CH(CH₃)₂), 3.15 (s, *J* = 0.6 Hz, 2H, CH₂), 3.02 (s, 3H, CH₃), 1.19 (d, *J* = 6.4 Hz, 12H, CH₃) ppm.

¹³C{¹H}-NMR (400 MHz, CDCl₃): δ = 166.9 (s, C=O), 139.4 (s, NCH), 104.8 (s, Ar-C), 67.0 (s, CH(CH₃)₂), 41.0 (NCH₃), 21.9 (s, CH(CH₃)₂) 21.3 (s, CH₂) ppm.

MS (EI, 70 eV) *m/z* (%) = 167 ([M-2*x*Pr]⁺, 62), 149 ([M-O^{*i*}Pr]⁺, 38).

Phenyl 3-carbamoylpyridine-1(4H)-carboxylate (133c)

To a solution of lithium tri-*tert*-butoxyaluminium hydride (1.1 M in THF, 0.57 mL, 0.51 g, 2.00 mmol, 3.00 eq.) in THF (5 mL) Cu(I)Br (0.43 g, 2.93 mmol, 4.40 eq.) was added at 0 °C. The reaction mixture was stirred at 0 °C for 30 min and the resulting suspension was cooled to –23 °C. Afterwards nicotinamide (122 mg, 1.00 mmol, 1.50 eq.) was added followed by dropwise addition of phenyl chloroformate (0.08 mL, 104 mg, 0.67 mmol, 1.00 eq.). The mixture was stirred vigorously at –23 °C for 1.5 h, and then 20% aqueous NH₄Cl-solution (10 mL) was added. The reaction mixture was filtered over Celite® and the organic phase was extracted with ether (3 x 20 mL). The combined organic layer was washed with water (1 x 20 mL) and brine (1 x 20 mL), dried over MgSO₄ and the solvent was removed under reduced pressure. Purification by column chromatography (SiO₂, 1 x 10 cm, EtOAc/cyclohexane 1:1) yielded the title compound **133c** as a colorless solid (50 g, 31%).

C₁₃H₁₂N₂O₃ (244.25 g mol⁻¹)

¹H-NMR (400 MHz, CDCl₃): δ = 7.39 (t, *J* = 7.7 Hz, 2H, Ar-*H*), 7.27 (t, *J* = 8.1 Hz, 1H, Ar-*H*), 7.15 (d, *J* = 7.4 Hz, 2H, Ar-*H*), 6.92-6.77 (m, 1H, NCH) 5.68-5.65 (m, 1H, NCH), 5.45 (br, 2H, NH₂), 5.18 (d, *J* = 19 Hz, 1H, NCHCH), 3.15-3.08 (m, 2H, CH₂) ppm.

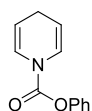
¹³C{¹H}-NMR (101 MHz, CDCl₃): δ = 168.7 (s, C=O), 167.6 (s, C=O), 158.3 (s, Ar-C), 150.4 (s, Ar CH), 126.6 (s, Ar-CH), 126.3 (s, Ar-CH), 121.4 (s, NCH), 120.1 (s, NCHCH), 115.4 (s, NCH), 107.9 (s, Ar-C), 22.7 (s, CH₂) ppm.

IR: $\tilde{\nu}$ = 3180w, 1743m, 1657m, 1575m, 1486w, 1288s, 1196s, 985m, 880w, 733m, 647w cm⁻¹.

HRMS (ESI-MS): calc. (*m/z*) for C₁₃H₁₂N₂O₃H⁺: 245.0921 [M+(H⁺)]⁺, found: 245.0919.

m.p.: 156-157 °C.

TLC (SiO₂, cyclohexane/EtOAc 1:1): R_f = 0.21.

Phenyl pyridine-1(4H)-carboxylate (133b)

The title compound **133b** was obtained following the procedure of **133c** using lithium tri-*tert*-butoxyaluminium hydride (1.1 M in THF, 0.55 mL, 500 mg, 1.97 mmol,

3.00 eq.), Cu(I)Br (422 mg, 2.88 mmol, 4.40 eq.), pyridine (80 μ L, 77.8 mg, 0.98 mmol, 1.50 eq.) and phenyl chloroformate (83 μ L, 103 mg, 0.65 mmol, 1.00 eq.) in THF (5 mL). Purification by column chromatography (SiO₂, 2 x 15 cm, EtOAc/cyclohexane 1:1) gave the desired product **133b** as a colorless solid (112 mg, 85%). The analytical data match the literature values.^[89]

C₁₂H₁₁NO₂ (201.22 g mol⁻¹)

¹H-NMR (400 MHz, CDCl₃): δ = 7.44-7.35 (m, 5H, Ar-H), 6.89 (dd, J = 8.5 Hz, J = 1.7 Hz, 2H, NCH), 5.05 (ddd, J = 8.7, 5.6, 3.4 Hz, 2H, NCHCH), 2.90 (tt, J = 3.6, 1.9 Hz, 2H, CH₂) ppm.

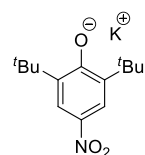
¹³C{¹H}-NMR (400 MHz, CDCl₃): δ = 129.5 (s, Ar-C), 126.3 (s, Ar-C), 123.6 (s, Ar-C), 121.6 (s, NCH), 121.5 (s, NCH), 107.03 (s, NCHCH), 106.8 (s, NCHCH), 22.4 (s, CH₂) ppm.

7.4.2 Phenolates

Formation of Phenolates

General Procedure C: Potassium hydride (1.00 eq.) was added to a solution of phenol (1.00 eq.) in THF (0.02 M) at 0 °C under an inert atmosphere. The mixture was stirred for 1 h and was allowed to warm to room temperature. The solvent was evaporated under high vacuum to give the desired product.

Potassium 2,6-di-*tert*-butyl-4-nitrophenolate (**114a**)



According to general procedure C, the title compound **114a** was obtained upon reaction of 2,6-di-*tert*-butyl-4-nitrophenol (250 mg, 1.00 mmol, 1.00 eq.) with potassium hydride (39.9 mg, 1.00 mmol, 1.00 eq.) as an orange solid (276 mg, 96%).

C₁₄H₂₀KNO₃ (289.11 g mol⁻¹)

¹H-NMR (500 MHz, DMSO-*d*₆): δ = 7.68 (s, 2H, Ar-H), 1.27 (s, 18H, C(CH₃)₃) ppm.

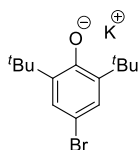
¹³C{¹H}-NMR (126 MHz, DMSO-*d*₆): δ = 180.6 (s, Ar-C), 137.8 (s, Ar-C), 125.4 (s, Ar-C), 122.2 (s, Ar-CH), 35.1 (s, C(CH₃)₃), 29.9 (s, C(CH₃)₃) ppm.

IR: $\tilde{\nu}$ = 2995w, 2328w, 1599w, 1554w, 1479w, 1386m, 1352m, 1281s, 1243s, 1194s, 1141w, 1087w, 907m 804w cm^{-1} .

MS (MALDI-TOF): m/z (%) = 250 ($[\text{M}-(\text{K}^+)]^-$), 100

HRMS (ESI-MS): calc. (m/z) for $\text{C}_{14}\text{H}_{20}\text{NO}_3^-$: 250.1449 $[\text{M}-(\text{K}^+)]^-$, found: 250.1452.

Potassium 4-bromo-2,6-di-*tert*-butylphenolate (**114b**)



According to general procedure C, the title compound **114b** was obtained upon reaction of 2,6-di-*tert*-butyl-4-bromophenol (284 mg, 1.00 mmol, 1.00 eq.) with potassium hydride (39.9 mg, 1.00 mmol, 1.00 eq.) as a brown solid (289 mg, 90%)

$\text{C}_{14}\text{H}_{20}\text{BrKO}$ (322.03 g mol^{-1})

$^1\text{H-NMR}$ (500 MHz, $\text{DMSO-}d_6$): δ = 7.16 (s, 2H, Ar-H), 1.35 (s, 18H, $\text{C}(\text{CH}_3)_3$) ppm.

$^{13}\text{C}\{^1\text{H}\}\text{-NMR}$ (126 MHz, $\text{DMSO-}d_6$): δ = 173.4 (s, Ar-C), 134.5 (s, Ar-C), 127.6 (s, Ar-C), 120.4 (s, Ar-CH), 35.2 (s, $\text{C}(\text{CH}_3)_3$), 30.5 (s, $\text{C}(\text{CH}_3)_3$) ppm.

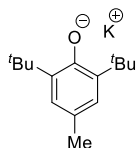
IR: $\tilde{\nu}$ = 3003w, 2957w, 2909w, 2867w, 1841m, 1603s, 1457m, 1386w, 1360s, 1289w, 1261m, 1199w, 1090s, 1042m, 969w, 932w, 898m, 844m, 819w cm^{-1} .

MS (MALDI-TOF): m/z (%) = 284 ($[\text{M}-(\text{K}^+)]^-$), 100

EA: calc.: C 52.01, H 6.24; found: C 52.41, H 6.34.

m.p.: 239-240 $^\circ\text{C}$.

Potassium 2,6-di-*tert*-butyl-4-methylphenolate (**114c**)



According to general procedure C, the title compound **114c** was obtained upon reaction of 2,6-di-*tert*-butyl-4-methylphenol (219 mg, 1.00 mmol, 1.00 eq.) with potassium hydride (39.9 mg, 1.00 mmol, 1.00 eq.) as a grey solid (250 mg, 98%)

$\text{C}_{15}\text{H}_{23}\text{KO}$ (258.14 mol^{-1})

$^1\text{H-NMR}$ (500 MHz, $\text{DMSO-}d_6$): δ = 6.38 (s, 2H, Ar-H), 1.99 (s, 3H, CH_3), 1.30 (s, 18H, $\text{C}(\text{CH}_3)_3$) ppm.

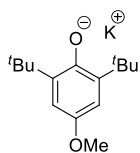
$^{13}\text{C}\{^1\text{H}\}$ -NMR (126 MHz, DMSO- d_6): δ = 169.5 (s, Ar-C), 134.8 (s, Ar-C), 123.9 (s, Ar-C), 107.9 (s, Ar-CH), 35.1 (s, CH₃), 30.5 (s, C(CH₃)₃), 22.1 (s, C(CH₃)₃) ppm.

IR: $\tilde{\nu}$ = 3064w, 2954m, 2911m, 2871m, 2362w, 1736w, 1656w, 1604w, 1444m, 1410s, 1377m, 1242m, 1274w, , 1209m, 1181m, 1129m, 1054m, 1030s, 930m, 887m cm⁻¹.

MS (MALDI-TOF): m/z (%) = 219 ([M-(K⁺)]⁻, 100)

m.p.: 253 °C.

Potassium 2,6-di-*tert*-butyl-4-methoxyphenolate (**114d**)



According to general procedure C, the title compound **114d** was obtained upon reaction of 2,6-di-*tert*-butyl-4-methoxyphenol (235 mg, 1.00 mmol, 1.00 eq.) with potassium hydride (39.9 mg, 1.00 mmol, 1.00 eq.) as a grey solid (258 mg, 95%)

C₁₅H₂₃KO₂ (274.13 mol⁻¹)

^1H -NMR (500 MHz, DMSO- d_6): δ = 6.35 (s, 2H, Ar-H), 3.19 (s, 3H, CH₃), 1.31 (s, 18H, C(CH₃)₃) ppm.

$^{13}\text{C}\{^1\text{H}\}$ -NMR (126 MHz, DMSO- d_6): δ = 172.3 (s, Ar-C), 135.8 (s, Ar-C), 128.8 (s, Ar-C), 106.9 (s, Ar-CH), 53.1 (s, CH₃), 37.1 (s, C(CH₃)₃), 29.9 (s, C(CH₃)₃) ppm.

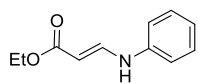
IR: $\tilde{\nu}$ = 2954w, 1604w, 1424m, 1404m, 1377w, 1242sm 1211s, 1181m, 1054m, 1029m, 930w, 875w cm⁻¹.

MS (MALDI-TOF): m/z (%) = 235 ([M-(K⁺)]⁻, 100)

7.5 Hantzsch Analogues in Pyridylidene Chemistry

7.5.1 Synthesis of *N*-Aryl Hantzsch esters

(*E*)-Ethyl 3-(phenylamino)acrylate (**178**)



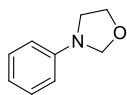
To a solution of ethyl propiolate (632 mg, 0.65 mL, 6.44 mmol, 1.20 eq.) in 1,2-dichloroethane (25 mL) was added copper(I)iodide (511 mg, 2.68 mmol, 0.50 eq.) and aniline (500 mg, 0.49 mL, 5.37 mmol, 1.00 eq.). The reaction mixture was stirred for 10 min and then heated at 60 °C overnight. The reaction mixture was filtered, evaporated and the residue was purified by column chromatography (silica, 3 x 20 cm, EtOAc/cyclohexane 1:15) to provide the desired product **178** (282 mg, 28%) as a colorless oil. The analytical data match the literature values.^[101]

C₁₁H₁₃NO₂ (191.23 g mol⁻¹)

¹H-NMR (400 MHz, CDCl₃): δ = 9.91 (d, *J* = 11.4 Hz, 1H, NH), 7.32-7.23 (m, 3H, =CHN and Ar-H), 7.02-6.95 (m, 3H, Ar-H), 4.85 (d, *J* = 8.2 Hz, 1H, CH=CHN), 4.17 (q, *J* = 7.1 Hz, 2H, OCH₂), 1.33 (t, *J* = 7.1 Hz, 3H, CH₃) ppm.

TLC (SiO₂, cyclohexane/EtOAc 15:1): R_f = 0.58.

3-Phenyloxazolidine (**174**)



2-Anilinoethanol (17.7 g, 12.5 mL, 0.10 mol, 1.00 eq.) and paraformaldehyde (3.30 g, 0.11 mol, 1.10 eq.) in toluene (50 mL) were heated under reflux using a Dean-Stark trap for 20 h. Concentration in vacuo and fractional distillation (88-92 °C, 10⁻¹ mbar), gave the title compound **174**, which solidified on cooling (11.2 g, 76%).

The analytical data match the literature values.^[99]

$C_9H_{11}NO$ (149.19 g mol⁻¹)

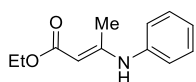
¹H-NMR (400 MHz, CDCl₃): δ = 7.27-7.23 (m, 2H, Ar-H), 6.77 (t, J = 7.3 Hz, 1H, Ar-H), 6.53 (d, J = 7.7 Hz, 2H, Ar-H), 4.88 (s, 2H, NCH₂O) 4.17 (t, J = 6.2 Hz, 2H, OCH₂CH₂), 3.43 (t, J = 6.5 Hz, 2H, NCH₂CH₂) ppm.

¹³C{¹H}-NMR (101 MHz, CDCl₃): δ = 145.6 (s, Ar-C), 129.4 (s, Ar-CH), 117.6 (s, Ar-CH), 112.6 (s, Ar-CH), 81.2 (s, NCH₂O), 67.4 (s, OCH₂CH₂), 46.1 (s, NCH₂CH₂) ppm.

m.p. = 28 °C.

b.p. = 88 °C, 10⁻¹ mbar.

(*E*)-Ethyl 3-(phenylamino)but-2-enoate (**172**)



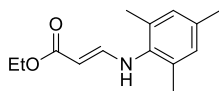
A mixture of ethylacetoacetate (1.30 g, 1.26 mL, 10.0 mmol, 1.00 eq.), aniline (931 mg, 0.91 mL, 10.0 mmol, 1.00 eq.) and acetic acid (60.0 mg, 0.60 mL, 1.00 mmol, 0.10 eq.) was heated to 90 °C for 3 h. After cooling to RT, the reaction mixture was diluted with ethanol (5 mL). The solution was dried over MgSO₄, filtered and concentrated under reduced pressure. The residue was purified by column chromatography (Si₂O, 2.5 x 25 cm, EtOAc/cyclohexane 1:10) to give the pure product **172** as a yellow oil (150 mg, 8%). The analytical data match the literature values.^[98]

$C_{12}H_{15}NO_2$ (205.25 g mol⁻¹)

¹H-NMR (400 MHz, CDCl₃): δ = 10.38 (br, 1H, NH), 7.34-7.30 (m, 2H, Ar-H), 7.17-7.07 (m, 3H, Ar-H), 4.69 (s, 1H, CH=CN), 4.14 (q, J = 7.1 Hz, 2H, OCH₂CH₃), 2.00 (s, 3H, NCCH₃), 1.29 (t, J = 7.1 Hz, 3H, OCH₂CH₃) ppm.

¹³C{¹H}-NMR (101 MHz, CDCl₃): δ = 170.2 (s, C=O), 158.6 (s, NHC), 139.5 (s, Ar-C), 128.8 (s, Ar-CH), 124.5 (s, Ar-CH), 124.1 (s, Ar-CH), 85.5 (s, CCO₂Et) 58.6 (s, CH₂), 20.0 (s, CH₃), 14.6 (s, CH₃) ppm.

TLC (SiO₂, cyclohexane/EtOAc 10:1): R_f = 0.66.

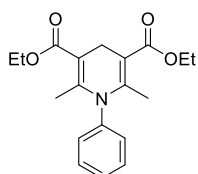
(E)-Ethyl 3-(mesitylamino)acrylate (179)

To a solution of ethyl propiolate (436 mg, 0.45 mL, 4.44 mmol, 1.20 eq.) in 1,2-dichloroethane (20 mL) was added copper(I)iodide (352 mg, 1.85 mmol, 0.50 eq.) and 2,4,6-trimethylaniline (500 mg, 0.52 mL, 3.70 mmol, 1.00 eq.). The reaction mixture was stirred for 10 min and then heated at 60 °C overnight. The reaction mixture was filtered, evaporated and the residue was purified by column chromatography (Si₂O, 3 x 20 cm, EtOAc/cyclohexane 1:10) to provide the desired product **179** (140 mg, 17%) as an orange solid.

C₁₄H₁₉NO₂ (233.31 g mol⁻¹)

¹H-NMR (400 MHz, CDCl₃): δ = 9.21 (d, *J* = 12.4 Hz, 1H, NH), 6.88 (s, 2H, Ar-*H*), 6.70 (dd, *J* = 12.4 Hz, 1H, =CHN), 4.71 (d, *J* = 8.1 Hz, 1H, CH=CHN), 4.17 (q, *J* = 7.1 Hz, 2H, OCH₂CH₃), 2.26 (s, 9H, CH₃), 1.31 (t, *J* = 7.1 Hz, 3H OCH₂CH₃) ppm.

TLC (SiO₂, cyclohexane/EtOAc 10:1): R_f = 0.66.

Diethyl 2,6-dimethyl-1-phenyl-1,4-dihydropyridine-3,5-dicarboxylate (175)

A solution of **178** (1.30 g, 6.33 mmol, 2.00 eq.) and **174** (472 mg, 3.17 mmol, 1.00 eq.) in anhydrous acetonitrile (11 mL) containing acetic acid (1.1 mL) was stirred at RT for 2.5 h. The reaction was basified with cold aqueous sodium carbonate solution (2 mL) and extracted with chloroform (3 x 10 mL). The combined organic layers were washed with cold water (10 mL) and dried over anhydrous MgSO₄, filtered and concentrated under reduced pressure. Purification by column chromatography (Si₂O, 4 x 25 cm, EtOAc/cyclohexane 1:10) gave the desired product **175** as a yellow solid (500 mg, 48%). The analytical data match the literature values.^[100]

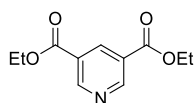
C₁₉H₂₃NO₄ (329.40 g mol⁻¹)

¹H-NMR (400 MHz, CDCl₃): δ = 7.44-7.38 (m, 3H, Ar-*H*), 7.16-7.14 (m, 2H, Ar-*H*), 4.18 (q, *J* = 7.1 Hz, 4H, OCH₂CH₃), 3.38 (s, 2H, CH₂), 1.91 (s, 6H, CH₃), 1.29 (t, *J* = 7.1 Hz, 6H, OCH₂CH₃) ppm.

$^{13}\text{C}\{^1\text{H}\}$ -NMR (101 MHz, CDCl_3): δ = 168.4 (s, C=O), 148.1 (s, NCCH_3), 140.8 (s, Ar-C), 130.6 (s, Ar-CH), 129.3 (s, Ar-CH), 128.4 (s, Ar-CH), 115.0 (s, CCO_2Et), 59.8 (s, OCH_2CH_3), 18.4 (s, CH_3), 14.4 (s, OCH_2CH_3) ppm.

TLC (SiO_2 , cyclohexane/EtOAc 10:1): R_f = 0.32.

Diethyl pyridine-3,5-dicarboxylate (**185b**)



Thionyl chloride (0.44 mL, 5.98 mmol, 2.00 eq.) was added dropwise to a stirred suspension of pyridine dicarboxylic acid (500 mg, 2.99 mmol, 1.00 eq.) in EtOH (15 mL) at 0 °C. The white suspension was then refluxed overnight. After cooling to room temperature, the reaction mixture was diluted with AcOEt (15 mL) and neutralized with aqueous NaHCO_3 -solution. The reaction mixture was extracted with AcOEt (3 x 15 mL), dried over Na_2SO_4 , filtered and concentrated to afford the title compound **185b** as a pale yellow oil (536 mg, 81%). The analytical data match the literature values.^[124]

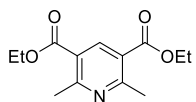
$\text{C}_{11}\text{H}_{13}\text{NO}_4$ (223.23 g mol⁻¹)

^1H -NMR (400 MHz, CDCl_3): δ = 9.37 (d, J = 1.9 Hz, 2H, Ar-H), 8.86 (t, J = 2.0 Hz, 1H, Ar-H), 4.44 (q, J = 7.1 Hz, 4H, OCH_2CH_3), 1.43 (t, J = 7.1 Hz, 6H, OCH_2CH_3) ppm.

$^{13}\text{C}\{^1\text{H}\}$ -NMR (101 MHz, CDCl_3): δ = 164.4 (s, C=O), 154.1 (s, Ar-CH), 137.9 (s, Ar-CH), 126.2 (s, Ar-C), 61.8 (s, OCH_2CH_3), 14.2 (s, OCH_2CH_3) ppm.

TLC (SiO_2 , cyclohexane/EtOAc 10:1): R_f = 0.18.

Diethyl 2,6-dimethylpyridine-3,5-dicarboxylate (**185**)



A solution of diethyl-1,4-dihydro-2,6-dimethyl-3,5-pyridinedicarboxylate (500 mg, 19.9 mmol, 1.00 eq.) in CHCl_3 (50 mL) was irradiated with a 200 W mercury lamp at room temperature for 6 h. The solvent was removed and the product **185** was obtained as a pale yellow solid (490 mg, 99%). The analytical data match the literature values.^[109]

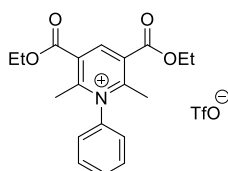
$C_{13}H_{17}NO_4$ (251.28 g mol⁻¹)

¹H-NMR (400 MHz, CDCl₃): δ = 8.77 (s, 1H, Ar-H), 4.42 (q, J = 7.1 Hz, 4H, OCH₂CH₃), 2.94 (s, 6H, CH₃), 1.41 (t, J = 7.1 Hz, 6H, OCH₂CH₃) ppm.

¹³C{¹H}-NMR (101 MHz, CDCl₃): δ = 165.1 (s, C=O), 161.7 (s, Ar-C), 142.2 (s, Ar-CH), 123.9 (s, Ar-C), 61.8 (s, OCH₂CH₃), 23.7 (s, CH₃), 14.2 (s, OCH₂CH₃) ppm.

TLC (SiO₂, cyclohexane/EtOAc 10:1): R_f = 0.25.

3,5-bis(Ethoxycarbonyl)-2,6-dimethyl-1-phenylpyridin-1-ium trifluoromethane sulfonate (165)



To a solution of Hantzsch ester **175** (50.0 mg, 0.15 mmol, 1.00 eq.) in toluene (1 mL) was added trifluoromethanesulfonic acid (22.8 mg, 13.5 μ L, 0.15 mmol, 1.00 eq.). The yellow solution was stirred for 1 h at RT. The

precipitate was separated by filtration and dried under high vacuum to give the desired product **165** as a yellow oil (63 mg, 85%).

$C_{20}H_{22}F_3NO_7S$ (477.45 g mol⁻¹)

¹H-NMR (400 MHz, CDCl₃): δ = 9.34 (s, 1H, Ar-H), 7.76-7.71 (m, 3H, Ar-H), 7.61-7.58 (m, 2H, Ar-H), 4.49 (q, J = 7.1 Hz, 2H, OCH₂CH₃), 2.77 (s, 6H, CH₃), 1.45 (t, J = 7.1 Hz, 6H, OCH₂CH₃) ppm.

¹³C{¹H}-NMR (126 MHz, CDCl₃): δ = 162.4 (C=O), 147.6 (s, Ar-CH), 139.2 (s, Ar-C), 131.8 (s, Ar-CH), 131.6 (s, Ar-CH), 128.9 (s, Ar-C), 125.7 (s, Ar-CH), 121.7 (s, Ar-C), 120.4 (q, J_{CF} = 320 Hz, CF₃), 63.4 (s, OCH₂CH₃), 21.5 (s, CH₃), 14.0 (s, OCH₂CH₃) ppm.

¹⁹F{¹H} NMR (376 MHz, CDCl₃): δ = -78.3 (s, TfO⁻) ppm.

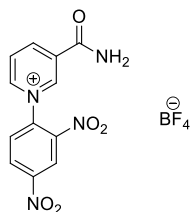
IR: $\tilde{\nu}$ = 2986w, 2662w, 1731m, 1591w, 1496w, 1373w, 1222s, 1170s, 1028s, 858w, 763m, 687m, 636s cm⁻¹.

MS (MALDI-TOF): m/z (%) = 328 ([M-(TfO⁻)]⁺, 100)

HRMS (ESI-MS): calc. (m/z) for C₁₉H₂₂NO₄⁺: 328.1543 [M-(TfO⁻)]⁺, found: 328.1546.

7.5.2 Synthesis of *N*-Aryl Nicotinamide derivatives

3-Carbamoyl-1-(2',4'-dinitrophenyl)pyridin-1-ium tetrafluoroborate (**195**)



A mixture of nicotinamide (500 mg, 4.09 mmol, 1.00 eq.) and 2,4-dinitrochlorobenzene (1.99 g, 9.83 mmol, 2.40 eq.) was stirred at to 105 °C under an inter atmosphere for 1 h to form a dark red solid. After cooling, the solid was dissolved in methanol (3 mL), followed by addition of Et₂O (5 mL).

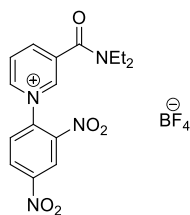
The liquid was decanted from the oily precipitate, and the procedure was repeated twice. The residue was dissolved in H₂O (12.5 mL), extracted with CHCl₃ (5 x 15 mL) and treated with activated charcoal (100 mg). After filtration through Celite[®], the solution was concentrated in vacuo at 30 °C to 3 mL was added to a solution of NaBF₄ (899 mg, 8.19 mmol, 2.00 eq.) in H₂O (2 mL). An oily material was formed, which was redissolved in H₂O (20 mL) by heating on a steam bath. After cooling, the product precipitated. The yellow solid was recrystallized twice from methanol to give the product **195** as fine pale yellow crystals, which were washed with Et₂O (5 mL) and dried in vacuo (1.05 g, 67%). The analytical data match the literature values.^[113]

C₁₂H₉BF₄N₄O₅ (376.03 g mol⁻¹)

¹H-NMR (400 MHz, DMSO-*d*₆): δ = 9.79-9.78 (m, 1H, Ar-*H*), 9.49 (dt, *J* = 6.2, 1.3 Hz, 1H, Ar-*H*), 9.28-9.24 (m, 1H, Ar-*H*), 9.13 (d, *J* = 2.5 Hz, 1H, Ar-*H*), 9.00 (dd, *J* = 8.7, 2.5 Hz, 1H, Ar-*H*), 8.67 (s, 1H, NH), 8.55 (ddd, *J* = 8.1, 6.1, 0.4 Hz, 1H, Ar-*H*), 8.42 (d, *J* = 8.7 Hz, 1H, Ar-*H*), 8.29 (s, 1H, NH) ppm.

¹³C{¹H}-NMR (126 MHz, DMSO-*d*₆): δ = 162.8 (s, C=O), 149.7 (s, Ar-C), 148.1 (s, Ar-CH), 147.0 (s, Ar-CH), 143.4 (s, Ar-C), 139.1 (s, Ar-CH), 134.0 (s, Ar-C), 132.4 (s, Ar-CH), 130.7 (s, Ar-CH), 128.2 (s, Ar-C), 121.8 (s, Ar-C) ppm.

¹⁹F{¹H} NMR (376 MHz, DMSO-*d*₆): δ = -148.3 (s, BF₄⁻) ppm.

3-(Diethylcarbamoyl)-1-(2',4'-dinitrophenyl)pyridin-1-ium tetrafluoroborate (205)

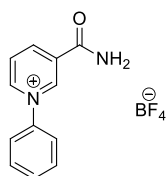
The title compound **205** was obtained following the procedure of **195** using *N,N*-diethylnicotinamide (500 mg, 2.81 mmol, 1.00 eq.), 2,4-dinitrochlorobenzene (1.36 g, 6.73 mmol, 2.40 eq.) and NaBF₄ (616 mg, 5.61 mmol, 2.00 eq.) as a beige solid (1.08 g, 90%). The analytical data match the literature values.^[125]

C₁₆H₁₇BF₄N₄O₅ (432.14 g mol⁻¹)

¹H-NMR (400 MHz, DMSO-*d*₆): δ = 9.64 (s, 1H, Ar-*H*), 9.41 (m, 1H, Ar-*H*), 9.13 (d, *J* = 2.5 Hz, 1H, Ar-*H*), 9.04-8.98 (m, 1H, Ar-*H*), 8.93 (d, *J* = 2.7 Hz, 1H Ar-*H*), 8.54-4.43 (m, 1H, Ar-*H*), 8.09 (d, *J* = 8.9 Hz, 1H Ar-*H*), 3.51 (q, *J* = 7.1 Hz, 2H, CH₂CH₃), 3.27 (q, *J* = 7.1 Hz, 2H, CH₂CH₃), 1.18 (t, *J* = 7.1 Hz, 3H, CH₂CH₃), 1.08 (t, *J* = 7.1 Hz, 3H, CH₂CH₃) ppm.

¹³C{¹H}-NMR (126 MHz, DMSO-*d*₆): δ = 163.6 (s, C=O), 149.7 (s, Ar-C), 147.0 (s, Ar-CH), 146.6 (s, Ar-CH), 144.4 (s, Ar-C), 143.5 (s, Ar-CH), 138.9 (s, Ar-CH), 136.8 (s, Ar-C), 132.5 (s, Ar-CH), 130.8 (s, Ar-CH), 129.0 (s, Ar-CH), 121.9 (s, Ar-CH), 43.6 (s, CH₂), 40.5 (s, CH₂), 14.3 (s, CH₃), 13.1 (s, CH₃) ppm.

¹⁹F{¹H} NMR (376 MHz, DMSO-*d*₆): δ = -148.3 (s, BF₄⁻) ppm.

3-Carbamoyl-1-phenylpyridin-1-ium tetrafluoroborate (197)

Aniline (2.42 mL, 2.47 g, 26.6 mmol, 40.0 eq.) was added to a solution of **195** (250 mg, 0.66 mmol, 1.00 eq.) in dry methanol (60 mL). The reaction mixture was heated to reflux overnight. After cooling to room temperature, the precipitate was removed by filtration. The filtrate was evaporated under reduced pressure and the residue was dissolved in H₂O (2 mL). The aqueous phase was then exhaustively washed with diethyl ether (3 x 5 mL). The aqueous layer was evaporated under reduced pressure to give a crude product, which was recrystallized from methanol to yield the desired product **197** as a beige solid (92 mg, 49%). The analytical data match the literature values.^[114]

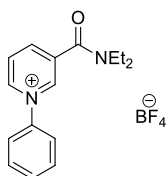
$C_{12}H_{11}BF_4N_2O$ (286.04 g mol⁻¹)

¹H-NMR (400 MHz, DMSO-*d*₆): δ = 9.59 (s, 1H, Ar-*H*), 9.47 (d, *J* = 6.1 Hz, 1H, Ar-*H*), 9.09 (d, *J* = 8.1 Hz, 1H, Ar-*H*), 8.58 (s, 1H, NH), 8.41 (dd, *J* = 7.7, 6.5 Hz, 1H, Ar-*H*), 8.23 (s, 1H, NH), 7.95 (dd, *J* = 6.3, 2.9 Hz, 2H, Ar-*H*), 7.82-7.72 (m, 3H, Ar-*H*) ppm.

¹³C{¹H}-NMR (126 MHz, DMSO-*d*₆): δ = 162.9 (s, C=O), 147.1 (s, Ar-CH), 145.4 (s, Ar-CH), 144.7 (s, Ar-CH), 143.2 (s, Ar-CH), 134.2 (s, Ar-C), 131.9 (s, Ar-CH), 130.7 (s, Ar-C), 128.5 (s, Ar-CH), 125.2 (s, Ar-CH) ppm.

¹⁹F{¹H} NMR (376 MHz, DMSO-*d*₆): δ = -148.3 (s, BF₄⁻) ppm.

3-(Diethylcarbamoyl)-1-phenylpyridin-1-ium tetrafluoroborate (206)



The title compound **206** was obtained following the procedure of **197** using **205** (100 mg, 0.23 mmol, 1.00 eq.), methanol (23 mL) and aniline (0.84 mL, 862 mg, 9.26 mmol, 40.0 eq.) as a yellow solid (65 mg, 83%).

$C_{16}H_{19}BF_4N_2O$ (342.14 g mol⁻¹)

¹H-NMR (400 MHz, CDCl₃): δ = 9.04 (dt, *J* = 6.2, 1.3 Hz, 1H, Ar-*H*), 8.74 (dd, *J* = 1.5, 1.1 Hz, 1H, Ar-*H*), 8.51 (dt, *J* = 8.1, 1.3 Hz, 1H, Ar-*H*), 8.32 (dd, *J* = 7.8, 6.4 Hz, 1H, Ar-*H*), 7.84-7.74 (m, 2H, Ar-*H*), 7.68-7.59 (m, 3H, Ar-*H*), 3.54 (q, *J* = 7.0 Hz, 2H, CH₂CH₃), 3.27 (q, *J* = 7.0 Hz, 2H, CH₂CH₃), 1.26-1.23 (m, 6H, CH₂CH₃) ppm.

¹³C{¹H}-NMR (126 MHz, CDCl₃): δ = 163.6 (s, C=O), 145.1 (s, Ar-CH), 143.8 (s, Ar-CH), 142.6 (s, Ar-CH), 142.1 (s, Ar-CH), 137.7 (s, Ar-C), 131.9 (s, Ar-C), 130.7 (s, Ar-CH), 129.4 (s, Ar-CH), 124.4 (s, Ar-CH), 43.7 (s, CH₂), 41.0 (s, CH₂), 14.1 (s, CH₃), 12.5 (s, CH₃) ppm.

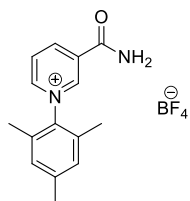
¹⁹F{¹H} NMR (376 MHz, CDCl₃): δ = -152.2 (s, BF₄⁻) ppm.

IR: $\tilde{\nu}$ = 3038w, 1629s, 1460m, 1386w, 1300w, 1216w, 1048s, 829w, 767m, 688m cm⁻¹.

MS (MALDI-TOF): *m/z* (%) = 255 ([M-(BF₄⁻)]⁺, 100)

HRMS (ESI-MS): calc. (*m/z*) for C₁₆H₁₉N₂O⁺: 255.1492 [M-(BF₄⁻)]⁺, found: 255.1496.

m.p.: 107-109 °C.

3-Carbamoyl-1-mesitylpyridin-1-ium tetrafluoroborate (201)

The title compound **201** was obtained following the procedure of **197** using **195** (120 mg, 0.32 mmol, 1.00 eq.), methanol (25 mL) and 2,4,6-trimethylaniline (1.8 mL, 1.73 g, 12.8 mmol, 40.0 eq.) as a pale brown solid (78 mg, 75%).

$C_{15}H_{17}BF_4N_2O$ (328.12 g mol⁻¹)

¹H-NMR (400 MHz, DMSO-*d*₆): δ = 9.45 (s, 1H, Ar-H), 9.27 (d, *J* = 5.8, 1H, Ar-H), 9.17 (d, *J* = 8.0 Hz, 1H, Ar-H), 8.55 (s, 1H, NH), 8.48 (t, *J* = 6.8 Hz, 1H, Ar-H), 8.22 (s, 1H, NH), 7.24 (s, 2H, Ar-H), 2.38 (s, 3H, CH₃), 2.00 (s, 6H, CH₃) ppm.

¹³C{¹H}-NMR (126 MHz, DMSO-*d*₆): δ = 162.8 (s, C=O), 148.5 (s, Ar-CH), 146.3 (s, Ar-CH), 145.9 (s, Ar-CH), 141.5 (s, Ar-C), 139.7 (s, Ar-C), 135.3 (s, Ar-C), 133.1 (s, Ar-C), 130.0 (s, Ar-CH), 129.5 (s, Ar-CH), 21.1 (s, CH₃), 17.2 (s, CH₃) ppm.

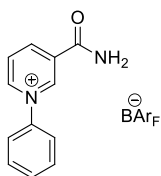
¹⁹F{¹H} NMR (376 MHz, DMSO-*d*₆): δ = -148.9 (s, BF₄⁻) ppm.

IR: $\tilde{\nu}$ = 3410 br, 3183w, 3103w, 1703m, 1641w, 1442w, 1394m, 1286w, 1234w, 1070s, 994s, 853w, 795w, 691m cm⁻¹.

MS (MALDI-TOF): *m/z* (%) = 241 ([M-(BF₄⁻)]⁺, 100)

EA: calc. (%) C 54.91, H 5.22, N 8.54; found C 54.25, H 5.63, N 8.20.

m.p.: 158-161 °C.

3-Carbamoyl-1-phenylpyridin-1-ium tetrakis-[3,5-bis(trifluoromethyl)phenyl]borate (202)

A solution of NaBAr_F (92.9 mg, 0.11 mmol, 1.00 eq.) in H₂O (2 mL) was added to a solution of **197** (30.0 mg, 0.11 mmol, 1.00 eq.) in H₂O (1.5 mL). The reaction mixture was stirred for 30 min at room temperature, and then the aqueous phase was extracted with dichloromethane (3 x 2 mL). The organic phase was separated, dried over MgSO₄ and concentrated under reduced pressure to give the product **202** as a beige solid (98 mg, 98%).

$C_{44}H_{29}BF_{18}N_2O$ (954.51 g mol⁻¹)

¹H-NMR (400 MHz, CDCl₃): δ = 9.31 (t, J = 1.3 Hz, 1H, Ar-H), 8.49 (dt, J = 6.1, 1.3 Hz, 1H, Ar-H), 8.38-8.35 (m, 2H, Ar-H), 7.81-7.77 (m, 2H, Ar-H), 7.69 (s, 8H, BAr_F-H), 7.68 (d, J = 2.5 Hz, 1H, Ar-H), 7.50 (s, 4H, BAr_F-H), 7.43-7.39 (m, 2H, Ar-H), 6.12 (s, 2H, NH₂) ppm.

¹³C{¹H}-NMR (126 MHz, CDCl₃): δ = 162.3 (s, C=O), 160.3 (q, J_{BC} = 49.7 Hz, Ar-C, BAr_F), 144.9 (s, Ar-CH), 144.3 (s, Ar-HC), 141.0 (s, Ar-CH), 134.9 (s, Ar-C), 134.7 (s, Ar-C, BAr_F), 131.7 (s, Ar-CH), 129.2 (s, Ar-C), 129.1 (qq, J_{FC} = 31.6 Hz, J_{BC} = 3.0 Hz, Ar-C, BAr_F), 128.5 (s, Ar-CH), 125.5 (q, J_{FC} = 272.5 Hz, CF₃, BAr_F), 127.7 (s, Ar-CH), 123.2 (s, Ar-CH) 117.6 (sept, J_{FC} = 3.5 Hz, Ar-C, BAr_F) ppm.

¹⁹F{¹H} NMR (376 MHz, CDCl₃): δ = -62.4 (s, BAr_F⁻) ppm.

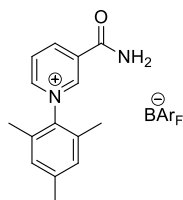
IR: $\tilde{\nu}$ = 3359w, 3199w, 1702m, 1615w, 1355s, 1274s, 1120s, 888m, 838w, 758w, 671m cm⁻¹.

MS (MALDI-TOF): m/z (%) = 199 ([M-(BAr_F⁻)]⁺, 100)

HRMS (ESI-MS): calc. (m/z) for C₁₂H₁₁BN₂O⁺: 199.0866 [M-(BAr_F⁻)]⁺, found: 199.0869.

m.p.: 79-81 °C.

3-Carbamoyl-1-mesitylpyridin-1-ium tetrakis-[3,5-bis(trifluoromethyl)phenyl]borate (**203**)



The title compound **203** was obtained following the procedure of **202** using **201** (50 mg, 0.15 mmol, 1.00 eq.), H₂O (1.5 mL) and NaBAr_F (135 mg, 0.15 mmol, 1.00 eq.) as a pale yellow solid (110 mg, 73%).

$C_{47}H_{35}BF_{18}N_2O$ (996.59 g mol⁻¹)

¹H-NMR (400 MHz, CDCl₃): δ = 9.07 (s, 1H, Ar-H), 8.38-8.32 (m, 3H, Ar-H), 7.75 (dd, J = 8.1, 6.3 Hz, 2H, Ar-H), 7.73 (s, 8H, BAr_F-H), 7.53 (s, 4H, BAr_F-H), 7.16 (s, 2H, NH₂), 2.44 (s, 3H, CH₃), 1.90 (s, 6H, CH₃) ppm.

¹³C{¹H}-NMR (126 MHz, CDCl₃): δ = 161.8 (s, C=O), 161.0 (q, J_{BC} = 49.45 Hz, Ar-C, BAr_F), 148.8 (s, Ar-CH), 145.9 (s, Ar-CH), 143.9 (s, Ar-CH), 141.2 (s, Ar-C), 138.9 (s, Ar-C), 135.3 (s, Ar-C), 134.7 (s, Ar-C, BAr_F), 132.8 (s, Ar-CH), 129.1 (s, Ar-C), 129.0 (qq, J_{FC} = 30.8 Hz, J_{BC} = 3.0 Hz, Ar-C, BAr_F), 125.6 (q, J_{FC} = 273.0 Hz, CF₃, BAr_F), 121.8 (s, Ar-CH), 117.6 (sept, J_{FC} = 3.5 Hz, Ar-C, BAr_F), 21.2 (s, CH₃), 16.8 (s, CH₃) ppm.

¹⁹F{¹H} NMR (376 MHz, CDCl₃): δ = -62.4 (s, BAr_F⁻) ppm.

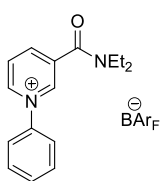
IR: $\tilde{\nu}$ = 3140w, 1705w, 1611w, 1452w, 1355m, 1277s, 1117s, 945w, 888m, 838m, 680m cm^{-1} .

MS (MALDI-TOF): m/z (%) = 241 ($[\text{M}-(\text{BAr}_F^-)]^+$, 100)

HRMS (ESI-MS): calc. (m/z) for $\text{C}_{15}\text{H}_{17}\text{N}_2\text{O}^+$: 241.1335 $[\text{M}-(\text{BAr}_F^-)]^+$, found: 241.1333.

m.p.: 176-178 °C.

3-(Diethylcarbamoyl)-1-phenylpyridin-1-ium tetrakis-[3,5-bis(trifluoromethyl)phenyl]-borate (207)



The title compound **207** was obtained following the procedure of **202** using **206** (50 mg, 0.15 mmol, 1.00 eq.), H_2O (1.5 mL) and NaBAr_F (130 mg, 0.15 mmol, 1.00 eq.) as a pale yellow solid (124 mg, 76%).

$\text{C}_{48}\text{H}_{37}\text{BF}_{18}\text{N}_2\text{O}$ (1010.62 g mol^{-1})

$^1\text{H-NMR}$ (400 MHz, CDCl_3): δ = 8.84 (s, 1H, Ar-H), 8.45-8.40 (m, 2H, Ar-H), 7.86-7.81 (m, 1H, Ar-H), 7.75-7.70 (m, 1H, Ar-H), 7.68 (s, 8H, $\text{BAr}_F\text{-H}$), 7.64-7.58 (m, 2H, Ar-H), 7.49 (s, 4H, $\text{BAr}_F\text{-H}$), 7.41-7.36 (m, 2H, Ar-H), 3.56 (q, J = 7.0 Hz, 2H, CH_2CH_3), 3.22 (q, J = 7.0 Hz, 2H, CH_2CH_3), 1.25 (t, J = 7.1 Hz, 3H, CH_2CH_3), 1.12 (t, J = 7.1 Hz, 3H, CH_2CH_3) ppm.

$^{13}\text{C}\{^1\text{H}\}\text{-NMR}$ (126 MHz, CDCl_3): δ = 161.9 (s, C=O), 161.5 (q, J_{BC} = 49.4 Hz, Ar-C, BAr_F), 143.2 (s, Ar-CH), 143.0 (s, Ar-CH), 141.6 (s, Ar-CH), 139.1 (s, Ar-C), 134.7 (s, Ar-C, BAr_F), 133.4 (s, Ar-CH), 131.6 (s, Ar-C), 128.4 (s, Ar-CH), 128.9 (qq, J_{FC} = 28.4 Hz, J_{BC} = 2.8 Hz, Ar-C, BAr_F), 125.5 (q, J_{FC} = 272.7 Hz, CF_3 , BAr_F), 123.3 (s, Ar-CH), 121.2 (s, Ar-CH), 117.6 (sept, J_{FC} = 3.5 Hz, Ar-C, BAr_F), 43.8 (s, CH_2), 40.6 (s, CH_2), 14.1 (s, CH_3), 12.4 (s, CH_3) ppm.

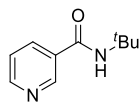
$^{19}\text{F}\{^1\text{H}\}\text{-NMR}$ (376 MHz, CDCl_3): δ = -62.4 (s, BAr_F^-) ppm.

IR: $\tilde{\nu}$ = 3078w, 2987w, 1647m, 1461w, 1434w, 1354s, 1272s, 110s, 1003w, 945w, 887m, 839m, 761w, 712m, 680m cm^{-1} .

MS (MALDI-TOF): m/z (%) = 297 ($[\text{M}-(\text{BAr}_F^-)]^+$, 100)

HRMS (ESI-MS): calc. (m/z) for $\text{C}_{16}\text{H}_{19}\text{N}_2\text{O}^+$: 255.1492 $[\text{M}-(\text{BAr}_F^-)]^+$, found: 255.1493.

m.p.: 46-48 °C.

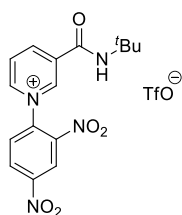
***N*-(*tert*-Butyl)nicotinamide (197a)**

To a solution of 3-cyanopyridine (0.35 mL, 406 mg, 3.90 mmol, 1.00 eq.) in *tert*-butyl acetate (2.89 mL, 2.50 g, 21.4 mmol, 5.50 eq.) was slowly added concentrated sulfuric acid (0.27 mL, 497 mg, 5.07 mmol, 1.30 eq.). The resulting solution was stirred at 40 °C for 5 h. The reaction mixture was cooled to room temperature and was poured into aqueous 20% KHCO₃ solution (20 mL) to neutralize the acid. The aqueous layer was extracted with EtOAc (3 x 20 mL) and the combined organic layers were dried over MgSO₄. The solvent was removed under reduced pressure to give the desired product **197a** as a white solid (643 mg, 93%). The analytical data match the literature values.^[126]

C₁₀H₁₄N₂O (178.11 g mol⁻¹)

¹H-NMR (400 MHz, CDCl₃): δ = 8.89 (d, *J* = 1.7 Hz, 1H, Ar-*H*), 8.67 (dd, *J* = 4.7, 1.7 Hz, 1H, Ar-*H*), 8.05 (dd, *J* = 7.8, 1.7 Hz, 1H, Ar-*H*), 7.34 (dd, *J* = 7.8, 4.7 Hz, 1H, Ar-*H*), 6.01 (br, 1H, NH), 1.47 (s, 9H, C(CH₃)₃) ppm.

¹³C{¹H}-NMR (400 MHz, CDCl₃): δ = 165.0 (s, C=O), 151.9 (s, Ar-CH), 147.7 (s, Ar-CH), 134.9 (s, Ar-CH), 131.5 (s, Ar-CH), 123.4 (s, Ar-C), 52.1 (s, C(CH₃)₃), 28.8 (s, C(CH₃)₃) ppm.

3-(*tert*-Butylcarbamoyl)-1-(2',4'-dinitrophenyl)pyridin-1-ium trifluoromethane sulfonate (197b)

A suspension of pyridine **197a** (1.00 g, 5.61 mmol, 1.00 eq.) and 1-chloro-2,4-dinitrobenzene (1.14 g, 5.61 mmol, 1.00 eq.) in EtOH (9 mL) was stirred at 86 °C for 86 h. After cooling to room temperature, the reaction mixture was diluted with pentane (20 mL). The reaction mixture was filtered and the residue was dried under reduced pressure to obtain a white solid. The solid was dissolved in CHCl₃ (55 mL) and silver trifluoromethanesulfonate (1.44 g, 5.61 mmol, 1.00 eq.) was added to the solution. The mixture was stirred at room temperature for one hour. The mixture was filtered and washed with CHCl₃ (3 x 20 mL). The solvent was concentrated under reduced pressure to afford the desired product **197b** as a yellow solid (2.20 g, 80%).

$C_{16}H_{17}F_3N_4O_8S$ (494.07 g mol⁻¹)

¹H-NMR (400 MHz, CDCl₃): δ = 9.30 (d, J = 1.6 Hz, 1H, Ar-H), 9.00 (d, J = 2.7 Hz, 1H, Ar-H), 8.76 (d, J = 2.6 Hz, 1H, Ar-H), 8.63 (dd, J = 5.2, 1.6 Hz, 1H, Ar-H), 8.53 (dd, J = 9.0, 2.7 Hz, 1H, Ar-H), 7.80 (d, J = 8.8 Hz, 1H, Ar-H), 7.58 (dd, J = 7.7, 5.3 Hz, 1H, Ar-H), 7.00 (br, 1H, NH), 1.48 (s, 9H, CH₃) ppm.

¹³C{¹H}-NMR (126 MHz, CDCl₃): δ = 160.24 (s, C=O), 152.26 (s, Ar-C), 149.65 (s, Ar-CH), 145.51 (s, Ar-CH), 142.97 (s, Ar-C), 138.25 (s, Ar-CH), 137.02 (s, Ar-C), 132.88 (s, Ar-C), 129.67 (s, Ar-CH), 122.74 (s, Ar-CH), 121.89 (s, Ar-CH), 121.67 (s, Ar-C), 121.1 (q, J_{CF} = 320 Hz, CF₃), 53.38 (s, CCH₃), 28.51 (s, CH₃) ppm.

¹⁹F{¹H} NMR (376 MHz, CDCl₃): δ = -78.23 (s, TfO⁻) ppm.

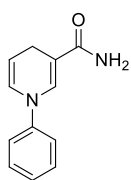
IR: $\tilde{\nu}$ = 3081w, 1668w, 1598m, 1531s, 1341s, 1289m, 1122m, 923w, 834m, 742w, 671w cm⁻¹.

MS (MALDI-TOF): m/z (%) = 345 ([M-(TfO⁻)]⁺, 100)

HRMS (ESI-MS): calc. (m/z) for $C_{16}H_{17}N_4O_5^+$: 345.1193 [M-(TfO⁻)]⁺, found: 345.1196.

m.p.: 153-155 °C.

1-Phenyl-1,4-dihydropyridine-3-carboxamide (208)



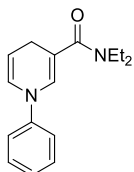
To a solution of **197** (40.0 mg, 0.14 mmol, 1.00 eq.) in cold degassed H₂O (1.4 mL) was added NaHCO₃ (58.7 mg, 0.70 mmol, 5.00 eq.) and Na₂S₂O₄ (73 mg, 0.42 mmol, 3.00 eq.). The reaction mixture was stirred under a stream of argon for 3 h. The aqueous phase was extracted with dichloromethane (3 x 1.5 mL) and the combined organic layers were dried over MgSO₄ and concentrated under vacuum. The desired product **208** was obtained as a beige solid (23 mg, 83%). The analytical data match the literature values.^[114]

$C_{12}H_{12}N_2O$ (200.24 mol⁻¹)

¹H-NMR (400 MHz, CDCl₃): δ = 7.55-7.52 (m, 1H, Ar-H), 7.37-7.30 (m, 2H, Ar-H), 7.15-7.08 (m, 3H, Ar-H, CH), 6.33 (ddd, J = 8.2, 3.5, 1.7 Hz, 1H, CH), 5.42 (br, 2H, NH₂), 4.97 (dt, J = 8.1, 3.5 Hz, 1H, CH), 3.22 (dd, J = 2.9, 1.7 Hz, CH₂) ppm.

$^{13}\text{C}\{^1\text{H}\}$ -NMR (126 MHz, CDCl_3): δ = 169.9 (s, C=O), 143.8 (s, Ar-C), 136.7 (s, NCH), 129.6 (s, Ar-CH), 127.6 (s, NCH), 124.4 (s, Ar-CH), 199.1 (s, Ar-CH), 104.7 (s, CCO_2NH_2), 102.3 (s, NCHCH), 23.0 (s, CH_2) ppm.

N,N-Diethyl-1-phenyl-1,4-dihydropyridine-3-carboxamide (**210**)



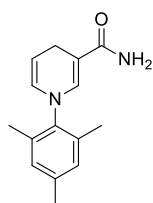
The title compound **210** was obtained following the procedure of **200** using **206** (22 mg, 0.06 mmol, 1.00 eq.), H_2O (0.6 mL), NaHCO_3 (27 mg, 0.32 mmol, 5.00 eq.) and $\text{Na}_2\text{S}_2\text{O}_4$ (33.6 mg, 0.19 mmol, 3.00 eq.) as a beige solid (14 mg, 85%).

$\text{C}_{16}\text{H}_{20}\text{N}_2\text{O}$ (256.35 mol^{-1})

^1H -NMR (400 MHz, CDCl_3): δ = 7.33-7.28 (m, 2H, Ar-*H*), 7.07-6.99 (m, 3H, Ar-*H*), 6.63 (dd, J = 2.5, 1.0 Hz, 1H, CH), 6.35 (dq, J = 8.2, 1.6 Hz, 1H, CH), 4.82 (dt, J = 8.2, 3.5 Hz, 1H, CH), 3.45 (q, J = 7.1 Hz, 4H, CH_2CH_3), 3.22-3.20 (m, 2H, CH_2), 1.81 (t, J = 7.1 Hz, 6H, CH_2CH_3) ppm.

$^{13}\text{C}\{^1\text{H}\}$ -NMR (126 MHz, CDCl_3): δ = 169.7 (s, C=O), 144.6 (s, Ar-C), 138.7 (s, NCH), 129.8 (s, Ar-CH), 126.6 (s, NCH), 125.8 (s, Ar-CH), 199.7 (s, Ar-CH), 106.2 (s, CCO_2NH_2), 103.3 (s, NCHCH), 22.8 (s, CH_2) 43.6 (s, CH_2), 41.2 (s, CH_2), 14.4 (s, CH_3), 12.5 (s, CH_3) ppm.

1-Mesityl-1,4-dihydropyridine-3-carboxamide (**209**)



The title compound **209** was obtained following the procedure of **200** using **201** (20 mg, 0.06 mmol, 1.00 eq.), H_2O (1.0 mL), NaHCO_3 (25.6 mg, 0.31 mmol, 5.00 eq.) and $\text{Na}_2\text{S}_2\text{O}_4$ (31.8 mg, 0.18 mmol, 3.00 eq.) as a beige solid (11 mg, 74%).

$\text{C}_{15}\text{H}_{18}\text{N}_2\text{O}$ (242.32 mol^{-1})

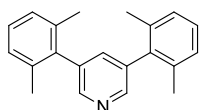
^1H -NMR (400 MHz, CDCl_3): δ = 6.94 (s, 1H, NCH), 6.89 (s, 2H, Ar-*H*), 5.67 (dd, J = 8.0, 1.6 Hz, 1H, NCH), 5.36 (br, 2H, NH_2), 4.83-4.79 (m, 1H, NCHCH), 3.26 (dd, J = 3.2, 1.6 Hz, 2H, CH_2), 2.26 (s, 3H, CH_3), 2.22 (s, 6H, CH_3) ppm.

$^{13}\text{C}\{^1\text{H}\}$ -NMR (126 MHz, CDCl_3): δ = 169.6 (s, C=O), 140.0 (s, Ar-C), 137.3 (s, NCH), 137.2 (s, Ar-CH), 136.1 (s, Ar-C), 129.9 (s, NCH), 129.5 (s, Ar-CH), 102.2 (s, CCO_2NH_2), 101.5 (s, NCHCH), 22.6 (s, CH_2), 21.0 (s, CH_3), 18.0 (s, CH_3) ppm.

7.6 Aryl Substituted Pyridylidenes in Dihydrogen Activation

7.6.1 Synthesis of Pyridinium Salts

3,5-bis(2',6'-Dimethylphenyl)pyridine (218)



A suspension of 3,5-dibromopyridine (1.92 g, 7.95 mmol, 1.00 eq.), 2,6-dimethylphenylboronic acid (2.78 g, 16.7 mmol, 2.1 eq.), $\text{Ba}(\text{OH})_2$ (5.45 g, 31.8 mmol, 4.00 eq.) and $\text{Pd}(\text{PPh}_3)_4$ (462 mg, 399 μmol , 0.05 eq.) in THF (100 mL) and H_2O (10 mL) was stirred at reflux for 24 h under inert atmosphere. After cooling to room temperature, the suspension was quenched with 50 mL of water, extracted with EtOAc (4 x 40 mL). The combined organic layers were dried over MgSO_4 and concentrated under reduced pressure. Purification by column chromatography (SiO_2 , 6 x 25 cm, EtOAc/cyclohexane, 1:10) gave the title compound **218** as a white solid (192 mg, 83%). The analytical data match the literature values.^[95]

$\text{C}_{21}\text{H}_{21}\text{N}$ (287.40 g mol^{-1})

^1H -NMR (400 MHz, CDCl_3): δ = 8.53 (d, J = 2 Hz, 2H, Ar-H), 7.87 (t, J = 2 Hz, 1H, Ar-H), 7.27 (t, J = 8 Hz, 2H, Ar-H), 7.17 (d, J = 8 Hz, 4H, Ar-H), 2.09 (s, 12H, CH_3) ppm.

$^{13}\text{C}\{^1\text{H}\}$ -NMR (101 MHz, CDCl_3): δ = 148.4 (s, Ar-CH), 137.8 (s, Ar-C), 136.4 (s, Ar-C), 136.3 (s, Ar-C), 127.9 (s, Ar-CH), 127.6 (s, Ar-CH), 21.0 (CH_3) ppm.

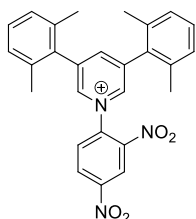
IR: $\tilde{\nu}$ = 3013w, 2950w, 2918w, 1461m, 1447m, 1380m, 775s, 731m cm^{-1} .

MS (EI, 70 eV) m/z (%): 287 (100), 272 (13), 245 (11), 129 (14), 128 (14), 155 (10).

m.p.: 132-134 $^\circ\text{C}$.

TLC (SiO_2 , cyclohexane/EtOAc 10:1): R_f = 0.24.

3,5-bis(2',6'-Dimethylphenyl)-1-(2,4-dinitrophenyl)pyridin-1-ium trifluoromethane sulfonate (220)



A suspension of diarylpyridine **218** (1.56 g, 5.43 mmol, 1.00 eq.) and 1-chloro-2,4-dinitrobenzene (1.10 g, 5.43 mmol, 1.00 eq.) in EtOH (11 mL) was stirred at 80 °C for 86 h under air atmosphere. After cooling to room temperature, the reaction mixture was diluted with pentane (20 mL). The reaction mixture was filtered and the residue was dried under reduced pressure to obtain a white solid. The solid was dissolved in CHCl₃ (50 mL) and silver trifluoromethanesulfonate (1.39 g, 5.43 mmol, 1.00 eq.) was added to the solution. The mixture was stirred at room temperature for one hour. The mixture was filtered and washed with CHCl₃ (3 x 20 mL). The solvent was concentrated under reduced pressure to give a colourless foam (2.91 g, 4.82 mmol, 88%). The analytical data match the literature values.^[95]

C₂₈H₂₄F₃N₃O₇S (603.58 g mol⁻¹)

¹H-NMR (400 MHz, CDCl₃): δ = 9.17 (d, *J* = 2 Hz, 1H, Ar-*H*), 8.88-8.82 (m, 2H, Ar-*H*), 8.76 (d, *J* = 1.6 Hz, 2H Ar-*H*), 8.38 (t, *J* = 1.6 Hz, 1H, Ar-*H*), 7.34 (t, *J* = 8 Hz, 2H, Ar-*H*), 7.25-7.12 (m, 4H, Ar-*H*), 2.28 (s, 6H, CH₃), 2.14 (s, 6H, CH₃) ppm.

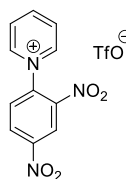
¹³C{¹H}-NMR (101 MHz, CDCl₃): δ = 150.6 (s, Ar-CH), 149.6 (s, Ar-CH), 143.8 (s, Ar-C), 143.1 (s, Ar-C), 142.6 (s, Ar-C), 138.3 (s, Ar-C), 136.4 (s, Ar-C), 135.9 (s, Ar-CH), 132.3 (s, Ar-CH), 132.0 (s, Ar-CH), 130.6 (s, Ar-CH), 130.1 (s, Ar-CH), 128.4 (s, Ar-CH), 128.3 (s, Ar-CH), 121.9 (q, *J*_{CF} = 320 Hz, CF₃), 122.1 (s, Ar-C), 20.8 (CH₃), 20.7 (CH₃) ppm.

¹⁹F{¹H} NMR (376 MHz, CDCl₃): δ = -78.23 (s, TfO⁻)ppm.

IR: $\tilde{\nu}$ = 3061w, 2922w, 2357w, 1613m, 1544s, 1456m, 1344s, 1253s, 1155s, 1029s, 908w, 836m, 779m, 738m, 703m, 639s cm⁻¹.

MS (MALDI-TOF): *m/z* (%) = 454 ([M-(TfO)]⁺, 100)

m.p.: 140-141 °C.

1-(2',4'-dinitrophenyl)pyridin-1-ium trifluoromethanesulfonate (225)

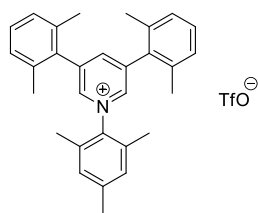
Pyridine (0.40 mL, 396 mg, 5.00 mmol, 1.00 eq.) and 1-chloro-2,4-dinitrobenzene (1.00 g, 5.00 mmol, 1.00 eq.) were heated together at 95 °C for 1 h. The precipitate was washed with acetone (15 mL) and dissolved in methanol (10 mL). Silver triflate (1.28 g, 5.00 mmol, 1.00 eq.) was added and the solution was stirred for 20 min at room temperature. The precipitate was filtered, washed with methanol (15 mL) and the solid was concentrated under reduced pressure to yield the product **225** as a colorless solid (395 mg, 20%). The analytical data match the literature values.^[114]

$C_{12}H_8F_3NO_7S$ (395.27 g mol⁻¹)

¹H-NMR (400 MHz, MeOD-*d*₄): δ = 9.33-9.00 (m, 2H, Ar-*H*), 9.28 (d, *J* = 2.5 Hz, 1H, Ar-*H*), 8.99-8.91 (m, 2H, Ar-*H*), 8.43-8.38 (m, 2H, Ar-*H*), 8.32 (d, *J* = 8.7 Hz, 1H, Ar-*H*) ppm.

¹³C{¹H}-NMR (101 MHz, MeOD-*d*₄): δ = 149.1 (s, Ar-C), 148.8 (s, Ar-C), 146.3 (s, Ar-C), 142.9 (s, Ar-C), 139.2 (s, Ar-C), 132.0 (s, Ar-C), 129.7 (s, Ar-C), 128.1 (s, Ar-C), 121.9 (q, *J*_{CF} = 320 Hz, CF₃), 121.4 (s, Ar-C) ppm.

¹⁹F{¹H} NMR (376 MHz, MeOD-*d*₄): δ = -78.3 (s, TfO⁻) ppm.

3,5-bis(2',6'-Dimethylphenyl)-1-mesitylpyridin-1-ium trifluoromethanesulfonate (214)

A mixture of Zincke salt **220** (500 mg, 0.83 mmol, 1.00 eq.) and 2,4,6-trimethylaniline (7 mL) was stirred at 150 °C for 2.5 h. After cooling to room temperature, the mixture was diluted with toluene and filtered. The solvent was evaporated and the crude mixture was purified by vacuum distillation (110-120 °C, 0.3 mbar). The brown residue was diluted with toluene (10 mL) and the precipitate was filtered. The precipitate was crystallized from CHCl₃ and toluene to obtain the title compound **214** as a colorless solid (150 mg, 33%). The analytical data match the literature values.^[95]

$C_{31}H_{32}F_3NO_3S$ (555.66 g mol⁻¹)

¹H-NMR (400 MHz, CDCl₃): δ = 8.78 (d, J = 2 Hz, 2H, Ar-*H*), 8.28 (s, 1H, Ar-*H*), 7.32 (t, J = 8 Hz, 2H), 7.24-7.21 (m, 4H, Ar-*H*), 7.17-7.13 (m, 2H, Ar-*H*), 2.38 (s, 3H, CH₃), 2.17 (s, 12H, CH₃), 2.15 (s, 6H, CH₃) ppm.

¹³C{¹H}-NMR (101 MHz, CDCl₃): δ = 148.8 (s, Ar-CH), 144.7 (s, Ar-CH), 143.1 (s, Ar-C), 142.4 (s, Ar-C), 138.8 (s, Ar-C), 137.9 (s, Ar-C), 135.4 (s, Ar-C), 132.1 (s, Ar-C), 131.8 (s, Ar-C), 130.4 (s, Ar-CH), 130.3 (s, Ar-CH), 129.1 (s, Ar-CH), 128.6 (s, Ar-CH), 125.3 (s, Ar-CH), 121.9 (q, J_{CF} = 320 Hz, CF₃), 21.5 (CH₃), 21.2 (CH₃), 21.1 (CH₃), 17.4 (CH₃) ppm.

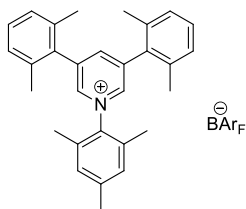
¹⁹F{¹H} NMR (376 MHz, CDCl₃): δ = -78.6 (s, TfO⁻) ppm.

IR: $\tilde{\nu}$ = 3061w, 3031w, 2916w, 2362w, 1598w, 1451m, 1382w, 1258s, 1221m, 1146s, 1029s, 787m, 738s, 635s cm⁻¹.

MS (MALDI-TOF): m/z (%) = 407 ([M-(TfO⁻)]⁺, 100)

m.p.: 207-208 °C.

3,5-bis(2',6'-Dimethylphenyl)-1-mesitylpyridin-1-ium tetrakis-[3,5-bis(trifluoromethyl)phenyl]borate (**221**)



To a solution of the pyridinium salt **214** (100 mg, 0.18 mmol, 1.00 eq.) in dichloromethane (2 mL) was added NaBAr_F (159 mg, 0.18 mmol, 1.00 eq.). The reaction mixture was stirred for 30 min at room temperature. The precipitate was filtered off and the solvent was

concentrated under reduced pressure. The desired product **221** was obtained as a yellow solid (223 mg, 98%).

$C_{62}H_{44}BF_{24}N$ (1269.81 g mol⁻¹)

¹H-NMR (400 MHz, CDCl₃): δ = 8.40 (t, J = 1.7 Hz, 1H, Ar-*H*), 8.33 (d, J = 1.7 Hz, 2H, Ar-*H*), 7.68 (s, 8H, BAr_F-*H*), 7.49 (s, 4H, BAr_F-*H*), 7.34 (t, J = 7.7 Hz, 2H, Ar-*H*), 7.21-7.19 (m, 4H, Ar-*H*), 7.11-7.09 (m, 2H, Ar-*H*), 2.34 (s, 3H, CH₃), 2.11 (s, 12H, CH₃), 2.04 (s, 6H, CH₃) ppm.

¹³C{¹H}-NMR (101 MHz, CDCl₃): δ = 161.9 (q, J_{BC} = 49.7 Hz, Ar-C, BAr_F), 149.8 (s, Ar-C), 144.1 (s, Ar-C), 143.6 (s, Ar-C), 143.5 (s, Ar-C), 138.4 (s, Ar-C, BAr_F), 135.0 (s, Ar-C), 134.8 (s, Ar-C), 131.2 (s, Ar-C), 131.3 (s, Ar-CH), 130.9 (s, Ar-CH), 130.7 (s, Ar-CH), 129.0 (qq, J_{FC} = 29 Hz, J_{BC} = 2.3 Hz,

Ar-C, BAr_F), 128.8 (s, Ar-CH), 128.2 (s, Ar-CH), 125.6 (q, $J_{FC} = 272.4$ Hz, CF₃, BAr_F), 117.5 (sept, $J_{FC} = 4.2$ Hz, Ar-C, BAr_F), 21.0 (CH₃), 20.8 (CH₃), 16.9 (CH₃) ppm.

¹⁹F{¹H} NMR (376 MHz, CDCl₃): $\delta = -62.4$ (s, CF₃, BAr_F) ppm.

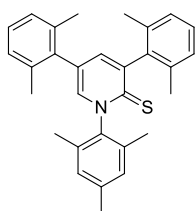
IR: $\tilde{\nu} = 2361w, 2326w, 1611w, 1452w, 1355m, 1277s, 1118s, 887m, 839m, 712m, 681m$ cm⁻¹.

MS (MALDI-TOF): m/z (%) = 407 ([M-(BAr_F⁻)]⁺, 100)

HRMS (ESI-MS): calc. (m/z) for C₃₀H₃₂N⁺: 406.2529 [M-(BAr_F⁻)]⁺, found: 406.2534.

m.p.: 158-159 °C.

3,5-bis(2',6'-Dimethylphenyl)-1-mesitylpyridine-2(1H)-thione (**222**)



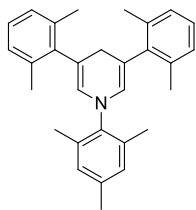
A mixture of pyridinium salt **214** (26.5 mg, 0.05 mmol, 1.00 eq.) and LiHMDS (1.0 M in toluene, 0.11 mL, 0.11 mmol, 2.25 eq.) in dry toluene (0.2 mL) was stirred for 5 min at RT. Then S₈ (12.2 mg, 0.05 mmol, 1.00 eq.) was added and the reaction mixture was stirred at room temperature for 1 h. Evaporation of the solvent yielded the product **222** as an orange solid (11.2 mg, 54%). The analytical data match the literature values.^[95]

C₃₀H₃₁NS (437.22 g mol⁻¹)

¹H-NMR (400 MHz, CDCl₃): $\delta = 7.33$ (d, $J = 2$ Hz, 1H, CH), 7.16 (dd, $J = 8$ Hz, 2H, Ar-H), 7.14 (d, $J = 2$ Hz, 1H, CH), 7.10 (d, $J = 7$ Hz, 2H, Ar-H), 7.00 (s, 2H, Ar-H), 2.32 (s, 3H, CH₃), 2.23 (s, 6H, CH₃), 2.21 (s, 6H, CH₃), 2.15 (s, 6H, CH₃) ppm.

¹³C{¹H}-NMR (101 MHz, CDCl₃): $\delta = 176.0$ (C=S), 144.1 (s, Ar-C), 138.9 (s, Ar-C), 137.0 (s, Ar-C), 136.4 (s, Ar-CH), 136.2 (s, Ar-C), 134.7 (s, Ar-CH), 133.8 (s, Ar-C), 133.0 (s, Ar-C), 132.9 (s, Ar-C), 130.6 (s, Ar-C), 127.2 (s, Ar-CH), 126.6 (s, Ar-CH), 125.9 (s, Ar-CH), 125.8 (s, Ar-CH), 125.4 (s, Ar-CH), 125.0 (s, Ar-C), 18.8 (CH₃), 18.5 (CH₃), 17.4 (CH₃), 15.6 (CH₃) ppm.

m.p.: 158-159 °C.

3,5-bis(2',6'-Dimethylphenyl)-1-mesityl-1,4-dihydropyridine (231b)

To a cooled solution of pyridinium salt **214** (105 mg, 0.19 mmol, 1.00 eq.) in THF was added sodium cyanoborohydride (12.5 mg, 0.19 mmol, 1.00 eq.). The solution was stirred at 0 °C for one hour. The crude reaction mixture was filtered over a disposable HPLC syringe filter (CHROMAFILL®0-20/15 MS, pore size 20 µm) and the solvent was removed under reduced pressure. Purification by column chromatography (*n*-alumina, 2 x 15 cm, cyclohexane) yielded the product **231b** as a pale yellow solid (68 mg, 88%). The analytical data match the literature values.^[95]

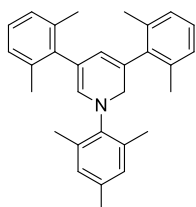
C₃₀H₃₃N (407.60 g mol⁻¹)

¹H-NMR (400 MHz, CDCl₃): δ = 7.04 (brs, 6H, Ar-H), 6.87 (brs, 2H, Ar-H), 5.64 (t, *J* = 1.1 Hz, 2H, NCH), 3.19 (t, *J* = 1.1 Hz, 2H, CH₂), 2.44 (s, 12H, CH₃), 2.34 (s, 6H, CH₃), 2.19 (s, 3H CH₃) ppm.

¹³C{¹H}-NMR (126 MHz, CDCl₃): δ = 140.6 (s, Ar-C), 137.2 (s, Ar-C), 136.6 (s, Ar-C), 135.3 (s, Ar-CH), 131.6 (s, Ar-C), 130.6 (s, Ar-C), 129.1 (s, Ar-C), 129.0 (s, Ar-C), 128.7 (s, Ar-C), 128.4 (s, Ar-C), 128.3 (s, Ar-C), 127.3 (s, Ar-C), 126.4 (s, Ar-C), 125.3 (s, Ar-CH), 107.4 (s, CH), 31.5 (s, CH₂), 21.1 (s, CH₃), 20.9 (s, CH₃), 19.8 (s, CH₃), 18.0 (s, CH₃), 17.3 (s, CH₃) ppm.

TLC (*n*-alumina, cyclohexane): R_f = 0.54.

m.p.: 138-140 °C.

3,5-bis(2',6'-Dimethylphenyl)-1-mesityl-1,2-dihydropyridine (231a)

To a cooled solution of pyridinium salt **214** (253 mg, 0.46 mmol, 1.00 eq.) in THF (3 mL) was added sodium borohydride (17.5 mg, 0.46 mmol, 1.00 eq.). The reaction mixture was stirred at 0 °C for 1 hour. The crude reaction mixture was filtered over a disposable HPLC syringe filter (CHROMAFILL®0-20/15 MS, pore size 20 µm) and the solvent was removed under reduced pressure. The product **231a** was obtained as a pale yellow solid (92 mg, 51%). The analytical data match the literature values.^[95]

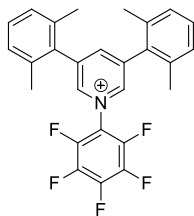
$C_{30}H_{33}N$ (407.60 g mol⁻¹)

¹H-NMR (400 MHz, CDCl₃): δ = 7.07-7.02 (m, 6H, Ar-H), 6.88 (d, J = 0.4 Hz, 2H, Ar-H), 5.85 (d, J = 1.2 Hz, 1H, C=CH), 5.63 (t, J = 1.2 Hz, 1H, NCH), 4.30 (d, J = 1.4 Hz, 2H, NCH₂), 2.40 (s, 6H CH₃), 2.39 (s, 6H CH₃), 2.37 (s, 6H CH₃), 2.26 (s, 3H CH₃) ppm.

¹³C{¹H}-NMR (126 MHz, CDCl₃): δ = 142.0 (s, Ar-C), 140.6 (s, Ar-C), 140.4 (s, Ar-C), 139.7 (s, Ar-C), 137.8 (s, Ar-C), 137.2 (s, Ar-C), 136.7 (s, Ar-C), 136.6 (s, Ar-C), 136.5 (s, Ar-C), 136.3 (s, Ar-C), 133.5 (s, Ar-CH), 129.4 (s, Ar-CH), 128.4 (s, Ar-C), 127.4 (s, Ar-CH), 127.3 (s, Ar-CH), 126.6 (s, Ar-CH), 126.4 (s, Ar-CH), 126.2 (s, Ar-CH), 126.0 (s, Ar-CH), 122.3 (s, Ar-C), 107.4 (s, CH), 106.9 (s, CH), 52.4 (s, CH₂), 21.1 (s, CH₃), 20.9 (s, CH₃), 20.8 (s, CH₃), 20.1 (s, CH₃), 19.8 (s, CH₃), 18.5 (s, CH₃) 18.0 (s, CH₃) ppm.

m.p.: 111-113 °C.

3,5-bis(2',6'-Dimethylphenyl)-1-(perfluorophenyl)pyridin-1-ium trifluoromethanesulfonate (229)



2,3,4,5,6-Pentafluoroaniline (1.00 g, 5.35 mmol, 40 eq.) and **220** (250 mg, 0.41 mmol 1.00 eq.) were mixed and the mixture was stirred at 150 °C for 2.5h. After the reaction was cooled to RT, the mixture was diluted with toluene and filtered. The solvent was evaporated and the crude mixture was purified by vacuum distillation (110-120 °C, 0.3 mbar). The brown residue was diluted with toluene (10 mL) and the precipitate was filtered. The precipitate was crystallized from CHCl₃ and toluene to obtain the title compound **229** as a colorless solid (230 mg, 92%).

$C_{28}H_{21}F_8NO_3S$ (603.53 g mol⁻¹)

¹H-NMR (400 MHz, CDCl₃): δ = 9.14 (d, J = 2.4 Hz, 1H, Ar-H), 8.73 (d, J = 1.6 Hz, 2H, Ar-H), 8.37 (t, J = 1.6 Hz, 1H, Ar-H), 7.24-7.16 (m, 6H, Ar-H), 2.28 (s, 6H, CH₃), 2.12 (s, 6H, CH₃) ppm.

¹³C{¹H}-NMR (126 MHz, CDCl₃): δ = 150.9 (s, Ar-C), 143.6 (s, Ar-C), 142.9 (s, Ar-C), 138.4 (s, Ar-C), 135.6 (s, Ar-C), 132.8 (s, Ar-C), 131.8 (s, Ar-C), 130.8 (s, Ar-C), 130.4 (s, Ar-C), 129.0 (s, Ar-C), 128.2 (s, Ar-C), 122.2 (q, J_{CF} = 320 Hz, CF₃), 121.9 (s, Ar-C), 20.9 (CH₃), 20.7 (CH₃) ppm.

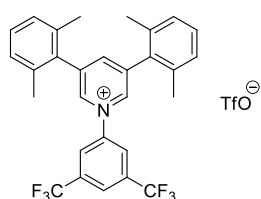
¹⁹F{¹H} NMR (376 MHz, CDCl₃): δ = -78.6 (s, TfO⁻) ppm.

IR: $\tilde{\nu}$ = 3071w, 1613w, 1545m, 1457w, 1341m, 1258s, 1153m, 1030s, 917w, 836w, 779w, 742m, 700m, 636s cm^{-1} .

MS (MALDI-TOF): m/z (%) = 454 ($[\text{M}-(\text{TfO})]^+$), 100

m.p.: 143-145 °C.

1-(3',5'-bis(Trifluoromethyl)phenyl)-3,5-bis(2'',6''-dimethylphenyl)pyridin-1-ium trifluoromethanesulfonate (230)



3,5-Bis(trifluoro)aniline (3.80 g, 2.58 mL, 16.6 mmol, 40 eq.) and **220** (250 mg, 0.41 mmol 1.00 eq.) were mixed and the mixture was stirred at 150 °C for 2.5 h. After the reaction was cooled to RT, the mixture was diluted with toluene and filtered. The solvent was evaporated and the

crude mixture was purified by vacuum distillation (110-120 °C, 0.3 mbar). The brown residue was diluted with toluene (10 mL) and the precipitate was filtered. The precipitate was crystallized from CHCl_3 and toluene to obtain the title compound **230** as a colorless solid (200 mg, 75%).

$\text{C}_{30}\text{H}_{24}\text{F}_9\text{NO}_3\text{S}$ (649.58 g mol^{-1})

$^1\text{H-NMR}$ (400 MHz, CDCl_3): δ = 9.09 (d, J = 2.4 Hz, 1H, Ar- H), 8.79 (d, J = 1.6 Hz, 2H, Ar- H), 8.69-8.61 (m, 2H, Ar- H), 8.33 (d, J = 1.6 Hz, 1H, Ar- H), 7.33-7.29 (m, 2H, Ar- H), 7.23-7.26 (m, 2H, Ar- H), 2.23 (s, 6H, CH_3), 2.12 (s, 6H, CH_3) ppm.

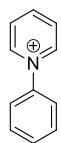
$^{13}\text{C}\{^1\text{H}\}$ -NMR (126 MHz, CDCl_3): δ = 150.7 (s, Ar-C), 149.7 (s, Ar-C), 143.7 (s, Ar-C), 143.2 (s, Ar-C), 142.7 (s, Ar-C), 138.4 (s, Ar-C), 136.4 (s, Ar-C), 135.7 (s, Ar-C), 132.8 (q, J_{CF} = 33 Hz, CF_3), 132.5 (s, Ar-C), 131.9 (s, Ar-C), 130.6 (s, Ar-C), 130.3 (s, Ar-C), 129.0 (s, Ar-C), 128.6 (s, Ar-C), 128.4 (s, Ar-C), 128.2 (s, Ar-C), 125.3 (s, Ar-C), 123.5 (q, J_{CF} = 274 Hz, CF_3), 122.0 (s, Ar-C), 121.6 (q, J_{CF} = 320 Hz, TfO^- , CF_3), 144.0 (q, J_{CF} = 4 Hz, CF_3), 20.9 (CH_3), 20.8 (CH_3) ppm.

$^{19}\text{F}\{^1\text{H}\}$ NMR (376 MHz, CDCl_3): δ = -78.7 (s, TfO^-), -64.6 (s, CF_3) ppm.

IR: $\tilde{\nu}$ = 3064w, 2921w, 1612m, 1454s, 1457m, 1341s, 1258s, 1154s, 1030s, 917m, 836m, 778m, 742s, 700m, 636s cm^{-1} .

MS (ESI-MS): m/z (%) = 500 ($[\text{M}-(\text{TfO})]^+$), 100

m.p.: 212-213 °C.

1-phenylpyridin-1-ium trifluoromethanesulfonate (226)

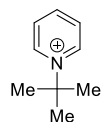
The title compound **226** was obtained following the procedure of **214** using Zincke salt **225** (365 mg, 0.92 mmol, 1.00 eq.) and aniline (3.37 mL, 3.44 g, 0.03 mol, 40.0 eq.) as a colorless solid (164 mg, 59%). The analytical data match the literature values.^[106]

$C_{12}H_{10}FNO_3S$ (305.03 g mol⁻¹)

¹H-NMR (400 MHz, CDCl₃): δ = 9.10 (d, J = 2.6 Hz, 2H, Ar-*H*), 8.68 (t, J = 7.9 Hz, 1H, Ar-*H*), 8.36-8.37 (m, 2H, Ar-*H*), 8.19 (dd, J = 9.3, 2.6 Hz, 2H, Ar-*H*), 7.78-7.66 (m, 3H, Ar-*H*) ppm.

¹³C{¹H}-NMR (101 MHz, CDCl₃): δ = 146.6 (s, Ar-CH), 145.0 (s, Ar-CH), 144.9 (s, Ar-C), 131.2 (s, Ar-CH), 128.1 (s, Ar-CH), 125.7 (s, Ar-CH), 121.8 (q, J_{CF} = 320 Hz, CF₃), 120.0 (s, Ar-CH) ppm.

¹⁹F{¹H} NMR (376 MHz, CDCl₃): δ = -78.7 (s, TfO⁻) ppm.

7.6.2 Synthesis of *N*-tert-Alkylpyridinium Salts**1-(*tert*-Butyl)pyridin-1-ium perchlorate (234)**

A solution of silver perchlorate (419 mg, 2.00 mmol, 1.00 eq.) in dry nitromethane (5 mL) was added to a solution of pyridine (0.48 mL, 475 mg, 6.00 mmol, 3.00 eq.) and 2-bromo-2-methylpropane (0.22 mL, 274 mg, 2.00 mmol, 1.00 eq.) in dry nitromethane (0.5 mL) over 2.5 h at 0 °C. The mixture was stirred at 0 °C for 4 h, and was then stirred further 12 h at room temperature. The reaction mixture was filtered and washed with nitromethane (10 mL). The combined organic phases were washed with water (3 x 10 mL), dried over MgSO₄ and concentrated *in vacuo*. Recrystallisation from ethanol gave the desired product **234** as colorless plates (119 mg, 26%). The analytical data match the literature values.^[117]

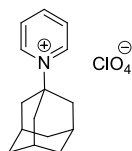
$C_9H_{14}ClNO_4$ (235.66 g mol⁻¹)

¹H-NMR (400 MHz, CDCl₃): δ = 9.12 (d, J = 5.8 Hz, 2H, Ar-*H*), 8.47 (t, J = 7.7 Hz, 1H, Ar-*H*), 8.23-8.5, 16 (m, 2H, Ar-*H*), 1.91 (s, 9H, CH₃) ppm.

$^{13}\text{C}\{^1\text{H}\}$ -NMR (101 MHz, CDCl_3): δ = 142.3 (s, Ar-C), 140.2 (s, Ar-C), 125.2 (s, Ar-C), 67.7 (s, NC), 28.8 (s, CH_3) ppm.

m.p.: 215-217 °C.

1-(Adamantan-1-yl)pyridin-1-ium perchlorate (236)



The title compound **236** was obtained following the procedure of **234** using perchlorate (419 mg, 2.00 mmol, 1.00 eq.), nitromethane (5 mL), pyridine (0.48 mL, 475 mg, 6.00 mmol, 3.00 eq.) and 1-bromoadamantine (430 mg, 2.00 mmol, 1.00 eq.) as colourless plates (315 mg, 51%). The analytical data match the literature values.^[117]

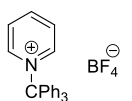
$\text{C}_{15}\text{H}_{20}\text{ClNO}_4$ (313.78 g mol⁻¹)

^1H -NMR (400 MHz, $\text{DMSO}-d_6$): δ = 9.31 (dd, J = 7.0, 1.1 Hz, 2H, Ar-*H*), 8.59 (t, J = 7.7 Hz, 1H, Ar-*H*), 8.16 (tt, J = 7.2, 1.0 Hz, 2H, Ar-*H*), 2.30 (s, 9H, CH_2 , CH), 1.75 (s, 6H, CH_2 , CH) ppm.

$^{13}\text{C}\{^1\text{H}\}$ -NMR (101 MHz, $\text{DMSO}-d_6$): δ = 145.3 (s, Ar-CH), 141.0 (s, Ar-CH), 135.3 (s, Ar-C), 127.2 (s, Ar-CH), 41.0 (s, CH_2), 34.3 (s, CH_2), 29.4 (s, CH) ppm.

m.p.: 256-258 °C.

1-(Triphenylmethyl)pyridin-1-ium tetrafluoroborate (235)



A solution of triphenylmethyl fluoroborate (355 mg, 1.08 mmol, 1.00 eq.) in dichloromethane (4 mL) was added to a solution of pyridine (0.2 mL, 196 mg, 2.47 mmol, 2.30 eq.) in dichloromethane (1 mL). The reaction mixture was stirred at room temperature for 30 min and the precipitate was filtered to give the desired compound **235** (358 mg, 82%). The analytical data match the literature values.^[118]

$\text{C}_{24}\text{H}_{20}\text{BF}_4\text{N}$ (409.23 g mol⁻¹)

^1H -NMR (400 MHz, CDCl_3): δ = 8.89 (m, 2H, Ar-*H*), 8.52 (t, J = 7.9 Hz, 1H, Ar-*H*), 8.02 (t, J = 5.4 Hz, 2H, Ar-*H*), 7.33-7.15 (m, 15H, Ar-*H*) ppm.

m.p.: 155-157 °C.

7.6.3 Activation at Elevated Pressure

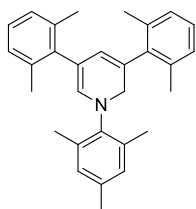
Reaction with H₂: In the glovebox, an oven dried 2 mL-glass vial was charged with a stirring bar and pyridinium salt (1.00 eq.) suspended in toluene (0.2 M). After addition of base (2.25 eq.), the vial was placed in an autoclave. The autoclave was then pressurized with H₂ (50 bar) and placed on a stirring plate for 5 h at 50 °C. After releasing the hydrogen pressure, the solvent was removed *in vacuo*. The residue was dissolved in the NMR solvent, filtered and analyzed by NMR.

Reaction with D₂: In the glovebox, an oven dried 2 mL-glass vial was charged with a stirring bar and pyridinium salt (1.00 eq.) suspended in toluene (0.2 M). After addition of base (2.25 eq.), the vial was placed in an autoclave. The autoclave was then pressurized with D₂ (50 bar) and placed on a stirring plate for 24 h at 50 °C. After releasing the deuterium pressure, the solvent was removed *in vacuo*. The residue was dissolved in the NMR solvent, filtered and analyzed by NMR.

7.6.4 Analytical Data for the Activation Products

Reaction with H₂

3,5-bis(2',6'-Dimethylphenyl)-1-mesityl-1,2-dihydropyridine (**231a**)



In the glovebox, an oven dried 2 mL-glass vial was charged with a stirring bar and pyridinium salt **214** (10.0 mg, 0.02 mmol, 1.00 eq.) suspended in toluene (0.2 mL). After addition of LiHMDS (1.0 M in toluene, 40.5 μ L, 0.04 mmol, 2.25 eq.), the vial was placed in an autoclave. The autoclave was then pressurized with H₂ (50 bar) and placed on a stirring plate for 5 h at 50 °C. After releasing the hydrogen pressure, the solvent was evaporated under high vacuum at 50 °C. The residue was dissolved in CDCl₃ (0.5 mL) filtered through a disposable HPLC filter (CHROMAFILL®0-20/15 MS, pore size 20 μ m) and transferred into an NMR tube. Analysis by NMR showed the

presence to the desired 1,2-dihydropyridine **231a** and full consumption of the pyridinium salt **214**.

$C_{30}H_{33}N$ (407.60 g mol⁻¹)

¹H-NMR (400 MHz, CDCl₃): δ = 7.07-7.02 (m, 6H, Ar-H), 6.88 (d, J = 0.4 Hz, 2H, Ar-H), 5.85 (d, J = 1.2 Hz, 1H, C=CH), 5.63 (t, J = 1.2 Hz, 1H, NCH), 4.30 (d, J = 1.4 Hz, 2H, NCH₂), 2.40 (s, 6H, CH₃), 2.39 (s, 6H, CH₃), 2.37 (s, 6H, CH₃), 2.26 (s, 3H CH₃) ppm.

¹³C{¹H}-NMR (126 MHz, CDCl₃): δ = 142.0 (s, Ar-C), 140.6 (s, Ar-C), 140.4 (s, Ar-C), 139.7 (s, Ar-C), 137.8 (s, Ar-C), 137.2 (s, Ar-C), 136.7 (s, Ar-C), 136.6 (s, Ar-C), 136.5 (s, Ar-C), 136.3 (s, Ar-C), 133.5 (s, Ar-CH), 129.4 (s, Ar-CH), 128.4 (s, Ar-C), 127.4 (s, Ar-CH), 127.3 (s, Ar-CH), 126.6 (s, Ar-CH), 126.4 (s, Ar-CH), 126.2 (s, Ar-CH), 126.0 (s, Ar-CH), 122.3 (s, Ar-C), 107.4 (s, CH), 106.9 (s, CH), 52.4 (s, CH₂), 21.1 (s, CH₃), 20.9 (s, CH₃), 20.8 (s, CH₃), 20.1 (s, CH₃), 19.8 (s, CH₃), 18.5 (s, CH₃) 18.0 (s, CH₃) ppm.

m.p.: 111-113 °C.

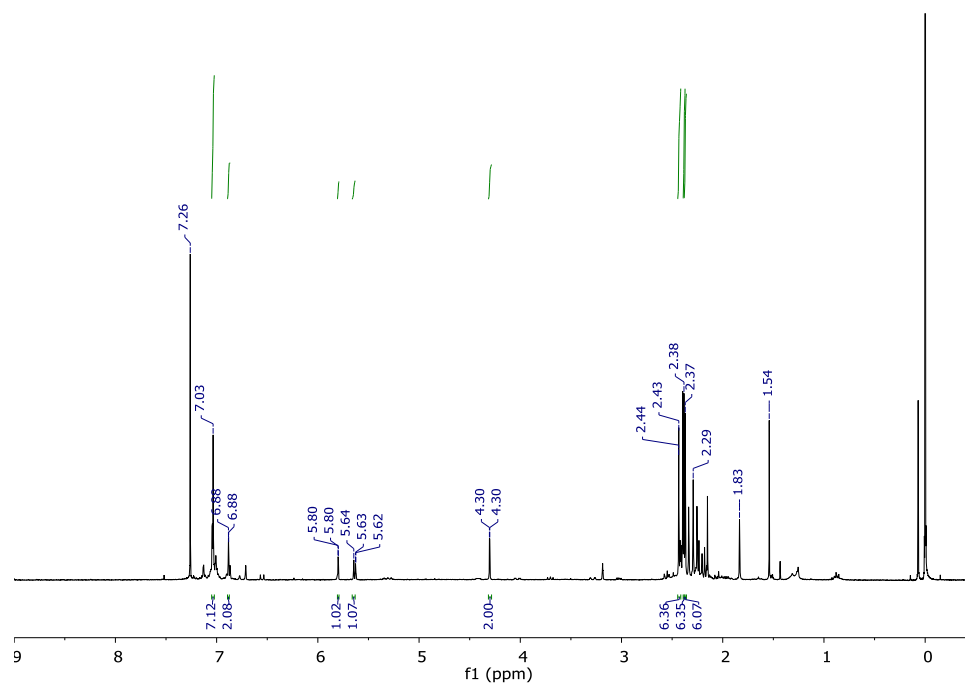
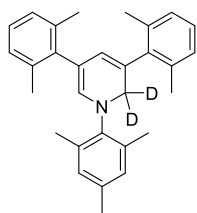


Figure 7.1 ¹H NMR of **231a** obtained after H₂ activation.

Reaction with D₂3,5-bis(2',6'-dimethylphenyl)-1-mesityl-1,2-dihydropyridine-2,2-d₂ (**231c**)

In the glovebox, an oven dried 2 mL-glass vial was charged with a stirring bar and pyridinium salt **214** (10.0 mg, 0.02 mmol, 1.00 eq.) suspended in toluene (0.2 mL). After addition of LiHMDS (1.0 M in toluene, 40.5 μ L, 0.04 mmol, 2.25 eq.), the vial was placed in an autoclave. The autoclave was then pressurized with D₂ (50 bar) and placed on a stirring plate for 24 h at 50 °C. After releasing the deuterium pressure, the solvent was evaporated under high vacuum at 50 °C. The residue was dissolved in CHCl₃ (0.5 mL + 1 μ L of CDCl₃ as internal standard), filtered through a disposable HPLC filter (CHROMAFILL®0-20/15 MS, pore size 20 μ m) and transferred into an NMR tube. Analysis by ²H NMR showed the signal of the CD₂ group of desired product **231c**.

C₃₀H₃₁D₂N (409.61g mol⁻¹)

²H-NMR (76.8 MHz, CDCl₃ in CHCl₃): δ = 4.30 (s, CD₂) ppm.

¹H-NMR (400 MHz, CDCl₃): δ = 7.07-7.02 (m, 6H, Ar-H), 6.88 (d, J = 0.4 Hz, 2H, Ar-H), 5.85 (d, J = 1.2 Hz, 1H, C=CH), 5.63 (t, J = 1.2 Hz, 1H, NCH), 4.30 (br s, 0.64H, NCH₂ and/or NCDH (32% H content)), 2.40 (s, 6H CH₃), 2.39 (s, 6H, CH₃), 2.37 (s, 6H, CH₃), 2.26 (s, 3H CH₃) ppm.

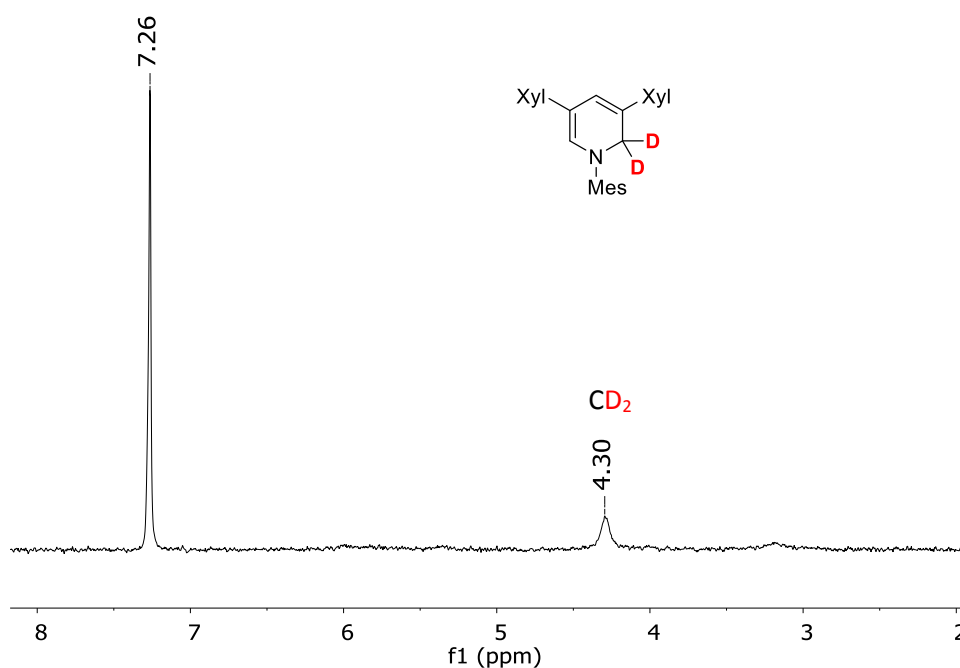
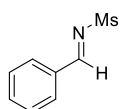


Figure 7.2: ²H NMR of deuterium splitting experiment; CDCl₃ (7.26 ppm) as internal standard in CHCl₃.

7.6.5 Synthesis of Substrates

Acetophenone (**142**), *trans-beta*-nitrostyrene (**191**), ethyl methylformate (**242**) and methyl benzoylformate (**148**) are commercially available and were used as received. Benzaldehyde (**139**), cinnamaldehyde (**150**) and *N*-benzylidene-*tert*-butylamine (**145**) are commercially available and were distilled prior to use.

(*E*)-*N*-benzylidenemethanesulfonamide (**243**)



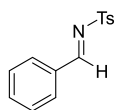
The imine was obtained according to literature procedure as a colorless solid (134 mg, 72%). The analytical data match the literature values.^[127]

$C_8H_9NO_2S$ (183.23 g mol⁻¹)

¹H-NMR (400 MHz, CDCl₃): δ = 9.04 (s, 1H, N=CH), 7.98-7.96 (m, 2H, Ar-H), 7.71-7.62 (m, 1H, Ar-H), 7.60-7.48 (m, 2H, Ar-H), 3.15 (s, 3H, CH₃) ppm.

TLC (SiO₂, cyclohexane/Et₂O 8:1): R_f = 0.36.

(*E*)-*N*-benzylidene-4-methylbenzenesulfonamide (**244**)

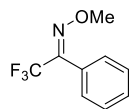


The imine was obtained according to literature procedure as a colorless solid (201 mg, 81%). The analytical data match the literature values.^[127]

$C_{14}H_{13}NO_2S$ (259.33 g mol⁻¹)

¹H-NMR (400 MHz, CDCl₃): δ = 9.03 (s, 1H, N=CH), 7.95-7.86 (m, 3H, Ar-H), 7.69-7.45 (m, 4H, Ar-H), 7.39-7.30 (m, 2H, Ar-H), 2.44 (s, 3H, CH₃) ppm.

TLC (SiO₂, cyclohexane/Et₂O 8:1): R_f = 0.32.

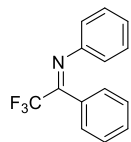
(E)-2,2,2-trifluoro-1-phenylethan-1-one O-methyl oxime (244a)

The oxime was obtained according to literature procedure as a colorless liquid (7.20 g, 84%). The analytical data match the literature values.^[128]

$C_9H_8F_3NO$ (203.16 g mol⁻¹)

¹H-NMR (400 MHz, CDCl₃): δ = 7.53-7.42 (m, 5H, Ar-H), 4.02 (s, 3H, CH₃) ppm.

b.p.: 95 °C (10⁻² mbar).

(E)-2,2,2-trifluoro-N,1-diphenylethan-1-imine (255)

The imine was obtained according to literature procedure as a yellow liquid (1.10 g, 63%). The analytical data match the literature values.

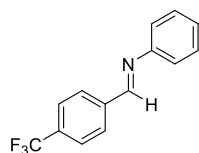
$C_{14}H_{10}F_3N$ (249.24 g mol⁻¹)

¹H-NMR (400 MHz, CDCl₃): δ = 7.38-7.27 (m, 3H, Ar-H), 7.24-7.16 (m, 4H, Ar-H), 7.09-7.00 (m, 1H, Ar-H), 6.77-6.71 (m, 4H, Ar-H) ppm.

¹⁹F{¹H} NMR (376 MHz, CDCl₃): δ = -70.0 (s, CF₃) ppm.

MS (EI, 70 eV) *m/z* (%): 249 (47) [M]⁺, 180 (100), 77 (85).

b.p.: 95 °C (10⁻¹ mbar).

(E)-N-Phenyl-1-(4-(trifluoromethyl)phenyl)methanimine (257)

The imine was obtained according to literature procedure as a yellow solid (156 mg, 63%). The analytical data match the literature values.^[129]

$C_{14}H_{10}F_3N$ (249.24 g mol⁻¹)

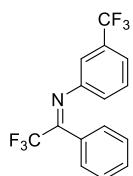
¹H-NMR (400 MHz, CDCl₃): δ = 8.52 (s, 1H, N=CH), 8.02 (d, J = 8.1 Hz, 2H, Ar-H), 7.75 (d, J = 8.1 Hz, 2H, Ar-H), 7.75 (d, J = 8.1 Hz, 2H, Ar-H), 7.44-7.41 (m, 2H, Ar-H), 7.28-7.24 (m, 2H, Ar-H) ppm.

¹⁹F{¹H} NMR (376 MHz, CDCl₃): δ = -63.0 (s, CF₃), -70.2 (s, CF₃) ppm.

MS (EI, 70 eV) m/z (%): 317 (27) [M]⁺, 248 (100), 145 (35), 77 (15).

TLC (SiO₂, cyclohexane/EtOAc 10:1): R_f = 0.53.

(E)-2,2,2-Trifluoro-1-phenyl-N-(3-(trifluoromethyl)phenyl)ethan-1-imine (246)



The imine was obtained according to literature procedure as a yellow oil (549 mg, 87%). The analytical data match the literature values.^[121]

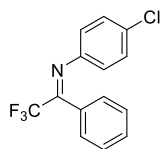
$C_{15}H_9F_6N$ (317.23 g mol⁻¹)

¹H-NMR (400 MHz, CDCl₃): δ = 7.38-7.36 (m, 5H, Ar-H), 7.21-7.18 (m, 2H, Ar-H), 7.04 (s, 1H, Ar-H), 6.91-6.85 (m, 1H, Ar-H) ppm.

¹⁹F{¹H} NMR (376 MHz, CDCl₃): δ = -62.8 (s, CF₃) ppm.

MS (EI, 70 eV) m/z (%): 249 (100) [M]⁺, 104 (132), 77 (95).

(E)-N-(4-Chlorophenyl)-2,2,2-trifluoro-1-phenylethan-1-imine (248)



The imine was obtained according to literature procedure as a brown oil (203 mg, 72%). The analytical data match the literature values.^[121]

$C_{14}H_9ClF_3N$ (283.68 g mol⁻¹)

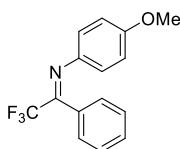
¹H-NMR (400 MHz, CDCl₃): δ = 7.43-7.29 (m, 3H, Ar-H), 7.18-7.15 (m, 4H, Ar-H), 6.71-6.68 (m, 2H, Ar-H) ppm.

¹⁹F{¹H} NMR (376 MHz, CDCl₃): δ = -70.1 (s, CF₃) ppm.

MS (EI, 70 eV) m/z (%): 283 (31) $[M]^+$, 214 (100), 111 (37), 77 (21).

TLC (SiO₂, cyclohexane/EtOAc 10:1): R_f = 0.71.

(E)-2,2,2-Trifluoro-N-(4-methoxyphenyl)-1-phenylethan-1-imine (247)



The imine was obtained according to literature procedure as a yellow oil (248 mg, 89%). The analytical data match the literature values.^[121]

C₁₅H₁₂F₃NO (279.26 g mol⁻¹)

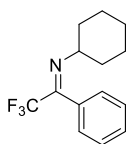
¹H-NMR (400 MHz, CDCl₃): δ = 7.48-7.31 (m, 3H, Ar-H), 7.25-7.20 (m, 2H, Ar-H), 6.73-6.70 (m, 4H, Ar-H) 3.74 (s, 3H, CH₃) ppm.

¹⁹F{¹H} NMR (376 MHz, CDCl₃): δ = -69.9 (s, CF₃) ppm.

MS (EI, 70 eV) m/z (%): 279 (44) $[M]^+$, 210 (100), 167 (13), 92 (14), 77 (28).

TLC (SiO₂, cyclohexane/EtOAc 10:1): R_f = 0.57.

(E)-N-Cyclohexyl-2,2,2-trifluoro-1-phenylethan-1-imine (249)



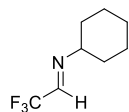
The imine was obtained according to literature procedure as a colorless oil (1.88 g, 52%). The analytical data match the literature values.^[128]

C₁₄H₁₆F₃N (255.28 g mol⁻¹)

¹H-NMR (400 MHz, CDCl₃): δ = 8.08 (ddt, J = 8.7, 2.3, 1.1 Hz, 1H, Ar-H), 7.59-7.52 (m, 1H, Ar-H), 7.50-7.42 (m, 3H, Ar-H) 3.22 (tt, J = 9.7, 4.8 Hz, 1H, NCH) 1.77-1.50 (m, 4H, CH₂), 1.31-0.94 (m, 6H, CH₂) ppm.

¹⁹F{¹H} NMR (376 MHz, CDCl₃): δ = -71.2 (s, CF₃) ppm.

MS (EI, 70 eV) m/z (%): 254 (5) $[M]^+$, 186 (63), 130 (12), 104 (100), 83 (18), 55 (32).

(E)-N-Cyclohexyl-2,2,2-trifluoroethan-1-imine (258)

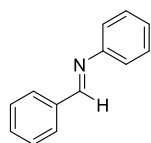
The imine was obtained according to literature procedure as a colorless oil (720 mg, 41 %). The analytical data match the literature values.^[130]

$C_8H_{12}F_3N$ (179.19 g mol⁻¹)

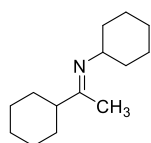
¹H-NMR (400 MHz, CDCl₃): δ = 7.63 (s, 1H, N=CH), 3.27 (ddt, J = 10.7, 9.5, 4.1 Hz, 1H, NCH), 1.85-1.81 (m, 2H, CH₂), 1.75-1.65 (m, 3H, CH₂), 1.56-1.49 (m, 2H, CH₂), 1.39-1.23 (m, 2H, CH₂) ppm.

¹⁹F{¹H} NMR (376 MHz, CDCl₃): δ = -71.6 (s, CF₃) ppm.

MS (EI, 70 eV) m/z (%): 178 (2) [M]⁺, 150 (71), 136 (36), 110 (35), 83 (91), 55 (100), 41 (50).

(E)-N-1-Diphenylmethanimine (253)

The amine was obtained from York Schramm, Pfaltz group, University of Basel.

(E)-N-1-Dicyclohexylethan-1-imine (250)

The amine was obtained from York Schramm, Pfaltz group, University of Basel.

7.6.6 Reduction with Authentic Samples

An oven-dried 2 mL glass vial was charged with with a stirring bar, 1,2-dihydropyridine (1.00 eq.), substrate (1.00 eq.) and was dissolved in toluene (0.2 mL). The vial was placed in a glass flask, which was kept under a nitrogen atmosphere. The flask was heated to given time

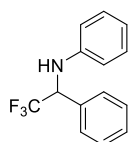
and temperature. Afterwards the solvent was removed *in vacuo* and the crude product was analyzed by NMR and MS.

7.6.7 *In-Situ* Reduction

In the glovebox, an oven dried 2 mL-glass vial was charged with a stirring bar, pyridinium salt (20-100 mol%), substrate (0.18-0.27 mmol) and was suspended in toluene (0.2 M). After addition of base (2.25 eq.), the vial was placed in an autoclave. The autoclave was then pressurized with H₂ (50 bar) and placed on a stirring plate for 5 h at 50 °C. After releasing the pressure the solvent was removed *in vacuo*. The conversion of imine **255** to amine **256** was determined by ¹⁹F NMR spectroscopy by integration of the ¹⁹F signals at -70.0 ppm (**255**) and -74.0 ppm (**256**).

7.6.8 Analytical Data for the Reduced Substrates

N-(2,2,2-Trifluoro-1-phenylethyl)aniline (**256**)



In the glovebox, an oven dried 2 mL-glass vial was charged with a stirring bar and pyridinium salt **214** (30.0 mg, 0.05 mmol, 0.20 eq.) and imine **255** (67.3 mg, 0.27 mmol, 1.00 eq.) suspended in toluene (0.6 mL). After addition of LiHMDS (1.0 M in toluene, 0.27 mL, 0.27 mmol, 1.00 eq.), the vial was placed in an autoclave. The autoclave was then pressurized with H₂ (50 bar) and placed on a stirring plate for 5 h at 50 °C. After releasing the hydrogen pressure, the solvent was evaporated under high vacuum at room temperature. Purification by column chromatography (SiO₂, 2 x 15 cm, EtOAc/cyclohexane 1:60 → 1:40) gave the desired compound **256** as a clear oil (55 mg, 82%). The analytical data match the literature values.^[24]

$C_{14}H_{12}F_3N$ (251.25 g mol⁻¹)

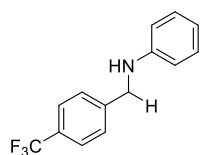
¹H-NMR (400 MHz, CDCl₃): δ = 7.45 (m, 5H, Ar-H), 7.16 (m, 2H, Ar-H), 6.77 (m, 1H, Ar-H), 6.65 (m, 2H, Ar-H), 5.02 (quin, J = 7.3 Hz, 1H, NCH), 4.34 (brs, 1H, NH) ppm.

¹⁹F{¹H} NMR (376 MHz, CDCl₃): δ = -74.0 (d, J = 2.0 Hz, CF₃) ppm.

MS (EI, 70 eV) m/z (%): 251 (40) [M]⁺, 182 (100), 109 (18), 104 (30), 90 (24), 77 (40).

TLC (SiO₂, cyclohexane/EtOAc 40:1): R_f = 0.36.

***N*-(4-(Trifluoromethyl)benzyl)aniline (256a)**



$C_{14}H_{12}F_3N$ (251.25 g mol⁻¹)

¹H-NMR (400 MHz, CDCl₃): δ = 7.58 (d, J = 8.2 Hz, 2H, Ar-H), 7.47 (d, J = 8.0 Hz, 2H, Ar-H), 7.21-7.12 (m, 2H, Ar-H), 6.73 (t, J = 7.3 Hz, 1H, Ar-H), 6.59 (dd,

J = 8.6, 1.1 Hz, 2H, Ar-H), 4.40 (s, 1H, NCH), 4.13 (brs, 1H, NH) ppm.

¹⁹F{¹H} NMR (376 MHz, CDCl₃): δ = -62.4 (s, CF₃) ppm.

MS (EI, 70 eV) m/z (%): 251 (100) [M]⁺, 159 (68), 109 (22), 106 (77), 104 (19), 77 (29), 65 (11).

Chapter 8

8. Appendix

8.1. Crystallographic Data

Compound	83
formula	$C_{24}H_{32}N_2O_5S$
Mr [g × mol ⁻¹]	460.20
shape	prism
color	colorless
space group	P2 1/N
crystal size	0.06 × 0.19 × 0.13 mm ³
<i>a</i> [Å]	8.6320
<i>b</i> [Å]	15.2841
<i>c</i> [Å]	17.2472
<i>V</i> [Å ³]	2237.97(18)
<i>Z</i>	4
radiation	Mo Kα
T [K]	123
absorption coeff. μ[mm ⁻¹]	0.184
measured reflections	7936
independent reflections	6574

8.2. List of Abbreviations

Å	Ångström (1 Å = 10 ⁻¹⁰ m)
Ac	acetyl
Alk	alkyl
Ar	aryl
BAr _F	tetrakis[3,5-bis(trifluormethyl)-phenyl]borate
Bn	benzyl
br	broad
c	concentration
calc.	calculated
cat.	catalyst
Cy	cyclohexyl
d	doublet (NMR)
δ	chemical shift
DBU	1,8-Diazabicyclo[5.4.0]undec-7-ene
DCE	dichloroethane
DCM	dichloromethane
DHP	dihydropyridine
DIPEA	<i>N,N</i> -diisopropylethylamine
DMF	<i>N,N</i> -dimethylformamide
DMSO	dimethylsulfoxide
<i>E</i>	opposite
EA	elemental analysis
<i>ee</i>	enantiomeric excess
EI	electron-impact ionisation
eq.	equivalent

ESI	electrospray ionisation
Et	ethyl
Et ₂ O	diethyl ether
FAB	fast atom bombardement
FTIR	Fourier transform infrared spectroscopy
GC	gas chromatography
h	hours
Hz	Hertz
HV	high vacuum
<i>i</i> Pr	2-propyl
<i>J</i>	coupling constant
LiHMDS	Lithiumhexamethyldisilazane
M	molar [mol/l]
m.p.	melting point
<i>m/z</i>	mass-to-charge ratio
Me	methyl
MeOH	methanol
Mes	2,4,6-trimethylbenzene
min	minute(s)
mL	mililiter
MS	mass spectrometry or mole-sieves
Ms	methanesulfonyl
<i>n</i>	normal
n.r.	no reaction
NMR	nuclear magnetic resonance
NOESY	nuclear Overhauser enhancement spectroscopy

<i>o</i>	ortho
<i>p</i>	para
Ph	phenyl
ppm	part per million
P ₁ - ^t Bu	<i>tert</i> -Butylimino-tris(dimethylamino)phosphorane
P ₄ -Oct	1- <i>tert</i> -Octyl-4,4,4-tris(dimethylamino)-2,2-bis[tris(dimethylamino)phosphoranylidenamino]-2λ5,4λ5-catenadi(phosphazene)
<i>R_f</i>	retention factor
RT	room temperature
T	temperature
t	triplet (NMR) or time
^t Bu	<i>tert</i> -butyl
TEA	triethylamine
THF	tetrahydrofuran
TFA	Trifluoroacetic acid
TfOH	Trifluoromethanesulfonic acid
TLC	thin layer chromatography
TMS	trimethylsilyl
Ts	toxyl
w	weak (IR)
Xyl	xylene
Z	together

Chapter 9

9. References

- [1] I. P. Freeman, in *Ullmann's Encyclopedia of Industrial Chemistry*, Wiley-VCH Verlag GmbH & Co. KGaA, **2000**.
- [2] W. Bonrath, J. Medlock, J. Schütz, B. Wüstenberg, T. Netscher, *Hydrogenation in the Vitamins and Fine Chemicals Industry – An Overview*, **2012**.
- [3] K. R. Westerterp, E. J. Molga, K. B. van Gelder, *Chemical Engineering and Processing: Process Intensification* **1997**, *36*, 17-27.
- [4] J. G. de Vries, C. J. Elsevier, in *The Handbook of Homogeneous Hydrogenation*, Wiley-VCH Verlag GmbH, **2008**.
- [5] S. Nishimura, *Handbook of Heterogeneous Catalytic Hydrogenation for Organic Synthesis*, Wiley-VCH Verlag GmbH, **2001**.
- [6] R. Noyori, *Angew. Chem. Int. Ed.* **2002**, *41*, 2008-2022.
- [7] W. S. Knowles, *Angew. Chem. Int. Ed.* **2002**, *41*, 1998-2007.
- [8] C. Walling, L. Bollyky, *J. Am. Chem. Soc.* **1964**, *86*, 3750-3752.
- [9] G. H. Spikes, J. C. Fettinger, P. P. Power, *J. Am. Chem. Soc.* **2005**, *127*, 12232-12233.
- [10] G. D. Frey, V. Lavallo, B. Donnadieu, W. W. Schoeller, G. Bertrand, *Science* **2007**, *316*, 439-441.
- [11] G. C. Welch, D. W. Stephan, *J. Am. Chem. Soc.* **2007**, *129*, 1880-1881.
- [12] G. C. Welch, R. R. S. Juan, J. D. Masuda, D. W. Stephan, *Science* **2006**, *314*, 1124-1126.
- [13] G. Erker, D. W. Stephan, *Frustrated Lewis Pairs I Uncovering and Understanding*, Springer Berlin Heidelberg, **2013**.
- [14] G. Erker, D. W. Stephan, *Frustrated Lewis Pairs II Expanding the Scope*, Springer Verlag Heidelberg, **2013**.
- [15] G. Wittig, E. Benz, *Chem. Ber.* **1959**, *92*, 1999-2013.
- [16] W. Tochtermann, *Angew. Chem. Int. Ed.* **1966**, *5*, 351-371.
- [17] H. C. Brown, H. I. Schlesinger, S. Z. Cardon, *J. Am. Chem. Soc.* **1942**, *64*, 325-329.
- [18] D. W. Stephan, *Org. Biomol. Chem.* **2008**, *6*, 1535-1539.
- [19] D. W. Stephan, G. Erker, *Angew. Chem. Int. Ed.* **2010**, *49*, 46-76.
- [20] A. L. Kenward, W. E. Piers, *Angew. Chem. Int. Ed.* **2008**, *47*, 38-41.
- [21] A. Berkessel, *Curr. Opin. Chem. Biol.* **2001**, *5*, 486-490.
- [22] P. A. Chase, G. C. Welch, T. Jurca, D. W. Stephan, *Angew. Chem. Int. Ed.* **2007**, *46*, 8050-8053.
- [23] P. Spies, G. Erker, G. Kehr, K. Bergander, R. Froehlich, S. Grimme, D. W. Stephan, *Chem. Commun.* **2007**, 5072-5074.
- [24] P. Spies, S. Schwendemann, S. Lange, G. Kehr, R. Frohlich, G. Erker, *Angew. Chem. Int. Ed.* **2008**, *47*, 7543-7546.
- [25] H. D. Wang, R. Frohlich, G. Kehr, G. Erker, *Chem. Commun.* **2008**, 5966-5968.
- [26] K. V. Axenov, G. Kehr, R. Fröhlich, G. Erker, *J. Am. Chem. Soc.* **2009**, *131*, 3454-3455.
- [27] P. A. Chase, T. Jurca, D. W. Stephan, *Chem. Commun.* **2008**, 1701-1703.
- [28] D. W. Stephan, *Org. Biomol. Chem.* **2012**, *10*, 5740-5746.
- [29] V. Sumerin, F. Schulz, M. Atsumi, C. Wang, M. Nieger, M. Leskelä, T. Repo, P. Pyykkö, B. Rieger, *J. Am. Chem. Soc.* **2008**, *130*, 14117-14119.
- [30] V. Sumerin, F. Schulz, M. Nieger, M. Leskelä, T. Repo, B. Rieger, *Angew. Chem. Int. Ed.* **2008**, *47*, 6001-6003.
- [31] G. Erős, H. Mehdi, I. Pápai, T. A. Rokob, P. Király, G. Tárkányi, T. Soós, *Angew. Chem. Int. Ed.* **2010**, *49*, 6559-6563.
- [32] Z. Lu, Z. Cheng, Z. Chen, L. Weng, Z. H. Li, H. Wang, *Angew. Chem. Int. Ed.* **2011**, *50*, 12227-12231.
- [33] M. Alcarazo, C. Gomez, S. Holle, R. Goddard, *Angew. Chem. Int. Ed.* **2010**, *49*, 5788-5791.
- [34] Z. M. Heiden, D. W. Stephan, *Chem. Commun.* **2011**, *47*, 5729-5731.
- [35] D. Chen, J. Klankermayer, *Chem. Commun.* **2008**, 2130-2131.

- [36] Y. W. Dianjun Chen, Jürgen Klankermayer, *Angew. Chem. Int. Ed.*, **49**, 9475-9478.
- [37] D. Chen, J. Klankermayer, *Chem. Commun.* **2008**, 2130-2131.
- [38] D. Chen, Y. Wang, J. Klankermayer, *Angew. Chem., Int. Ed.* **2010**, *49*, 9475-9478.
- [39] D. Chen, V. Leich, F. Pan, J. Klankermayer, *Chemistry* **2012**, *18*, 5184-5187.
- [40] G. Ghattas, D. Chen, F. Pan, J. Klankermayer, *Dalton Trans.* **2012**, *41*, 9026-9028.
- [41] Y. Liu, H. Du, *J. Am. Chem. Soc.* **2013**, *135*, 6810-6813.
- [42] D. J. Scott, M. J. Fuchter, A. E. Ashley, *J. Am. Chem. Soc.* **2014**, *136*, 15813-15816.
- [43] T. Mahdi, D. W. Stephan, *J. Am. Chem. Soc.* **2014**, *136*, 15809-15812.
- [44] S. J. Geier, D. W. Stephan, *J. Am. Chem. Soc.* **2009**, *131*, 3476-3477.
- [45] P. A. Chase, D. W. Stephan, *Angew. Chem. Int. Ed.* **2008**, *47*, 7433-7437.
- [46] D. Holschumacher, T. Bannenberg, C. G. Hrib, P. G. Jones, M. Tamm, *Angew. Chem. Int. Ed.* **2008**, *47*, 7428-7432.
- [47] G. C. Welch, D. W. Stephan, *J. Am. Chem. Soc.* **2007**, *129*, 1880-1881.
- [48] F. Bertini, V. Lyaskovskyy, B. J. J. Timmer, F. J. J. de Kanter, M. Lutz, A. W. Ehlers, J. C. Slootweg, K. Lammertsma, *J. Am. Chem. Soc.* **2012**, *134*, 201-204.
- [49] T. Wang, D. W. Stephan, *Chem. Eur. J.* **2014**, *20*, 3036-3039.
- [50] L. Greb, C.-G. Daniliuc, K. Bergander, J. Paradies, *Angew. Chem. Int. Ed.* **2013**, *52*, 5876-5879.
- [51] S. Grimme, H. Kruse, L. Goerigk, G. Erker, *Angew. Chem. Int. Ed.* **2010**, *49*, 1402-1405.
- [52] B. Schirmer, S. Grimme, *Chem. Commun.* **2010**, *46*, 7942-7944.
- [53] T. A. Rokob, I. Bakó, A. Stirling, A. Hamza, I. Pápai, *J. Am. Chem. Soc.* **2013**, *135*, 4425-4437.
- [54] J. L. T. J. M. Berg, L. Stryer, *Biochemie*, Spektrum Akademischer Verlag, Heidelberg, **2007**.
- [55] U. Eisner, J. Kuthan, *Chem. Rev.* **1972**, *72*, 1-42.
- [56] D. Mauzerall, F. H. Westheimer, *J. Am. Chem. Soc.* **1955**, *77*, 2261-2264.
- [57] J. Kuthan, A. Kurfurst, *Ind. Eng. Chem. Res.* **1982**, *21*, 191-261.
- [58] D. M. Stout, A. I. Meyers, *Chem. Rev.* **1982**, *82*, 223-243.
- [59] R. Lavilla, *J. Chem. Soc., Perkin Trans. 1* **2002**, 1141-1156.
- [60] M. Fujii, K. Kawaguchi, K. Nakamura, A. Ohno, *Chem. Lett.* **1992**, *21*, 1493-1496.
- [61] A. Ohno, Y. Ishihara, S. Ushida, S. Oka, *Tetrahedron Lett.* **1982**, *23*, 3185-3188.
- [62] S. Obika, T. Nishiyama, S. Tatematsu, K. Miyashita, C. Iwata, T. Imanishi, *Tetrahedron* **1997**, *53*, 593-602.
- [63] T. J. Van Bergen, R. M. Kellogg, *J. Am. Chem. Soc.* **1976**, *98*, 1962-1964.
- [64] A. Hantzsch, *Justus Liebigs Ann. Chem.* **1882**, *215*, 1-82.
- [65] S. Tasaka, H. Ohmori, N. Gomi, M. Iino, T. Machida, A. Kiue, S. Naito, M. Kuwano, *Bioorg. Med. Chem. Lett.* **2001**, *11*, 275-277.
- [66] M. Suárez, Y. Verdecia, B. Illescas, R. Martínez-Alvarez, A. Alvarez, E. Ochoa, C. Seoane, N. Kayali, N. Martín, *Tetrahedron* **2003**, *59*, 9179-9186.
- [67] S. G. Ouellet, J. B. Tuttle, D. W. C. MacMillan, *J. Am. Chem. Soc.* **2004**, *127*, 32-33.
- [68] J. W. Yang, M. T. Hechavarria Fonseca, B. List, *Angew. Chem. Int. Ed.* **2004**, *43*, 6660-6662.
- [69] S. G. Ouellet, A. M. Walji, D. W. C. Macmillan, *Acc. Chem. Res.* **2007**, *40*, 1327-1339.
- [70] E. R. Clark, M. J. Ingleson, *Angew. Chem.* **2014**, *126*, 11488-11491.
- [71] L. Leclercq, I. Suisse, G. Nowogrocki, F. Agbossou-Niedercorn, *Green Chem.* **2007**, *9*, 1097-1103.
- [72] A. Pyrko, *Chem. Heterocycl. Compd.* **1999**, *35*, 688-694.
- [73] A. F. Abdel-Magid, C. A. Maryanoff, K. G. Carson, *Tetrahedron Lett.* **1990**, *31*, 5595-5598.
- [74] O. Mitsunobu, *Synthesis* **1981**, 1-28.
- [75] C. M. Martínez-Vituro, D. Domínguez, *Tetrahedron Lett.* **2007**, *48*, 1023-1026.
- [76] P. Bohn, N. Le Fur, G. Hagues, J. Costentin, N. Torquet, C. Papamicael, F. Marsais, V. Levacher, *Org. Biomol. Chem.* **2009**, *7*, 2612-2618.
- [77] G. W. Gribble, D. C. Ferguson, *J. Chem. Soc., Chem. Commun.* **1975**, 535-536.
- [78] J. i. Uenishi, M. Hamada, S. Aburatani, K. Matsui, O. Yonemitsu, H. Tsukube, *J. Org. Chem.* **2004**, *69*, 6781-6789.

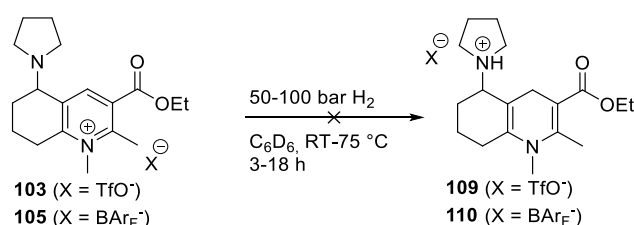
- [79] K. Worm, D. G. Weaver, R. C. Green, C. T. Saeui, D.-M. S. Dulay, W. M. Barker, J. A. Cassel, G. J. Stabley, R. N. DeHaven, C. J. LaBuda, M. Koblisch, B. L. Brogdon, S. A. Smith, R. E. Dolle, *Bioorg. Med. Chem. Lett.* **2009**, *19*, 5004-5008.
- [80] N. G. J. Clayden, S. Warren, P. Wothers, *Organic Chemistry*, Oxford University Press, Oxford, **2001**.
- [81] M. N. Burnett, C. K. Johnson, *ORTEP-III: Oak Ridge Thermal Ellipsoid Plot Programm for Crystal Structure Illustration*, Oak Ridge National Laboratory Report ORNL-6895, **1996**.
- [82] M. F. Dubreuil, N. G. Farcy, E. J. Goethals, *Macromol. Rapid Commun.* **1999**, *20*, 383-386.
- [83] T. Hayashida, H. Kondo, J.-i. Terasawa, K. Kirchner, Y. Sunada, H. Nagashima, *J. Organomet. Chem.* **2007**, *692*, 382-394.
- [84] I. Krossing, I. Raabe, *Angew. Chem. Int. Ed.* **2004**, *43*, 2066-2090.
- [85] H. Fiege, H.-W. Voges, T. Hamamoto, S. Umemura, T. Iwata, H. Miki, Y. Fujita, H.-J. Buysch, D. Garbe, W. Paulus, in *Ullmann's Encyclopedia of Industrial Chemistry*, Wiley-VCH Verlag GmbH & Co. KGaA, **2000**.
- [86] J. A. King, G. L. Bryant, *J. Org. Chem.* **1992**, *57*, 5136-5139.
- [87] J. H. Cooley, E. J. Evain, *Synthesis* **1989**, *1989*, 1-7.
- [88] A. P. Shaw, B. L. Ryland, M. J. Franklin, J. R. Norton, J. Y. C. Chen, M. L. Hall, *J. Org. Chem.* **2008**, *73*, 9668-9674.
- [89] D. L. Comins, A. H. Abdullah, *J. Org. Chem.* **1984**, *49*, 3392-3394.
- [90] J.-L. Vasse, V. Levacher, J. Bourguignon, G. Dupas, *Tetrahedron* **2003**, *59*, 4911-4921.
- [91] J. W. Runyon, O. Steinhof, H. V. R. Dias, J. C. Calabrese, W. J. Marshall, A. J. Arduengo, *Aust. J. Chem.* **2011**, *64*, 1165-1172.
- [92] O. Schuster, L. Yang, H. G. Raubenheimer, M. Albrecht, *Chem. Rev.* **2009**, *109*, 3445-3478.
- [93] J. S. Owen, J. A. Labinger, J. E. Bercaw, *J. Am. Chem. Soc.* **2004**, *126*, 8247-8255.
- [94] M. Albrecht, H. Stoeckli-Evans, *Chem. Commun.* **2005**, 4705-4707.
- [95] K. Hata, Y. Segawa, K. Itami, *Chem. Commun.* **2012**, *48*, 6642-6644.
- [96] T. J. Van Bergen, T. Mulder, R. A. Van Der Veen, R. M. Kellogg, *Tetrahedron* **1978**, *34*, 2377-2383.
- [97] S.-L. You, *Chem. Asian J.* **2007**, *2*, 820-827.
- [98] Q. Dai, W. Yang, X. Zhang, *Org. Lett.* **2005**, *7*, 5343-5345.
- [99] H. Heaney, G. Papageorgiou, R. F. Wilkins, *Tetrahedron* **1997**, *53*, 14381-14396.
- [100] H. Singh, K. Singh, *Tetrahedron* **1989**, *45*, 3967-3974.
- [101] T. Sirijindalert, K. Hansuthirakul, P. Rashatasakhon, M. Sukwattanasinitt, A. Ajavakom, *Tetrahedron* **2010**, *66*, 5161-5167.
- [102] B. C. Hamann, J. F. Hartwig, *J. Am. Chem. Soc.* **1998**, *120*, 7369-7370.
- [103] A. Singer, S. M. McElvain, *Org. Syn.* **1934**, *30*.
- [104] J. Kuthan, *Collect. Czech. Chem. Commun.* **1962**, 2175.
- [105] N. R. Davis, R. A. Anwar, *J. Am. Chem. Soc.* **1970**, *92*, 3778-3782.
- [106] M. Saunders, E. H. Gold, *J. Org. Chem.* **1962**, *27*, 1439-1441.
- [107] E. H. Huntress, E. N. Shaw, *J. Org. Chem.* **1948**, *13*, 674-681.
- [108] E. E. Ayling, *J. Chem. Soc.* **1938**, 1014-1023.
- [109] M.-Z. Jin, L. Yang, L.-M. Wu, Y.-C. Liu, Z.-L. Liu, *Chem. Commun.* **1998**, 2451-2452.
- [110] A. Ohno, S. Ushida, S. Oka, *Bull. Chem. Soc. Jpn.* **1984**, *57*, 506-509.
- [111] Y. Ohnishi, M. Kitami, *Tetrahedron Lett.* **1978**, *19*, 4035-4036.
- [112] Y. Ohnishi, *Tetrahedron Lett.* **1977**, *18*, 2109-2112.
- [113] N. Goulioukina, J. Wehbe, D. Marchand, R. Busson, E. Lescrinier, D. Heindl, P. Herdewijn, *Helv. Chim. Acta* **2007**, *90*, 1266-1278.
- [114] M. E. Brewster, A. Simay, K. Czako, D. Winwood, H. Farag, N. Bodor, *J. Org. Chem.* **1989**, *54*, 3721-3726.
- [115] X.-Q. Zhu, Y. Liu, B.-J. Zhao, J.-P. Cheng, *J. Org. Chem.* **2000**, *66*, 370-375.
- [116] W.-C. Cheng, M. J. Kurth, *Org. Prep. Proced. Int.* **2002**, *34*, 585-608.
- [117] A. R. Katritzky, O. Rubio, M. Szadja, B. Nowak-Wydra, *J. Chem. Research (S)* **1984**, 234-235.

- [118] R. E. Lyle, C. B. Boyce, *J. Org. Chem.* **1974**, *39*, 3708-3711.
- [119] T. Ishikawa, *Superbases for Organic Synthesis: Guanidines, Amidines, Phosphazenes and Related Organocatalysts*, John Wiley & Sons, Chichester, **2009**.
- [120] S. Brandau, A. Landa, J. Franzén, M. Marigo, K. A. Jørgensen, *Angew. Chem.* **2006**, *118*, 4411-4415.
- [121] M. Abid, M. Savolainen, S. Landge, J. Hu, G. K. S. Prakash, G. A. Olah, B. Török, *J. Fluorine Chem.* **2007**, *128*, 587-594.
- [122] S. Singh, V. K. Sharma, S. Gill, R. I. K. Sahota, *J. Chem. Soc., Perkin Trans. 1* **1985**, 437-440.
- [123] M. Litvic, M. Filipan, I. Pogorelic, I. Capanec, *Green Chem.* **2005**, *7*, 771-774.
- [124] J. C. Speelman, R. M. Kellogg, *The Journal of Organic Chemistry* **1990**, *55*, 647-653.
- [125] M. Gangapuram, K. K. Redda, *J. Heterocycl. Chem.* **2006**, *43*, 709-718.
- [126] A. Takács, A. Szilágyi, P. Ács, L. Márk, A. F. Peixoto, M. M. Pereira, L. Kollár, *Tetrahedron* **2011**, *67*, 2402-2406.
- [127] K. Y. Lee, C. G. Lee, J. N. Kim, *Tetrahedron Lett.* **2003**, *44*, 1231-1234.
- [128] P. Beak, A. Basha, B. Kokko, D. Loo, *J. Am. Chem. Soc.* **1986**, *108*, 6016-6023.
- [129] J. L. García Ruano, J. Alemán, I. Alonso, A. Parra, V. Marcos, J. Aguirre, *Chem. Eur. J.* **2007**, *13*, 6179-6195.
- [130] S. S. Szinai, G. Crank, D. R. K. Harding, *J. Med. Chem.* **1970**, *13*, 1212-1215.

Summary

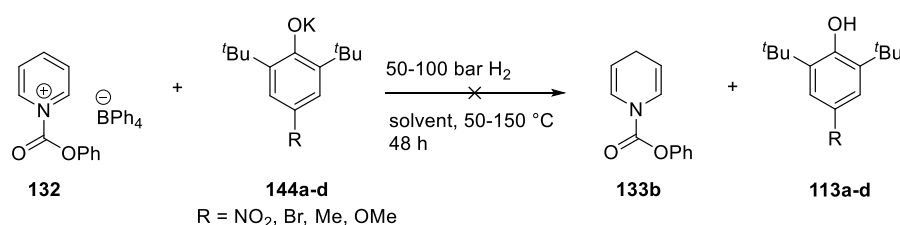
10 Summary

The work presented in this thesis was dedicated to the development of novel systems based on pyridinium salts for the heterolytic dihydrogen activation and evaluation of their suitability as catalysts for catalytic hydrogenation. These systems contain a pyridinium salt as hydride acceptor and a basic nitrogen or oxygen function as proton acceptor. Initially, an intramolecular system was envisioned, in which the pyridinium salt is linked with a basic amine and the hydrogen cleavage should occur through a concerted transition state. Due to the low stability of the starting materials, mainly decomposition products were observed after test reactions at high temperatures and hydrogen pressures ranging from 50-100 bar (Scheme 10.1).



Scheme 10.1. Attempted dihydrogen activation by an intramolecular pyridinium-amine system.

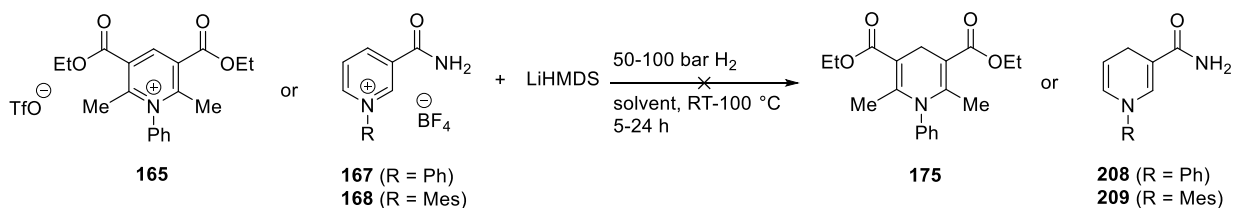
As a next step, a bimolecular system based on pyridinium salts and sterically hindered alcoxides was evaluated. For this purpose, electrophilic *N*-acyl ammonium salts and phenolates derived from commercially available BHT derivatives were prepared. However, in the presence of hydrogen gas no reaction was observed and starting materials were recovered (Scheme 10.2).



Scheme 10.2. Attempted dihydrogen activation by a bimolecular system.

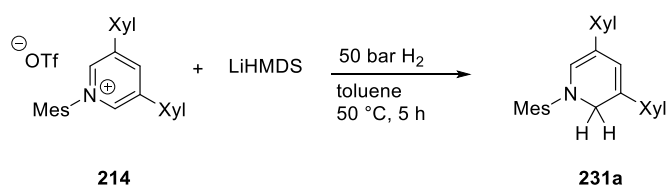
ITAMI and co-workers^[95] demonstrated the formation of pyridylidenes from pyridinium salts in the presence of a strong base. These highly reactive intermediates could then undergo formal

addition of H₂. Known pyridinium salt/dihydropyridine systems are Hantzsch esters and nicotinamide derivatives. Both classes of pyridinium salts were tested for H₂ activation reactions. Although the formation of the corresponding dihydropyridines was observed, deuteration experiments proved that the reaction did not proceed *via* dihydrogen splitting. Furthermore, the ability of these *N*-protected pyridinium salts to reduce selected substrates was rather poor (*Scheme 10.3*).



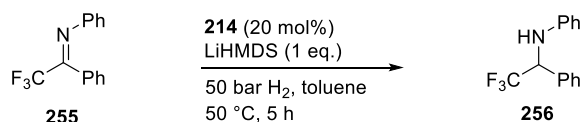
Scheme 10.3. Attempted dihydrogen activation by *N*-phenyl Hantzsch esters and *N*-aryl nicotinamides.

Finally, the activation of dihydrogen was achieved by reaction of a pyridinium salt as described by *ITAMI* in the presence of base.^[95] First, a 1,3,5-triarylpyridinium salt was synthesized, which could be transformed into the corresponding pyridylidene in the presence of LiHMDS. This intermediate was trapped by quenching with S₈. Reaction with H₂ led to its activation and the corresponding 1,2-dihydropyridine was formed (*Scheme 10.4*).



Scheme 10.4. Dihydrogen activation by reaction of a pyridinium salt and LiHMDS.

Dihydrogen activation was confirmed by reaction with deuterium gas, as the ²H NMR spectra showed the signal of the corresponding CD₂ group. Studies towards catalytic applications of that system showed that imine **255** was reduced to the corresponding amine in the presence of stoichiometric amounts of base and 20 mol% of catalyst loading (*Scheme 10.5*).



Scheme 10.5. *In-situ* reduction of imine **25**

